CELLULAR ACTIONS OF PEROXYNITRITE IN PULMONARY ARTERY ENDOTHELIAL AND SMOOTH MUSCLE CELLS: RELEVANCE TO PULMONARY HYPERTENSION

By

EJAIFE ONO AGBANI [B.Pharm, M.Sc]

A thesis submitted in fulfilment of the requirements

for the degree of Doctor of Philosophy

Strathclyde Institute of Pharmacy and Biomedical Sciences

University of Strathclyde

Glasgow, United Kingdom

2009

This thesis is the result of the author's original research. It has been composed by the author and has not been previously submitted for examination, which has led to the award of a degree.

Signed: Date: 2nd December 2009

ACKNOWLEDGEMENTS

"To be sure, this was not an easy path for me to tread. I owe it to my God Jehovah – the giver of life and the sustainer of it that I did come off victorious"

Very special thanks to Professor Roger Martin Wadsworth, my PhD research supervisor and academic mentor. There was just so much to learn from you Prof. You skilfully drove my learning cycle to my benefit. Your criticisms were constructive; your recommendations were insightful, always cushioned with commendations. I could not have had it better. I thank you and I thank Dr Paul Coats my 2nd research supervisor.

I am grateful to the Universities UK and the University of Strathclyde for the funding that has made this project a reality and a success.

And how better to close this chapter than to thank my darling wife Naomi Temitope Agbani who stood by me while peroxynitrite decayed so quickly and cared for my kids while I watched pulmonary artery cells grow slowly. I was brave only because I had your full support. I dedicate this work to you and to our inheritance during the period of this work – Ejoyovwi and Oghenemine.

.

PUBLICATIONS

Agbani, E.O., Coats P., Mills A., and Wadsworth RM (2009). Peroxynitrite Stimulates Proliferation of Pulmonary Artery Smooth Muscle and Endothelial Cells Via ERK 1/2 Activation. Am. J. Respir. Crit. Care Med., Apr 2009; 179: A1810. http://ajrccm.atsjournals.org/cgi/reprint/ Conference of American Thoracic Society. San Diego, California, USA. May 15-20, 2009.

Agbani, E.O., Coats P., Mills A., and Wadsworth RM (2009). Hypoxia and Peroxynitrite Act Synergistically To Stimulate Pulmonary Artery Smooth Muscle and Endothelial Cell Proliferation. Am. J. Respir. Crit. Care Med., Apr 2009; 179: A1801. http://ajrccm.atsjournals.org/cgi/reprint/. Conference of American Thoracic Society. San Diego, California, USA. May 15-20, 2009.

Agbani, E.O., Coats P., Mills A., and Wadsworth RM (2009) Peroxynitrite impairs pulmonary artery cell function through JNK and p38 MAP kinase. E-journal of British pharmacological society: Volume 7 Issue 2. Conference of British Pharmacological Society, Edinburgh, Scotland, UK. July 8-10, 2009.

.

ABSTRACT

BACKGROUND: Pulmonary artery hyperplasia and the up-regulation of peroxynitrite (ONOO-) have been independently associated with pulmonary hypertension; accordingly, this study hypothesized a role for the anion in the pathogenesis of the disease. **METHODS:** The life and activity of authentic and 3-morpholinosydnonimine (SIN-1) generated ONOO- were investigated by absorbance spectroscopy and NADH fluorescence quenching. Cytotoxicity was investigated by Trypan blue dye exclusion and LDH assays. Cell proliferation determination involved cell counting, ^{3}H-thymidine incorporation and MTT assays. Protein biochemistry was by western blot analysis. **RESULTS:** Primary isolates of bovine pulmonary artery endothelial (PAEC) and smooth muscle cell (PASMC) were obtained from bovine lungs. Peroxynitrite half life was 1.38s at pH 7.4. Decomposing via a pH and oxygen dependent mechanism, 20μM SIN-1 generated ONOO- at the rate of 0.11μM min^{-1}. Peroxynitrite was cytotoxic at and above 2μM; at which apoptotic cell death may be caspase-3 dependent but independent of p38 or JNK activation. Cell death at >2μM ONOO- may involve activation of caspase-3 in both apoptotic and necrotic pathways. However, transient exposure of PASMC in 0.1% foetal bovine serum (FBS) to 0.2nM ONOO- caused 117.8±6% increase in DNA synthesis ($p<0.05$). Similarly, at 2.5% FBS, PASMC cells were stimulated by 2nM ONOO- (136.2±10%; $p<0.01$) and by 0.2μM ONOO- (199.6±22%; $p<0.01$). PAEC were stimulated to proliferate by slightly higher concentrations of ONOO-; 0.2μM ONOO- (137±4%; $p<0.01$) and by 2μM SIN-1 (188±16 %; $p<0.01$). This is the first report of these findings. Moreover, acute exposure to experimental hypoxia (5% O_2) induced the intracellular formation of peroxynitrite and significantly stimulated pulmonary artery cell proliferation. In addition, ONOO- activated ERK via a MEK/Raf-1/Ras dependent pathway and the proliferative response to ONOO- was abolished by selective tyrosine kinase inhibition. **CONCLUSION:** This study demonstrates a potential role for ONOO- in pulmonary artery cell hyper-proliferation and vascular remodelling in pulmonary hypertension.

.

TABLE OF CONTENTS

.

CHAPTER 1
GENERAL INTRODUCTION

.

1.0: PULMONARY HYPERTENSION

Pulmonary hypertension (PH) is a spectrum of progressive diseases in which the pulmonary vasculature appears to be the exclusive target. The disorder involves the narrowing of the pulmonary arterioles within the lung, leading to increased vascular resistance and pressure on the heart. Other features include pulmonary vascular proliferation and remodelling (Rabinovitch, 2008). Clinical manifestations include dyspnea, fatigue, severe respiratory distress, cyanosis and right ventricular hypertrophy/ failure and death (Runo and Loyd, 2003). Abnormally thickened pulmonary arteries, endothelial dysfunction, reduced production of nitric oxide and prostacyclin, over-expression of vasoconstrictors, the generation of superoxide and peroxynitrite, vasoconstriction and thrombosis have been reported as pathophysiological features of the disease (Voelkel *et al.*, 1997). The World Health Organization (WHO) in 2004 reclassified pulmonary hypertension into five clinical groups/categories sharing similarities in pathophysiological mechanisms, clinical presentation, and therapeutic options (Simonneau *et al.*, 2004). In general, patients show similar response to treatment (Liu *et al.*, 2006), though variable conditions exist between groups. The 5 main groups are (i) pulmonary arterial hypertension (PAH) (ii) pulmonary venous hypertension (iii) pulmonary hypertension associated with disorders of the respiratory system or hypoxemia (iv) pulmonary hypertension caused by chronic thrombotic or embolic disease (v) pulmonary hypertension caused by disorders directly affecting the pulmonary vasculature (Simonneau *et al.*, 2004). Broad incidence and prevalence data for populations of PAH have not been reported in the UK. In France however, a comprehensive registry has determined the prevalence of PAH to be 15 cases per million, with an average age at the time of diagnosis of 50 ± 15 years, a female predisposition of 2:1, an average mean PA pressure of 55 mmHg (Humbert *et al.*, 2006) (normal = 12-16mmHg, PH=mean pulmonary artery pressure becomes greater than 25mmHg at rest or 30mmHg with exercise; Humbert *et al.*, 2006). The main hazard for patients is the abnormal RV pressure, which causes high morbidity and mortality.

1.1. THE PATHOBIOLOGY OF PULMONARY HYPERTENSION

The spectrum of pathological changes in pulmonary hypertension is extraordinarily varied (Rubin *et al.*, 2007; Mooi and Grünberg, 2006). However, all forms of the disease feature a raised pulmonary arterial blood pressure. Also, for the most part they share common pathobiology with pulmonary arterial hypertension (PAH). The pathology of PAH is characterised by luminal obliteration of small pulmonary arteries. This process of vascular remodelling involves proliferation of smooth muscle cells, fibroblasts and endothelial cells in the vessel wall (Jeffery and Morrell, 2002; Pietra *et al.*, 1989). In severe forms of pulmonary hypertension, the formation of a neointima is observed forming concentric intimal lesions. Abnormal endothelial cell proliferation results in the formation of plexiform lesions (Fig. 1). The most severe forms of precapillary pulmonary hypertension are usually pathologically indistinguishable (Consensus, 2008). In older children and adults, in addition to loss of distal vessels and enhanced distal arterial muscularization, there is progressive intimal hyperplasia leading to occlusive changes in the pulmonary arteries and plexiform lesions (Rabinovitch, 2008); Fig. 1). There is medial hypertrophy of muscular pulmonary arteries (Mooi and Grünberg, 2006) and the muscularization of distal wall pulmonary arteries has been associated with differentiation of pericytes into smooth muscle cells that subsequently proliferate (Meyrick and Reid, 1980). The progressive thickening of the wall of more proximal muscular arteries and the obliteration associated with neointimal formation has been attributed to increased proliferation and migration of cells considered to be SMCs cells (Jones *et al.*, 1997). In these patients alterations in endothelial functions have been reported and shown to precede the development of muscularization of pulmonary arteries (Rabinovitch *et al.*, 1986). The pathobiology of pulmonary hypertension associated with lung diseases also involve slight medial hypertrophy of veins (Mooi and Grünberg, 2006) and the mechanisms underlying the thickening of the pulmonary vascular medial layer have been linked mostly to cell proliferation (Rubin *et al.*, 2007). In addition, animal models show increased growth factors and markers of cell multiplication in pulmonary hypertension (Balasubramaniam *et al.*, 2003; Humbert *et al.*, 1998). The consensus in recent times suggests that the disease is proliferative in nature. Accordingly, anti-proliferative therapy has been shown to reverse vascular remodelling and cor pulmonale in severe experimental pulmonary hypertension regardless of the initiating stimulus (Schermuly *et al.*, 2005)

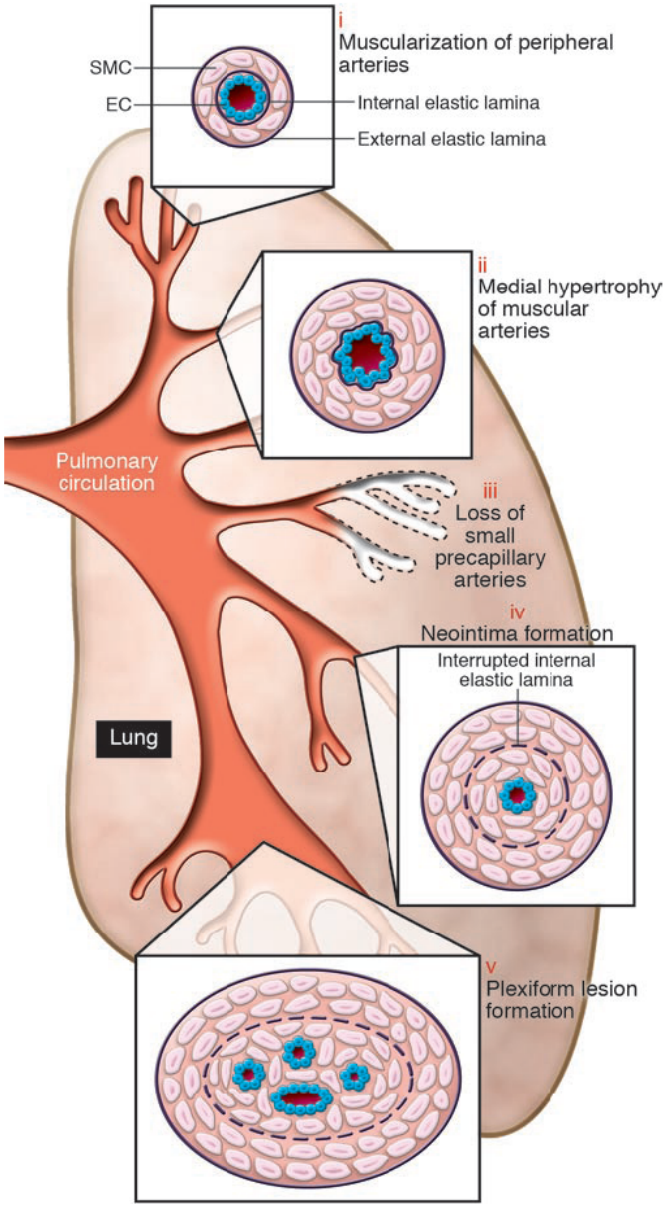

Figure 1: Vascular Pathobiology of Pulmonary Hypertension. The figure illustrates the different vascular abnormalities compared associated with pulmonary hypertension. These include but not limited to (i) abnormal muscularization of distal precapillary arteries, (ii) medial hypertrophy (thickening) of large pulmonary muscular arteries, (iii) loss of precapillary arteries, (iv) neointimal formation that is particularly occlusive in vessels 100–500μM, and (v) formation of plexiform lesions (Mooi and Grünberg, 2006); Figure from Rabinovitch, 2008)

1.2. CONTEMPORARY THERAPIES FOR PULMONARY HYPERTENSION

The aim of therapies for pulmonary hypertension is to improve right ventricular function, patients' functional class and mortality by reducing pulmonary vascular resistance. Randomised controlled clinical trials (RCT) have evaluated several available treatment options for the management of PAH using simple and reliable clinical end points. The Six-Minute Walk Test (6MW) in which the patient walks as far as possible in 6 min (Miyamoto *et al.*, 2000) is used as a primary clinical endpoint for the assessment of current therapy; independently, it is a good predictor of mortality in patients with pulmonary hypertension. Patients' functional class as indicated by the New York Heart Association (NYHA) or the WHO functional classification of patients with pulmonary hypertension is also used (D'alonzo *et al.*, 1991).

The treatment of pulmonary hypertension is as varied as its aetiology. In general, this has involved conventional therapy such as the use of anticoagulants such as warfarin, diuretics, digoxin, nifedipine and oxygen. Diuretics and digoxin provide symptomatic relief by reducing the workload on the heart but do not affect the course of pulmonary hypertension. Anticoagulant therapy with warfarin might improve survival but its contribution is difficult to estimate (Johnson *et al.*, 2006). Oxygen administered acutely has been demonstrated to reduce PVR in both hypoxic and non-hypoxic patients with PH (Consensus, 2008). Limited evidence from studies with chronic obstructive pulmonary disorder (COPD) patients also confirm the benefits of oxygen in this subgroup of pulmonary hypertensive patients (Mrc, 1981). However, there are no randomised data available to suggest that long term oxygen therapy (LTOT) is beneficial (Consensus, 2008). Nifedipine offer considerable benefits to patients who response to calcium channel blockers, but these account for only 6% of PAH patients (Rubin, 1985). Treatment guidelines thus stipulate the use of therapies targeted more directly at the pathology of pulmonary hypertension (Consensus, 2008). Currently, three classes of drugs (prostanoids, endothelin receptor antagonists, and phosphodiesterase-5 inhibitors) are approved for this.

1.2.1. Prostanoids: synthetic prostacyclin and its analogues

These have been used extensively to manage pulmonary hypertension. Prostacyclin is a potent vasodilator in the pulmonary and systemic circulations, it is endogenously produced by the vascular endothelium and is a metabolite of arachidonic acid with antiplatelet aggregatory activity. It is not known whether a deficiency of prostacyclin contributes to the pathogenesis of pulmonary hypertension though this has been suggested (Tuder *et al.*, 1999; Christman *et al.*, 1992). Prostacyclin (epoprostenol) administered intravenously showed significant improvements in 6MW for patients treated with epoprostenol compared with placebo within 3 months (Badesch *et al.*, 2000; Barst *et al.*, 1996; Rubin *et al.*, 1990). However, epoprostenol therapy requires continuous intravenous infusion since the drug has a systemic half-life of 6 min; therefore treatment is complicated, uncomfortable for patients and costly, besides the numerous adverse effects and life threatening complication of regimen and delivery systems (Liu *et al.*, 2006). Iloprost is another chemically stable prostacyclin analogue (half-life 20–25 min) that can be delivered by inhaler to patients with pulmonary hypertension. Its clinical and adverse effects are considered to be similar to those of epoprostenol (Higenbottam *et al.*, 1998). A 12-week trial (Olschewski *et al.*, 2002) showed significant improvement in hemodynamic values, improvement in the NYHA class and quality of life with iloprost inhalation. However, a recent cochrane review (Paramothayan *et al.*, 2008) could not ascertain long term efficacy owing to the short duration of studies. Treprostinil is a stable prostacyclin analogue with a half-life of 3h and is delivered subcutaneously. It thus avoids some of the drawbacks of epoprostenol; however, its clinical effectiveness is in doubt given reports showing no significant improvement in 6MW (Mclaughlin *et al.*, 2003). Beraprost is an orally active prostacyclin analogue, for which pooled data from randomised controlled trials do not show a significant improvement of NYHA/WHO function class in patients treated compared with placebo (Barst *et al.*, 2003; Galiè *et al.*, 2002).

1.2.2 Endothelin receptor antagonists (ERA)

These are potent vasodilators and antimitotic substances, and may specifically dilate and remodel the pulmonary arterial system. Two endothelin (ET) receptors have been identified, ET-A and ET-B. ET-A is commonly found on vascular smooth-muscle cells,

and stimulates vasoconstriction by increasing intracellular calcium. ET-B receptors are located on endothelial cells and promote the release of vasodilating agents such as nitric oxide and prostacyclin. However, ET-B receptors also appear on vascular smooth muscle cells, where they stimulate vasoconstriction. It has been shown that, either selective block of ET-A receptors alone or non-selective block of ET-A and ET-B receptors together can dilate the local vessels (Liu *et al.*, 2006). Randomised controlled trials have shown that either a non-selective ERA (bosentan) or a selective ET-A receptor antagonist (sitaxsentan) significantly improved 6MW distance and NYHA/WHO functional status by 12 weeks of therapy relative to placebo (Barst *et al.*, 2004; Rubin *et al.*, 2002; Channick *et al.*, 2001). However, it should be noted that the ERA have the potential for hepatic toxicity which may limit their clinical use.

1.2.3. Sildenafil (Phosphodiesterase (PDE)-type 5 inhibitor)

This selectively dilate pulmonary arteries via the enhancing of nitric oxide-dependent, cyclic guanosine monophosphate (CGMP) mediated pulmonary vasodilatation by inhibition of the breakdown of CGMP (Fig. 1.2) Pooled data from randomised controlled trials on 6MW or improvement in NYHA functional class suggest only marginal clinical gains up to 6 weeks of treatment (Liu *et al.*, 2006; Galie *et al.*, 2005; Bharani *et al.*, 2003). All the leading drugs used in pulmonary hypertension give only small improvement, but nevertheless this is important to the patient and is considered a worthwhile object of treatment. Therapies remain complicated, contentious, poorly effective, enormously expensive and potentially unsafe (Nauser and Stites, 2001). The need for novel therapeutic approaches for the treatment of pulmonary hypertension remains very important.

1.2.4. Emerging future therapeutic target: Tyrosine kinases

Recent developments in pulmonary hypertension research include the use of drugs originally developed for the treatment of cancer. This perhaps highlights that uncontrolled cell growth and increase growth factor receptors and or tyrosine kinase activity are common to both diseases. Recent studies have demonstrated the promise that anti-proliferative therapy hold for the management of pulmonary hypertension. An

agent showing positive benefit in pulmonary hypertension patients is imatinib- a tyrosine kinase receptor inhibitor used for the treatment of chronic myeloid leukaemia. Following a 3-month imatinib therapy, a rapidly-deteriorating patient was reported to have shown improvements in 6 minute walk test, haemodynamics and NYHA class; these gains were sustained at 6 months' follow-up (Ghofrani *et al.*, 2005). However, the use of imatinib in clinical practice may be limited as cardiotoxic effects have been associated with its long-term use. Imatinib has frequently caused left-ventricular dysfunction and heart failure (Kerkela *et al.*, 2006). These notwithstanding, the use imatinib as lead molecule will enable the development of potent drugs with improved pharmacodynamic profile for the treatment of pulmonary hypertension.

1.3. HYPOXIA IN PULMONARY HYPERTENSION

Group 3 of the WHO Evian clinical classification of pulmonary hypertension highlights the involvement of hypoxia in pulmonary hypertension (Simonneau *et al.*, 2004). Hypoxia is associated with adult respiratory distress syndrome and has major impact on the pulmonary circulation (Orfanos *et al.*, 2004). It induces the up-regulation of superoxide forming enzymes and initiates hypoxic pulmonary vasoconstriction as well as conditions predisposing to pulmonary hypertension. Under pathological conditions, hypoxic pulmonary vasoconstriction may occur as an acute episode during a rapidly progressive critical illness or as a sustained response associated with vascular remodelling and pulmonary arterial hypertension (Demiryürek and Wadsworth, 1999; Dumas *et al.*, 1999).

1.3.1 Hypoxic Pulmonary Vasoconstriction

Demonstrated in all the species so far examined in the international literature, hypoxic pulmonary vasoconstriction (HPV) is a physiological mechanism, intrinsic to the lung, which matches local blood flow to local alveolar ventilation (Dumas *et al.*, 1999); HPV is preserved even after lung transplantation (Robin *et al.*, 1987). It acts to reduce the perfusion of poorly ventilated regions of the lung by diverting blood to well-ventilated regions; thus optimising alveolar gaseous exchange (Orchard *et al.*, 1983; Marshall *et al.*, 1981; West *et al.*, 1964). This contrasts with the vasodilation effect observed in most vascular beds, including the coronary, skeletal muscle, cerebral, and gastrointestinal

circulations, following reduction in arterial PO_2. Wadsworth (1994) thus concluded that the response of a particular vascular bed to hypoxia is determined by the requirements of the tissue that it perfuses (Wadsworth, 1994). Hypoxic pulmonary vasoconstriction has been shown to be important in improving transitory gas exchange and oxygenation during acute lung injury (Brimioulle *et al.*, 2002). However, sustained vasoconstriction can lead to increased pulmonary vascular resistance, increased pulmonary arterial pressure, vascular remodelling, smooth muscle hypertrophy, decreased perfusion and increased right ventricular workload (Thompson *et al.*, 1993) .

Precapillary pulmonary arteries play an important role in hypoxic vasoconstriction (Dumas *et al.*, 1999; Nagasaka *et al.*, 1984; Kato and Staub, 1966). In addition, evidence of human and animal studies from this laboratory showed that the main pulmonary artery responds similarly to "resistance" pulmonary arteries (Demiryurek *et al.*, 1993; Demiryurek *et al.*, 1991). It has been demonstrated that the vasoconstriction response to hypoxia depends largely on the endothelium and is partly due to inhibition of a vasodilator cyclooxygenase products (prostacyclin) and limited by release of endothelium-derived nitric oxide (Demiryurek *et al.*, 1993; Demiryurek *et al.*, 1991)

HPV seen in different lung preparations differs in time course and response to pharmacological intervention (Emery *et al.*, 2003). Pulmonary vascular resistance has been observed to increase by up to 50% pre hypoxia level when the alveolar PO_2 drops below 50 mm Hg in humans (Harris and Heath, 1986). The trigger for HPV appears to be the oxygen tension of the pulmonary arterial vascular smooth muscle. Cotes (1993) indicated that this is determined by the oxygen tensions of the alveolar gas, the mixed venous blood, and the blood in the bronchial arteries that supplies the vasa vasorum in the walls of the pulmonary arteries (Cotes, 1993).

There seem to be agreement that pulmonary artery smooth muscle cell mitochondria act as the sensor for decline in ambient oxygen (Ward and Mcmurtry, 2009). In addition, Rho kinase-mediated Ca^{2+} sensitisation and the release of Ca^{2+} from ryanodine-sensitive stores are believed to be essential for sustained HPV. Also, increase in intracellular Ca^{2+} by voltage-dependent or independent pathways may play a role (Aaronson *et al.*, 2006). There is, however, no agreement on the signalling pathways that link oxygen sensing to

vasoconstriction. Evans and Ward (2009) identified three main hypotheses. The AMP-activated protein kinase (AMPK) hypothesis proposes that hypoxic inhibition of mitochondrial function increases the AMP/ATP ratio and thus activates AMPK, which in turn stimulates the production of an endogenous activator of ryanodine receptors (RyRs; cyclic ADP ribose (cADPR), (Ward and Mcmurtry, 2009; Evans, 2006). This mediates cADPR-dependent mobilisation of ryanodine-sensitive sarcoplasmic reticulum Ca^{2+} stores. The ROS hypothesis holds that HPV is due to increased ROS generation under hypoxic conditions; and ROS is here advocated to be the signalling moiety (Hodyc *et al.*, 2008; Ward, 2007). The 3rd hypothesis is the Redox hypothesis; this suggests that hypoxia causes a decrease in mitochondria function, decreased mitochondrial ROS generation and a more reduced cellular redox state. This is believed to be associated with $K_{v1.5}$ channel inhibition and Ca^{2+} influx (Ward and Mcmurtry, 2009; Wu *et al.*, 2007).

1.3.2. Hypoxia and the proliferation of pulmonary artery cells

Chronic hypoxia is associated with obstructive pulmonary diseases and pulmonary hypertension. Alone, hypoxia can stimulate cell proliferation and lead to vascular wall thickening, reduction in vessel lumen and increased vascular resistance (Leach and Treacher, 1995; Groves *et al.*, 1987; Fishman, 1976). Under hypoxic conditions (2-5% O_2), endothelial cells are capable of the release of basic fibroblast growth factor, pro-mitogenic prostanoids (Michiels *et al.*, 1994) and factor(s) that enhances SMC proliferation (Vender, 1992) and typifies pulmonary hypertension (Naeije and Rondelet, 2004; Tuder *et al.*, 2001; Durmowicz and Stenmark, 1999; Mecham *et al.*, 1987; Mckenzie *et al.*, 1984)

1.4. THE VITAL ROLE OF THE VASCULAR ENDOTHELIUM

The vascular endothelium has been described as an active organ with paracrine, endocrine, and autocrine activities and crucial for the regulation of vascular tone and the maintenance of vascular homeostasis (Hampl and Herget, 2000; Liaudet *et al.*, 2000; Moncada *et al.*, 1991). Amongst other vasodilating and contracting agents, the endothelium produces nitric oxide ($NO^{\bullet}$) through endothelial $NO^{\bullet}$ synthase (eNOS), a homodimeric oxidoreductase. The process involves the terminal nitrogen atom of L-

arginine in the presence of O_2 and the cofactors nicotinamide adenine dinucleotide phosphate (NADPH), flavin adenine dinucleotide (FAD), flavin mononucleotide (FMN), haem and tetrahydrobiopterin (BH_4) (Hampl and Herget, 2000). Along with endothelin, $NO^{\bullet}$ is an important signalling molecule in the endothelium, together they maintain vascular homeostasis and play a central role in the pathophysiology of pulmonary hypertension (Napoli and Loscalzo, 2004). Nitric oxide causes smooth muscle relaxation by the activation of soluble guanylate cyclase followed by cyclic GMP accumulation (Fig. 1.2; Moncada *et al.*, 1991).

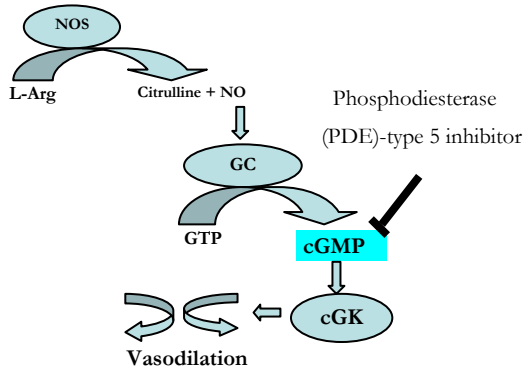

Figure 1.2: Downstream targets of nitric oxide. NO, produced by NOS, activates the target enzyme (soluble guanylyl cyclase) and increases tissue levels of cGMP. cGMP activates a cGMP-dependent protein kinase that mediates vasorelaxation. NOS, nitric oxide synthase; GC, soluble guanylyl cyclase; cGK, cGMP-dependent protein kinase; VASP, vasodilator stimulated phosphoprotein (Figure concept from Szöcs, 2004)

.

1.4.1. Nitric oxide and synthases in the pathophysiology of pulmonary hypertension

Studies using NOS isoforms knockout models suggest that eNOS-derived NO is an important modulator of basal pulmonary vascular tone as it attenuates the development of pulmonary hypertension (Fagan *et al.*, 1999a; Fagan *et al.*, 1999b; Steudel *et al.*, 1998; Steudel *et al.*, 1997). On the other hand, in experimental pulmonary hypertension, eNOS levels are often paradoxically raised in the pulmonary vascular endothelium (Demiryürek *et al.*, 2000; Le Cras *et al.*, 1996a; Le Cras *et al.*, 1996b) although without a concomitant increase in NO levels in hypoxic model of pulmonary hypertension (Demiryürek *et al.*, 2000; Nakazawa *et al.*, 1999) and thus suggesting possible eNOS dysfunction in the disease. Evidence from this laboratory indicated that endothelium-dependent relaxation of intrapulmonary vessels from hypoxic animals was impaired due to a reduced $NO^{\bullet}$ generation, determined by means of a microsensor (Weerackody *et al.*, 2009). This was despite an increase in eNOS expression (Weerackody *et al.*, 2009). The study involved the use of sprague-Dawley rats exposed to 2 wk hypobaric hypoxia, which resulted in the development of pulmonary hypertension and vascular remodelling (Weerackody *et*

al., 2009). Increases in eNOS levels may be unique to hypoxic models of pulmonary hypertension since such have not been observed in chemically induced or genetic models of the disease. Still, such increases have not prevented the development of vascular disorders in this models (Bauersachs *et al.*, 1999; Sato *et al.*, 1999; Tyler *et al.*, 1999; Bouloumie *et al.*, 1997). Unlike eNOS and neuronal NOS (nNOS) isoforms of $NO^{\bullet}$ synthase, inducible NOS (iNOS) is non constitutive and independent of intracellular calcium (Moncada *et al.*, 1991). Formation of iNOS protein can be induced by cytokines in many cells such as macrophages and smooth muscle cells. The expression of iNOS protein is also up-regulated in the pulmonary artery of chronically hypoxic rats (Le Cras *et al.*, 1996a; Xue and Johns, 1996). In rats exposed to chronic hypoxia, administration of $NO^{\bullet}$ synthesis inhibitors did not aggravate pulmonary hypertension and remodelling (Hampl *et al.*, 1993). Work by Carville et al., (1997) suggests that basal $NO^{\bullet}$ released by iNOS is little during pulmonary hypertension and is not enough to prevent the development of pulmonary hypertension (Carville *et al.*, 1997). Thus in spite of the up-regulation of both eNOS and iNOS in hypoxic pulmonary hypertension the pulmonary vasculature is deficient in NO.

1.5. OXIDATIVE STRESS IN CARDIOVASCULAR DISEASE

Cellular oxidants, derivatives of oxygen include reactive oxygen species (ROS) such as superoxide (O_2^-), hydrogen peroxide (H_2O_2), hydroxyl radical (-OH.) as well as reactive nitrogen species (RNS) such as nitrogen dioxide (NO_2^-) and peroxinitrite ($ONOO^-$; Salganik, 2001). Superoxide, $O_2^{\cdot-}$ was considered a vasoconstrictor agent derived from endothelial cells (Rey *et al.*, 2001; Vanhoutte, 2000) following the discovery that superoxide dismutase (SOD) augmented endothelium-dependent relaxation (Rubanyi and Vanhoutte, 1986). ROS production is low and endogenous antioxidant systems are often sufficient to maintain the balance between $O_2^{\cdot-}$ production and elimination, thus preventing the breakdown of $NO^{\bullet}$ under physiological conditions (Szöcs, 2004). However, ROS production has been found to increase with or without a decrease in the capacity of the vessels to produce antioxidant. The result is the conversion of $NO^{\bullet}$ into peroxynitrite (ONOO-) and an inhibition of $NO^{\bullet}$ dependent vascular relaxation (Szöcs, 2004; Salganik, 2001; O'donnell *et al.*, 1997; Adnot *et al.*, 1991). Peroxynitrite is a powerful oxidant that reacts with different biomolecules including amino acids such as cysteine, methionine, tryptophan, and tyrosine, thiol groups in proteins leading to

changes in protein structure and function (Alvarez and Radi, 2003). $ONOO^-$ thus exhibits a wide array of tissue damaging effects which include lipid peroxidation, DNA fragmentation, inactivation of enzymes and ion channels via protein oxidation and nitration, inhibition of mitochondrial respiration and reduction in cellular defences by oxidation of thiol pools (Szabó, 2003; Virág *et al.*, 2003; Lin *et al.*, 1997; Lopez *et al.*, 1997; Radi *et al.*, 1991a; Radi *et al.*, 1991b). Research has revealed some targets of peroxynitrite that could be modulated, as a result of oxidant stress, to produce the characteristic cellular changes occurring in pulmonary hypertension (Ronson *et al.*, 1999).

There are a number of sources of superoxide in the lungs; it can be formed under basal conditions and has been detected on the lung surface and in isolated pulmonary rings (Demiryürek and Wadsworth, 1999). Nitric oxide synthase is capable of generating superoxide when cellular L-arginine has been depleted and many oxidase enzymes present in the endothelium, namely xanthine oxidase, arachidonic acid peroxidases and eNOS, are capable of forming superoxide (Demiryürek and Wadsworth, 1999). ROS are also generated by mitochondria of the lung tissue via the release of electrons from the electron transport chain and the reduction of oxygen molecules to superoxides (O_2.-). Other sources of ROS, located in the endoplasmic reticulum, are cytochrome P_{450} complexes and phagocytes which produce superoxides, hydrogen peroxide and hydroxyl radicals to kill infectious cells. ROS are capable of oxidizing cell constituents such as DNA, proteins, and lipids, leading to impairment of cell functions and the development of morbid conditions (Szöcs, 2004; Ames *et al.*, 1993).

1.6. CLINICAL EVIDENCE: ONOO- IN PULMONARY HYPERTENSION

A few studies investigating the role of oxidative stress in pulmonary hypertension have demonstrated the up-regulation of ONOO- in the disease. One clinical study used immunohistochemistry to localize markers of peroxynitrite and oxidative stress (nitro-tyrosine and 8-OH guanosine, respectively) in lung tissue sections of patients with primary and secondary pulmonary hypertension and observed the ubiquitous expression of nitro-tyrosine (Bowers *et al.*, 2004). The formation of nitro-tyrosine is a footprint for ONOO-, revealing previous history of cumulative exposure to the anion, since it preferentially nitrates the tyrosine moieties of protein to form nitro-tyrosine

(Demiryürek *et al.*, 2000; Haddad *et al.*, 1994). Similarly, there was over-expression of 8-OH- guanosine in endothelial cell of pulmonary hypertension lungs (Bowers *et al.*, 2004). The conversion of guanine to 8-OHG is a frequent result of reactive oxygen species and may be indicative of the presence a strong oxidant such as ONOO-. These findings are supported by the analysis of lung lavage sample of patients with pulmonary hypertension (Kaneko *et al.*, 1998). In both studies, the patients have had PH for several years. It was therefore unclear whether or not there was an early involvement of ONOO- in pulmonary hypertension. Independently, this laboratory studied the lung tissue from infants who had died from pulmonary hypertension of the newborn and compared these to age-matched control patients who had no pulmonary or cardiovascular illness (Wadsworth *et al.*, 2004). The study demonstrated a 4-fold increase in staining intensity for nitro-tyrosine in the endothelium of small pulmonary arteries in patients with pulmonary hypertension. This is indicative of the up-regualtion of ONOO- and oxidative stress in the disease (Wadsworth *et al.*, 2004). Together, these findings demonstrate the presence of ONOO- in early and advanced stage of pulmonary hypertension. Unfortunately, the amount of ONOO- present in these patients cannot be determined from these studies.

1.7. THE IN-VIVO FORMATION AND DECAY OF PEROXYNITRITE

Peroxynitrite (ONOO–) is formed by reaction between superoxide (O_2^-) and nitric oxide ($NO^\bullet$) (Liaudet *et al.*, 2000; Beckman and Crow, 1993; Darley-Usmar *et al.*, 1992).

$O_2^- + NO^\bullet \Rightarrow O{=}N\text{-}O\text{-}O^-$. The rate constant for the reaction of superoxide and nitric oxide ($\sim 10^{10} M^{-1} s^{-1}$) makes it the fastest reaction known in biology and virtually assures that peroxynitrite will be formed in any cell or tissue where both radicals exist simultaneously (Crow, 2002). The mitochondria thus constitute a primary locus for the intracellular formation of ONOO-. Since $NO^\bullet$ is constitutively produced in vivo and is uncharged and freely diffusible, production of peroxynitrite is more likely to be governed by local production of superoxide. It may be a function of $NO^\bullet$ diffusing into a cellular compartment where superoxide is being generated and retained due to its negative charge (Crow, 2002). Peroxynitrite formation in-vivo may also be due to the combined action of superoxide producing enzyme like NADPH oxidase and a nitric oxide synthase generating $NO^\bullet$ (Squadrito and Pryor, 1995).

Peroxynitrite can undergo target molecule reactions with various cell constituents as well as react with carbon dioxide to yield secondary radicals capable of interaction with cells and sub cellular constituents (Radi *et al.*, 2002). The biological targets of ONOO- are illustrated in Figure 1.3. Decay of ONOO- is complicated; it is postulated to decay by over 40 reaction pathways the majority of which may not be physiologically relevant (Kissner *et al.*, 1997). The decay is very rapid (1.5 seconds at pH 7.4; Beckman *et al.*, 1990)

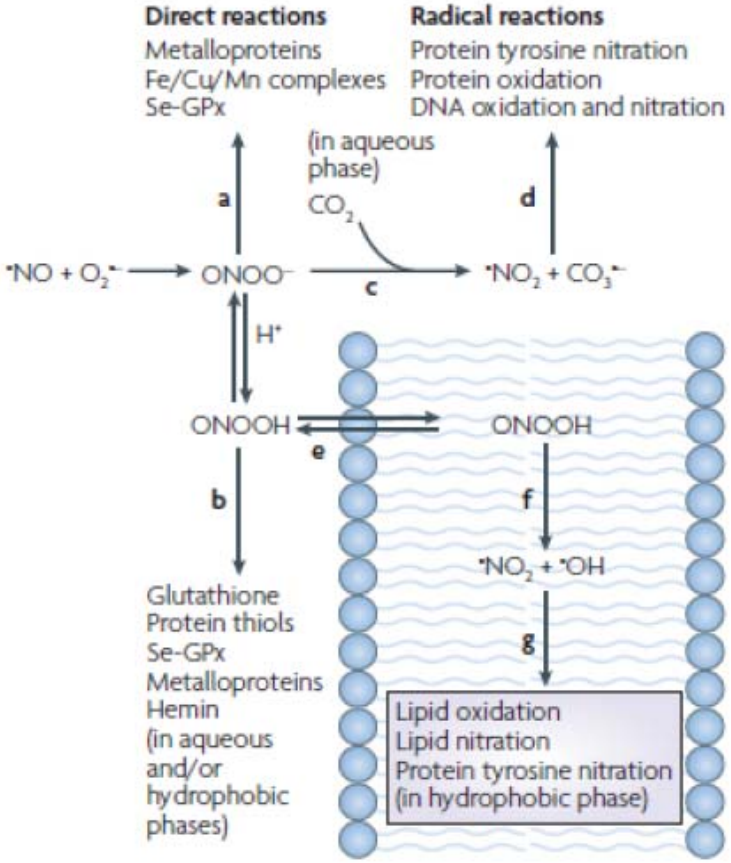

Figure 1.3: Targets of peroxynitrite reaction: Peroxynitrite anion (ONOO–) is in equilibrium with peroxynitrous acid (ONOOH; pKa = 6.8) and either one can undergo direct reactions with biomolecules as indicated (a and b). A fundamental reaction of ONOO– in biological systems is its fast reaction with carbon dioxide (in equilibrium with physiological levels of bicarbonate anion; c), which leads to the formation of carbonate ($CO_3^{\bullet-}$) and nitrogen dioxide ($^{\bullet}NO_2$) radicals, which are good one-electron oxidants (d) that can readily oxidize amino acids such as cysteine and tyrosine to yield the corresponding cysteinyl and tyrosyl radicals. In addition, $^{\bullet}NO_2$ can undergo diffusion-controlled termination reactions with biomolecule-derived radicals, resulting in nitrated compounds (d). Alternatively, ONOOH can undergo homolytic fission to generate one-electron oxidants hydroxyl ($^{\bullet}OH$) and $^{\bullet}NO_2$ radicals However, this reaction is slow in biological systems compared with the other reactions of ONOO- and ONOOH and therefore is a modest component of the in vivo reactivity of peroxynitrite in aqueous compartments. However, ONOOH readily crosses lipid bilayers (f) and its decomposition to •OH and •NO2 radicals seems to become relevant in hydrophobic phases to initiate lipid peroxidation and lipid and protein nitration processes (g). Moreover, ONOOH in the membranes may undergo direct reactions with metal centres such as hemin or membrane associated thiols (Szabo *et al.*, 2007)

1.8. CELL SIGNALLING VIA MITOGEN ACTIVATED PROTEIN KINASES

The mitogen activated protein kinases (MAPKs) are a family of intracellular protein kinases; together, they form a cascade that is highly conserved in all eukaryotes. The MAPKs pathway is one of the fundamental signalling systems controlling such essential cellular processes as proliferation, differentiation, survival and apoptosis in response to external stimuli (Chen *et al.*, 2001; Schaeffer and Weber, 1999). A large number of growth factors including epidermal (EGF) or platelet derived growth factor (PDGF) are known to activate MAPKs. About 5 MAPK pathways have been identified; these include the extracellular signal-regulated kinase 1 and 2 (ERK1/2) cascade, which preferentially regulates cell growth and differentiation, as well as the c-Jun N-terminal kinase (JNK) and p38 MAPK cascades, which function mainly in stress responses like inflammation and apoptosis (Ip and Davis, 1998; Robinson and Cobb, 1997). The others are the ERK5 and ERK3 pathways (Brown and Sacks, 2008). They typically are organized in a three-kinase architecture consisting of a MAPK, a MAPK activator (MEK, MKK, or MAPK kinase), and a MEK activator (MEK kinase [MEKK] or MAPK kinase kinase). Transmission of signals is achieved by sequential phosphorylation and activation of the components specific to a respective cascade (Schaeffer and Weber, 1999). Individual MAPK modules generally can signal independently from each other, and this specificity is manifested in distinct physiologic responses.

1.8.1. The ERK pathway

Several growth stimuli cause tyrosine phosphorylation of various cellular proteins through receptors, either directly or indirectly coupled to tyrosine kinases, which is believed to play an essential role in proliferation (Geer *et al.*, 1994). Typically, cell surface receptors such as tyrosine kinases (RTK) and G protein-coupled receptors transmit activating signals to the Raf/MEK/ERK cascade through different isoforms of the small GTP-binding protein Ras (Fig. 1.4) (Schaeffer and Weber, 1999). The MEK/ERK pathway is activated in response to protein tyrosine kinase receptors such as EGF or PDGF receptors. Acting as ligand, these bind to the receptors and induce receptor dimerisation (Fig. 1.5A) and the phosphorylation of the cognate receptor by intrinsic tyrosine kinases (Brown and Sacks, 2008; Pearson *et al.*, 2001). Tyrosine

phosphorylation of the receptor leads to the recruitment of proteins that contain the SH2 (Src homology) domains as well as the adapter protein Grb2 which is cytosolic and constitutively bound to Ras activator Sos (son of sevenless) (Fig. 1.5B). Sos is a Ras-activating guanine nucleotide exchange factor. Sos stimulates Ras to change GDP to GTP, allowing it to interact with a wide range of downstream effector proteins, including isoforms of the serine/threonine kinase Raf. It is the relocation to membrane which activates Sos which in turn activates Ras (Brown and Sacks, 2008; Mor and Philips, 2006).

1.8.2. The ERK pathway- regulation of Ras activity

The ras protein belongs to a large super-family of proteins known as low-molecular weight G-proteins; they are also referred to as GTPase since they essentially hydrolyses guanosine triphosphate (GTP) to guanosine diphosphate (GDP). Only 3 Ras isoforms have been identified, H-Ras, K-Ras, and N-Ras. In order to activate down-stream effectors and allow propagation of signals, Ras need be bound to GTP, hence the control of Ras activity is achieved by the regulation of the GTP/GDP bound state of Ras (Brown and Sacks, 2008) (Fig 1.5C). Enzymes such as GTPase activating protein (GAP) reduce Ras activity by increasing the rate of GTP hydrolysis, thus reducing thr pool of GTP-bound/activated Ras. The guanine-nucleotide exchange factors (GEFs) act in opposition to this and increase the pool of GTP-bound Ras. (Brown and Sacks, 2008). At their C-terminal ends, Ras protein contains a CAAX motif, here a cysteine (C) is followed by 2 aliphatic amino acids (A) and any other amino acid (X). This motif is farnesylated by farnesyl transferase, resulting the membrane localisation of Ras GTPase (Brown and Sacks, 2008; Mor and Philips, 2006). Activated Ras can bind to Raf-1 with high affinity; and several observations has implicated Raf-1 as an essential effector of Ras-induced cell transformation (Schaeffer and Weber, 1999; Kolch *et al.*, 1991).

1.8.3. The ERK pathway- signalling via Ras

Once bound to GTP, Ras is able to recruit the kinase Raf to the membrane, where is becomes activated. The Raf proteins (A-Raf, B-Raf, and C-Raf also called Raf-1) have distinct function but all function as serine/threonine kinases in the protein kinase cascades important for mitogenic signaling (Wellbrock *et al.*, 2004; Avruch *et al.*, 1994).

Raf-1 phosphorylates and activates MAP kinase kinase (MKK, also known as MEK), the specific activator of MAP kinase; both of which are dual specificity kinases. MEK is the physiological substrate of Raf-1 (Kyriakis *et al.*, 1992). Binding of MEK to the C-terminal end of activated Raf-1 results in the phosphorylation and subsequent activation of MEK (Dent *et al.*, 1992). MEK are able to activate the extracellular signal regulated kinases, ERK1 and ERK2 (ERK 1/2)- MAP kinase (Fig. 1.4). Once activated, ERK is dimerises and translocates to the nucleus where it phosphorylates transcription factors such as c-Myc, c-Fos, c-jun, STAT3, Elk-1 (Brown and Sacks, 2008; Roux and Blenis, 2004; Robinson and Cobb, 1997). Following MEK-induced ERK activation, ERK may remain in the cytosol and catalyse the phosphorylation of subtrates which includes various membrane proteins (CD120a, Syk, and calnexin), and several mitogen kinases (RSKs, MSKs, and MNKs) (Roux and Blenis, 2004; Frödin and Gammeltoft, 1999). Ribosome S6 kinases (RSKs), mitogen and stress activated kinases (MSKs), and MNKs represent three kinase subfamilies of ERK1/2 substrates (Frödin and Gammeltoft, 1999). The main effect of the MEK/ERK signalling pathway is cell differentiation and proliferation

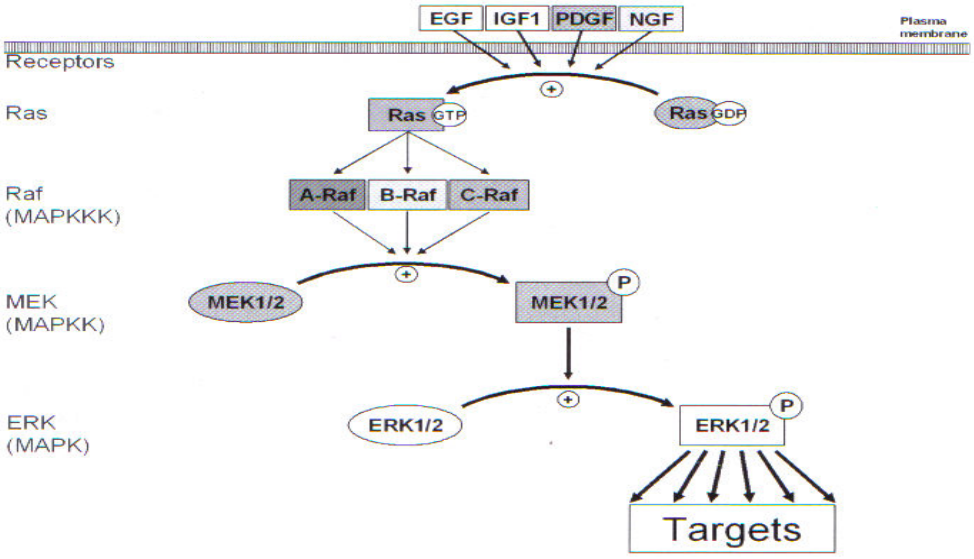

Figure 1.4: The MEK/ERK module of the MAPK signalling pathway. Growth factors such as EGF and PDGF cause Ras activation by inducing the exchange of GDP for GTP on Ras. GTP-Ras activates Raf kinases which in turn activates MEK1/2 downstream. MEK1/2 causes the phosphorylation of ERK1/2. In turn, ERK activates both cytosolic and nuclear substrates by catalysing their phosphorylation. Figure from Brown and Sacks (2008).

.

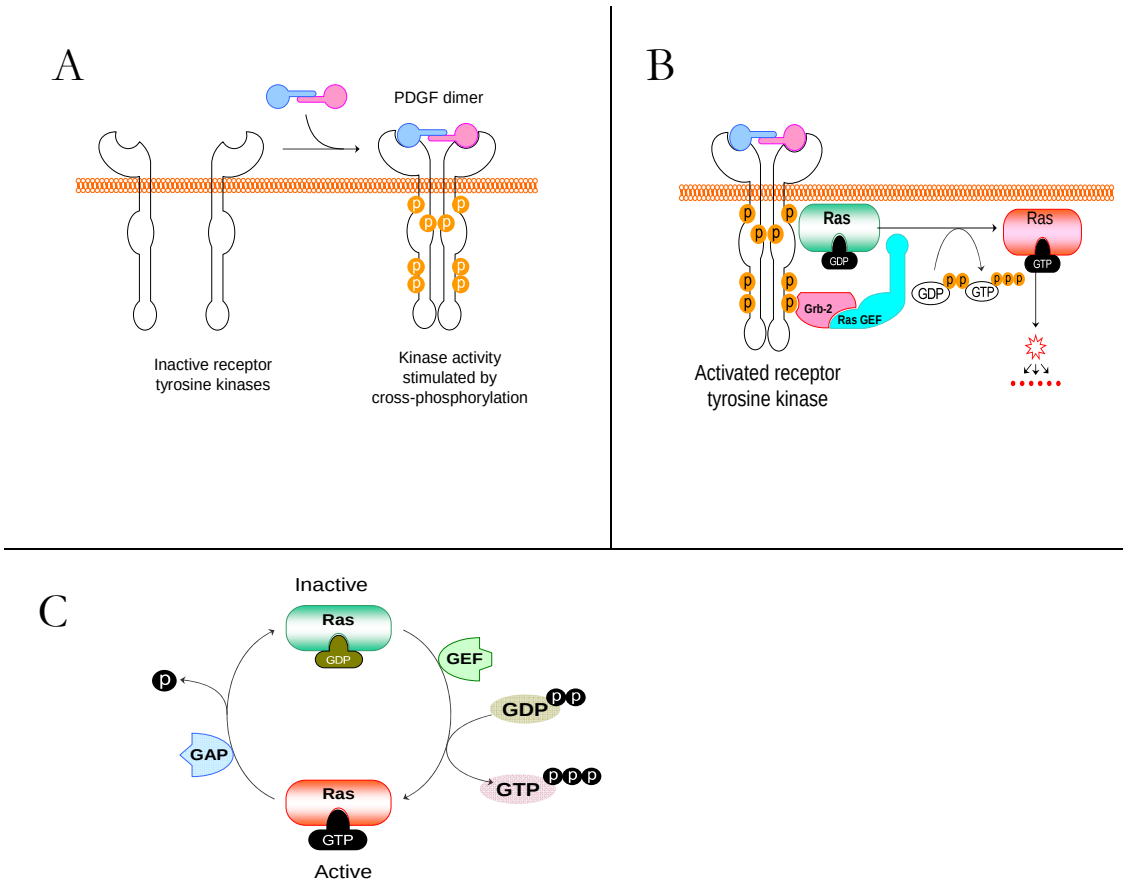

Figure 1.5: Features of the MAPK signalling pathway: (A) shows normal receptors dimerize in response to ligand binding. Growth factor binding induces homo- and/or heterodimerization of the receptor, leading to trans-autophosphorylation and subsequent activation of SH2 domain-dependent downstream signaling pathways (Dawson *et al.*, 2005) (B): shows the activation of Ras. Tyrosine phosphorylation of the receptor leads to the recruitment of the adapter protein Grb2 which is cytosolic and constitutively bound to Ras activator Sos (son of sevenless). Sos is a Ras-activating guanine nucleotide exchange factor (GEF). Sos stimulates Ras to change GDP to GTP, allowing it to interact with a wide range of downstream effector proteins, including isoforms of the serine/threonine kinase Raf. It is the relocation to membrane which activates Sos which in turn activates Ras (Brown and Sacks, 2008; Mor and Philips, 2006) (C): Illustrates the regulation of Ras activity. Ras need be bound to GTP, hence the control of Ras activity is achieved by the regulation of the GTP/GDP bound state of Ras. Enzymes such as GTPase activating protein (GAP) reduce Ras activity by increasing the rate of GTP hydrolysis, thus reducing thr pool of GTP-bound/activated Ras. The guanine-nucleotide exchange factors (GEFs) act in opposition to this and increase the pool of GTP-bound Ras.

.

1.8.4. The p38 MAPK pathway

The p38 kinase family include α, β, γ, and δ isoforms. They are frequently activated by G-protein coupled receptors and cell stress, heat as well as osmotic shock will activate these proteins. As a group, p38 are targets of both MEK3 and MEK6. MEK4 (also known as MKK4) is a known JNK kinase that possesses some MAPKK activity toward p38, suggesting that MEK4 represents a site of integration for the p38 and JNK pathways (Roux and Blenis, 2004). While MEK6 activates all p38 isoforms, MEK3 is somewhat selective, as it preferentially phosphorylates the p38α and p38β isoforms (Roux and Blenis, 2004). Substrates for p38 include MAPK interacting kinases (Mnk) Mnk-1 and Mnk-2. Signal transduction via the p38 module of the MAPK pathway regulates angiogenesis, cell proliferation, inflammation and cytokine production (Brown and Sacks, 2008; Pearson *et al.*, 2001).

1.8.5. The JNK pathway

The JNK (c-Jun N-terminal kinases) family of kinases are ubiquitously expressed. The family consist of JNK1, JNK2 and JNK3. They are activated in response to stress stimuli and selected G-protein coupled receptors (GPCR). Extracellular or intracellular signals inhibiting DNA synthesis will activate JNK. These kinases are phosphorylated by upstream kinases MEK4 or MEK7, MLK2/3 and DLK. This is followed by the translocation of JNK to the nucleus where it phosphorylates and up-regulates several transcription factors such as c-jun, ATF-2, STAT3 and HSF-1. The activation of JNK play a key role in controlled cell death and in the development of multiple cell types in the immune system (Brown and Sacks, 2008; Roux and Blenis, 2004)

.

1.8.6. Specificity of the MAPK signalling

An array of environmental, chemical and biological factors can activate the MAPK cascade. Cells are able to filter signals from various sources and elicit a specific response for a specific activator. The mechanisms underlying the specificity of the MAPK signalling pathway is poorly understood. Current understanding however provides some explanation. These include concepts of the integration of multiple pathways, receptor specific pathways, signalling kinetics and the presence of tissue specific down-stream effects (Brown and Sacks, 2008). Cells have been shown to integrate diverse input and produce a coordinated response by allowing several pathways to converge on a single transcriptor factor to regulate gene expression. Signalling pathways may also intersect on a single protein such as the oestrogen receptor. This was shown to require oestrogen binding and the phosphorylation of MAPK for maximal activation (Kato *et al.*, 1995). Signalling pathways generally cross-talk, leading to synergism or inhibition of an agonist effect. For example, transforming growth factor-β signals via SMAD1; ERK can phosphorylate SMAD1 and inhibit nuclear translocation and transcriptional activity (Kretzschmar *et al.*, 1997). Hence, the activation of MEK/ERK pathway by PDGF or EGF will abrogate TGF-β signalling. It is also possible that signalling specificity occur at the receptor level. This notion holds that a specific response is linked to the activation of a specific receptor in a specific tissue/cell (Sacks, 2006). Distinct cellular response may arise from the discreet interpretation of the signalling kinetics. The duration and or intensity of signal may underlie the specific response of the cells. Marshall (1995) showed that while P12 cell proliferated in response to EGF, they differentiated in response to nerve growth factor (NGF). Although both responses are mediated via MER/ERK pathway, the divergent response was due to the signalling kinetics. EGF signalling was transient lasting minutes while NGF caused sustained activation lasting hours (Marshall, 1995). It is also supposed that tissue specific expression of down stream effector and transcription factor is another way by which MAPK specificity is achieved (Tan and Kim, 1999). Smith et al (1997) provided some evidence in support of this. The authors showed that in certain IL-3 dependent cell types activation of JNKs induced cell proliferation (Smith *et al.*, 1997); even though ERKs generally regulate cell growth and cell differentiation and JNKs participate in a stress response (Roux and Blenis, 2004; Schaeffer and Weber, 1999).

1.8.7. Compartmentalisation and control of the MAPK pathway

Increasing evidence suggest that MAPK signalling is initiated from discrete subcellular domains and organelles (Brown and Sacks, 2008). This compartmentalisation allows for the regulation of the different modules of the pathway and for the discretionary execution of signalling from different sources. Compartmentalisation and control of the MAPK pathway is achieved through apparatus such as plasma membrane, lipid rafts, caveolae and endosomes, golgi bodies and endoplasmic reticulum and molecular scaffold. Plasma membrane contains multiple compartments that serve as nucleation sites for signalling complexes. Invaginations of the cell membrane (caveolae) can also provide platforms for the efficient propagation of MAPK signalling from the external stimuli to intracellular effectors. Caveolae are known to concentrate EGF, VEGF and insulin transmembrane receptors and intracellular molecules such as Ras, Grb2 and Sos (Brown and Sacks, 2008). Lipid rafts are freely diffusing stable assemblies of sphingolipids and cholesterol (Hancock, 2006) and have been said to act as platform for MAPK signalling by allowing components of the signalling pathway to congregate and efficiently propagate the cascade. In addition, recent studies have shown that endosomes can serve to propagate MAPK cascade. After activation, growth factor receptors are internalised into endosomes. This may serve to recycle the receptors but can also enhance the specificity and propagation of the signalling since endosomes can be transported by retrograde motion to specific sites within the cell (Charles and William, 2004). Molecular scaffold bind to multiple members of the MAPK pathway, thus bringing them into close proximity to one another and enhancing the efficient propagation of signal along the cascade. In addition, the scaffold may contain the inactivating protein phosphatases for the MAPK members. Regulation of signal source and intensity can be achieved by scaffold proteins. They confer spatial and temporal regulation of the MAPK pathway. Several scaffold proteins have been recognised and characterised. These includes but not limited to kinase suppressor of Ras (KSR) which binds to C-Raf, MEK1/2 and ERK 1/2, then there is MEK partner-1 which promote association of MEK and ERK and thus facilitate ERK activation and β-arrestin which are regulators of the GPCR (Kolch, 2005; Morrison and Davis, 2003).

.

1.8.8. MAPK- bone morphogenetic protein signalling in pulmonary hypertension

Several studies have investigated the molecular basis of the pulmonary arterial hypertension. Together they have revealed that PAH can be caused by mutations in the bone morphogenetic protein receptor type 2 (BMPR2) signalling pathway (Morrell, 2006; Runo and Loyd, 2003). BMPR2 is a cell-surface protein belonging to the TGF-β receptor super family, which binds a variety of protein, peptides or glycoproteins acting as signalling molecules. These include TGF-β, bone morphogenetic protein (BMP). The BMP-BMPR2 signalling is now known to be important for cell proliferation, differentiation and apoptosis. BMPR activation leads to the phosphorylation of a family of signalling molecules (Smad proteins) which translocates and interacts with specific nuclear transcription factors. In pulmonary vascular smooth muscle cells, BMPR2 signalling causes inhibition of smooth muscle cells proliferation and favours apoptosis. Thus, in the absence of such signalling, it is believed that there will be smooth muscle cell multiplicity, vascular obliteration and remodelling that characterize pulmonary hypertension (Morrell, 2006; Richter *et al.*, 2004). This has been demonstrated in some cases (Naeije and Rondelet, 2004). However, mutations of BMPR have been found in some but not all patients with primary pulmonary hypertension. Only about 55% of familiar cases and 10-26% of idiopathic pulmonary hypertension are associated with BMPR-2 mutation (Newman *et al.*, 2004; Thomson *et al.*, 2000). In addition alterations in BMPR are not found in all patients with non-primary pulmonary hypertension; the significance of the role of BMPR is therefore not settled.

The work of Du and co-workers provide support for the hypothesis that all forms of PAH may be linked by defects in the signalling pathway involving angiopoietin-1 (a protein involved in the recruitment of smooth-muscle cells around blood vessels), BMPR1A, and BMPR2 (Du *et al.*, 2003). In this study the type-I receptor BMPR-IA was down-regulated in the lung tissue of the patients and the authors demonstrated a reciprocal relationship between BMPR-IA expression and potential recruitment of smooth-muscle cells. This suggests that intact BMP signalling is important for the maintenance of normal pulmonary vasculature. The findings of Du and co-workers are interesting in that it was based on heterogeneous group of patients with pulmonary hypertension. The authors had performed lung biopsy in patients with thromboembolic pulmonary hypertension (22), idiopathic/primary pulmonary hypertension (5),

pulmonary hypertension with scleroderma (3), pulmonary hypertension with mitral regurgitation (9) and 19 patients without pulmonary hypertension (Du *et al.*, 2003). As a whole, the work of Du and co-authors do not represent all types of pulmonary hypertension (Simonneau *et al.*, 2004) and the sample size of this study limits the generalisability of its findings even within represented groups of pulmonary hypertension patients. Nonetheless, a recently published work confirm that most heterogenous BMPR-2 mutations are associated with defective Smad signaling compensated for by an activation of p38MAPK signalling and this accounted for apoptosis deficient and proliferation of PASMC (Dewachter *et al.*, 2009).

Human pulmonary artery smooth muscle cells and endothelial cells express a wide range of TGF-β superfamily receptors, including BMPR-II and BMPR-IB. Activation of these receptors by BMPs leads to phosphorylation of Smad1 and induction of mRNAs for Smad6 and Smad7 (Humbert *et al.*, 2004). There is increasing evidence that TGF-β and BMPs can activate ERK, p38MAPK, and JNK kinases (reviewed in Massague and Chen, 2000). In addition, a feature common to all mutants is a gain of function involving p38MAPK activation (Humbert *et al.*, 2004). Accordingly a recent study presented evidence that p38 MAPK is an important intermediary in the functional consequences of acute hypoxia in the pulmonary circulation and in experimental pulmonary hypertension (Weerackody *et al.*, 2009). Hypoxia-induced pulmonary artery endothelial depression and dysfunction were found to be p38 MAPK dependent (Weerackody *et al.*, 2009). The study also demonstrated that p38 MAPK activation stimulated the generated of superoxide production (Weerackody *et al.*, 2009). Taken together, the classical MAPK pathway already discussed appears to cross-talk with BMP signaling and may account for pulmonary hypertension in some patients; it is expected that future work will elucidate on the nature of this relationship. In conclusion, the entire interaction linking BMPR mutation with the development of pulmonary hypertension is incompletely understood. The presence of BMPR mutation confers only a 15-20% lifetime risk of developing pulmonary hypertension (Newman *et al.*, 2004), a 'second hit' is thus said to be required to complete the link between BMPR mutation and the development of pulmonary hypertension (Davies and Morrell, 2008; Song *et al.*, 2005).

.

1.9. PEROXYNITRITE SIGNALLING

A number of studies on the cellular effects of peroxynitrite (ONOO-) suggest a degree of varying biological effects depending on the concentrations involved. High (>100μM) peroxynitrite concentrations have been shown to readily nitrate tyrosine residues and inhibit tyrosine kinase receptor signalling (Bassil *et al.*, 2008; Estévez *et al.*, 1995). Accordingly, a decrease in ERK1/2 and p38 MAP kinase phosphorylation has been reported with 0.5mM ONOO- (Klotz *et al.*, 2002; Mallozzi *et al.*, 1997). On the other hand, lower concentrations (≤ 100μM) would favour bio-oxidation reactions, thus activating tyrosine kinase receptor signalling through the inhibition of phosphatase induced dephosphorylation (Klotz *et al.*, 2000; Reiter *et al.*, 2000); this will potentially stimulate cell proliferation. Fittingly, 10-100μM peroxynitrite has been shown to activate the anti-apoptotic kinase Akt (Minetti *et al.*, 2002; Reiter *et al.*, 2000) and kinases of the nonreceptor tyrosine kinases (src family), important for the regulation of cell communication, proliferation, migration, differentiation, and survival (El-Remessy *et al.*, 2007). Also, independent work confirm that an estimated 1-10μM ONOO- peroxynitrite was involved in transducing VEGF's angiogenic signal via nitration-independent and oxidation-mediated tyrosine phosphorylation (Ichikawa *et al.*, 2008). In addition, a recent study demonstrated that 1 and 10μM ONOO- augmented the differentiation of lung fibroblasts to myofibroblast (Ichikawa *et al.*, 2008). In the same study, these concentrations of ONOO- were found to enhance the release of TGF-β by lung fibroblast, implying a key role for ONOO- in airways remodelling.

1.9.1. Peroxynitrite activation of ERK, p38 and JNK MAPK

The several in-vitro studies reporting on the effects of peroxynitrite on vascular as well as other cells and sub-cellular components show that the molecule has potent cytotoxic effects. It noteworthy however, that the concentrations of peroxynitrite in these studies have ranged mainly from 10μM-50mM and may be classified as non physiological and improbable in established diseases. Using increasing concentrations of ONOO- (1–1000 μM) in western blotting experiments targeted at extracellular signal-regulated kinases (ERKs), Zhang et al (2000) showed some and maximal activation of ERK at 1 and 100μM in rat lung myofibroblasts, respectively. Pesse et al (2005) also demonstrated that ONOO– acted as a potent inducer of MAP kinase family of signalling proteins.

Peroxynitrite (50-500μM) elicited a concentration and time-dependent activation of ERK, secondary to the upstream activation of MEK 1 (ERK kinase). The study also showed that ONOO- activated two additional members of the MAP kinase family of signalling proteins, JNK and p38. The mechanism of peroxynitrite activation of ERK in cardiomyocytes was found to be through an unusual signalling cascade involving Raf-1 and MEK 1, independently from EGFR and p21 Ras. Using 25μM and 500μM ONOO- Bapat co-workers (2001) also showed that ONOO- activated ERK via a MEK-independent pathway. Separate evidence from Kaji and co-workers (2002) also showed that the Ras–MAPK–p19ARF pathway has an essential role in p53-dependent apoptosis triggered by peroxynitrite in neural cells. Together, these studies show that peroxynitrite can activate ERK1/2 as well as other members of MAPK family and that this activation is non cell specific. Even though these studies demonstrate activation of key transducers in the signalling cascade mediating cell proliferation in response to growth factors such as platelet-derived growth factor and EGF, the concentrations being used would not have caused cell proliferation but cell death. These authors thought they were studying the mechanism of ONOO- induced cell toxicity.

.

1.9.2. Peroxynitrite induced cytotoxicity- a role for PARP

In damaging DNA, ONOO- also triggers the activation of DNA repair systems. Virág et al., (2003) postulated a model in which a DNA nick sensor enzyme, poly(ADP-ribose) polymerase-1 (PARP-1) also becomes activated upon sensing DNA breakage. Activated PARP-1 cleaves NAD^+ into nicotinamide and ADP-ribose and polymerizes the latter on nuclear acceptor proteins (Fig. 1.4) Peroxynitrite-induced overactivation of PARP consumes NAD^+ and consequently ATP culminating in cell dysfunction, apoptosis or necrosis- depending on whether the cascade of events was initiated by low or high concentration ONOO- , respectively (Fig. 1.7) (Virág *et al.*, 2003).

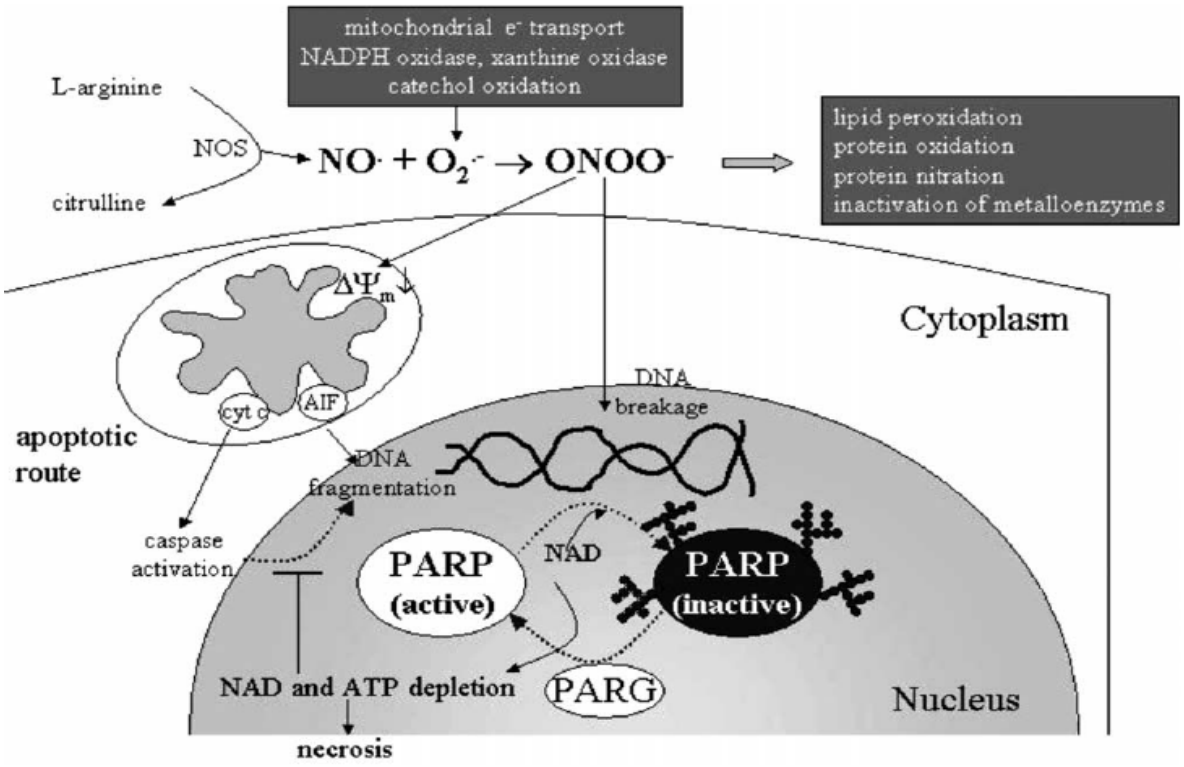

Figure 1.6: Peroxynitrite-induced cytotoxic pathways: Nitric oxide and superoxide react to form peroxynitrite which damages cells via a variety of deleterious effects such as lipid peroxidation, inactivation of metalloenzymes and other proteins by oxidation and nitration. Peroxynitrite also acts on mitochondria triggering the release of proapoptotic factors such as apoptosis-inducing factor (AIF) and cytochrome c. These factors mediate caspase dependent and independent apoptotic death pathways. Moreover, peroxynitrite-induced DNA breakage activates PARP leading to NAD and ATP depletion and consequently to necrosis (Figure from Virág *et al.*, 2003).

.

1.10. IN-VITRO PRODUCTION OF PEROXYNITRITE FROM SIN-1

Peroxynitrite has in recent times been generated from SIN-1 (3-morpholino-sdynonimine), a metabolite of the vasodilator molsidomine. SIN-1 decomposes spontaneously in neutral aqueous media consuming oxygen to release NO and the superoxide anion simultaneously (Kita *et al.*, 1994; Bohn and Schönafinger, 1989). It has thus been frequently used as a model compound for continuous release of superoxide and nitric oxide and thus for the continuous formation of ONOO (Cao *et al.*, 2004; Cao and Li, 2004; Bao and Liu, 2002; Robinson *et al.*, 2001; Lomonosova *et al.*, 1998; Brunelli *et al.*, 1995). The first step in the transformation of SIN-1 appears to be the hydroxyl ion dependent conversion to SIN-1A that occurs almost immediately at neutral pH (Bohn and Schonafinger 1989). Bohn and Schonafinger (1989) also showed that an oxidative process is essential for the release of $NO^{\bullet}$ from SIN-1. This is associated with one-electron reduction and oxidation of dioxygen (O_2) and SIN-1 to form superoxide and an intermediate cation which dissociates to release NO, respectively. While the electron acceptor in buffer solutions is oxygen, under biological conditions other molecules such as heme proteins can compete with oxygen for this role, thus changing the ratio of $NO^{\bullet}$/ONOO- produced by SIN-1. Also, at the relatively low in-vivo oxygen concentrations, SIN-1 is likely to behave more like an NO donor than a peroxynitrite donor (Singh *et al.*, 1999). Accordingly, decomposition of SIN-1 by human plasma resulted in the formation of $NO^{\bullet}$ (Singh *et al.*, 1999).

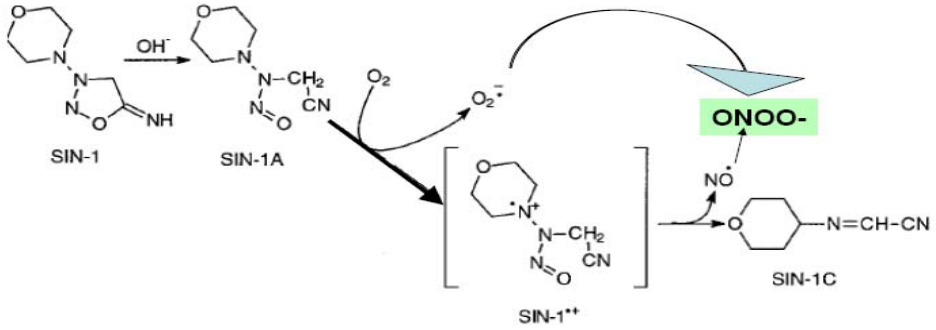

Scheme 1.1: The mechanism of SIN-1 decomposition in oxygenated solution follows the following steps: (i) The sydnonimine ring opens, by a base-catalyzed mechanism, to give SIN-1A; (ii) SIN-1A reduces oxygen, in a one-electron transfer reaction, to give superoxide and SIN-1•+, a cation radical. (iii) SIN-1•+ decomposes to form SIN-1C and NO (Feelisch *et al.*, 1989). It is believed that the NO from SIN-1 will react with superoxide generated in step ii. When brought together exogenously added from separate sources, NO reacts with superoxide with a rate constant of 3–6 x 10^{-9} M^{-1} s^{-1} (Huie and Padmaja, 1993), close to the diffusion limit, NO is rapidly scavenged (Modified from Singh Singh *et al.*, 1999).

.

Peroxynitrite generation from from SIN-1 has been demonstrated and measured albeit under test tube conditions (Holm *et al.*, 1998). Holm and co-workers measured oxygen consumption and demonstrated the quantitative formation of superoxide by means of a chemical assay. Using nitro-tyrosine as marker for ONOO- the study showed that SIN-1 released both $NO^{\bullet}$ and superoxide radical in aqueous solutions resulting in the formation of peroxynitrite (Holm *et al.*, 1998). The mechanism of decomposition of SIN-1 to generate peroxynitrite (ONOO-) is illustrated in Scheme 1.1 and 2.2 of chapter 2.

1.11. MODELLING PULMONARY HYPERTENSION

A variety of stimuli models have been used to study the changes in pulmonary hypertension. Pathophysiological stimuli include acute and chronic hypoxia, increased blood flow, vascular obstruction (air embolism, synthetic microspheres); chemical and toxic models involve the use of monocrotalline (pyrrole), α-naphthythiourea and bleomycin; genetic models include vascular endothelial growth factor receptor 2 (VEGFR-2) inhibition + hypoxia and angiopoietin-1 over-expression; and inbred strains with undefined molecular abnormalities in rats, chicken and mouse (Marsboom and Janssens, 2004). The rat model is commonly used as a model for hypoxic pulmonary hypertension and it is well characterized from several years of use in our laboratory. However, the rat pulmonary artery is unsuitable for the culture of endothelial cells by the widely used mechanical method. It was therefore aimed to use the bovine pulmonary artery as a model for key features of pulmonaty hypertension. Several studies investigating signalling or treatment options in pulmonary hypertension have involved the use endothelial and smooth muscle cells of the bovine pulmonary artery (Chakraborti *et al.*, 2009; Hicham *et al.*, 2009; Lu *et al.*, 2009; Bogatcheva *et al.*, 2006; Garg *et al.*, 2006). In addition, other authors have used these cells as model of hypoxic lung conditions (Kolluru *et al.*, 2008; Tucci *et al.*, 1997; Farber and Barnett, 1991). Still others have focused on the response of the bovine pulmonary artery to vaso-active agents (Alapati *et al.*, 2007; Gruetter and Lemke, 1988; Tracey and Eyre, 1988). Prelimary works in the current study confirmed that the bovine pulmonary artery mimicked key features of the human pulmonary artery. It was therefore considered a suitable model to explore the role of the pulmonary artery/cells in the pathogenesis of pulmonary hypertension.

1.12. HYPOTHESIS

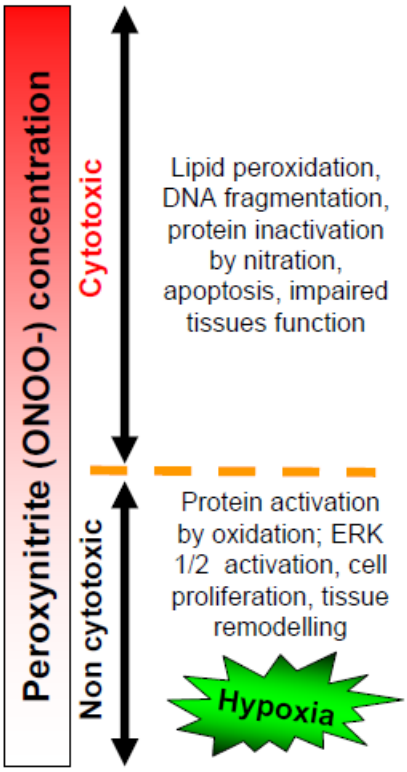

Endothelial dysfunction and oxidative stress are hallmarks of pulmonary hypertension. There is evidence for increased peroxynitrite (ONOO-) formation in both the endothelium and smooth muscle layers of the pulmonary vasculature. It has been reported that peroxynitrite can activate extracellular signal-regulated MAP kinases (ERK) which is a key regulator of cell proliferation. Therefore it has been hypothesized that local formation of peroxynitrite leads to proliferation of endothelial (PAEC) and smooth muscle cells (PASMC) and hence pulmonary vascular remodelling in pulmonary hypertension. In addition, it is supposed that ONOO- can aggravate the proliferative response of pulmonary cells under hypoxic lung conditions. However, current research literature has not demonstrated that peroxynitrite can stimulate proliferation of pulmonary artery cells. Thus, it was aimed to determine the threshold of ONOO- cytotoxicity in PAEC and PASMC and to investigate the proliferative effects of the anion at concentrations no more than the lower limits for the widely reported cytotoxic effects. The ONOO- generator, 3- morpholinosydnonimine (SIN-1) was used to mimic the in-vivo sustained generation of the anion. It is also important to discover what cellular mediator pathways are important for this pro tissue-remodelling action.

1.13. MODEL OF STUDY

Bovine Pulmonary Artery

.

CHAPTER 2

THE LIFE AND ACTIVITY OF PEROXYNITRITE IN PULMONARY CELL CULTURE MEDIUM: AUTHENTIC AND IN-SITU GENERATED UPON SIN-1 DECOMPOSITION

2.1. INTRODUCTION

Several lines of evidence support the in-vivo formation of peroxynitrite in the pulmonary vasculature, this study therefore sought to investigate the role of this anion in the cellular hyper-proliferation and vascular remodelling associated with pulmonary hypertension. However, working with authentic peroxynitrite (ONOO-) as a drug is challenging; the half-life is reported to be 1.9s at physiological pH (Beckman *et al.*, 1990) and there are but few data on the life and profile of the molecule in cell culture medium. In addition, whether supplied commercially or prepared extemporaneously, ONOO- is stabilised and stored under strongly alkaline conditions (Konorev *et al.*, 1998; Kissner *et al.*, 1997) and the exposure of cells to this form of ONOO- will in tandem lead to increase in culture media pH. Most studies have reported results in this area using control containing alkaline solution but have not reported the associated increase in pH or designed experiments to quantify solvent/pH effects on cellular activities (Pesse *et al.*, 2005a; Walia *et al.*, 2003; Bapat *et al.*, 2001; Zhang *et al.*, 2000; Salgo *et al.*, 1995a; Salgo *et al.*, 1995b; Tarpey *et al.*, 1995). This study therefore aimed to characterise the activity and life of ONOO- under various storage and pH conditions as well as in cell culture media.

Several researchers have sought alternative means of generating peroxynitrite while retaining physiological pH conditions (Kim *et al.*, 2003; Malan *et al.*, 2003; Ruan, 2002; Cai *et al.*, 2000). 3-morpholinosydnonimine (SIN-1) the active metabolite of the vasodilatory drug molisdomine has been reported to generate both nitric oxide and superoxide anion, thus suggesting that SIN-1 may be a peroxynitrite generator (Holm *et al.*, 1998; Haddad *et al.*, 1994; Feelisch *et al.*, 1989). A currently accepted mechanism for this process is illustrated in Scheme 1.1 (Chapter 1). It is worthy of note, that consistent with the original use of SIN-1, the molecule can decompose primarily to yield NO under physiological conditions or in the presence of electron acceptors which may include those other than oxygen found in biological systems (Singh *et al.*, 1999). However, recent evidences from newer techniques confirm earlier findings that SIN-1 can generate ONOO- under aerobic conditions. Martin-Romero et al., (2004) quantitatively assessed the production of peroxynitrite during real time SIN-1 decomposition, with a sensitivity of about 0.1 μM, from the kinetics of reduced nicotinamide adenine dinucleotide (NADH) fluorescence quenching in phosphate and other buffers commonly used with cell cultures. The authors showed that maximum

concentration of ONOO- generated and quantified by this method may range from 1.2-3.6% of added SIN-1. A hallmark reaction of ONOO- is the nitration of tyrosine moiety of proteins; the formation of nitro-tyrosine is thus widely used as a footprint for the production of ONOO- (Bowers *et al.*, 2004; Bao and Liu, 2003). Trackey and co-workers (2001) had showed that SIN-1 caused a concentration-dependent increase in cortical cell injury associated with a parallel increase in the release of cellular proteins containing 3-nitro-tyrosine into the culture medium (Trackey *et al.*, 2001). In addition, the concentrations of ONOO- generated from SIN-1 have also been determined from the concentrations of formed nitro-tyrosine in in-vivo experiments (Bao and Liu, 2003). Similarly, Holm et al., (1998) directly estimated the production of ONOO- by quantifying the formation of nitro-tyrosine, from a SIN-1 solution that had been supplemented with free tyrosine. Taken together, these evidences confirm that SIN-1 is also a peroxynitrite generator.

The slow and sustained generation of peroxynitrite from SIN-1 decomposition under physiological pH conditions is expected to mimic the in-vivo formation of the anion; SIN-1 has therefore been widely used as a model for the continuous formation of peroxynitrite in chemical and biological systems investigating peroxynitrite-mediated biological effects (Kim *et al.*, 2003; Malan *et al.*, 2003; Darley-Usmar *et al.*, 1992; Hogg *et al.*, 1992). Indirect evidence of the in-situ formation of peroxynitrite from SIN-1 may be deduced from studies using superoxide dismutase (SOD) to scavenge superoxide and thus prevent the formation and action attributed to peroxynitrite during SIN-1 decomposition (Konorev *et al.*, 1998). Reported peroxynitrite-like effects of SIN-1 include oxidation of low-density lipoproteins (Darley-Usmar *et al.*, 1992), degradation of deoxyribose (Hogg *et al.*, 1992), and inhibition of glyceraldehyde-3-phosphate-dehydrogenase (Dimmeler *et al.*, 1992). Indeed, the cytotoxic effects of SIN-1 are comparable with those of authentic peroxynitrite have been reported in various cell types (Cao and Li, 2004; Brunelli *et al.*, 1995; Lipton *et al.*, 1993). In the present chapter, this study aimed to determine whether or not authentic peroxynitrite was generated following the decomposition of SIN-1, and if so, to characterise such formation under pulmonary artery cell culture conditions.

2.2. OBJECTIVES

(1) To determine the stability, suitable mode of administration and storage conditions of authentic peroxynitrite. (2): To understand the concentration and time course of ONOO- when added to pulmonary cell culture medium. (3): To characterise the continuous formation of peroxynitrite by 3-morpholinosydnonimine (SIN-1)- a peroxynitrite generator under conditions mimicking physiological pH. This was expected to mimic physiological release of the anion.

2.2.1. Acknowledgment to Professor Andrew Mills and Dr Michael Mcfarlane

The findings reported in this chapter of the study were borne from experiments carried out in the laboratory of Professor Andrew Mills (Department of Applied Chemistry). and co-supervised by Dr Michael Mcfarlane. The expert advice and skilful direction of these scientists enabled a furtherance of current knowledge of the life and activity of peroxynitrite

2.3. METHODS

2.3.1. Studies by light absorbance spectroscopy

2.3.1.1. Real time decay and stability study of peroxynitrite: Calibration line

Peroxynitrite was supplied (Calbiochem, United Kingdom and Ireland) as a 170mM solution in 4.7% NaOH. Dilutions of this solution were made ($1:10^{-3}$ and $1:10^{-4}$) in NaOH 1M and stored at -80^{o}C. Further dilutions were made in NaOH 1M to give a range of concentrations in 1cm cuvettes and their absorbance was read at 302nm.

2.3.1.2. Stability study of peroxynitrite

Solutions of peroxynitrite at 2 concentrations ($1.7\ 10^{-3}$M and $1.7\ 10^{-4}$ M) in NaOH 1M were kept on the shelf at room temperature or at 4^{0} or at -80^{0}C for 50 days. Absorbance was measured at intervals by placing the peroxynitrite solution in a cuvette into a UV/Visible spectrophotometer (Ultrospec 2000; Pharmacia Biotech), and readings made repeatedly at 302nm.

2.3.1.3. Decay of Peroxynitrite authentic (ONOO-)

Real time decay of peroxynitrite under conditions of varying pH was evaluated using the Cary50Bio® UV-Visible spectrophotometer (Varian). Using quartz cuvettes, the kinetics of ONOO- were monitored at 302nm every 10 seconds. Control experiments were also conducted to obtain absorbance spectra of the vehicle (NaOH), pulmonary cell culture medium used for the cell culture as well as the spectra of peroxynitrite in these media.

2.3.1.4. Decay of 3-morpholinosdynonimine (SIN-1)

Real time decay of SIN-1 under conditions of varying pH was monitored at several wavelengths using quartz cuvettes and Cary50Bio® UV-Visible spectrophotometer (Varian). The spectra and kinetics of SIN-1 were evaluated overnight in pulmonary cell culture medium. The kinetics of formed authentic peroxynitrite were monitored at 302nm, the decomposition of SIN-1 and the formation of SIN-1C were monitored at 292nm at 280nm nm as anticipated from the literature (Shown in Scheme 1.1, Chapter 1; Thome *et al.*, 2003; Singh *et al.*, 1999)

2.3.2. Studies by stopped-flow spectroscopy

2.3.2.1. Activity and life of authentic and in-situ generated peroxynitrite

Kinetic data on dynamic processes in chemical and biochemical reactions can be obtained by stopped-flow spectroscopy; a representation of the system is shown in scheme 2.1. The experiments have been performed as previously described (Kissner et al., 1999). Stock solution of peroxynitrite supplied as described above was kept on ice, and diluted into distilled water and immediately used to fill one of the stopped-flow apparatus syringes. In experiments involving SIN-1, one of the stopped flow syringes was filled with double strength of the desired SIN-1 solution concentration while the other was filled with appropriate buffer of a double strength solution of interest. All reagents were freshly prepared. Solutions were purged with nitrogen in some experiments. For any experiment, sufficient volume of SIN-1 and NaOH or buffer of interest was pushed through filler ports into the drive syringes or internal tubing; the dead volume is filled and the reaction is initiated in the quartz cell.

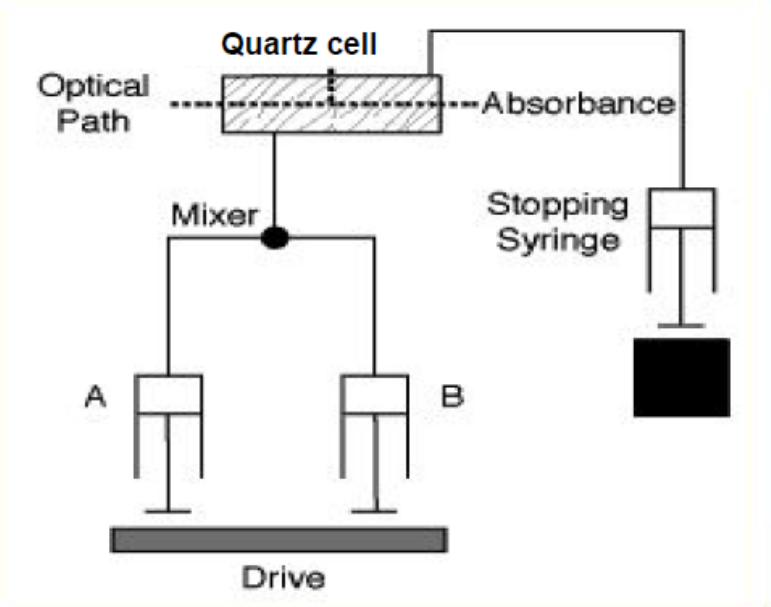

Scheme 2.1: Single mixing stopped-flow system: Small volumes of solutions are rapidly driven from syringes (A & B) into a high efficiency mixer to initiate a fast reaction. The resultant reaction volume then displaces the contents of an observation cell and fills it with freshly mixed reagents. The volume injected is limited by the stop syringe which provides the "stopped-flow". Just prior to stopping, a steady state flow is achieved and the solution entering the flow cell is only milliseconds old. As the solution fills the stopping syringe, the plunger hits a block, causing the flow to be stopped instantaneously. Using coupled UV/Vis detection techniques, Absorbance was measured as the reactions proceeded in the spectrophotometric cell. Single wavelength kinetic monitoring was possible at the rate of 1 scan /0.1s, while 200-450nm spectral analysis was possible at every 0.6s.

2.3.3. Studies by fluorimetry

Peroxynitrite generated from SIN-1 was quantified by fluorimetry. Fluorescence measurements were carried out with a spectrofluorometer (LS 45 Luminescence Spectrometer, PerkinElmer Instruments). NADH fluorescence was measured with excitation and emission wavelengths of 340 and 460 nm, respectively. In most experiments, the production of peroxynitrite during 3-morpholinosydnonimine (SIN-1) decomposition was continuously monitored in large vessel endothelial cell basal medium-prf (TCS cell works; Cat # ZHM-2959). Solution of authentic peroxynitrite was purchased from Calbiochem (United Kingdom and Ireland; Cat # 516620), split into aliquots and frozen at -80^{0}C until use. Based on an extinction coefficient of 1670 M-1cm^{-1} at 302 nm in 1M NaOH, concentration of peroxynitrite solution was determined spectrophotometrically in aliquots thawed just before use.

.

2.3.4. Materials

3-morpholinosdynonimine (SIN-1) was purchased from Sigma (UK; Cat # M184-25mg). Peroxynitrite was supplied (Calbiochem, United Kingdom and Ireland; Cat # 516620) as a 170mM solution in 4.7% NaOH. Nicotinamide adenine dinucleotide (β-NADH; Cat # N7410-15VL) and superoxide dismutase from bovine erythrocytes (Cat # S2515-75KU) were obtained from Sigma UK. Cell culture media included Large vessel endothelial cell basal medium-prf (TCS cell works; Cat # ZHM-2959) and Leibovitz's L-15 medium (Invitrogen® Cat #: 21083-027); both of these medium are colourless. Other mediums such as Waymouth's MB 752/1 + L-glutamine (Invitrogen® Cat #: 31220-072) and F-12 (Ham) Nutrient mixture medium + L-Glutamine (Invitrogen® Cat #: 21765-037) were red in colour due to the presence of phenol red indicator.

.

2.4. RESULTS

2.4.1. Determination of the stability and half-life of peroxynitrite

2.4.1.1. Investigating peroxynitrite stability under varying storage conditions

It was confirmed that peroxynitrite (ONOO-) is relatively stable in strongly alkaline conditions (Fig. 2.1A; Kissner *et al.*, 1999). The absorbance spectrum (λ_{max} 302nm) of peroxynitrite in aqueous NaOH (Fig 2.1A) was similar to what has been reported in the literature (Thome *et al.*, 2003) Absorbance was linear down to 10^{-4} M ONOO- (Fig. 2.1B).

The stability of ONOO- in 1M NaOH was investigated under various storage and intermittent exposure to room temperature conditions. At room temperature ONOO- decay was approximately log-linear with a 10-fold decay after approximately 5 days (Fig. 2.2A). At 4^0C, the decay appeared approximately linear with 10-fold decay in approx 7 days (Fig 2.2B). At -80^0C, decay of ONOO- appeared curvilinear and fell by approximately half in 14 days (Fig 2.2C). This decay rate indicates that at storage condition of -80^0C, higher concentration aliquots of ONOO- can be stored for up to 3 weeks (Fig. 2.2C); it will however be necessary to obtain fresh calibration data for each experiment more than a week apart. The experiments of the study involved the use of ONOO- supplied in 1M NaOH, stored at -80^0C and quantified spectrophotometrically (λ_{max}= 302n) on the day of each experiment.

.

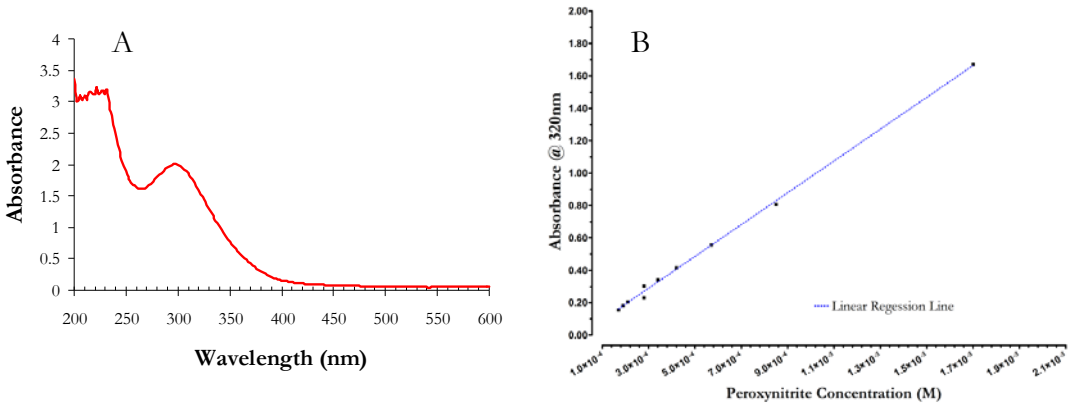

Figure 2.1: Peroxynitite in 1M NaOH. (A): The spectrum of 10^{-3}M peroxynitrite in 1M NaOH; (B): Concentration Dependent Absorbance of Peroxynitite @ 320nm. Absorbance was measured at 320nm and room temperature by placing peroxynitrite in a plastic cuvette into a UV/Visible spectrophotometer (Ultrospec 2000; Pharmacia Biotech). Experiments were conducted in triplicates

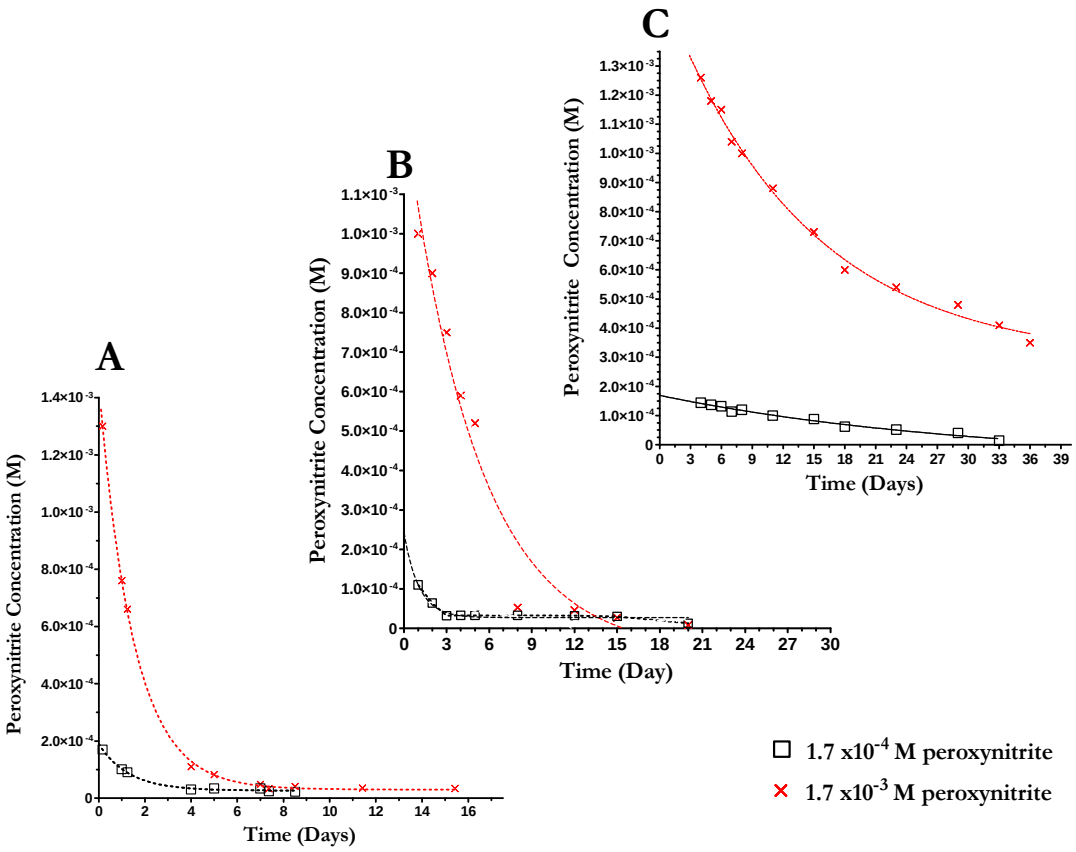

Figure 2.2: Peroxynitrite (ONOO-) In 1M NaOH:-Decay Under Various Storage Conditions (A): Room temperature. ONOO- was stored on shelf, exposed to room light and temperature. (B): Peroxynitrite stored at 4^0C. (C): Peroxynitrite stored at -80^0C, thawed at each point of measurment. Decay of ONOO- fitted well when modelled with one phase exponential decay equation which assumed decay rate was proportion to ONOO- concentration. During the 50-day study period, absorbance was measured periodically at 320nnm wavelength using a plastic cuvette place within UV/Visible spectrophotometer at room temperature (Ultrospec 2000; Pharmacia Biotech). Experiments were conducted in triplicates

2.4.2. The decay of peroxynitrite in cell culture media

2.4.2.1. ONOO- decay in 50:50 mix of Ham F-12 and Waymouths MB725 medium

For the most part, this study utilised a general cell culture medium for the growth of pulmonary cells. This medium (50:50 mix of Ham F-12 and Waymouths MB725) contained phenol red for pH indication; the red appearance indicated that the medium absorbed light within the yellow and blue region of the UV-spectrum. It was therefore considered un-suitable for the assessment of the activity of ONOO- within the UV light range of the UV-Visible spectrum. Un-coloured (phenol-red free) medium was therefore used for the study of the life and activity of ONOO- in cell culture medium. The data from the red-medium however showed that albeit the interference due to red phenol, the results were essentially similar to those observed in the general purpose medium (50:50 mix of Ham F-12 and Waymouths MB725). Some kinetic data of the decay of peroxynitrite in phenol-red medium (+ 15% Foetal Bovine Serum) was obtained and shown in Figure 2.4A. The final pH of a 1ml culture medium containing carbonate buffers was 7.93±0.1 following the addition of 0.6μL of strongly alkaline peroxynitrite solution. However, under conditions of pulmonary cell culture, this was reversed to 7.4 following the equilibration of the medium with incubator CO_2 levels.

2.4.2.1. ONOO- decay in phenol-red free medium

Spectrophotometric detection of peroxynitrite (ONOO-) added to phenol-red free culture medium suitable for the growth of human endothelial cells (LVEC Basal medium, TCS cell work Ltd) showed a prominent absorbance maximum at about 302 nm as expected (Fig 2.3). This was similar to the spectrum of ONOO- in aqueous alkaline solution although the latter condition was not associated with significant decay (Fig. 2.1). Peroxynitrite was seen to decay rapidly in phenol-red free cell culture medium with the appearance of an isosbestic point evident at a wavelength of 410nm (Fig 2.3). The isobestic point is suggestive of the formation of new species (i.e. products) which have not been identified and may or may not be involved in the biological effects elicited by ONOO-. Further experimentation is necessary to fully understand the formation and effects of these species in cell culture medium. The absorbance spectra of nitrates and nitrites indicate that these breakdown products of peroxynitrite did not show appreciable absorbance at 302nm. Similarly, the absorbance spectrum of sodium hydroxide (ONOO- solvent) did not show appreciable absorbance at 302 or 320nm.

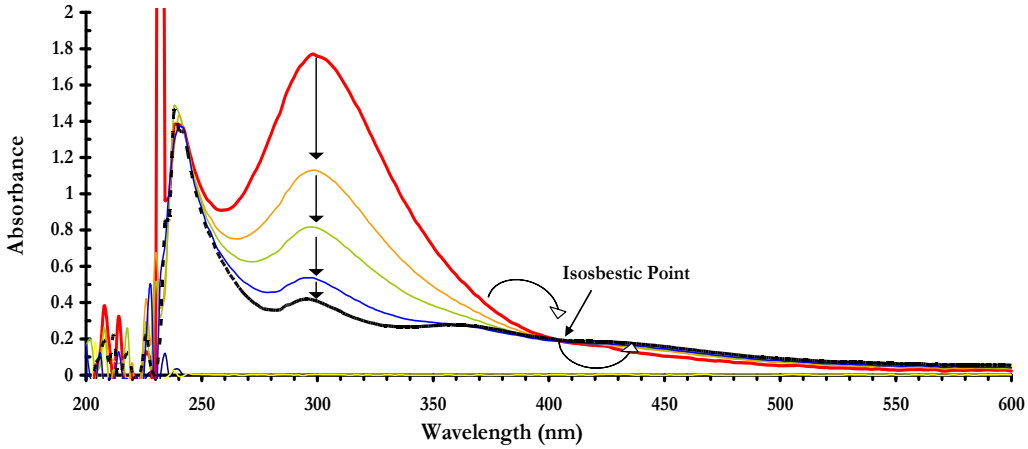

Figure 2.3: Spectra of the decay of 10^{-3}M Peroxynitrite Added 'Large Vessel' Human Endothelial Cell Culture Medium. Peroxynitrite was supplied in 1M Sodium Hydroxide Solution. Scan was conducted at room temperature every 10 seconds for 15min using the Cary50Bio® UV-Visible spectrophotometer (Varian). First (Red) line represents absorbance measured within first second after injecting peroxynitrite into quartz curvette; subsequent coloured lines are selected decay spectra in the direction of the arrow. The isosbestic point represents the spectroscopic wavelength at which the absorbance of peroxynitrite and a decay product, to which it is being converted, is the same. Experiments were conducted in triplicates

.

The decay of peroxynitrite in the red cell culture medium routinely used in this study was compared with the life of the anion under conditions mimicking pH of 1.5, 7.4, 11, 11.6, and 13.8 (Fig. 2.4A; buffers were prepared as described in Robbinson and Stokes, 2002). The conditions were chosen to represent strongly acidic, strongly basic and intermediate pH states. As shown in Figure 2.4A, ONOO- remained stable in strongly alkaline solution. The rate of decay however increased with decrease in pH with the anion possessing only a fleeting existence at pH 7.4 and 1.5 (Fig. 2.4A, B). If authentic peroxynitrite solution at pH 11.05 (Fig. 2.4B) or 14, the pH in which it is supplied commercially) is added to a buffered solution to give an abrupt change to pH 7.4, the peroxynitrite is destroyed rapidly (Fig. 2.4B). Half life of authentic peroxynitrite was calculated to be 1.38 seconds at pH 7.4 (Fig 2.4B), close to the 1.9s value reported by Beckman et al, (1990).

2.4.2.2. Estimate of the life of authentic ONOO-

In some experiments, bovine endothelial and smooth muscle cells were exposed to authentic peroxynitrite solution in volumes ranging from 0.3-0.6µl (chapter 3, 4, 5, 6); this resulted in increase in culture medium pH up to 7.93. At pH 7.93 and room temperature, ONOO- decayed to 60 and 50% initial level of activity within 5 and 10min, respectively (Fig. 2.4A). Also, during experimentation with pulmonary cells, it was typical for culture plates to be kept under this condition for period of 5-10min after ONOO- administration. Culture medium pH reversed to 7.4 when culture plates/flasks were returned to CO_2 incubator (5% CO_2, 37^0C). The return of medium pH to 7.4 will essentially terminate the life of ONOO- (Fig. 2.4B). It was therefore expected that the pulmonary cells of this study were exposed to substantial levels of ONOO- only within 5-10min period post ONOO- administration when plates were kept out of the incubator.

.

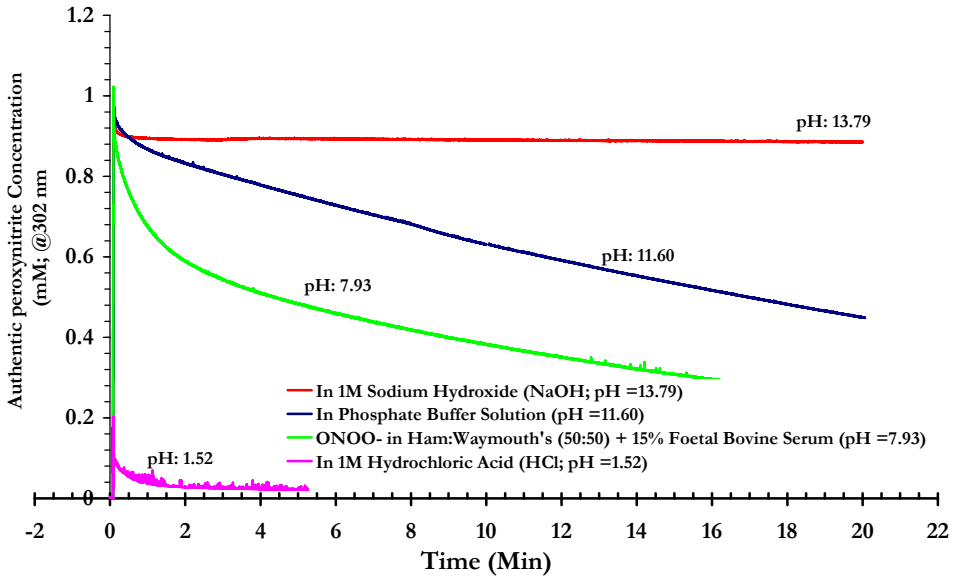

Figure 2.4A: Kinetic Profile of 10^{-3}M Peroxynitrite Decay in various pH conditions. Peroxynitrite was supplied in 1M Sodium Hydroxide Solution. Scan was conducted at room temperature every 0.1 seconds at 302nm for 15min using the Cary50Bio® UV-Visible spectrophotometer (Varian). Experiments were conducted in triplicates

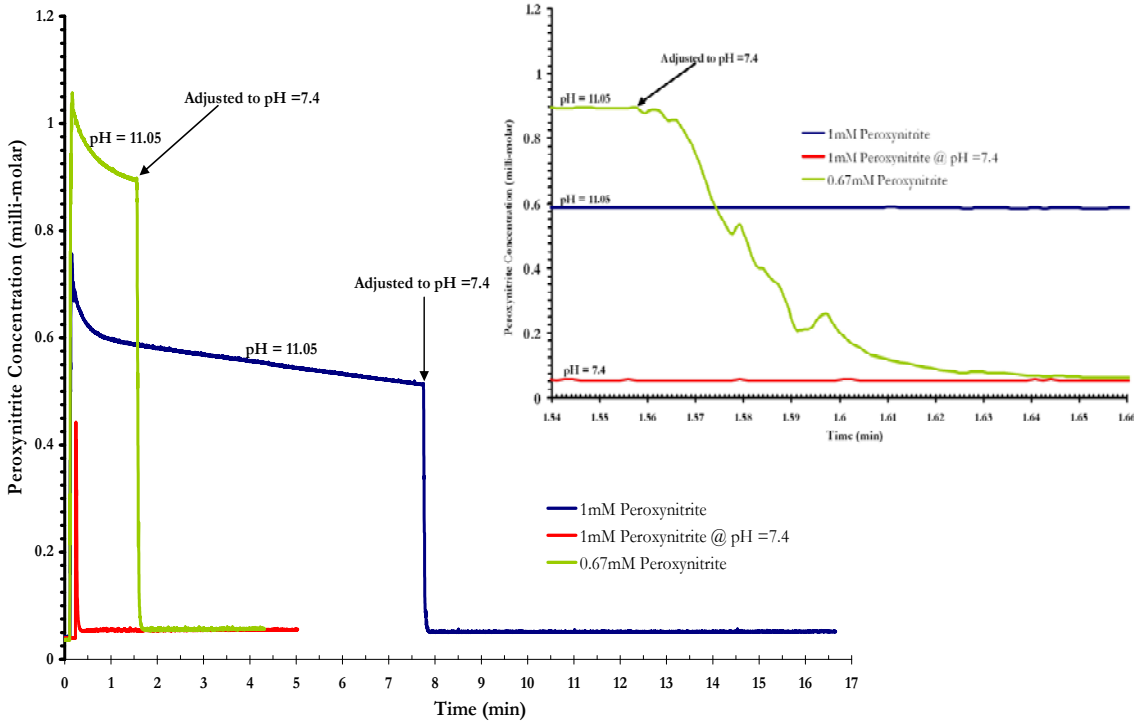

Figure 2.4B: Kinetic Profile of the Decay 10^{-3}M Peroxynitrite at pH =7.4 and pH 11.05 adjusted to 7.4 in phosphate buffer solution. Peroxynitrite was supplied in 1M Sodium Hydroxide Solution. Light absorbance spectrophotometry was conducted at room temperature every. Absorbance at 302nm was measured every 0.1 for 15min using the Cary50Bio® UV-Visible spectrophotometer (Varian). Experiments were conducted in triplicates.

2.4.3. Generation of peroxynitrite by SIN-1: evidence from conventional spectrophotometry

2.4.3.1. SIN-1: stable at acidic pH

Decomposition kinetics of SIN-1 was measured by conventional light absorbance spectroscopy at room temperature; SIN-1 showed maximum absorbance (λ_{Max}) at 291±2nm (Fig. 2.5), close to the reported 290nm value earlier reported (Asahi *et al.*, 1971). Figure 2.5 show the spectra of a 3-week old stock solution of SIN-1 ($2x10^{-4}$M; stored at -20^0C) further reconstituted in phosphate buffer solution, distilled water and 1M hydrochloric acid. The solutions were analysed for absorbance between 200 and 450nm; for 60 cycle spectrum at the rate of 10s per spectra. The results showed that at 10^{-4}M SIN-1 was stable in these media; 10^{-4}M SIN-1 caused a minute decrease in pH of the phosphate buffer solution and distilled water from 7.51±0.1 to 7.45±0.02 and 5.6±0.04 to 5.1±0.01, respectively. This is expected since SIN-1 is reported as a salt of the strong base 3-morpholinosydnonimine and has an acid dissociation constant of pk_1 9.1 at 25^0C. Also SIN-1 is known to be very stable at pH 1-2 (Thome *et al.*, 2003; Singh *et al.*, 1999) and this study demonstrates no significant decrease in absorbance at pH 5.1 over a 15 min period (Fig. 2.5B). Figure 2.5A showed the typical spectra of SIN-1; in addition, it showed that SIN-1 did not undergo a spontaneous reaction nor form any product under the conditions described (Fig. 2.5B).

2.4.3.2. SIN-1: decomposition under alkaline condition

Under alkaline condition, SIN-1 dissociated rapidly to form end products (Fig. 2.6). The rapid decomposition of SIN-1 was associated with a shift in absorbance maximum from 291±2nm to 279±2nm (Fig. 2.6, 2.8) which is the λ_{max} of SIN-1C (Thome *et al.*, 2003; Singh *et al.*, 1999). SIN-1 remained stable at λ_{max} 292nm in distilled water until the addition of 10^{-3}M NaOH which catalyses the decomposition of the molecule (Fig. 2.6). The addition of 10^{-3}M NaOH caused a rapid decline in absorbance at 292nm reaching a minimum within 10s; this was followed by an increase in absorbance at 279±2nm. Simultaneously, there was a decrease in absorbance at 230nm (Fig. 2.6). Previous researchers have shown that these sequences of events under this condition represent the formation of SIN-1C (Fig. 2.6; Thome *et al.*, 2003; Singh *et al.*, 1999).

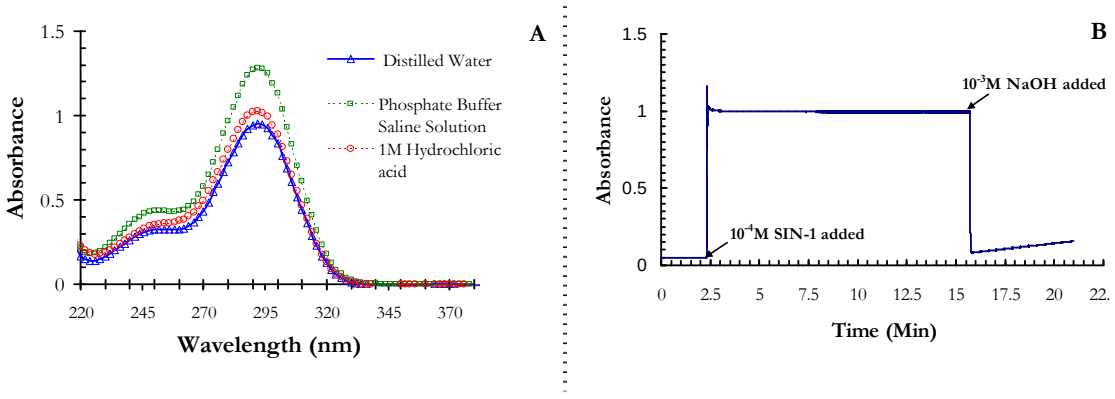

Figure 2.5: SIN-1 is stable at acidic pH (A) Spectra of 10^{-4}M SIN-1 in Water, acid and buffer solution; 60 cycles @ 10s/Cycle was conducted (B). Kinetics of 10^{-4}M SIN-1 in water (pH 5.1±0.037) showing the effect of alkalinising the medium with 10^{-3}M NaOH: Scan was conducted every 0.1 seconds at 292nm for 23min. Figure A and B experiments were conducted in triplicates at room temperature using the Cary50Bio® UV-Visible spectrophotometer (Varian).

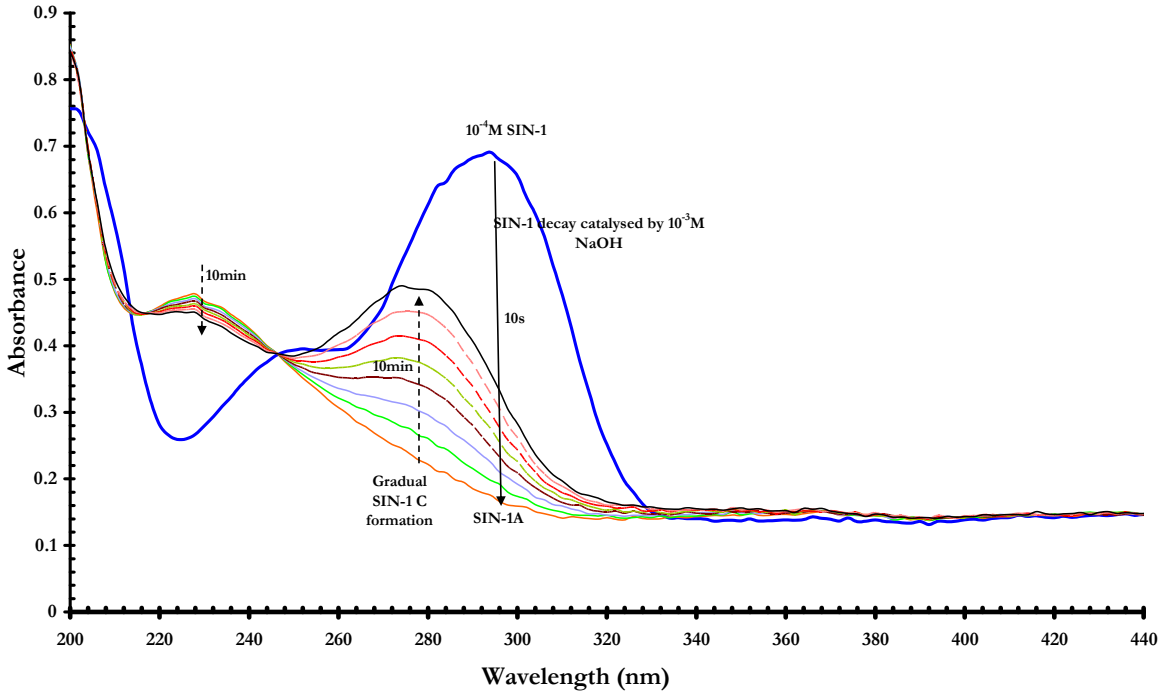

Figure 2.6: Spectra of 10^{-4}M SIN-1 in Water and Real Time Effect of the Addition of 10^{-3}M NaOH (60 cycles @ 10s/Cycle): Scan was conducted at room temperature using the Cary50Bio® UV-Visible spectrophotometer (Varian). SIN-1 remained stable until the addition of NaOH to the quartz cuvette. The solid arrow indicates rapid decay of SIN-1 while the dashed arrow show the increases in absorbance and the concentration of specie/s formed at 279±2nm immediately after the addition of 10^{-3}M NaOH. Experiments were conducted in triplicates

.

2.4.3.3. SIN-1: Spontaneous decomposition in endothelial cell culture medium

The spectrum of SIN-1 in cell culture medium was similar to that obtained for SIN-1 in water and buffer (Fig. 2.5, 2.6). The pH of 10^{-4}M SIN-1 was determined to be 7.53±0.1 (Fig. 2.7A, 2.7B). SIN-1 decayed slowly in endothelial cell culture medium (Fig. 2.7A); based on the kinetics of the decay, the half-life of SIN-1 was calculated to be 80min (Fig. 2.7B). However, the decomposition could be made to proceed rapidly with the addition of 10^{-3}M NaOH (final pH= 10.04; Fig. 2.7C), this indicated that further increase in pH will enhance the decay of the molecule as earlier observed under aqueous conditions (Fig. 2.6). The spectral changes in SIN-1 reported in buffer (Fig. 2.6) were also observed in cell culture media. The slow decay of SIN-1 was similarly associated with a shift in absorbance maximum from 291±2nm to 279±2nm (Fig. 2.6, 2.7A) which is the λ_{max} of SIN-1C (Thome *et al.*, 2003; Singh *et al.*, 1999). Without the catalyst effect of 10^{-3}M NaOH, 10^{-4}M SIN-1 decayed in cell culture media until a stable concentration of an intermediate product was reached at 90-100 minutes (Fig. 2.7B); following this was a phase of slight increase in absorbance observed for an additional 7 hours (Fig. 2.7B). The kinetic of SIN-1 decay in cell culture medium were essentially similar at 292 and 302nm (Fig. 2.7B, C). Although SIN-1C has λ_{max} at 279±2nm; the shoulders of the peak absorbance were detectable also at 290-302nm. Hence, the slight increase in absorbance at 292nm and 302nm over a 7h extended period (Fig. 2.7B) was likely indicative of the formation of stable SIN-1C. SIN-1C showed some absorbance and a maximum absorbance (λ_{max}) at 302 and 279±2nm, respectively (Fig. 2.6).

.

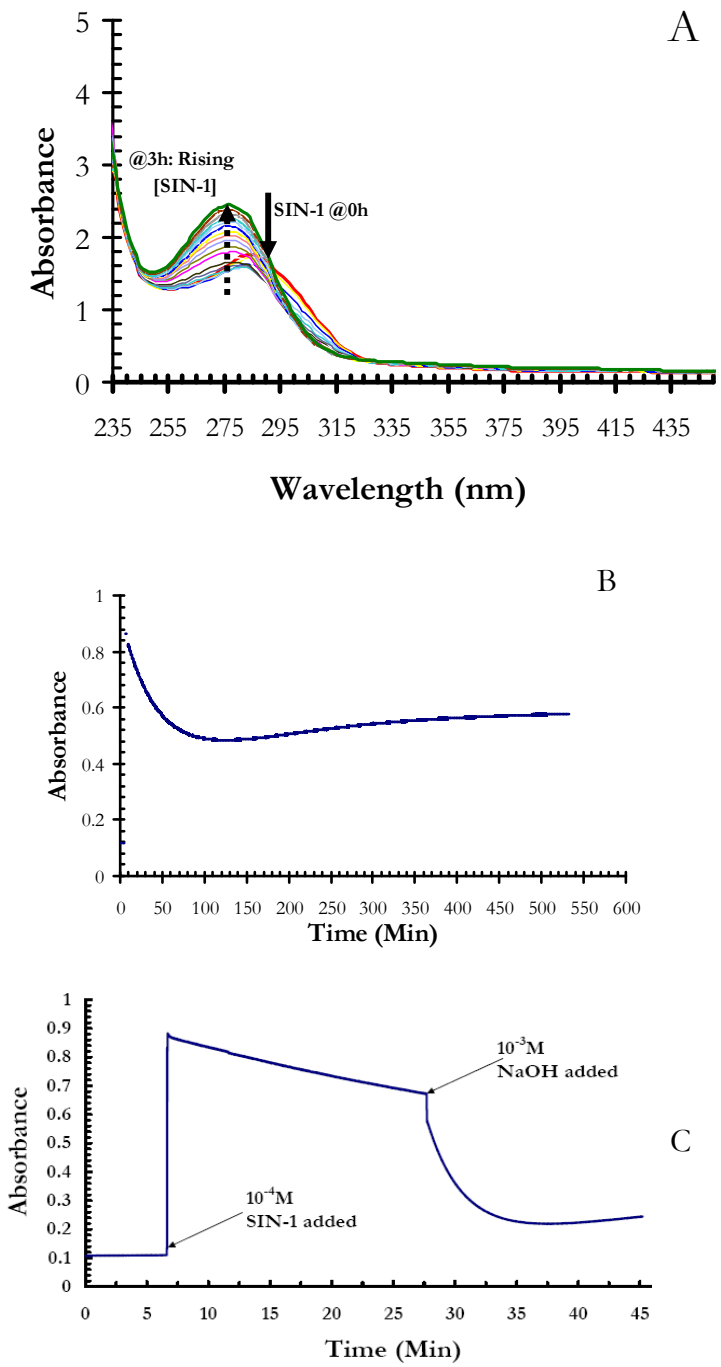

Figure 2.7: The Decomposition Spectra and Kinetics of 10^{-4}M SIN-1 in Endothelial Cell Culture Medium (A) Spectra of 90 cycles @ 2min/Cycle; the solid arrow indicated the decline in SIN-1 concentration between 0 and 32min real time period while the broken arrow showed the increases in absorbance and the concentration of a specie formed at 279±2nm between the 33rd min and 3rd hour of experimentation. (B) Every 2min scan at 292nm for 12h. (C) Decomposition kinetics of 10^{-4}M SIN-1 in endothelial cell culture medium showing effect of further increase in pH by 10^{-3}M NaOH. Scan was conducted every 0.1 seconds at 302nm for 50min. The slow yet steady decline in SIN-1 absorbance was accelerated by the addition of 10^{-3}M NaOH. For Figures A, B and C, experiment was conducted in triplicates at room temperature using the Cary50Bio® UV-Visible spectrophotometer (Varian).

.

The formation of SIN-1C following the decomposition of SIN-1 has been monitored at wavelengths between 270 and 280nm in other studies (Thome *et al.*, 2003; Schrammel *et al.*, 1998). Therefore, the increases in concentration at these wavelengths, as observed in this study, confirm the formation of this stable end product according scheme 1.1 and the comprehensive scheme 2.2 produced by this study. SIN-1C formation was later shown to be impaired under nitrogen purged conditions (see section 2.4.4.3). Hence, the formation of SIN-1C under aerobic condition is indirect evidence that superoxide was produced in the process and that SIN-1 isomerised and formed an intermediate product (SIN-1A) and later dissociated to yield nitric oxide (Singh *et al.*, 1999; Feelisch *et al.*, 1989; Asahi *et al.*, 1971). The study at this stage did not observe several of these steps. The reactions had occurred too quickly to enable monitoring by the current approach. The conventional spectroscopy instrument required at least 10s to scan between 200 and 450nm for activity/absorbance by which time the formation of SIN-1A may have been completed. Also, it was impossible to assess the activity of SIN-1 within the first 1s, which was crucial to plotting the transition to SIN-1A or SIN-1C. The use of stopped-flow spectroscopy was thereon considered a suitable approach to further the progress in the area since the stopped-flow system can monitor changes in absorbance between 200-450nm in increments of 0.6s.

2.4.4. Generation of peroxynitrite by SIN-1: evidence from stopped-flow spectroscopy

2.4.4.1. SIN-1 decay: The formation of SIN-1A can be [$^{-}$OH] catalysed

As shown from experiments with conventional spectroscopy (Fig. 2.5, 2.6, 2.7), SIN-1 is stable only in a strongly acidic medium (pH 1-2), it decomposes in a pH dependent manner to form the stable active metabolite- SIN-1C (Fig. 2.8A-F) as medium pH increases. Stopped-flow spectroscopy results summarized in Figure 2.8 showed that an aqueous solution of SIN-1 (pH 5.1$\pm$0.04) decays only slowly throughout the period of experimentation; there were no changes in absorbance maximum within a 120s period (Fig. 2.8A). However, as medium pH increased from 6.2 to 11.9, the time taken for the formation of the intermediate product (SIN-1A) decreased from 7.5min to 0.6s, respectively (Fig. 2.8). This was further illustrated in Figure 2.9A. At pH 6.7, the decay of SIN-1 was slow and the formation of SIN-1C was detectable after 5h. There were

decreases in absorbance at 240nm (Fig. 2.8b); this coincided with the decay of SIN-1 monitored at 292nm thus suggesting that at slightly acidic pH the decay of SIN-1 may be monitored at 240 or 292nm (Fig. 2.8b). A hint at the complex nature of SIN-1 decomposition was seen as medium pH was increased from 6.7 to 8.6 (Fig. 2.8c). For the first time, the study observed clear evidence of the broadening of SIN-1 peak from 325nm (Fig. 2.8a) to 380nm on the right hand shoulder of the SIN-1 spectrum (Fig. 2.8c). In addition, 2 absorbance peaks were visible, namely at 290 and 330nm recorded at pH 8.6 (Fig. 2.8c). Decline in absorbance at these points was 2-phased. Firstly, within 4.8s SIN-1 absorbance declined to form an intermediate (SIN-1A) with trough absorbance at 270nm and an isobestic point at 285nm (Fig. 2.8c). This was immediately followed by 2nd decay phase characterised by further decline in absorbance at 292 and 330nm but with simultaneous increase in absorbance at 270nm with the isobestic point remaining at 285nm (Fig. 2.8c), thus indicating the formation of SIN-1C. At pH 9.7, much of this insight into the multi-phased decay of SIN-1 was not apparent. Under the same scan settings as in Figure 2.8c, the formation of SIN-1A appeared to have been completed within 35s. The 2 absorbance peaks of the broadened SIN-1 spectrum noticed at pH 8.6 (Fig. 2.8c) were also observed at 290 and 330nm in addition to the early stages of SIN-1C formation (Fig. 2.8d). The spectral changes at pH 10.0, 10.2, 10.8 and 11.9 were similar to that reported at pH 9.7; however, SIN-1A formation appeared to have occurred within 11, 8, 3 and 0.6s respectively (Fig. 2.8 e-h). In all 5 pH conditions, the formation of SIN-1C was evident at 280nm (Fig. 2.8d-h). These results suggest that the formation of SIN-1A can be modified by pH changes; with the hydroxyl ion ($^{-}$OH) serving as a catalyst for this phase of SIN-1 decay (Fig. 2.8; Scheme 2.2). The results also demonstrate that formation of SIN-1A and the generation of stable SIN-1C are mutually exclusive events in which the latter proceeds only after the completion of the former (Fig. 2.8). In summary, the gradual decay of SIN-1 to SIN-1A has occurred in pH dependent time frames; at all pH levels investigated, this was accompanied for the most part with decline in absorbance at 291±2 nm and with increases in absorbance at 279±2 nm which indicated the formation of stable SIN-1C (Fig. 2.8).

.

2.4.4.2. SIN-1 decay: the de-protonation sub-phase of SIN-1A formation

Beginning at pH 8.6, the sharp SIN-1 peak seen normally at 291±2 nm was broadened to have a right shoulder extending from 325nm (Fig. 2.6, 2.8A) to 375nm (Fig. 2.8A-E). The presence of an isobetic point at approximately 315nm represented a pKa transition (Fig. 2.9B); thus suggesting the existence of 2 directly related species.

A possible explanation is the formation of a de-protonated intermediate (see Scheme 2.2) before the formation of SIN-1A (Fig. 2.9B). This phenomenon appeared to have occurred so fast that it is hardly seen even at 0.6s of SIN-1 in a pH 11.9 medium (compare Fig. 2.8A-E with Fig. 2.8F).

.

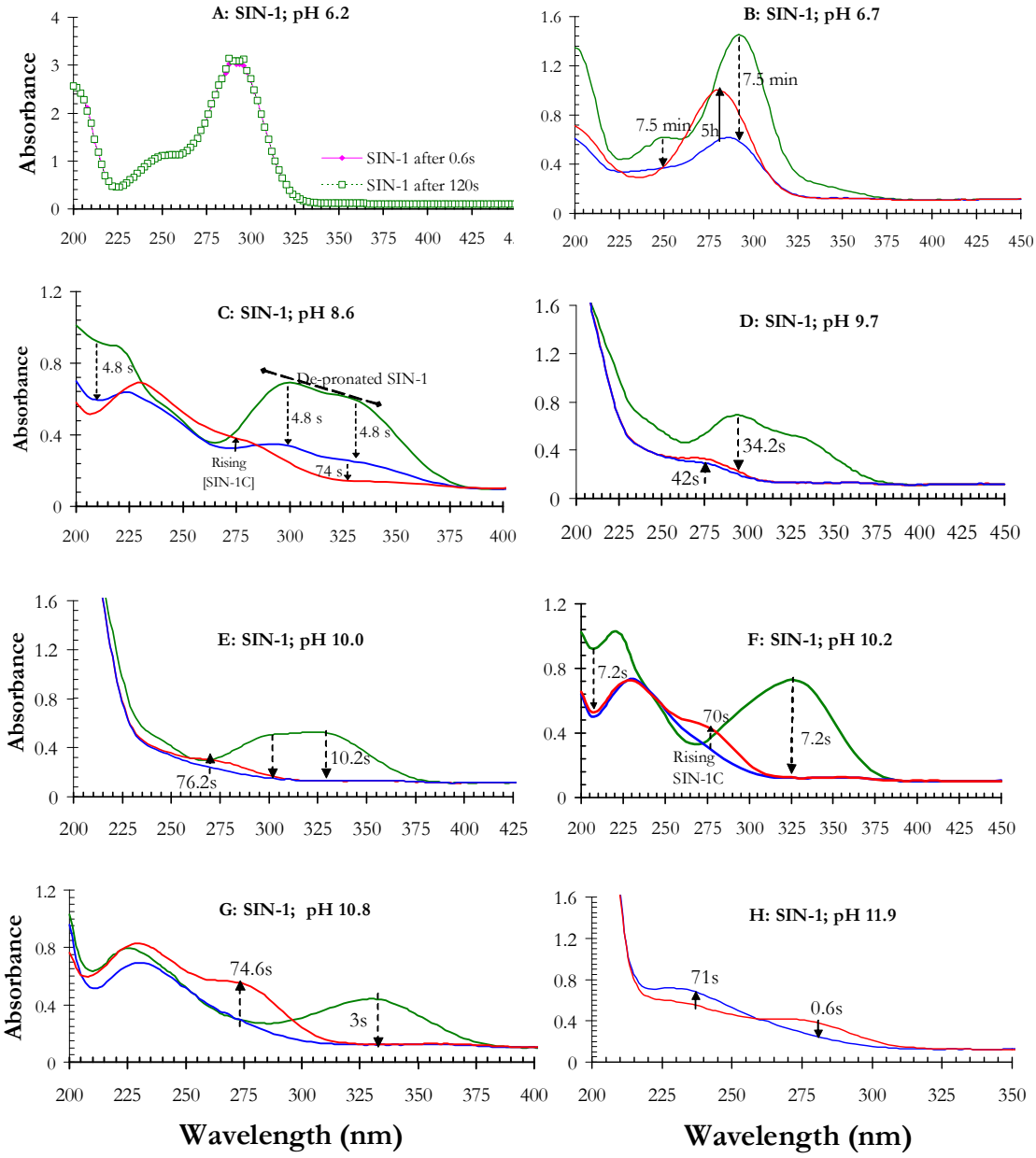

Figure 2.8: Significant Time Points Selected From the Real Time Stopped-Flow Spectra of Aqueous 10-4M SIN-1 Solution Alone or Mixed with Equal Volume Buffer or NaOH. The selected time points highlight the decay of SIN-1 (Green line) to an intermediate product (Blue lines) followed by the gradual formation of stable SIN-1C (red line) (A): $2x10^{-4}$M SIN-1 mixed with equal volume $2x10^{-4}$M SIN-1 solution (pH 6.2) Scan setting: 200 cycles @ 0.6s/Cycle. (B): $2x10^{-4}$M SIN-1 solution mixed with equal volume $2x10^{-5}$M NaOH (pH = 6.5; setting: 128 cycles @ 2.5min/Cycle). (C): $2x10^{-4}$M SIN-1 solution mixed with equal volume $5x10^{-5}$M NaOH; pH = 8.6). (D): $2x10^{-4}$M SIN-1 solution at pH 9.7 (Carbonates/NaOH Buffer); pH = 9.7) (E): 10^{-4}M SIN-1 solution at pH 10 (Carbonates/NaOH Buffer; actual pH 10.0) (F): Mixture of aqueous $2x10^{-4}$M SIN-1 solution + $1x10^{-4}$M NaOH (pH 10.2). (G): Mixture of aqueous $2x10^{-4}$M SIN-1 solution + 2x10-4M NaOH (pH 10.8) (H): $2x10^{-4}$M SIN-1 solution mixed with $2x10^{-3}$M NaOH. (pH= 11.9) Experiments were conducted in triplicates at room temperature using the Cary50Bio® UV-Visible stopped-flow spectrophotometer (Varian). Scan setting for C-H: 128 cycles @ 0.6s/Cycle. The gradual decay of SIN-1 to SIN-1A and the subsequent increase in SIN-1C (280nm) absorbance were monitored in real time. Experiments were conducted in triplicates

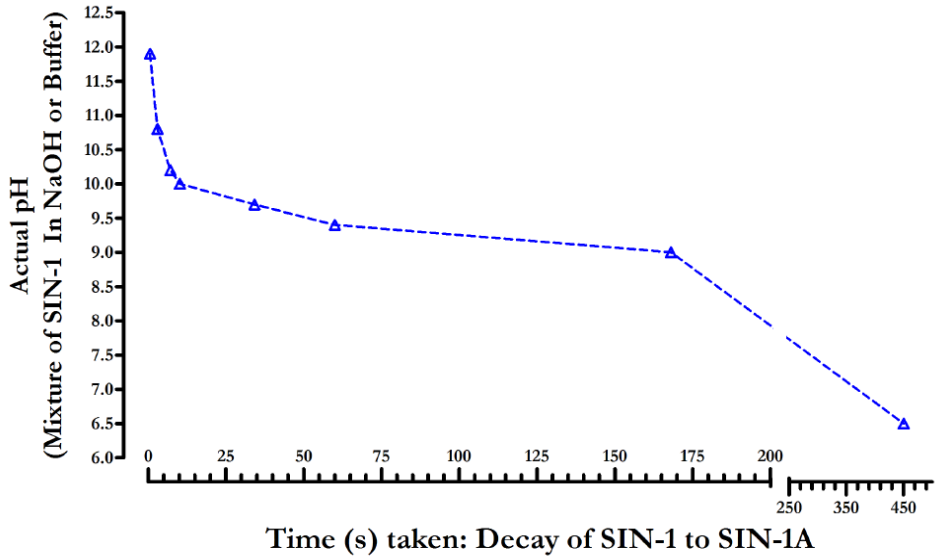

Figure 2.9A: Selected Time Point From Real Time Stopped-Flow Spectra Of 2x10^{-4}M SIN-1 Mixed With Equal Volume NaOH or Suitable Buffers. Time taken for SIN-1 to decay to SIN-1A was determined from UV-spectroscopy data and illustrated by the down-pointing arrows in Figure 2.8. Experiments were conducted in triplicate at room temperature using the Cary50Bio® UV-Visible stopped-flow spectrophotometer (Varian).

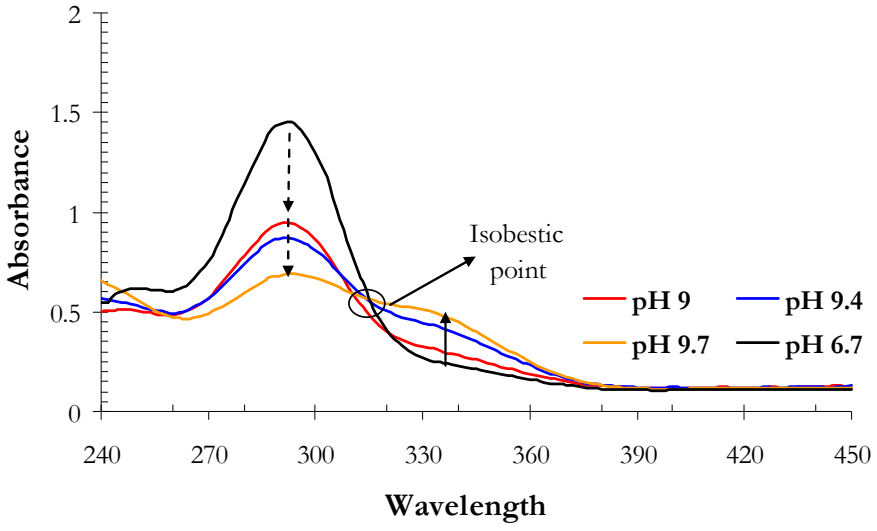

Figure 2.9B: Putative Evidence For The Deprotonation Of SIN-1. The initial (time, t=0) spectral of SIN-1 at different pH have been pooled to demonstrate the presence of an isobestic point at approximately 315nm. This indicated the absorbance of two substances, one of which was being converted into the other. The observed change in spectrum with pH represents a pKa transition likely caused by the deprotonation of SIN-1. Experiments were conducted in triplicates at room temperature using the Cary50Bio® UV-Visible stopped-flow spectrophotometer (Varian).

2.4.4.3. Oxygen dependence of 2nd Phase SIN-1 decay: the formation of SIN-1C

The formation of SIN-1C was significantly impaired under nitrogen purged conditions (Fig. 2.10; $p < 0.05$; t-test). At pH 9.0 and using nitrogen purged SIN-1/buffer mixtures, SIN-1 decayed to intermediate SIN-1A within 2.8min; this was monitrored at 292nm (Fig. 2.10, N1). This was immediately followed by a steady increase in SIN-1C concentration at 280nm (Fig. 2.10, N1). Repeating the experiments with air saturated SIN-1/buffer mixtures showed that the final concentration of SIN-1C increased from 54.7±3.3% under nitrogen purged conditions to 71.4 ±4.6% initial SIN-1 concentration under air saturated conditions over the same time period (Fig. 2.10 A1, N1). The results were similar in trend at pH 9.4 (Fig. 2.10 A2, N2). In this study, it was not possible to create oxygen free medium or saturate SIN-1/buffer mixtures with pure oxygen, however the amount of SIN-1C formed during these period increased significantly under air saturated conditions (Fig. 2.10). This supposes an important role for oxygen in this phase of SIN-1 decay.

In this set of experiments, NaOH was utilized to provide the $^{-}$OH ion needed to catalyse the decay of SIN-1. The stopped-flow spectroscopy data confirmed that the decay of SIN-1 to SIN-1A (Phase 1) can be accelerated by hydroxyl ion, while the subsequent formation of SIN-1C from SIN-1A can be catalysed by oxygen. This study therefore concluded that the SIN-1 → SIN-1C transformation was the result of the $^{-}$OH catalyzed hydrolytic decomposition (Fig. 2.8, 2.9) which occurred under cell culture medium condition (Fig. 2.7). The broadened (pH 8.6, 9.7. 10, 10.2, 10.8; Fig. 2.8C-G) and characteristic double peak (pH 8.6, 9.7. 10; Fig. 2.8D-E) seen during the decay of SIN-1 to SIN-1A was an indication that SIN-1 formed a putative de-protonation species during the process. Based on the results of this and earlier studies, a pathway for the decomposition of SIN-1 in cell culture medium was proposed (scheme 2.2)

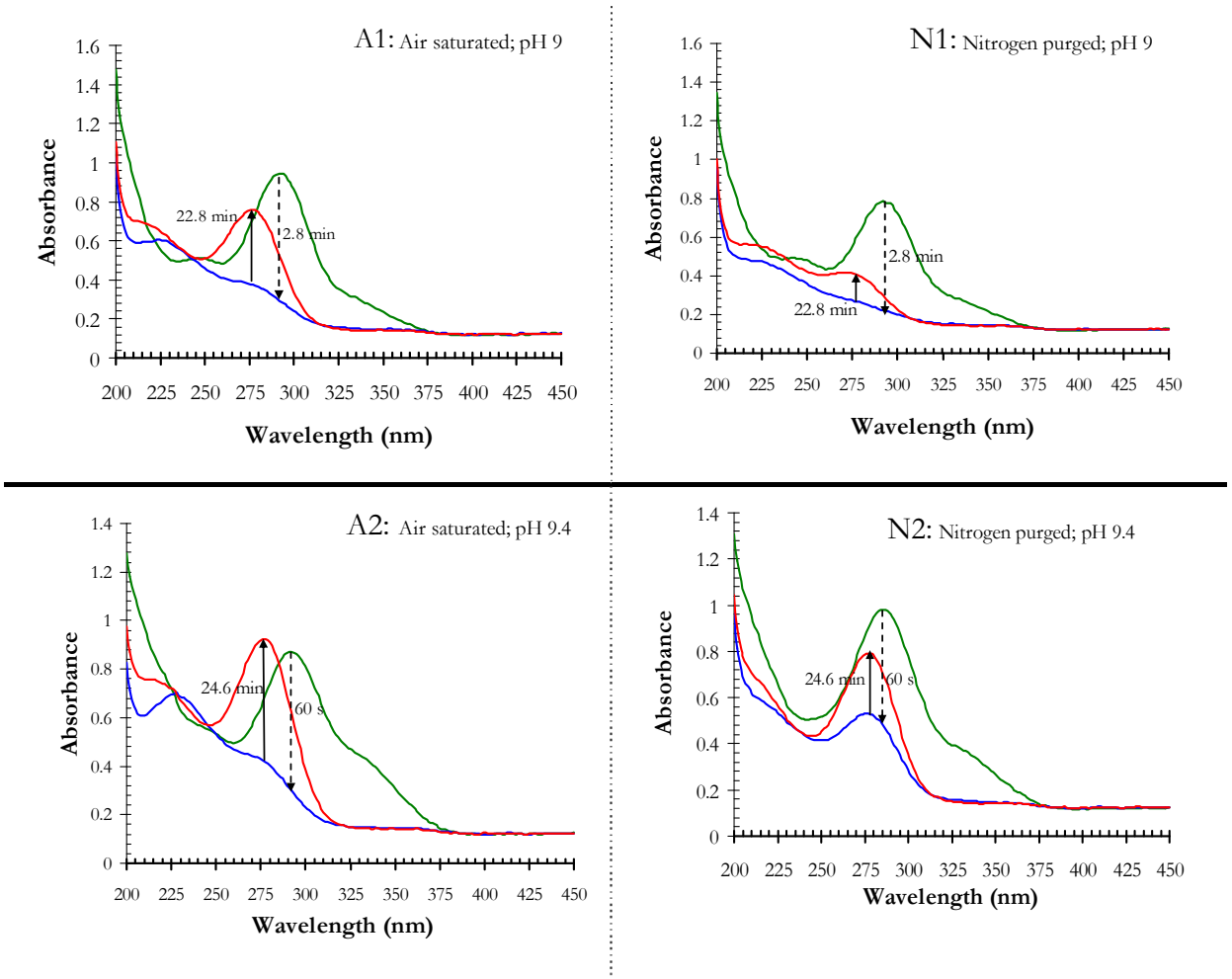

Figure 2.10: Significant time points selected from real time stopped-flow spectra of aqueous air saturated or nitrogen purged 10^{-4}M SIN-1 solution at pH 9.0 (Borax/HCl Buffer) and 9.4 (Borax/NaOH Buffer). Experiments were conducted in triplicate (128 cycles @ 12s/Cycle) with air saturated (Fig. A1 & A2) and nitrogen purged (Fig. N1 & N2) SIN-1 samples at pH 9 and 9.4, respectively. Scan was conducted in triplicates at room temperature using the Cary50Bio® UV-Visible stopped-flow spectrophotometer (Varian).

.

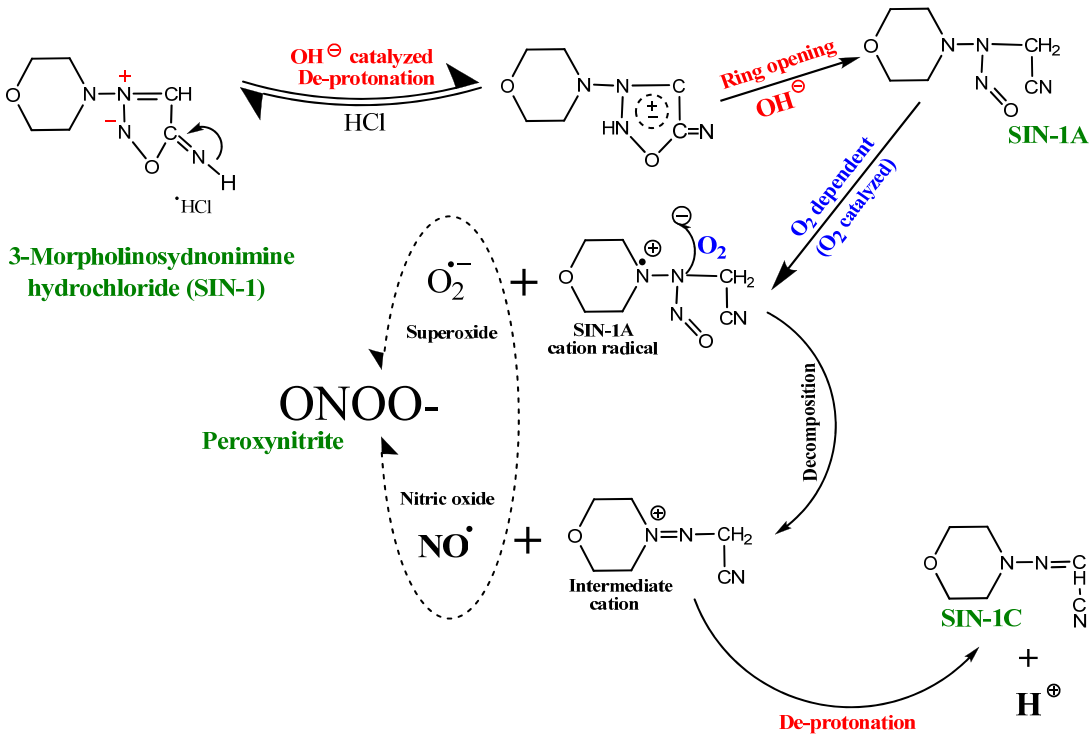

Scheme 2.2: A Schematic Representation of the Generation of Peroxynitrite from 3-Morpholinosdynonimine (SIN-1): SIN-1 isomerises and undergoes ring opening to form SIN-1A. Under aerobic condition, Dioxygen undergoes one electron reduction to form superoxide. This is may have been initiated by the one electron oxidation of SIN-1A to form an intermediate radical cation of SIN-1A. This decomposed to release NO• and form stable SIN-1C. This study has demonstrated that (1) the rate of SIN-1 decomposition is pH dependent (2) the rate and amount of SIN-1C formation is oxygen dependent. The timing of the appearance and increases of the absorbance peak at 279±2nm in aqueous confirmed the formation of SIN-1C and provide indirect evidence for the release of NO•. (3) For the first time, this study provided stopped-flow spectroscopic evidence that SIN-1 is de-protonated in the initial phase of the reaction leading up to SIN-1A formation in a pH dependent manner. This reaction may be the initiator of SIN-1 decay.

.

2.4.5. Peroxynitrite from SIN-1: Quantification by NADH fluorescence quenching

2.4.5.1. Selection of cell culture medium for optimal NADH fluorescence

NADH was found to fluoresce between emission wavelengths of 420 and 520nm with a peak at 460nm (Fig 2.11a). Leibovitz's L-15 non phenol-red (Fig. 2.11B) and Waymouth/F-12 (Fig. 2.11D) culture media showed significant background fluorescence; such that NADH 30 μM caused either no increase or only a 2 fold increase in fluorescence over background (Fig. 2.11B, D). However large vessel endothelial cell basal medium (LVEC medium) had a lower background fluorescence and a satisfactory 5 fold increase (measured at 460 nm) on addition of NADH 30 μM (Fig. 2.11C), and was therefore chosen for future experiments.

NADH fluorescence at 460nm was approximately linear with NADH concentration up to 35μM in both cell culture medium and de-ionised water (result not shown). Thereafter the relationship was curvilinear, possibly suggesting some self-quenching of emission (result not shown). Most experimentations in cell culture medium therefore involved the use of 30 μM NADH in LVEC medium.

2.4.5.2. SIN-1 induced quenching of NADH fluorescence emission

Bolus addition of authentic peroxynitrite caused a concentration dependent rapid quenching of NADH fluorescence without significant distortion of the fluorescence emission spectra (result not shown). This though was associated with an increase in fluorescence emission at approximately 410nm due likely to a fluorescing adduct (result not shown). Loss of NADH fluorescence was due likely to the conversion of NADH to NAD^+ (Martin-Romero *et al.*, 2004). Also, it was confirmed that NADH underwent slight air oxidation giving a gradual decline in fluorescence at 460 nm, as previously found by Martin-Romero *et al.*, 2004) (Fig 2.12). Over a period of 120 minutes, fluorescence diminished from 22.11 to 20.15, a decline of 9% due to air oxidation (Fig 2.12).

.

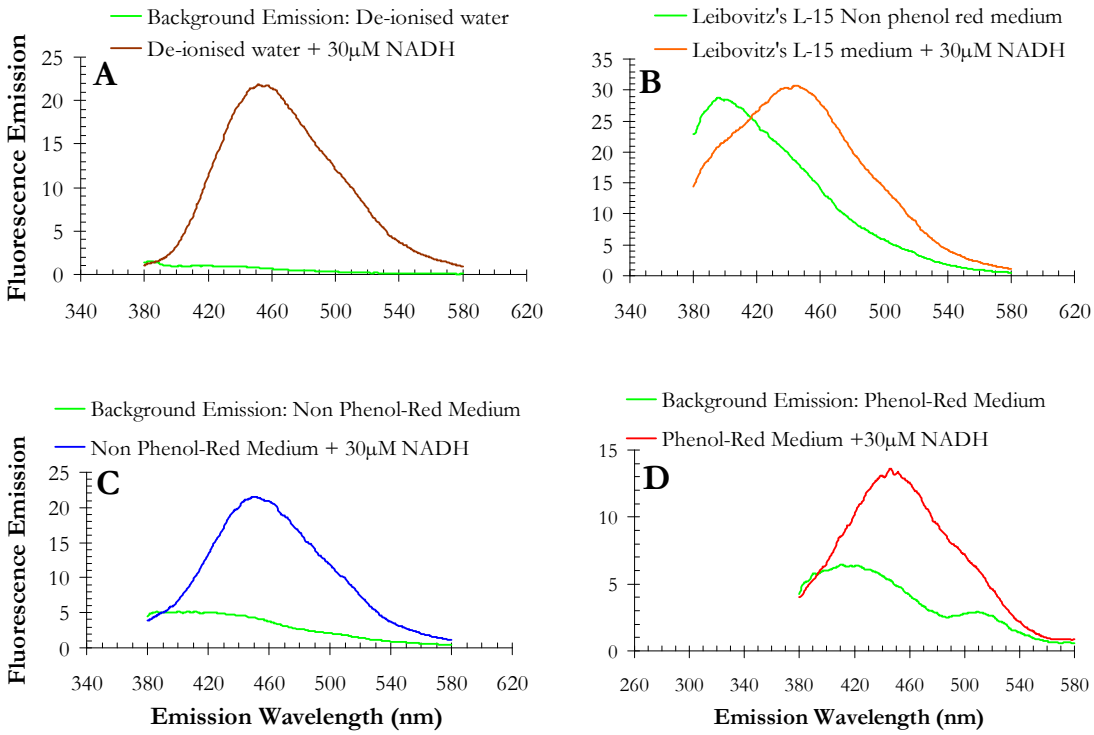

Figure 2.11: Background and NADH fluorescence in pulmonary cell culture media. Fluorescence measurements were carried out with a spectrofluorometer (LS 45 Luminescence Spectrometer, PerkinElmer Instruments). Fluorescence spectrum is shown in (A) De-ionised water (B) Leibovitz's L-15 Non phenol red medium (C) Large vessel endothelial cell basal medium (D) 50:50 mix of Waymouth's MB 752/1 + L-glutamine and F-12 (Ham) Nutrient mixture medium + L-Glutamine. Measurement were taken following a rapid mixing period of approximately 10s. Experiments were conducted in triplicates

.

SIN-1 20μM caused a gradual decline in NADH fluorescence over a period of approximately 2 hours (Fig. 2.12). Increasing SIN-1 concentration 5 fold caused a more rapid decline in NADH fluorescence; this was similar to background medium fluorescence within 90 minutes. These effects were blocked by the co-addition of superoxide dismutase, a superoxide scavenger (Fig. 2.13), consistent with the reaction mechanism that showed the release of a superoxide intermediate from SIN-1 (scheme 2.2).

With the addition of 1mM SIN-1, the fluorescence emission of 30μM NADH diminished to the level of the culture medium basal fluorescence in approximately 30min. Thus it appears that 1 mM SIN-1 generated more ONOO- than was required to react with 30μM NADH (Fig. 2.13).

Subtraction of the decline due to air oxidation of NADH from the results in Figure 2.12 generated the true rate of ONOO- formation shown in Fig 2.14. This showed close to linear formation of ONOO-. At 20μM, SIN-1 caused a 2.20 unit decline in fluorescence emission over a period of 88.85min (Fig. 2.14). The rate of NAD+ formation by 20μM SIN-1 which also corresponded to the rate of ONOO- formation was therefore calculated to be 0.025 fluorescence unit/min.

Under the same conditions, the effect of authentic peroxynitrite on NADH fluorescence was further investigated by step-wise titration experiments involving the addition of pre-synthesised ONOO- to cuvette containing 30μM NADH in LVEC medium. The results of preliminary experiments (not shown) confirmed that the number and volume of the pulses of authentic peroxynitrite used in these experiments did not cause significant change in cell culture medium pH (Fig. 2.15). The real time tracing of these experiments (Fig. 2.15) showed that quenching of NADH fluorescence due to ONOO- was rapid and cumulative. In addition, control experiments showed the real time air-oxidation of 30μM NADH (Fig. 2.15).

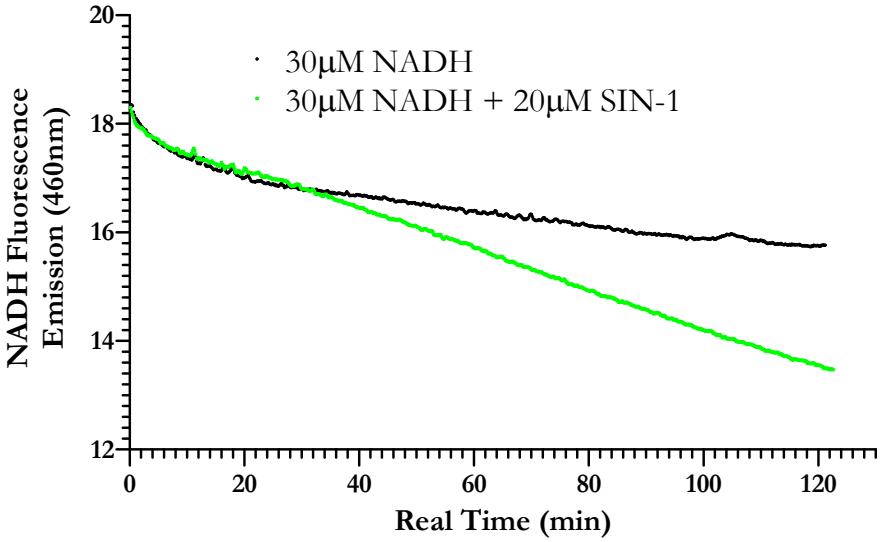

Figure: 2.12. Kinetics of SIN-1 induced quenching of 30μM NADH fluorescence. NADH fluorescence was investigated in large vessel endothelial cell basal medium to which SIN-1 was added (pH = 7.41±0.23 at 25^{0}C) and measured with excitation and emission wavelengths at 340 and 460 nm, respectively. Separate experiments investigated the quenching of 30μM NADH fluorescence in the presence of 20 (above) and 100μM SIN-1 (not shown) in a cuvette. Measurements were taken following a rapid mixing period of approximately 10s. Experiments were conducted in triplicates

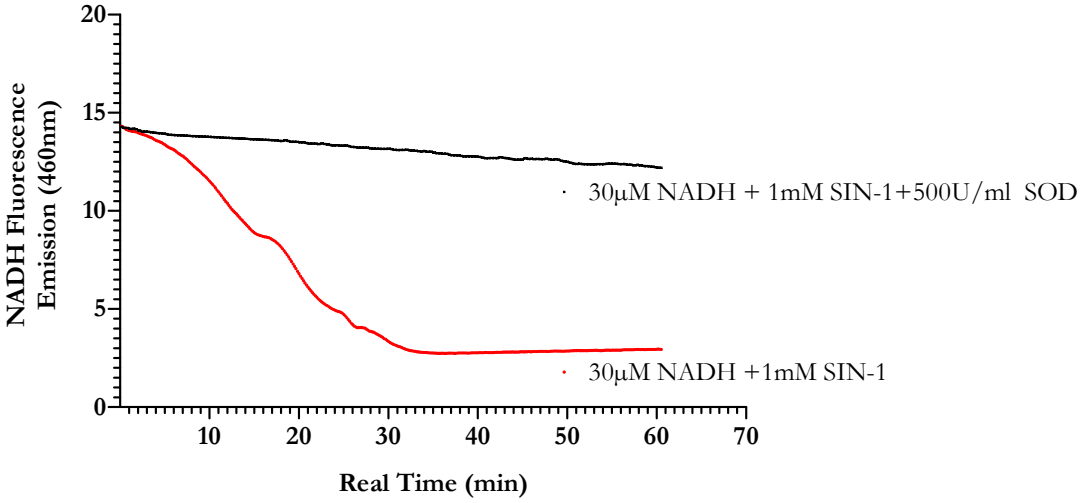

Figure 2.13: Attenuation of SIN-1 induced oxidation of 30μM NADH fluorescence by superoxide dismutase (SOD). NADH fluorescence was investigated in large vessel endothelial cell basal medium to which SIN-1 and SOD were added (pH = 7.41±0.23 at 25^{0}C) and measured with excitation and emission wavelengths at 340 and 460 nm, respectively. Measurement were taken following a rapid mixing period of approximately 10s. Experiments were conducted in triplicates

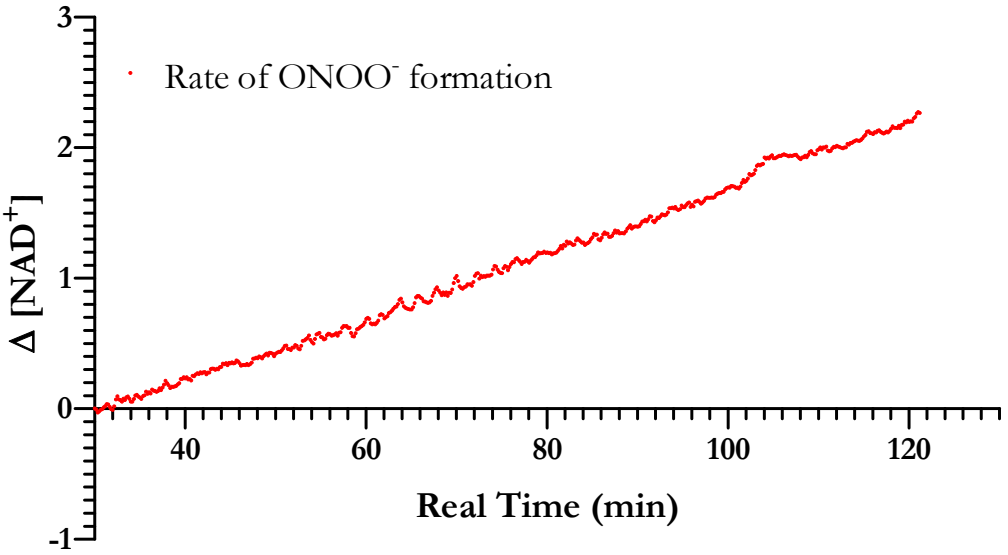

Figure 2.14: The production of peroxynitrite during SIN-1 decomposition. Loss is NADH fluorescence correlates with increased NAD^+ formation (Martin-Romero *et al.*, 2004). The figure shows increase in NAD^+ formation in the presence of 20μM SIN-1 in large vessel endothelial cell basal medium (pH = 7.41±0.23 at 25^{0}C) and measured with excitation and emission wavelengths at 340 and 460 nm, respectively. Oxidation of NADH to NAD^+ was due to peroxynitrite (ONOO-) generated from SIN-1. The data was derived from Fig 2.13 following correction for NADH air-oxidation.

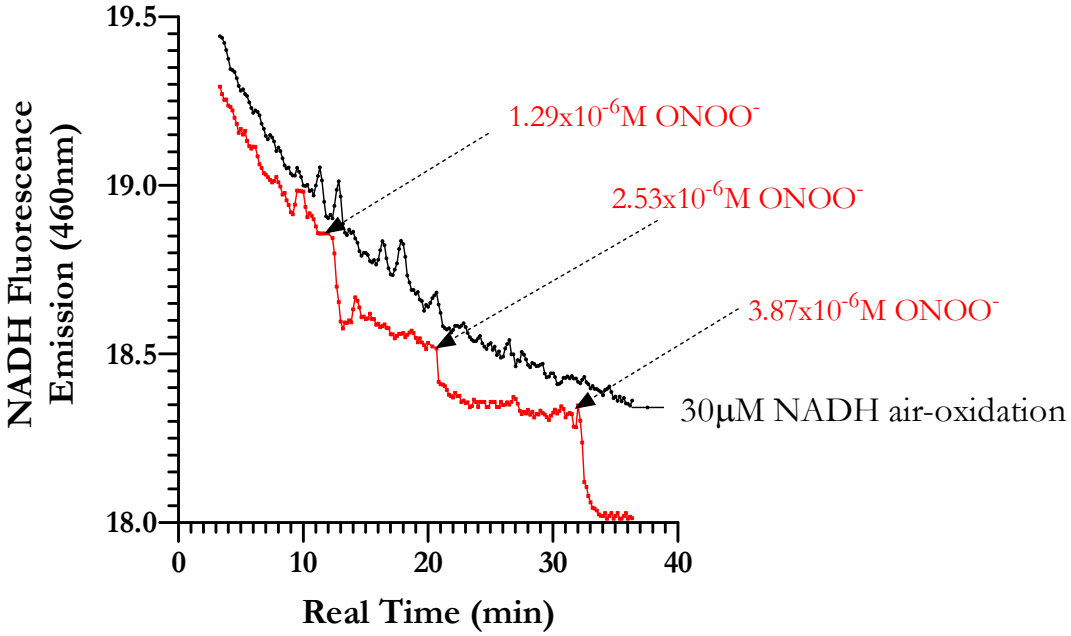

Figure 2.15: Stepwise titration of 30μM NADH fluorescence with authentic peroxynitrite. The tracing shows the quenching of the fluorescence of 30μM NADH by the sequential addition of 1μL volume pulses of authentic peroxynitrite from 3.87x10^{-3}M stock solutions to 3ml NADH/Medium in a cuvette. Cumulative authentic peroxynitrite concentrations are indicated by the arrow at each point of addition. NADH fluorescence was investigated in large vessel endothelial cell basal medium to which authentic ONOO- was added (pH = 7.47±0.2 at 25^{0}C) and measured with excitation and emission wavelengths at 340 and 460 nm, respectively. Experiments were conducted in triplicates

The fluorescence decline at each step in Figure 2.15 was measured, and plotted against cumulative ONOO- added to give Fig 2.16. (Fig 2.16A shows the data without correction for air oxidation, and Fig 2.16B includes correction for air oxidation). This showed an approximately linear relationship between ONOO- formation and fluorescence quenching. From Figure 2.16 it can be seen that decline by 1 fluorescence unit occurred with addition of 4.6μM of ONOO-. Since decline in NADH fluorescence with 20μM SIN-1 was 0.025 fluorescence unit per min, 20μM SIN-1 was thus generating 1.9nM ONOO- per second or 0.11μM min^{-1}. Introducing this figure into the rate of fluorescence decline with 20μM SIN-1 (Fig 2.12) gives an estimate for ONOO- generation of 10μM over approximately 90min period. Comparing SIN-1 induced NADH fluorescence quenching (Fig. 2.12, 2.14) and the **s**tepwise titration of NADH fluorescence with authentic peroxynitrite (Fig. 2.15, 2.16B) showed that 20μM SIN-1 was generating ONOO- at 0.11μM min^{-1} over approx. 90min period.

.

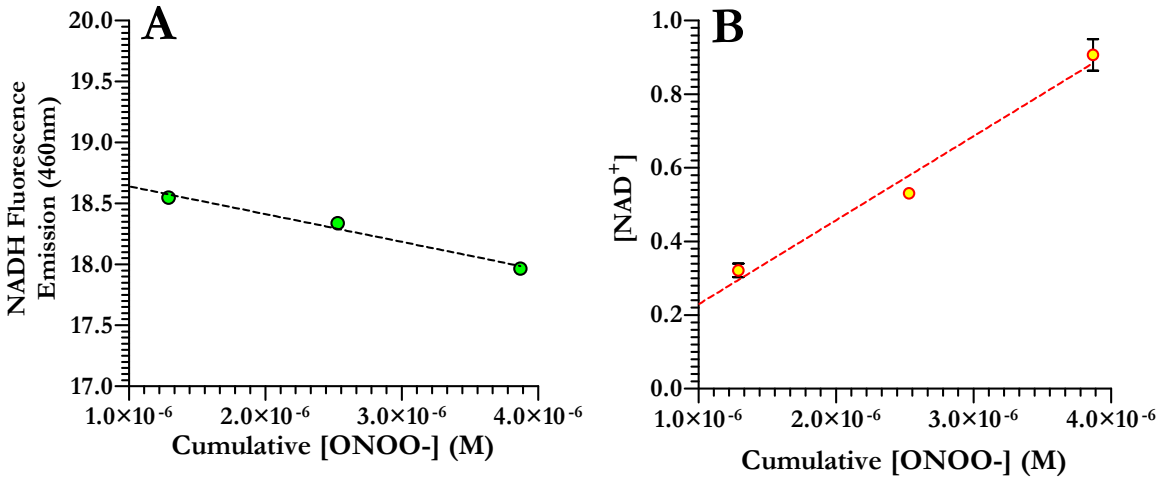

Figure 2.16: Analysis of stepwise titration of 30µM NADH fluorescence with authentic peroxynitrite. Loss is NADH fluorescence correlates with increased NAD^+ formation (Martin-Romero *et al.*, 2004)**.** NADH fluorescence was investigated in large vessel endothelial cell basal medium to which authentic ONOO- was added (pH = 7.47±0.21 at 25^0C) and measured with excitation and emission wavelengths at 340 and 460 nm, respectively. Figure 2.18A shows the cumulative quenching of the fluorescence of 30µM NADH achieved by cumulative authentic peroxynitrite concentration. Figure 2.18B show the increase in NAD^+ with cumulative [ONOO-]

.

2.5. DISCUSSION

2.5.1. Working with authentic peroxynitrite solution

Although peroxynitrite is stable in strongly alkaline solution, working with the molecule at physiological pH poses a major challenge because of its unstable nature and fleeting existence at physiological pH. This study confirmed earlier findings that $ONOO^-$ is short-lived at physiological pH; ONOO- half-life was calculated to be 1.38s at pH 7.4 similar to the findings of other investigators (Beckman *et al.*, 1990). Also, studies involving bolus and direct addition of ONOO- to cells engender significant loss of ONOO- before reaching the cells. It has however been argued that this method of adding ONOO- simulate the physiologically relevant steady state ONOO- concentration in-vivo (Alvaro *et al.*, 1999; Salgo *et al.*, 1995b). In addition, this study showed that the slight increase in pH of buffered cell culture medium to 7.93 following the addition of strongly alkaline solution ONOO- sustained the activity of the anion for a much longer period (Fig. 2.4A).

2.5.2. The peroxynitrite from SIN-1

2.5.2.1. Confirming the evidence, elucidating on the mechanism of SIN-1 decay

This study confirms published evidence for the accepted mechanism for the generation of ONOO- from SIN-1 (Feelisch *et al.*, 1989) and provides additional evidence to further the understanding of the decay process. This study has demonstrated that (1) the rate of SIN-1 decomposition can be catalysed by -OH ions (Fig. 2.8), (2) the rate and amount of SIN-1C formation during this process was oxygen dependent (Fig. 2.8, 2.10; scheme 2.2). For the first time, this study provided stopped-flow spectroscopic evidence that SIN-1 is de-protonated in a pH dependent manner during the phase of the reaction leading up to SIN-1A formation (Fig. 2.8A-D). It is possible that the depronation of SIN-1 under physiological pH initiated its decay. In addition, studies on the mechanism of nitric oxide release from SIN-1 showed a positive correlation between O_2 consumption and superoxide formation (Bohn and Schönafinger, 1989). As confirmed by this study (Fig. 2.10), the formation SIN-1C during SIN-1 decay was reported to be oxygen dependent (Feelisch *et al.*, 1989). Under aerobic condition, oxygen initiated SIN-1A decay. This was thought to have occurred via the one electron abstraction from the nitrogen connected to the N-NO group as shown in scheme 2.2 (Feelisch *et al.*, 1989);

oxygen is thereafter reduced to superoxide and the SIN-1A is oxidized to an unstable radical cation that further decomposes to release $NO^{\bullet}$ (Singh *et al.*, 1999). In this study, the timing of the appearance and increases of the absorbance peak at 279±2nm in aerobic condition (Fig. 2.8) confirmed the formation of SIN-1C and provide indirect evidence for the release of $NO^{\bullet}$ (scheme 2.2). It has been proven under this condition that $NO^{\bullet}$ and superoxide combine to form peroxynitrite (Haddad *et al.*, 1994; Feelisch *et al.*, 1989). Previous work has showed that decay of SIN-1 and formation of ONOO- can be sustained at physiological or pH 7.4 under aerobic condition (Martin-Romero *et al.*, 2004). In this study, this was confirmed by experiments showing the decay of SIN-1 under in-vitro pulmonary artery cell culture conditions (Fig. 2.7). The formation of peroxynitrite under this condition may have in the present study occurred over a period in excess of 75min (Fig. 2.7).

2.5.2.1. Quantifying ONOO- from SIN-1: NADH Fluorescence quenching

Although useful in elucidating the decay mechanism for the release of ONOO- from SIN-1, absorbance spectroscopy was unsuitable for the determination of the amount of ONOO- released per unit time or molecule from SIN-1. A key reason being that SIN-1 and ONOO- show considerable overlap in absorbance at both 292 and 302nm (Fig 2.3; 2.6). The use of another method was thus indicated. The work of Martin-Romero et al (2004) showed that the production of peroxynitrite during 3-morpholinosydnonimine (SIN-1) decomposition can be continuously monitored from the loss in fluorescence associated with the ONOO- oxidation of nicotinamide adenine dinucleotide (NADH) to NAD^{+}. This reaction was claimed to be specific for peroxynitrite and provided a cumulative record of peroxynitrite formation. Unlike the Dihydrorhodamine 123 method, this approach was more specific for ONOO- and was not affected by the influence of hydrogen peroxide or other oxidants. The kinetics of NADH fluorescence quenching by SIN-1 was shown to overlap with the kinetics of NADH oxidation to NAD^{+}, monitored by the decay of absorbance at 340 nm (Martin-Romero *et al.*, 2004). Thus this study employed this method to demonstrate the release and to quantify the yield of ONOO- from SIN-1 in pulmonary artery cell culture medium.

.

The decay rate of 20μM (Fig. 2.12), 100μM (not shown) and 1mM SIN-1 (Fig. 2.13) suggests that the process was governed by 1st order kinetics. This implied that the half-life of the anion= 0.693/k, where k is the decay constant of ONOO-. The half-life of ONOO- was determined to be 1.38s in pulmonary artery cell culture medium (Fig. 2.4B); hence $k=0.5s^{-1}$. In addition, the study estimated that under this condition, 20μM SIN-1 generated ONOO- at the rate of 0.11μM min^{-1}. Dividing this production rate by the decay constant amounted to a steady state ONOO- concentration of 0.95nM over 90min period (Fig. 2.15, 2.16). This takes into cognisance that ONOO- is concurrently being generated and destroyed. The sensitivity of the NADH fluorescence quenching method did not allow for reproducible estimation of ONOO- formation by lower SIN-1 concentration. Peroxynitrite formation by 100μM SIN-1 was calculated to be 3.2μM ± 0.2 min^{-1} in DMEM-F12 medium containing phenol red indicator; this medium being similar in composition to that used for the growth of pulmonary cells in this study. This confirmed that the rate ONOO- generation from SIN-1 depended on SIN-1 concentration.

2.5.3 CONCLUSION

This study provides data on the life and activity of SIN-1 and $ONOO^-$ in pulmonary artery cell culture medium to which their biological actions can be related. The formation of ONOO- was demonstrated by the qualitative and quantitative determination of its in-situ generation from the decay of 3-morpholinosydnonimine (SIN-1).

.

CHAPTER 3
DETERMINATION
OF THE THRESHOLD OF
PEROXYNITRITE CYTOTOXICITY

3.1. INTRODUCTION

Studies have shown that ONOO- is extremely cytotoxic at 10μ-50mM (Li *et al.*, 2002; Szabo *et al.*, 2001; Alvaro *et al.*, 1999; Virag *et al.*, 1998b). In addition, the cytotoxic effects of ONOO- appear to be at odds with clinical evidence for the up-regulation of the anion in pathological conditions of oxidative stress such pulmonary hypertension (Rabinovitch, 2008), since ONOO- induced cytotoxicity does not account for the unique vascular changes evident in the patho-biology of the disease. This variance may be explained by the observation that most laboratory studies on the biological actions of ONOO- have often involved the use of concentrations (10μ-50mM) irrelevant to the pathological formation of the anion. If ONOO- were important in the development and or progression of pulmonary hypertension, lower concentration of ONOO- may stimulate pulmonary cell proliferation, similar to the vascular changes seen in pulmonary hypertension. In addition, the stimulatory response of pulmonary artery cells must occur at ONOO- concentrations not more than the lower limits of cytotoxicity. Peroxynitrite (ONOO-) is known to cause DNA fragmentation, activation and inactivation of enzymes and ion channels via protein oxidation and nitration, inhibition of mitochondrial respiration, apoptosis and impaired tissue function (Szabo *et al.*, 2007; Virág *et al.*, 2003; Szabo *et al.*, 2001). However, it is unclear which of these actions is important. This phase of the study therefore aimed to confirm ONOO- induced cytotoxicity and to determine the threshold concentration for such effect in pulmonary artery endothelial (PAEC) and smooth muscle cells (PASMC). In addition, the study sought to elucidate on the signal mechanism involved in the impairment of pulmonary artery cell function by ONOO-.

3.2. OBJECTIVES

(1): To isolate and characterise primary culture of PAEC and PASMC from bovine lung (2): To investigate the effect of a range of peroxynitrite concentrations on PAEC and PASMC viability under normoxic growth (21% oxygen) conditions (3): To investigate the role of caspase-3, PARP and the mitogen/stress activated protein kinase (p38 and JNK, respectively) on ONOO- induced impairment of pulmonary artery cell function.

3.3.0. METHOD

3.3.1. Cell Harvest and culture: PAEC

Bovine pulmonary artery endothelial cells were obtained by a method described by Ryan and Maxwell (1986). Lungs of cows under 24 months of age were obtained from a local abattoir within 1h of slaughter. Lungs were dissected to free main and large lobular (>5-2cm diameter) pulmonary arteries. Extraneous fatty and connective tissues were then gently removed. The arteries were sliced opened in a sterile petri dish, so that they laid flat with initimal surface upwards. Endothelial cells were thereafter harvested by gently scraping and scooping (into culture flasks) the luminal surface of the longitudinally opened pulmonary arteries with a sterile scapel (no. 10 blade, blunt end). This was done using light, single strokes, covering each area only once. Cells were thereafter subcultured in medium comprising a 50:50 mix of Ham F-12 (cat.#: 21765-037, Invitrogen) and Waymouth MB752 media (cat.#: 31220-072, Invitrogen) to which 15% foetal bovine serum (FBS) and 5% penicillin (5000U/ml):streptomycin (5000μg) (PEN-STREP® BioWhittaker™) were added. Endothelial cells were maintained at 37°C in a humidified atmosphere containing 5% CO_2, and used between passages 2 and 6.

3.3.2. Cell Harvest and culture: PASMC

Bovine PASMC were cultured from explants. The intimal cell layer and residual adventitial tissue were stripped off lobular pulmonary arteries (diameter: 5–10 mm) using scapel and forceps respectively. The vessels were cut into small rings (3–5 mm), and transferred into a 25cm^2 cell culture flasks containing culture medium as described above. After 21 days of incubation, artery rings were discarded and the seeded PASMC were transferred into new cell-culture flasks. Cultured PASMC were used between passages 2 and 6.

.

3.3.3. Cell characterisation by immunocytochemistry: PAEC

Endothelial cells were cultured overnight on labelled treated slides, the cells adhered to the slides and were fixed with 4% paraformaldehyde, and this is henceforth referred to as 'cell slide'. Cell slides were stored at 4^0C in 2% azide solution until needed. A peroxidase conjugated streptavidin method was used in this study. Briefly, endothelial nitric oxide antibody was selected and the optimum dilution was tried out in pre-tests. Cell slide processing began with the quenching of endogenous peroxidise using CH_3OH with 0.3% H_2O_2 for 10 min after which cell slides were washed with Phosphate Buffered Saline (PBS: NaCl 8g/L, KCl 0.2g/L, Na_2HPO_4 1.44g/L, and KH_2PO_4 0.24g/L in distilled water, pH 7.4) for 5 min. Antigen retrieval process involved boiling of cell slides dipped into Tris/EDTA Buffer solution (Trisma Base 0.55g/L, EDTA 0.37g/L in distilled water, pH 9.0) for 1 min in a microwave oven. The heating chamber was depressurised, allowed to cool and cell slides were washed with PBS for 5 min. Non-specific binding to primary tissue was blocked by incubating cell slides with 20% normal goat serum in PBS (S-1000; Dako, UK) for 20 min. Primary antibody (Primary antibody against eNOS: rabbit polyclonal, cat.#: 610298, BD transduction laboratories, UK) diluted to 1:200 with Dakocytomation antibody diluent (S0809; Dako, UK) was added and incubated with cells overnight at 4^0C. Thereafter, cells slides were washed with PBS for 5min. A secondary antibody (Secondary antibody: polyclonal goat anti-rabbit Ig: cat.#: E0432, Dako, UK) diluted to 1:200 with Dakocytomation antibody diluent (S0809; Dako, UK) was added for 20 min and cell slides were washed with PBS for 5min. This was followed by the addition of 150ul streptavidin-Horse Radish Peroxidase (HRP: Ready to use product, SA-5704; Dako, UK for 20 minutes and the addition of DAB [containing 11 drops of DAB chromogen (cat.#: K5207; Dako, UK) in 11ml of diluting solution] for 12min. Cell were counterstained in the following protocol: haematoxylin (12 min) → acidic alcohol (1 min) → water rinse (1 min) → STWS (2 min) → water rinse (2 min) → absolute alcohol →absolute alcohol → absolute alcohol (2 min each) → Histoclear → Histoclear → Histoclear → Histoclear (2 min each). Sections were mounted using DPX mounting solution; cell slides were thereafter viewed under bright field objective (Nikon microscope, Japan).

3.3.4. Immunocytochemistry slides analysis: Image intensity semi-quantification

Images were obtained using CoolSnap-Pro RS Photometric (Media Cybernetics®) and CoolSnap-Pro Software. The white balance and colour calibration was corrected in conjunction with intensity of backlight and remained constant for each group of slides with same antibody concentration. Slides were photographed using constant setting for exposure time (20ms) at magnification 40x objective lenses. Images obtained were saved in .tiff format and processed for quantification using Image-Pro Plus version 6.0 (Media Cybernetics®). Colour segmentation was performed using Hue, Saturation and Intensity settings to mask all but the DAB staining on each slide or selected portions. The settings used for eNOS 1 in 200 antibody dilution were as follows: Hue 5 to 50; Saturation 0 to 230; Intensity 11 to 255. These were the settings shown in preliminary experiments to best identify the characteristic eNOS brown staining. The settings were saved as eNOS and reloaded for each analysis. The areas which were not stained were masked by black colouring with intensity value = 0 (Transparent on black option). The eNOS stained and total area were derived in pixels with and without the 'eNOS' macro setting, respectively. The intensity of eNOS and the mean intensity of the selected area were also derived accordingly. The intensity of eNOS expression per pixel was calculated in control and test slides as shown below

$$\textbf{Intensity of eNOS expression (IEE)} = \frac{\textbf{(MI x SA) - SISA}}{\textbf{TA}}$$

Where:
SA = eNOS Stained Area
MI = Mean Intensity of slide without image
SBI = Sum Background Intensity = Mean Intensity x Area Stained
SISA = Sum Intensity of Stained Area
TA = Total Selected Area

.

3.3.5. Cell characterisation by immunofluorescense: PAEC and PASMC

To determine the phenotypic characteristics of cultured PAEC and PASMC from bovine lungs, the cells were assessed for expression of endothelial or smooth muscle-specific proteins, respectively. PAEC and PASMC were assessed for total actin and vimentin for cell structure elucidation; the expression of eNOS or α-smooth muscle actin was used to positively identify PAEC or PASMC, respectively. In some experiments human umbilical cord endothelial cells (HUVEC) were used as positive or negative control for eNOS or α-smooth muscle actin expression, respectively. PAEC or PASMC were allowed to seed on plain cover slips and fixed by aspirating the culture medium and applying 4% paraformaldehyde for 10 min. This was followed by a 10min exposure to cold methanol. The slides were then washed with PBS (x3 washes) and exposed to 0.01% Triton-X for 10min. Non specific binding was blocked using 1% BSA in PBS for 1 h at room temperature and then primary antibody total actin, (Rabbit anti-actin, cat.#: A2066 sigma) or vimentin (mouse monoclonal, cat.#: SC 32322, Santa Cruz laboratory) was added without washing at concentrations of 1:50; 1:100, 1:250, 1:500 and 1: 1000 made in 1% BSA in PBS and the cells were incubated overnight at 4°C. The total actin and vimentin primary antibodies used were raised in rabbit and mouse respectively. In separate experiments cells were stained with purified mouse anti-eNOS/NOS (cat#: 610296; BD Transduction Laboratories™) or mouse monoclonal anti-actin, α-smooth muscle antibody (cat#: A5228; Sigma®). The secondary antibody raised against rabbit and mouse IgG bound to Texas red (Vector labs, cat#: TI-1000) and fluorescein isothiocyanate-FIT-C (Sigma®, cat# F2012) respectively were applied at a dilution of 1:200 in sterile PBS and followed by incubation at room temperature for 1 hour. After washing, cover slips were mounted using Vectashield® mounting medium containing DAPI (Vecta laboratory®, cat#: H1200) and stored in the dark at 4°C until they were viewed and photographed. The DAPI in the mounting medium stained the cells' nucleus blue. Pictures were taken using Nikon Eclipes™ E600 Oil Immersion microscope (magnification 40x) connected to a photometrics (CoolSnap™ Fx) digital camera managed by MetaMorph™ software (Universal Imaging Corporation, West Chester, PA).

.

3.3.6. Pulmonary cell viability assessment: Trypan blue dye exclusion assay

In order to determine the viability of bovine PAEC or PASMC after exposure to authentic or in-situ generated peroxynitrite (ONOO-) from SIN-1 under normal growth condition (15% FBS), the percentage PAEC or PASMC cell becoming non-viable after treatment with 0.02, 0.2. 2 and 20μM peroxynitrite for 24 was estimated. Cells were detached by trypsin, centrifuged and re-suspended in phosphate buffer solution (PBS). The cells were then stained with 0.4% Trypan blue dye (cat.#: T-0776, Sigma) and the number of cells stained blue from the nucleus to cell membrane ("non-viable" cells) was counted and noted against the number of cells unstained ("viable"). Cells were counted with the aid of a haemocytometer mounted on a phase contrast microscope (Nikon, Japan) at x10 magnification. Parallel experiments involved the use of exposure of cells to 0.2, 2, 20 and 200μM SIN-1 for 24. These concentrations of SIN-1 have been reported to cause similar biological effects as 0.02, 0.2, 2 and 20 μM authentic peroxynitrite respectively (Cao *et al.*, 2004; Cao and Li, 2004)

3.3.7. Pulmonary cell viability assessment: Lactate dehydrogenase (LDH) assay

Following treatment with authentic ONOO- or SIN-1, the release of lactate dehydrogenase (LDH) into pulmonary artery cell culture medium was detected by colorimetric enzyme-linked assay. This study employed the cytotoxicity detection kit from Roche® (cat.#: 04-744-926-001), according to manufacturers' instructions.

3.3.8. Assessment of pulmonary artery cell DNA synthesis

3.3.8. DNA synthesis measured by [^{3}H] Thymidine incorporation assay

DNA synthesis was used as a measure of PAEC and PASMC proliferation. Cells were grown to approximately 70% confluency in 24-well plates at 37^0C and were quiesced with 0.1% foetal bovine serum (FBS) for 24h. The quiescent cells were maintained at 0.1, 0.5, 1, 1.5, 2.5 and 15% FBS baseline stimulation for 24h and stimulated with either 2, or 20μM authentic peroxynitrite during the same period. Simultaneous control experiments involving these FBS concentrations without ONOO- were used to determine the effect of FBS alone on PAEC and PASMC proliferation. In separate experiments, the quiescent cells were stimulated with either 2, 20 or 200μM of SIN-1 at

each of the baseline FBS stimulation used namely 0.1, 0.5, 1, 1.5, 2.5 and 15% for 24h. The concentrations of SIN-1 used in the present experiments were based on Cao et al., (2004) from which it may be estimated that the effects of 0.2, 2 and 20μM SIN-1 will be similar to 0.02, 0.2 and 2μM authentic peroxynitrite. The PAEC and PASMC were pulsed with [methyl-^{3}H] thymidine aqueous solution (GE Healthcare® Cat #: TRK 120) at 0.1 μCi/well for 5-6h before the end of the 24h of stimulation to allow estimation of DNA synthesis by the PAEC and PASMC incorporation of ^{3}H-thymidine into newly formed DNA. At 24h the medium was removed and the cells were washed twice with 1ml PBS. This was followed by 4-6 1ml washes with 10% trichloroacetic acid (TCA) at intervals of 15min. The remaining cell contents were dissolved in 250μL 0.1% NaOH/Sodium lauryl sulphate solution. The contents of each well were then transferred to scintillation vials, to which was added 2ml of Emulsifier-safe™ scintillation fluid (PerkinElmer, Boston, USA). Vials were vortexed thoroughly before radioactive counts were measured by scintillation counter (Packard 1500 TRI-CARB®). Counts were converted to DPMs (disintegrations per minute); each experiment had 4 replicates.

3.3.9. Mechanism of peroxynitrite induced cytotoxicity: Western blot technique

3.3.9.1. Preparation of whole cell extracts

Cells were plated onto appropriate tissue culture plastic dishes, made quiescent and stimulated with peroxynitrite for 15min or for the duration relevant to each experiment and then placed on ice to stop the reaction. Other experiments involved stimulation with selective agonists for the required time periods. The culture dishes were then washed twice with ice cold PBS before 100-200μl of 4x SDS-PAGE sample buffer (63mM Tris-HCl pH6.8, 2mM Na4P2O7, 5mM EDTA, 10% (v/v) glycerol, 2% (w/v) SDS, 50mM DTT, 0.007% (w/v) bromophenol blue) was added. The cells were scraped and sheared by repeatedly passing through a 21-gauge needle. Samples were then transferred to eppendorf tubes and boiled for 5 minutes, to denature cellular proteins, before storing at –20°C until required for SDS-polyacrylamide gel electrophoresis.

.

3.3.9.2. SDS-Polyacrylamide Gel Electrophoresis (SDS-PAGE)

Resolving gels were prepared containing an appropriate percentage (7.5%, 10% or 12.5%) acrylamide: N,N'-methylenebis-acrylamide (30:0.8), 0.375M Tris pH 8.8, 0.1% (w/v) SDS and 0.05% (w/v) ammonium persulfate (APS). Polymerisation was initiated by the addition of 0.05% (v/v) N, N, N, N', N'-tetramethylethylenediamine (TEMED). The solution was then mixed thoroughly and poured between 2 assembled glass plates, allowing enough space at the top for stacking gel after which they were overlaid with 150 µl of 0.1% (w/v) SDS. Once polymerised, the 0.1% SDS was poured off and the gel surface rinsed with distilled water to remove excess polyacrylamide, then the stacking gel containing 10% (v/v) acrylamide. N,N'-methylenebisacrylamide (30:0.8), in 125 mM Tris, pH 6.7, 0.1% (w/v), SDS, 0.05% APS and 0.05% (v/v) TEMED was poured on top of the resolving gel, and an appropriate Teflon spacer comb inserted into the stacking gel. Following the complexion of polymerisation, the comb was removed and the polyacrylamide gels were assembled in a Bio-Rad Mini-PROTEAN®-3 electrophoresis tank, with both upper and lower reservoirs filled with electrophoresis buffer (25mM Tris, 192mM glycine, 0.1% (w/v) SDS). Aliquots of samples were then loaded into the wells of the stacking gel using a microsyringe. A prestained SDS-PAGE molecular weight marker of known molecular weights was run concurrently in order to identify the polypeptide of interest. This was usually the broad range prestained protein marker (7-175 KDa; Cat.#: P7708V, New England Biolabs or the high molecular weight (211-49 KDa; Biorad®; Cat.#: 161-0309) prestained protein marker. Samples were electrophoresed at a constant voltage of 200V, for 45min by which time the dye had reached the bottom of the gel.

3.3.9.3. Electrophoretic Transfer of Proteins to Nitrocellulose Membrane

The proteins separated by SDS-PAGE were transferred to nitrocellulose membranes by electrophoretic blotting. The gel was pressed firmly against a nitrocellulose sheet and assembled in a transfer cassette sandwiched between Whatmann 3MM paper and two sponge pads. The cassette was immersed in blotting buffer (25mM Tris, 195mM glycine, 20% (v/v) methanol) in a Bio-Rad Mini Trans-BlotTM tank and a constant voltage of 100v was applied for 1 hour, whilst the tank was cooled by inclusion of an ice reservoir.

3.3.9.4. Immunological Detection of Proteins

Following transfer of the proteins to the nitrocellulose membrane, the membrane was removed and incubated with of 3% (w/v) BSA in Tween tris-base solution (TTBS) (150mM NaCl, 20mM Tris base pH 7.4, 0.02-0.03% (v/v) Tween-20) for 1 hour with gentle agitation on a platform shaker. The blocking buffer was removed and membranes incubated overnight with antiserum specific to the target protein (see Table 3.1) appropriately diluted in TTBS containing 1% (w/v) BSA. Thereafter, membranes were washed 4-5times for 10-15min with TTBS. The membranes were then incubated for a further 1 hour at room temperature with secondary horseradish peroxidase-conjugated IgG directed against the first immunoglobulin diluted in TTBS according to manufacturer's instruction. After 3 10-15min additional washes in TTBS, immunoreactive protein bands were detected by enhanced chemiluminescence (ECL). Membranes were blotted on a paper towel and exposed to ECL reagent for 90 seconds. The membranes were blotted again, mounted in an exposure cassette and covered with cling film. Blots were then exposed to Kodak X-OMAT LS film for periods ranging 5s - 5min under darkroom conditions and developed by a KODAK M35-M X-OMAT processor.

#	Name of antibody	Source	Manufacturer	Dilution	Catalogue number/
1	Phospho JNK	Rabbit polyclonal;	New England Biolabs, UK	1:5000	9251S
2	Total JNK	Rabbit polyclonal	Santa Cruz Biotechnology, Germany	1:5000	Sc-571
3	Phospho p38	Rabbit polyclonal,	Biosource, UK	1:15000	44-684G
4	Total p38	Rabbit polyclonal,	Santa Cruz biotechnology, Germany	1:15000	sc-728
5	CleavedCaspase-3 (Asp 175)	Rabbit monoclonal	Cell Signaling, Boston, USA	1:1000	9664
6	Total Caspase-3	Rabbit polyclonal,	Cell Signaling, Boston, USA	1:1000	9662
7	PARP antibody	Rabbit polyclonal,	Cell Signaling, Boston, USA	1:1000	9542

Table 3.1: Details of antibodies used in elucidating the mechanism of peroxynitrite induced cytotoxicity

3.3.10. Method of adding peroxynitrite

Authentic peroxynitrite (ONOO-) is stable and commercially supplied in strongly alkaline solvents which are potentially toxic to cells; the method of ONOO- application to cells is therefore vital to cell viability and the interpretation of ONOO- effects. Several investigations into the effect of ONOO- on biological cellular response and cell signalling pathways have involved the application of peroxynitrite through direct addition to cell culture medium (Walia *et al.*, 2003; Virag *et al.*, 1998a; Virag *et al.*, 1998b;

Salgo *et al.*, 1995a; Salgo *et al.*, 1995b) direct addition made to one side of culture flasks, or direct addition followed by rapid swirling (Pesse *et al.*, 2005a; Bapat *et al.*, 2001; Zhang *et al.*, 2000). Preliminary studies showed that pre-diluting authentic $ONOO^-$ to desired concentration in cell culture medium prior to exposing cells to the mixture or its direct addition to cell culture medium followed by rapid swirling gave nil solvent effects. These methods were therefore used to administer $ONOO^-$ in this study.

3.3.11. Excluding the solvents effects of ONOO- solution

Several authors investigating the effects of peroxynitrite on different cell types have worked with the molecule supplied in strongly alkaline solution usually about 1M NaOH and most studies have involved concentrations of ONOO- between 15μM and 1mM (Walia *et al.*, 2003; Virag *et al.*, 1998a; Virag *et al.*, 1998b; Salgo *et al.*, 1995a; Salgo *et al.*, 1995b). Since these papers have not stated that the final pH of their solutions were neutralized to pH 7.4, nor included appropriate vehicle/alkaline solution controls, it is likely that the resulting solutions were slightly alkaline, at the least. Some authors used controls treated with phosphate buffer saline and or decomposed peroxynitrite neutralized to pH 7.2-7.4 (Virag et al, 1998a; Virag et al, 1998b; Salgo et al, 1995) which would not give alkaline pH conditions comparable to ONOO- solution. Addition of authentic ONOO- solution even at low concentrations and volumes was in tandem associated with addition of significant amount of 1M NaOH (0.3-6μL) resulting in a transient increase in cell culture medium pH from 7.4±0.04 to 7.93±0.04 (see chapter 2). In this study, the experiments involving authentic peroxynitrite have thus involved controls groups exposed to equal volume of the peroxynitrite vehicle.

3.3.12. Statistics

Paired Student's T- tests were used to compare treatment groups and matched controls in some experiments. Statistical analysis was by the Prism software package (Prism 5; GraphPad Software, San Diego, CA). Differences at $P<0.05$ were considered statistically significant.

.

3.4. RESULTS

3.4.1. Pulmonary artery endothelial Cell: Isolation, Culture and Characterisation

3.4.1.1. Endothelial cell culture yield

Colonies of nascent endothelial cells were visible within 3 days of harvesting and culturing of PAEC from the bovine pulmonary artery (Fig. 3.1). The cells attained monolayer confluency in a conventional 25cm^2 cell culture flask within 12-15 days depending on the number of viable cells collected during harvesting (Fig. 3.1). The endothelial cells maintained characteristic cobblestone morphology (Fig. 3.1) through passages 1-8. This was similar to the morphology of bovine pulmonary artery endothelial cells in published photos (Farber and Barnett, 1991). Thriving bovine pulmonary artery endothelial cells are shown at day 2-13 from harvesting (Fig. 3.1).

3.4.1.2. Characterisation of bovine pulmonary endothelial cells - Immunocytochemistry

It is known that cells obtained from primary sources can undergo loss of differentiated characteristics after repeated passage (Anderson, 1970). This study therefore investigated the possible change in endothelial nitric oxide synthase (eNOS) expression with repeated passages by comparing eNOS expression at passages 2, 4, 6 and 8. Slides of cells at passage 2, 6 and 8 were processed for immunocytochemistry in the same batch of experiment and shown in Fig. 3.2; in addition, the expression of eNOS was quantified (Fig 3.2B). The expression of eNOS declined gradually with increasing passage number; this change was significant at passage 8. (Fig. 3.2A and 3.2B). Using eNOS as a marker, it was concluded from these experiments that bovine pulmonary artery endothelial cells retain their differentiated characteristics up to passage 6, and therefore in all subsequent experiments, cell were not used beyond passage 6.

.

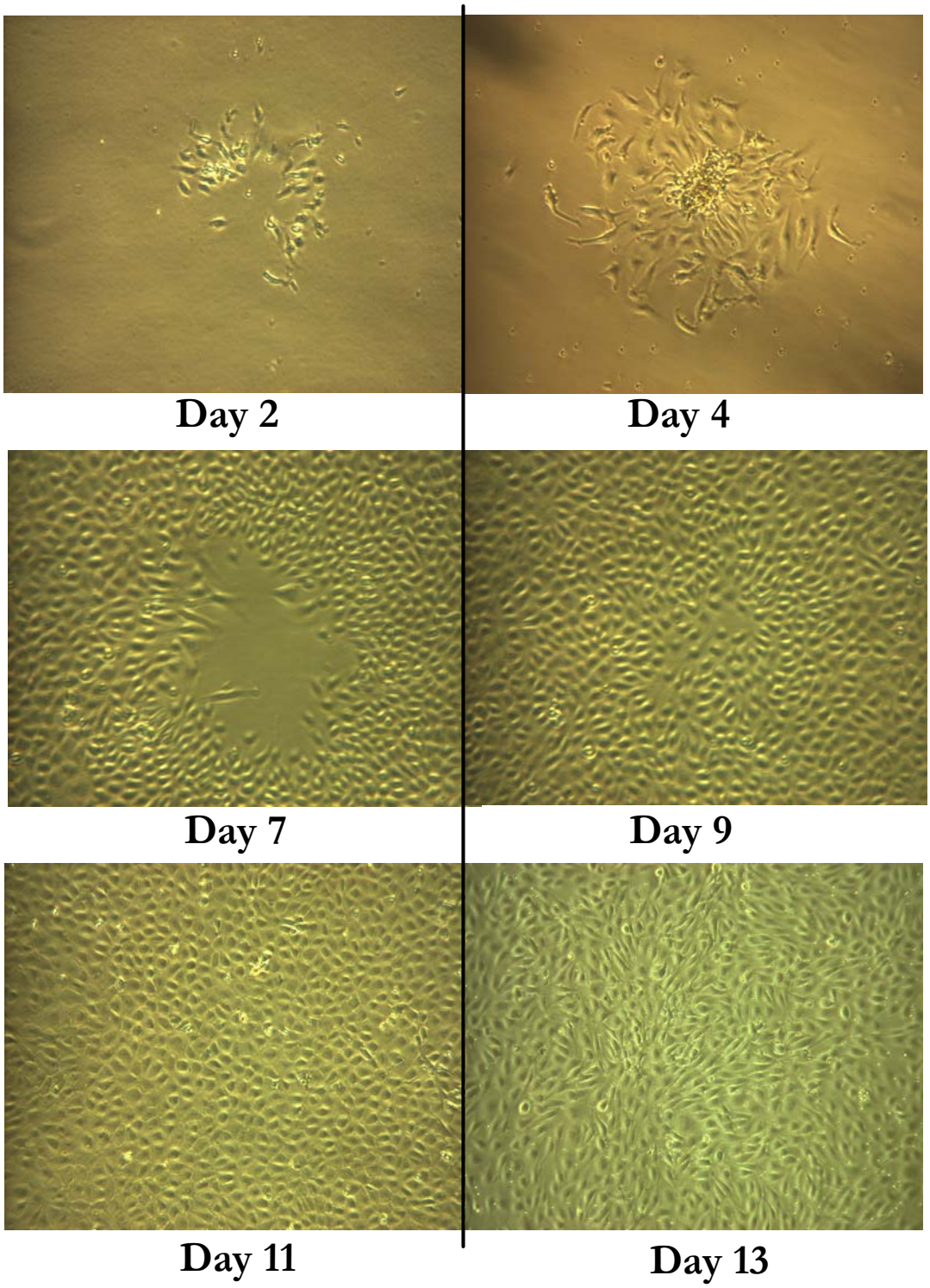

Figure 3.1: Ph**ase contrast microscopic appearance of thriving bovine pulmonary artery endothelial cells in cell culture medium** (x10). Cells were sub-cultured in medium comprising a 50:50 mix of Ham F-12 and Waymouth MB752 media (Invitrogen) to which 15% foetal bovine serum and 5% penicillin (5000U/ml):streptomycin (5000µg) (PEN-STREP® BioWhittaker™) were added. Endothelial cells were maintained at 37°C in a humidified atmosphere containing 5% CO_2.

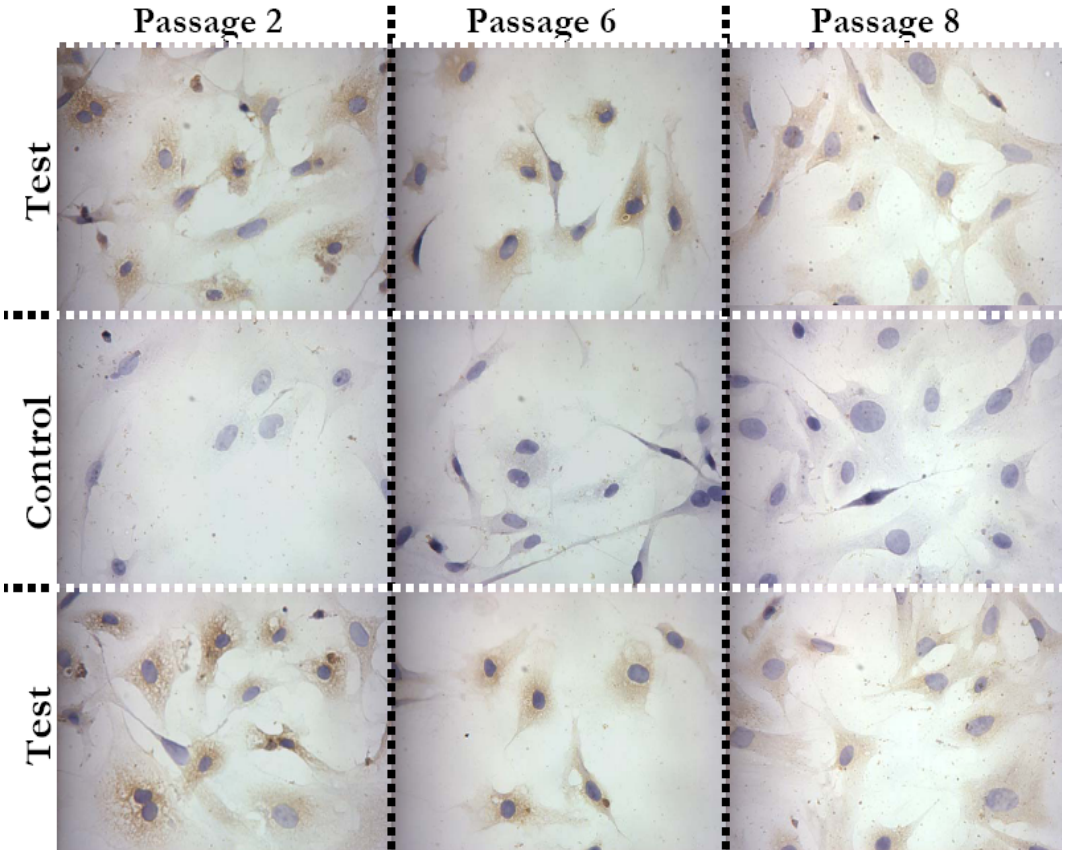

Figure 3.2A: Passage Dependent Decline in eNOS Expression in Bovine Pulmonary Artery Endothelial Cells: Bovine pulmonary endothelial cells were allowed to seed on slides and thereafter stained for endothelial nitric oxide synthase (eNOS) by immunocytochemistry. The intensity of brown staining of the cells indicates the expression of eNOS. The purple stains show the location and shape of the nucleus; these have been counterstained with haematoxylin. Comparisons of stains were done in cells of different passages processed in a single experiment. This was done to eliminate the variation in staining due to minute inter-experiment variations in processing conditions. Figure shows phase contrast microscopic appearance of eNOS stained and unstained cells (Nikon Japan; Magnification, x200).

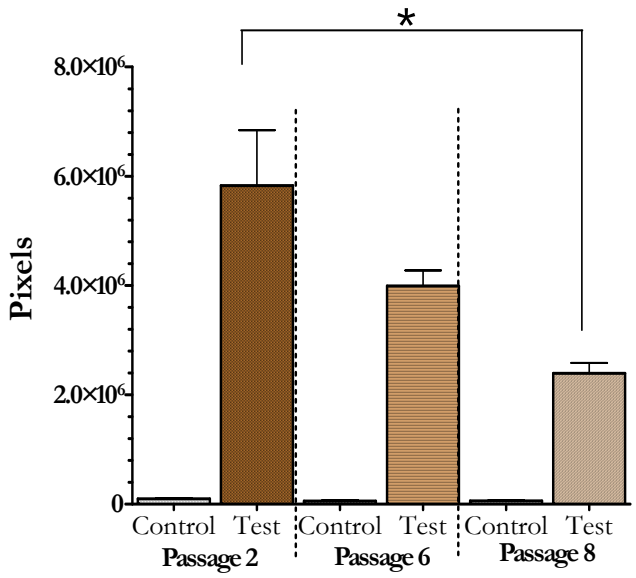

Figure 3.2B: Chart Illustration of Passage (P) Dependent Decline in eNOS Expression in Bovine Pulmonary Artery Endothelial Cell: Images were obtained using CoolSnap-Pro RS Photometric Adapter (Media Cybernetics®) and CoolSnap-Pro Software. The intensity of eNOS expression per pixel was calculated as reported in Image intensity quantification protocol; mean eNOS intensity ±SEM are shown. Statistical evaluations were by 1-way analysis of variance; post hoc investigations were by Bonferroni's Multiple Comparison Test. P2 was not significantly different from P6. *= $p < 0.05$ was considered significant; n=3.

3.4.1.3. Characterisation of bovine pulmonary endothelial cells - Immunofluorecence

Bovine pulmonary artery endothelial cells were stained for total actin and vimentin for structure elucidation. The results showed that PAEC lack staining for α-actin but stained for total actin with intensity (results not shown) similar to control smooth muscle cells. However, the expression of vimetin in endothelial cells was markedly reduced in endothelial cells compared with smooth muscle cells. The expression of total actin in both cell types enhanced the visibility of macro-structure of the cells and showed that the cobble stone morphology of endothelial cells was distinct from the spindle shaped smooth muscle control cells. Dual staining experiments using PAEC showed some co-localisation of vimentin and actin proteins (results not shown); the results demonstrated that vimentin was more prevalent in the central regions of PAEC than in the cell periphery as earlier reported (Pesen and Hoh, 2005).

In other experiments bovine PAEC were characterised for eNOS localisation using immunofluorescence. Endothelial nitric oxide synthase (eNOS) was found to reside in different intracellular localizations such as the plasma membrane, at the golgi complex, in the cytosol and at cell-cell contacts (Fig. 3.3A). This was in good agreement with published reports (Govers, 2002). Figure 3.3B showed the quantification of eNOS in PAEC compared with bovine smooth muscle cell and human umbilical cord endothelial cells used as negative and positive controls, respectively. The result showed the significant abundance of eNOS in PAEC (Fig. 3.3B).

Taken together, the results of PAEC characterisation by immunocytochemistry and immunofluorescence provide a measure of quality assurance for the PAEC used in this study and exclude phenotypic changes that would otherwise confound the interpretations of the results from the use of these cells.

.

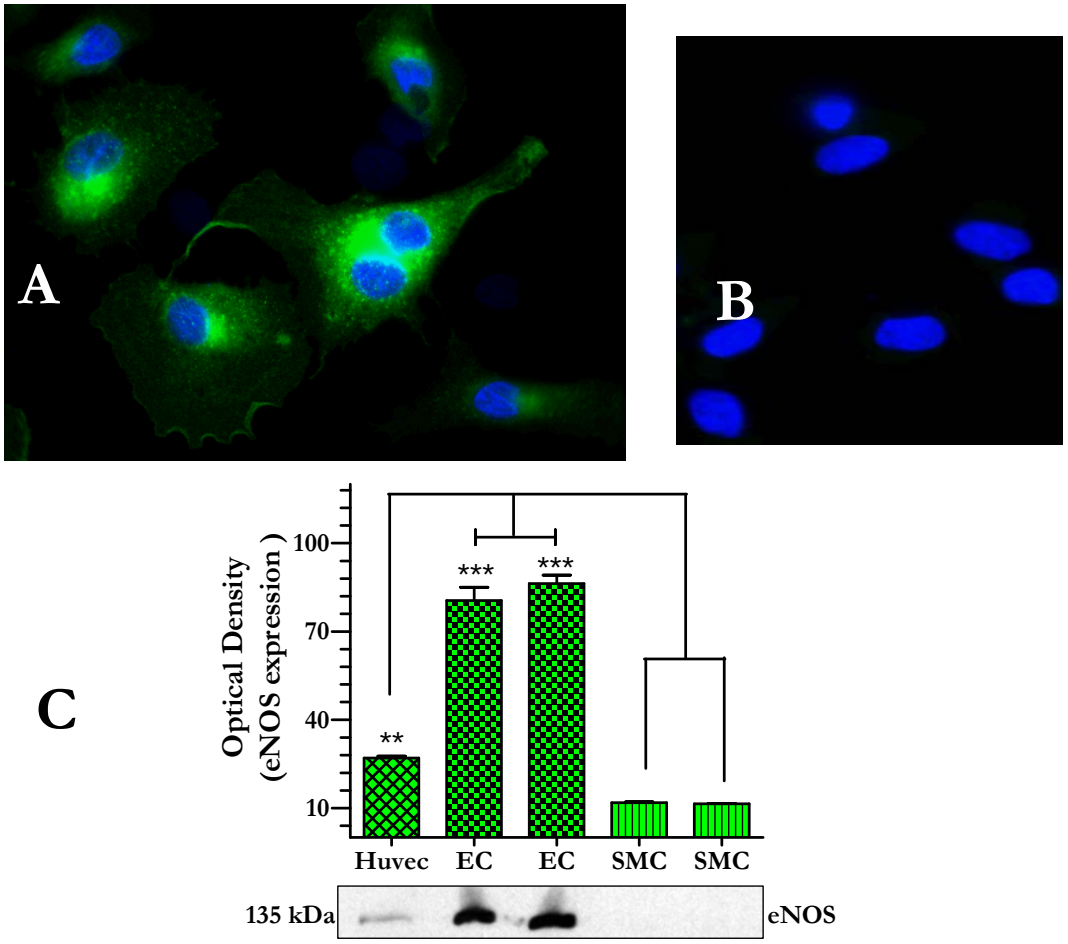

Figure 3.3: Immunofluorecence and Western Blot Probe for Endothelial Nitric Oxide Synthase (Enos) in Bovine Pulmonary Artery Endothelial Cell (BPAEC). (A): The immunofluorescence collage (x400) show BPAEC nucleus stained with Dapi (Blue) while the green pigments indicate the localisation of eNOS. The eNOS antibody was applied at 1:1000 dilution (n=6). (B): Show the nucleus of cells treated without the primary antibody; these did not stain for eNOS. (C): The graph show analysis of western blot results obtained when Huvec (human umbilical vein endothelial cells), EC (BPAEC) and SMC (bovine pulmonary artery smooth muscle cells) were probed for the expression of eNOS using a 7.5% gel. Quantification was by densitometry, statistical analysis was by 1-way ANOVA following by Bonferroni's multiple test. $P < 0.001$ (***) or < 0.01 (**) were considered significant (n=3).

.

3.4.2. Pulmonary artery smooth muscle cell: Isolation, Culture and Characterisation

3.4.2.1. Smooth muscle cell: culture

Bovine pulmonary artery smooth muscle cells (PASMC) thrived under growth conditions described above (3.3.2). Figure 3.4 show photographs of cells at approximately 15, 75 and 100% confluency; PASMC were identified by their characteristic "hill and valley" pattern of organisation (Fig. 3.4; Kocher *et al.*, 1991; Majack, 1987). This morphology was distinct from the characteristic cobble stone morphology of bovine endothelial cells earlier reported (Fig. 3.1).

3.4.2.2. Characterisation of pulmonary artery smooth cells - Immunofluorescence

The study investigated the expression of total actin – a major component of both the cytoskeletal and contractile structures of cells; actins are highly conserved proteins and are ubiquitously expressed in all eukaryotic cells. In this study, bovine pulmonary artery smooth muscle cells stained for total actin with intensity similar to control endothelial cells following the exposure of both cells types to graded concentration of the actin antibody. However, the structure of PASMC was seen to be clearly distinct from PAEC (Fig. 3.5A). When both control and test cell were treated with graded vimentin antibody concentration, the expressions of vimetin were markedly higher in smooth muscle cells compared to endothelial cells treated with same concentrations of the antibody (compare Fig. 3.3A with Fig. 3.5B).

The dual staining (Fig. 3.5B) showed co-localisation of vimentin and total actin proteins and indicated that vimentin were prevalent both in the cytoplasm and nuclear periphery regions of the smooth muscle cells. This location is in keeping with the function of vimentin as intermediate-sized filaments in smooth muscle cell (Gabbiani *et al.*, 1981). Since α-smooth muscle actin is one of few genes whose expression is relatively restricted to vascular smooth muscle cells, further characterisation by probing for α-smooth muscle actin confirmed PASMC. The results showed PASMC stained ubiquitously for α-smooth muscle actin (Fig. 3.5C).

.

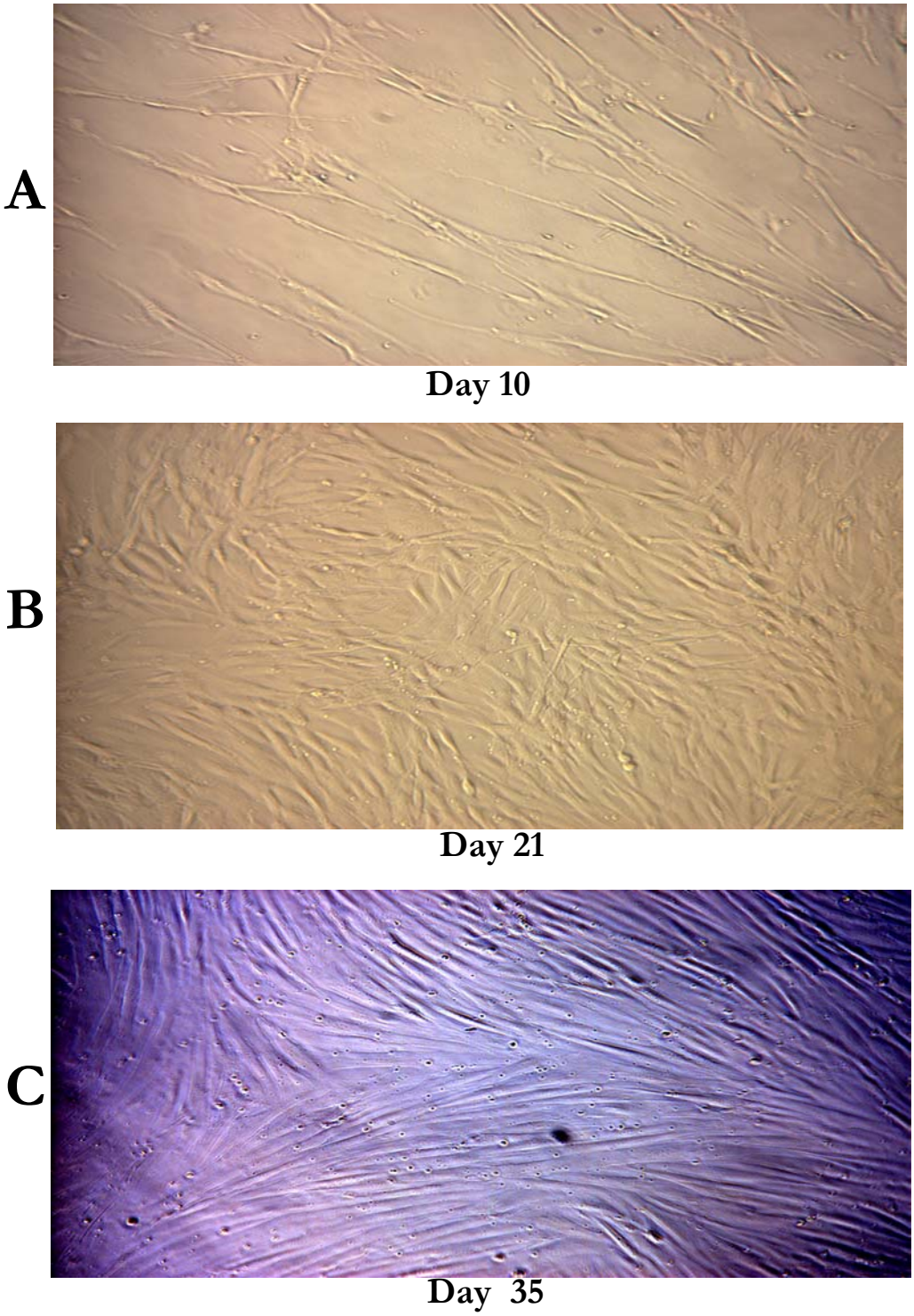

Figure 3.4: Bovine Pulmonary Artery Smooth Muscle Cells As Seen Under Phase Contrast Microscope (x100). A and B: Show cells at estimated 15 and 75% confluency on day 10 and 16 respectively. (C) Shows 100% confluent cell population on day 28. Cells were maintained in culture medium comprising a 50:50 mix of Ham F-12 and Waymouth MB752 media (Invitrogen) to which 15% foetal bovine serum and 5% penicillin (5000U/ml):streptomycin (5000µg) (PEN-STREP® BioWhittaker™) were added. Smooth muscle cells were maintained at 37°C in a humidified atmosphere containing 5% CO_2.

.

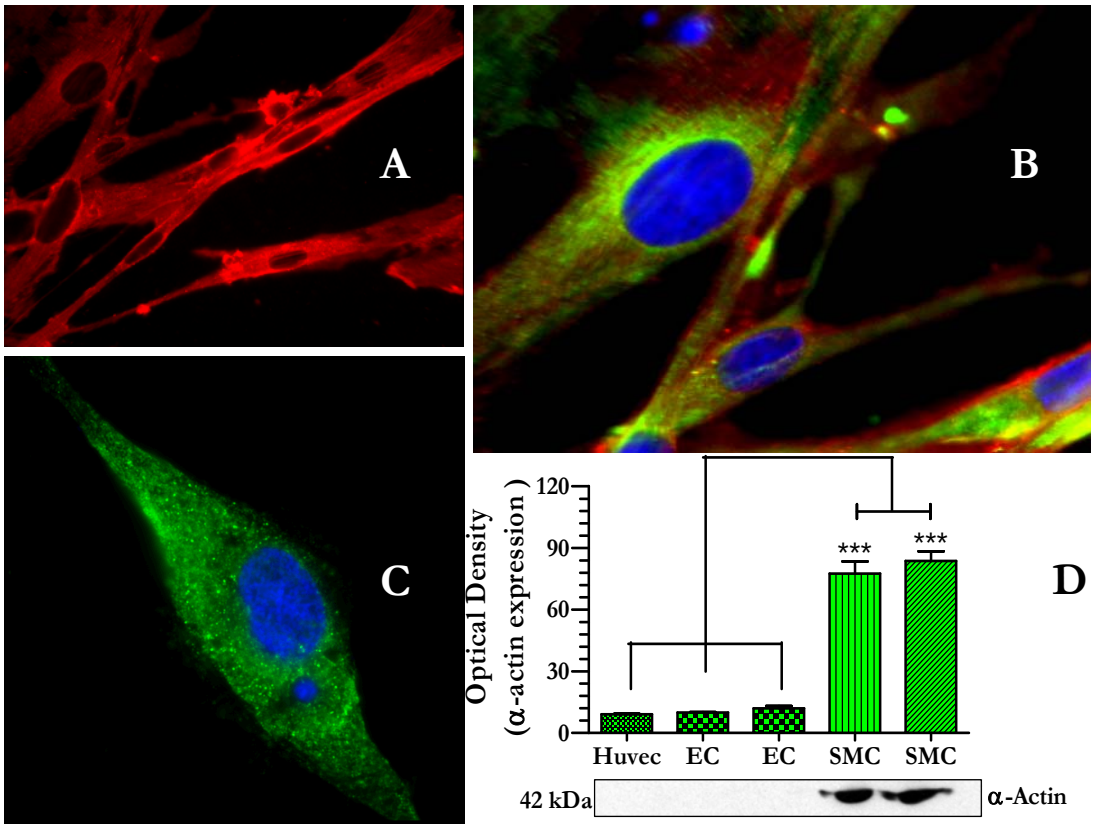

Figure 3.5: Immunofluorecence and western blot probe for alpha smooth muscle actin (α-actin) in bovine pulmonary artery smooth muscle cells (PASMC). The immunofluorescence collage (x400) Picture A showed PASMC stained for total actin. In Picture B, PASMC nucleus stained with blue with Dapi while the green and red pigments indicate the localisation of intermediate filament protein vimentin and total actin, respectively. In Picture C, α-smooth muscle actin (Green) localisation was shown. The α-actin antibody was applied at 1:1000 dilution (n=4). Total actin and vimentin were applied at 1/100 and 1/250, respectively; n=6. (D) Show the graph of western blot results obtained when Huvec (human umbilical vein endothelial cells), EC (PAEC) and SMC (PASMC) were probed for the expression of α-smooth muscle actin. Quantification was by densitometry, statistical analysis was by 1-way ANOVA following by Bonferroni's multiple test. P< 0.001 (***) was considered very significant (n=3).

.

3.4.3. Cytotoxicity of authentic peroxynitrite

3.4.3.1. Effect of authentic ONOO- on PAEC and PASMC viability

The cytotoxic effect of authentic peroxynitrite (ONOO-) on pulmonary artery endothelial (PAEC) and smooth muscle cells (PASMC) was investigated using the trypan blue dye exclusion methods. In these experiments, cells with ruptured or impaired membrane were visibly stained blue (Fig. 3.6) while cells with intact membrane excluded the dye and were judged as 'viable' (Fig. 3.6). Control cells showed 15% mean loss in viability (Fig. 3.7). The cells were detached by trypsinizing and spunned in a centrifuge; it is possible that either or both of these steps contributed to loss in cell viability. Twenty-four hour exposure to peroxynitrite at 0.02 or 0.2μM or to peroxynitrite solvent (NaOH) did not significantly affect endothelial cell viability in comparison with untreated cells over the same period (Fig 3.7A; $p>0.05$). Relative to control groups however, 25.1% endothelial cells became non-viable after 24h exposure to 2μM ONOO-; this was statistically significant (Fig 3.7A; $p<0.01$). Total cell number indicated that the numbers of PAEC in 2μM ONOO- treated group were similar to untreated and vehicle treated controls (Fig. 3.7A) The results were similar when PASMC were treated with authentic peroxynitrite; in these experiments, 20μM ONOO- caused further cell membrane damage (Fig. 3.8). When observed at 48h, PAEC and PASMC damaged by treatment with ≥2μM ONOO- detached from the culture flask base and floated. In this study, these results were the first indication of ONOO- induced cytotoxicity; in addition, the results showed that 2μM was the threshold concentration for ONOO- induced cytotoxicity. Interestingly, treatment of PAEC with lower concentration ONOO- caused increase in cell number; this was significant at 0.2μM (Fig 3.7B; $P<0.01$) and further investigated (see Chapter 4).

3.4.3.2. Effect of authentic ONOO- on pulmonary cell function: DNA synthesis assay

The impact of ONOO- at threshold and higher concentration on pulmonary artery cell function was investigated by the evaluation of the proliferative potential of cells following treatment with these ONOO- concentrations. The results indicated an impairment of DNA synthesis in ONOO- treated cells; 2 and 20μM authentic ONOO- caused significant 23 and 98% reduction in normal DNA sysnthesis in PASMC (Fig. 3.9; $p<0.01$). This effect was similar in PAEC.

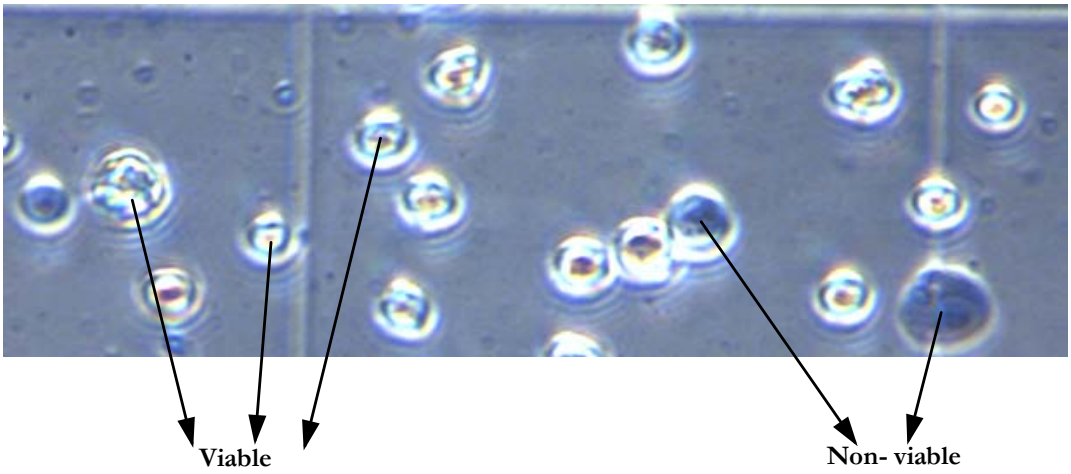

Figure 3.6: Microscopic View on Haemocytometer Slide of the Cytotoxic Effect of 2μM peroxynitrite on Bovine Endothelial Cell. Trypan blue exclusion assay was conducted 24h after one time addition of peroxynitrite. Endothelial cells were maintained under maximal growth conditions (15% foetal bovine serum). Pictures were taken by Phase contrast microscope (x100)

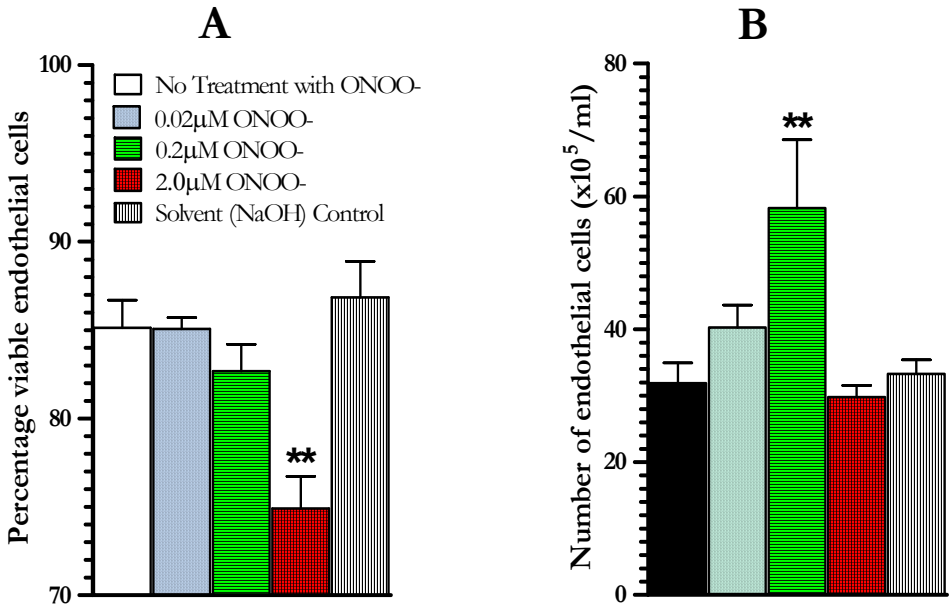

Figure 3.7: Cytotoxic Effect of Peroxynitrite on Bovine Pulmonary Artery Endothelial Cells. Trypan blue assay was conducted 24h after peroxynitrite treatment. Statistical evaluations were by 1-way analysis of variance and post hoc investigations were by Dunnett's test that compares treatment with control values. ** = $p < 0.01$ was considered significant relative to untreated cells; endothelial cells were maintained at 15% foetal bovine serum; n=8-10).

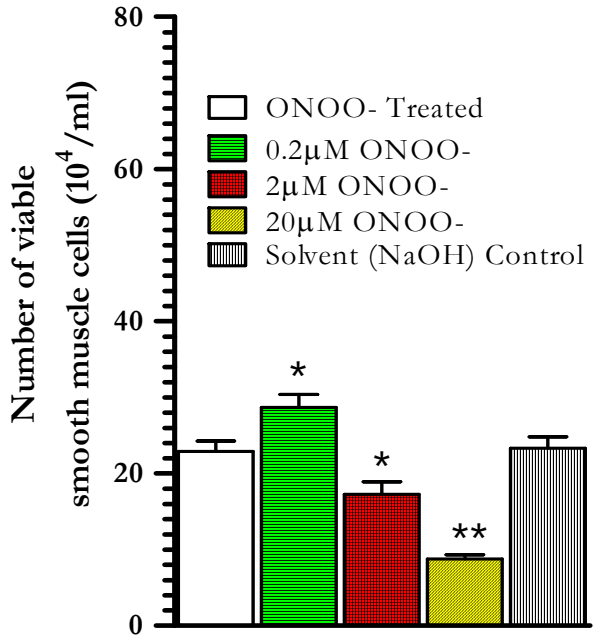

Figure 3.8: Cytotoxic Effect of Peroxynitrite on Bovine Pulmonary Artery Smooth Muscle Cells. Trypan blue assay was conducted 24h after peroxynitrite treatment. Statistical evaluations were by 1-way analysis of variance and post hoc investigations were by Dunnett's test that compares treatment with control values. ** = p< 0.01 or * p<0.05 were considered significant relative to untreated cells. Cells were maintained under maximal growth conditions (15% foetal bovine serum); n=6-7).

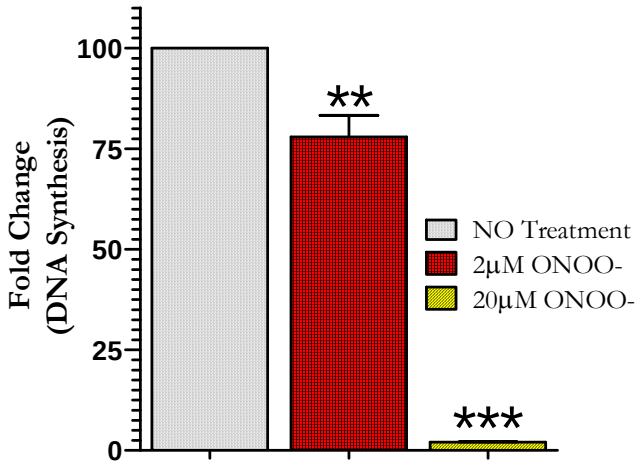

Figure 3.9: Effects of 2 and 20μM authentic ONOO on pulmonary artery smooth muscle cell proliferation: Cells were at basal stimulus from 2.5% foetal bovine serum. Proliferation was determined by ^{3}H-thymidine incorporation assay: Counts were measured in DPM (disintegrations per minute ± SEM) and normalised to relevant controls. Statistical evaluations were by 1-way analysis of variance and post hoc investigations were by Dunnett's test that compares treatment with control values. * p<0.05 were considered significant relative to untreated cells. Experiments were conducted in quadruplicates, n= 3-6.

3.4.4. Cytotoxicity of peroxynitrite generated from SIN-1 decomposition

3.4.4.1. Effect of SIN-1 on cell viability

The peroxynitrite generator caused significant membrane impairment after 24h exposure period (Fig. 3.10; $p<0.01$). At 0.2-20μM SIN-1, cytotoxicity remained largely unchanged (Fig. 3.10A) and it is uncertain whether the exact amount of ONOO- generated from these range of SIN-1 concentration increased accordingly. In cells treated with 0.2, 2, or 20μM SIN-1, percent viable PAEC reduced by approximately 18% relative to controls (Fig. 3.10A). Observably in PAEC, SIN-1 was cytotoxic at the lowest concentration investigated (0.2μM).

Interestingly, yet consistent with results obtained from the exposure of PAEC to 0.2μM authentic ONOO- (Fig. 3.7B), 2μM SIN-1 significantly stimulated the proliferation of PAEC (Fig. 3.10B). This was further investigated (see chapter 4). The proliferative response of PAEC to 2μM SIN-1 was similar in PASMC (Fig. 3.11B); although there was marked differences in susceptibility of PAEC (Fig. 3.10) compared to PASMC (Fig. 3.11). The decrease in PASMC number following treatment with 200μM SIN-1 (Fig. 3.11B) was due to cell loss. In this study, it was observed that severely damaged PASMC detached from the culture flask, floated within 24h and were aspirated before the evaluation of adhering cells for viability.

.

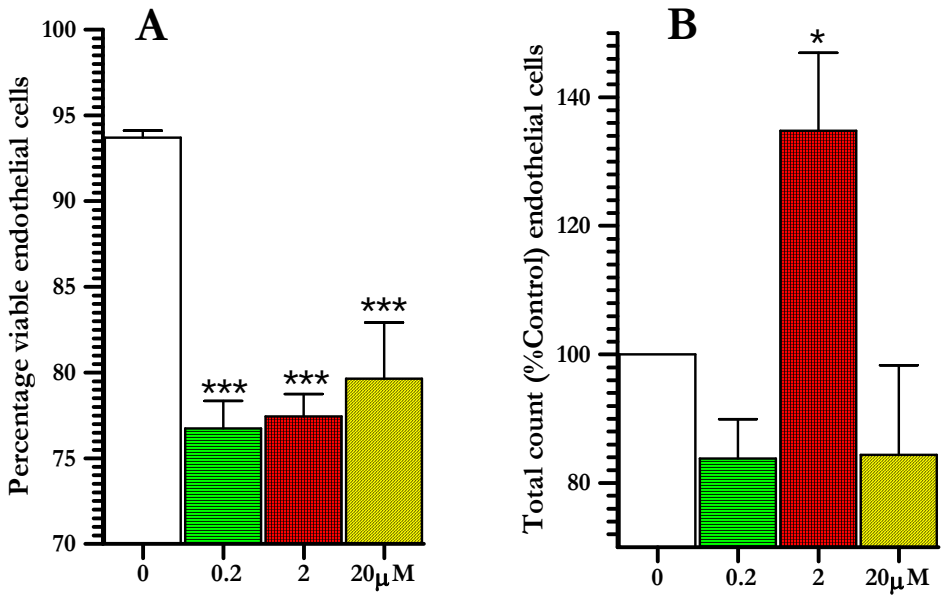

Figure 3.10: Cytotoxic Effect of 0.2, 2 and 20μM 3-Morpholinosydnonimine (SIN-1: Peroxynitrite (ONOO*) Generator) on Endothelial Cell. Trypan blue assay was conducted 24h after peroxynitrite treatment. Statistical evaluations were by 1-way analysis of variance and post hoc investigations were by Dunnett's test that compares treatment with control values. $p<0.05$ was considered significant relative to untreated cells. Cells were maintained under maximal growth conditions (15% foetal bovine serum); n=7

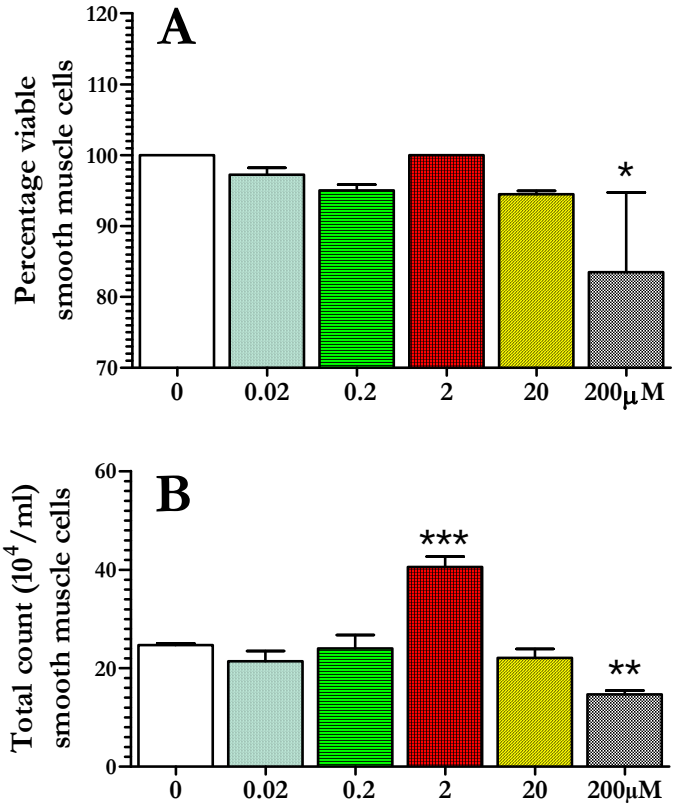

Figure 3.11: Cytotoxic effect of 0.2, 2, 20 and 200μM 3-Morpholinosydnonimine (SIN-1: peroxynitrite (ONOO*) Generator) on pulmonary artery smooth muscle cells. Assay was by Trypan blue dye exclusion method. Statistical evaluations were by 1-way analysis of variance and post hoc investigations were by Dunnett's test that compares treatment groups with control. Values are mean ± SEM; * = $p< 0.05$ was considered significant; n=5.

.

3.4.4.2. Effect of SIN-1 on pulmonary cell function: assessment of DNA synthesis

SIN-1 20μM significantly impaired DNA synthesis in PAEC (Fig. 3.12) and a higher concentration (200μM) caused similar effects in PASMC (Fig. 3.13). In PAEC this effect was evident at basal conditions of 1.5, 2.5 and 15% but not lower serum levels of 0.1, 0.5 or 1% (Fig. 3.12). PAEC appeared to be more sensitive to the toxic effects of SIN-1 than PASMC (compare Fig. 3.10 with 3.11) and inhibition of cell proliferation may be considered as a consequence of cell toxicity. Parallel experiments in PAEC and PASMC showed that impairment of DNA synthesis by 2μM authentic ONOO- was unaffected by serum concentration of the culture medium (see chapter 4). This suggests while ONOO- cytotoxicity in non serum-dependent, SIN-1 induced cytotoxicity may be dependent on serum concentration. Further work will be required to establish this possibility.

.

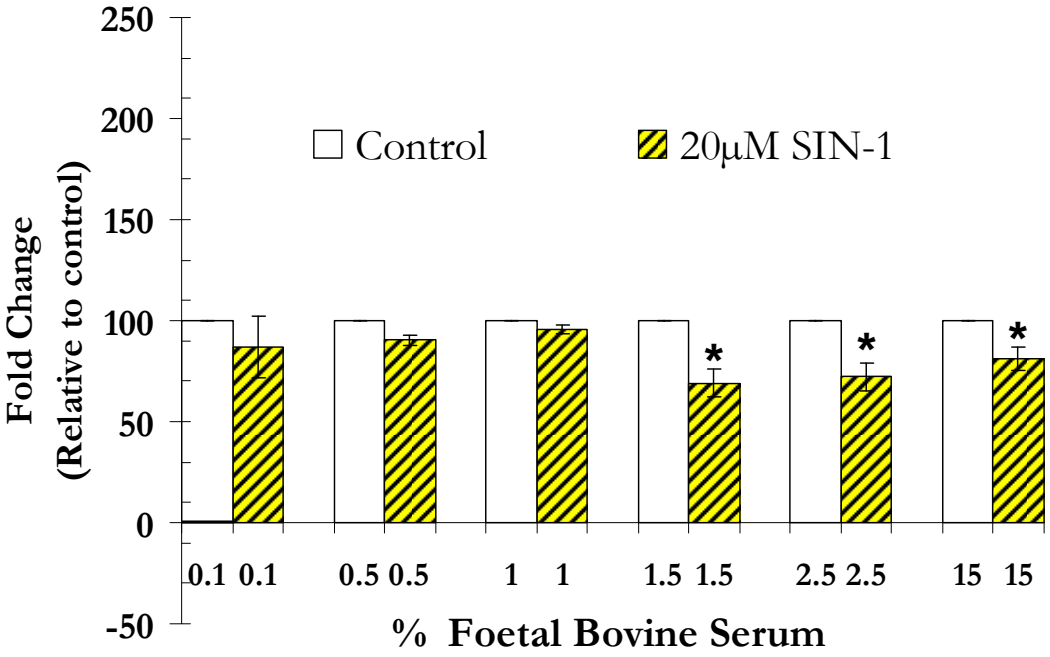

Figure 3.12: The Effect 20μM 3-Morpholinosydnonimine (SIN-1: Peroxynitrite (ONOO-) Generator) on Endothelial Cell Proliferation. DNA synthesis was evaluated by ^{3}H-thymidine incorporation assay. Counts were recorded in DPM (disintegrations per minute) and normalised to relevant controls (± SEM). Pair-wise comparison by paired t-test was used to analyse the statistical significance of the fold changes in DNA synthesis in cell treated with SIN-1 relative to their controls. Experiments were done in quadruplicate, n=5

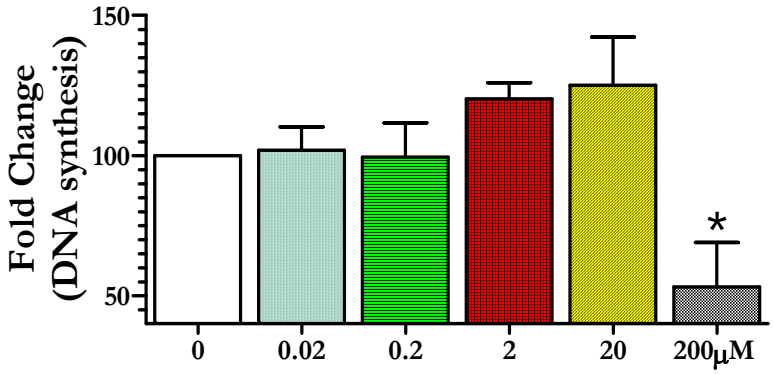

Figure 3.13: The Effect 3-Morpholinosydnonimine (SIN-1: Peroxynitrite (ONOO-) Generator) on Smooth Muscle Cell Proliferation. DNA synthesis was evaluated by ^{3}H-thymidine incorporation assay. Counts were recorded in DPM (disintegrations per minute) and normalised to 'no treatment'. Statistical evaluations were by 1-way analysis of variance and post hoc investigations were by Dunnett's test that compares treatment groups with control. Cell were maintained under 2.5% serum; Values are mean ± SEM; * = $p < 0.05$ was considered significant. Experiments were done in quadruplicates, n=5

.

3.4.5. Peroxynitrite induced cytotoxicity: the role of p38 MAPK and JNK

Using pulmonary artery cell, the study investigated the role of mitogen activated protein kinase p38 MAPK and stress activated protein kinase (JNK) in the mechanisms of ONOO- induced cell function impairment or death. The results showed that exposure to 2μM ONOO- did not activate p38 MAPK activation (Fig. 3.14A) In addition, in PASMC, 2μM or lower ONOO- concentration did not activate p38 MAPK; however, 20μM ONOO- significantly activated p38 MAPK similar to 10μM anisomycin a well known p38 MAPK stimulant (Fig. 3.14A). Similarly exposure of bovine PAEC to serum, 2nM, 0.02μM or 0.2μM ONOO- for 15min did not stimulate the phosphorylation of p38 MAPK (Fig. 3.15). Also, 0.2μM ONOO- did not stimulate p38 MAPK in PAEC following exposure for up to 3h (not shown). However, 15min treatment of PAEC with 20μM ONOO- caused a 3-fold increase in p38 MAPK activation relative to untreated cells (Fig. 3.15). Preliminary experiments showed that 15min exposure to up to 20μM ONOO- did not activate JNK in PAEC or PASMC (Fig 3.16).

.

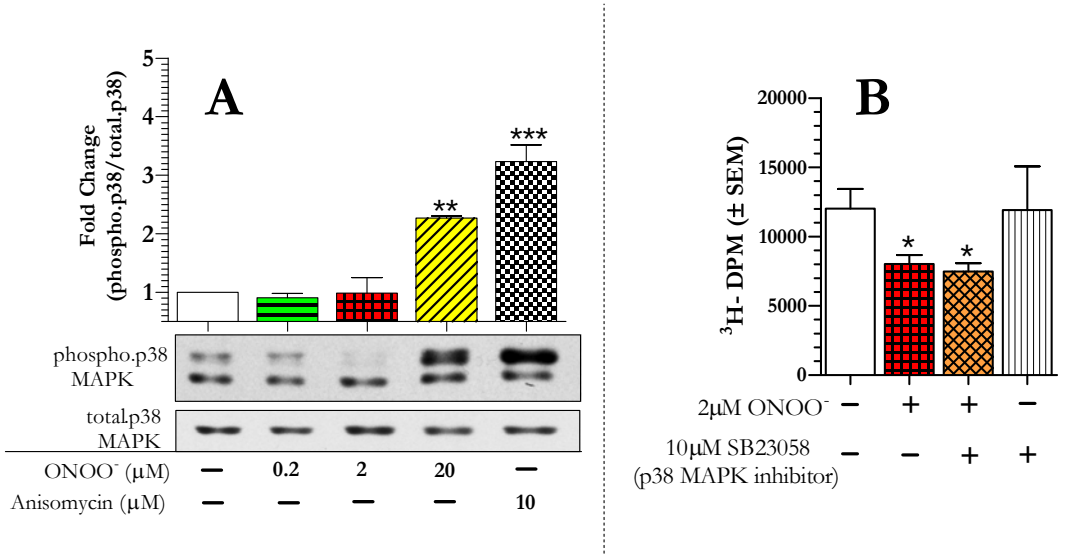

Figure 3.14: The Effect of Peroxynitrite on p38 MAPK Phosphorylation and DNA Synthesis in Pulmonary Artery Smooth Muscle Cells. Figure A: PASMC treated with bolus addition of ONOO- were processed for western blot analysis after 15min; quantification was by densitometry. (n=3). Figure B: Cells were evaluated for DNA synthesis 24h after treatment. Counts were measured and expressed in DPM (disintegrations per minute) ± SEM. Statistical evaluations were by 1-way analysis of variance and post hoc investigations were by Dunnett's test that compares treatment groups with control. Cell were maintained under 2.5% serum; Values are mean ± SEM; * = p< 0.05 was considered significant. Experiments were done in quadruplicates, n=5

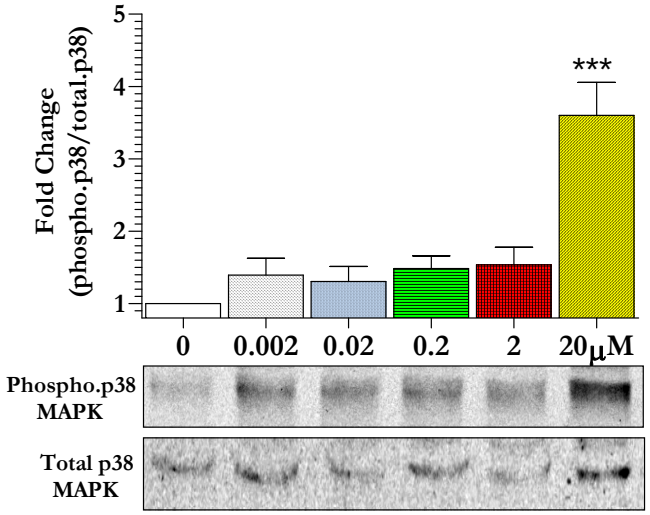

Figure 3.15: The Effect of Peroxynitrite Concentration on p38 MAPK Phosphorylation in Bovine Pulmonary Artery Endothelial Cells. Cells were at 0.1% bovine foetal serum condition. Expression of total and phosphorylated p38 of mitogen activated protein kinase family was determined by western blotting; quantification was by densitometry. Statistical analysis was by 1-way ANOVA, post hoc test by Dunnett's test that compares treatment groups with relevant control p<0.01 (**) were considered significant. n=3-4

.

3.4.6. Activation of Caspase-3 and LDH activity

This study demonstrated that 2μM ONOO- caused significant release of cytosolic LDH in PASMC; this increased with 20μM treatment to levels comparable to the cytotoxic effect of the apoptotic agent staurosporine (Fig. 3.17). Lower concentration ONOO- did not cause LDH release (Fig. 3.17). These results correlated with the cleavage of pro-apoptotic caspase-3 following 15min treatment of PASMC with 0.002nM-20μM ONOO- or 100nM stautosporine (Fig. 3.17). Works involving PAEC showed similar results (results not shown). Experiments investigating nuclear activation of poly ADP ribose polymerase (PARP) showed that PARP was significantly activated following 15min 20μM ONOO- treatment of PAEC (Fig. 3.18). Taken together, these results showed that 2 or 20μM ONOO- induced PASMC and PAEC death may involve necrotic and apoptotic mechanisms.

.

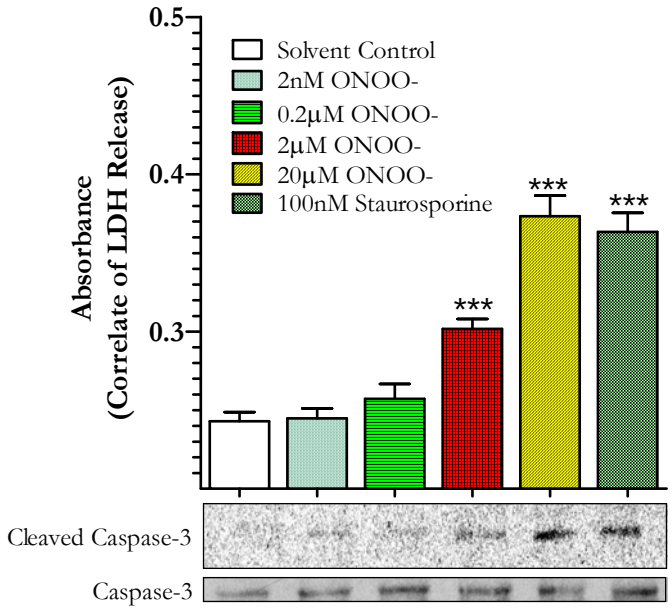

Figure 3.17: Peroxynitrite concentration dependent release of cytosolic lactate dehydro-genase correlates with caspase 3- cleavage in pulmonary artery smooth muscle cells. Release of cytosolic lactate dehydrogenase was evaluated by Roche® kit (n=4). Statistical analysis was by 1-way ANOVA, post hoc test by Dunnett's test that compares treatment groups with relevant control $p<0.001$ (***) were considered significant. For the assessment of caspase-3 activation (n=3), cell were treated with bolus ONOO- for 15min and prepared for western blot analysis. Results were quantified by densitometry

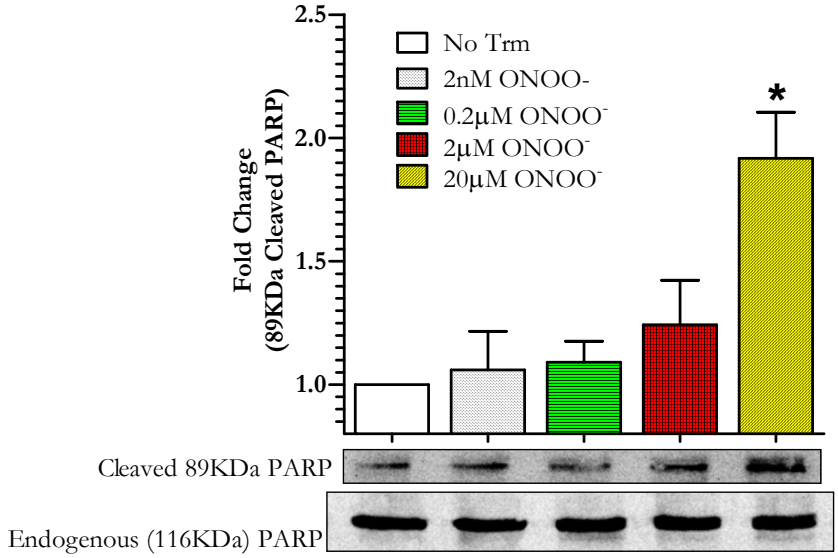

Figure 3.18: Peroxynitrite concentration dependent Activation of Poly ADP Ribose Polymerase **in Pulmonary Artery Endothelial Cells.** PASMC treated with bolus addition of ONOO- were processed for western blot analysis after 15min; quantification was by densitometry (n=2). Statistical analysis was by 1-way ANOVA, post hoc test by Dunnett's test that compares treatment groups with relevant control $p<0.05$ (*) was considered significant.

.

3.5. DISCUSSION

3.5.1. The primary isolates of the pulmonary artery

Experiments aimed at characterising the primary isolates of bovine pulmonary arteries confirmed that PAEC and PASMC were isolated. PAEC confirmation was based on the expression and localisation of eNOS (Fig. 3.2A, 3.3B), the characteristic cobble stone morphology (Fig. 3.1), low intensity of vimentin protein expression as well as the distribution of the intermediate filament protein (results not shown). In support of the immunofluorecence data (Fig. 3.3A), a recent study into the architecture of bovine pulmonary endothelial cells showed that actin was the most significant component of endothelial cells whereas vimentin was less prevalent (Pesen and Hoh, 2005). The scraping method described by Ryan and Maxwell 1986 was therefore suitable for the isolation of bovine PAEC. In contrast to PAEC, the abundance of vimentin served to identify cell isolated by explant method (Gabbiani *et al.*, 1981). As observed in this study, other authors have reported that smooth muscle cells tend to develop high concentrations of vimentin during proliferation (Tom-Moy *et al.*, 1985; Lazarides, 1982). The characteristic hill and valley formation (Fig. 3.4) as well as the ubiquitous presence of the specific α-smooth muscle actin (Fig. 3.5C) served to positively identify the cells as PASMC.

3.5.2. Cytotoxic effects of authentic peroxynitrite: PAEC and PASMC

It is well established that 5-50μM peroxynitrite is cytotoxic by multiple mechanisms (reviewed in Szabo *et al.*, 2007; Szabó, 2003). This study has utilized a range of ONOO- concentration and has confirmed these cytotoxic effects in pulmonary artery cells. In addition, for the first time, this study reports a threshold concentration of 2μM. Cytotoxicity at this concentration was mild affecting less than 20% of cells (Fig. 3.7, 3.8).

Several studies implicate mitogen activated protein kinase p38 and stress activated protein kinase (JNK) in the impairment of cell function or mechanisms of cell death (Ali *et al.*, 2008; Pesse *et al.*, 2005a; Nabeyrat *et al.*, 2003; Oh-Hashi *et al.*, 1999). The results of this study showed that PASMC membrane damage (Fig. 3.8) or the decrease in PASMC DNA synthesis (Fig. 3.9) associated with 24h exposure to 2μM ONOO- were not

mediated by early onset p38 MAPK activation (Fig. 3.14A) nor attenuated by 24h p38 MAPK inhibition (Fig. 3.14B). Similarly the study results showed that the significant damage in PAEC membrane (Fig. 3.7A) following 24h exposure to 2μM ONOO- may not involve the activation of p38 MAPK. The study however demonstrated caspase-3 activation in PAEC and PASMC (Fig. 3.17) in addition to the release of cytosolic LDH following treatment with 2μM ONOO-. The executional phase of apoptosis has been shown to be via caspases likely activated by mitochondria-derived apoptogenic factors in peroxynitrite treated cells (Green and Kroemer, 1998). Although the exact mechanism of peroxynitrite-induced apoptosis is unclear, independent studies have also reported caspase-3 cleavage during the course of peroxynitrite induced apoptosis (Zhuang and Simon, 2000; Lin *et al.*, 1998; Virag *et al.*, 1998b). The Leakage of LDH from pulmonary cells into the surrounding milieu (Fig. 3.17) is evidence of cell death via necrosis. At 20μM ONOO-, this was associated with the activation of p38 MAPK in PAEC and PASMC (Fig. 3.14A, 3.15). In addition, this study provides initial evidence for the activation of PARP in PAEC following exposure to 20μM ONOO- (Fig. 3.18). This likely is the result of DNA single strand breakage as seen in other cell types (Virag and Szabo, 2002). Studies have shown that upon DNA cleavage by enzymes involved in cell death (such as caspases), PARP can deplete the ATP of a cell in an attempt to repair the damaged DNA. ATP depletion in a cell leads to lysis and cell death (Virág *et al.*, 2003; Virag *et al.*, 1998b). This will at best simulate lung injury due to necrosis since apoptotic cells are rapidly cleared from the tissues by macrophages. Taken together, the results provide evidence for apoptotic and necrotic mechanisms of pulmonary cell death in ≥ 2μM ONOO-treated cells.

In both PAEC and PASMC it not clear whether stress activated protein kinase JNK mediated ONOO- cytotoxicity at 20μM concentration (Fig. 3.16). Using 50-500μM ONOO- however, Pesse and co-workers (2005) demonstrated concentration dependent JNK activation in primary ventricular cardiomyocytes. It is thus possible that cytotoxicity in PAEC and PASMC is not JNK linked at the concentrations investigated.

.

3.5.3. Cytotoxic effects of SIN-1: PAEC and PASMC

With SIN-1, cytotoxicity was seen at a lower threshold concentration compared to authentic ONOO-. The extent of cytotoxicity remained unchanged even when SIN-1 concentration increased 10 or a 100-fold (Fig. 3.10A). It is expected that SIN-1 generated ONOO- over a longer duration of time (see chapter 2), this may account for the cytotoxicity of 0.2μM SIN-1 (Fig. 3.10A). However, the reason cytotoxicity remained similar in 0.2, 2 and 20μM SIN-1 treated cells is not clear. It is however possible that cytotoxicity in these groups was mediated by another factor. A recent study showed that SIN-1 or SIN-1 derived reactive species can react with components of serum in cell culture medium to cause the formation of unstable yet potent cytotoxic substances (Konishi *et al.*, 2009). At higher ONOO- concentrations (0.2-3mM), the potencies of ONOO- cytotoxicities were found to be concentration dependent but to be also considerably less when compared to SIN-1 of similar concentration range (Konishi *et al.*, 2009). The presence of other cytotoxic agents in SIN-1/serum experiments is supported by the observation that while cell death was approximately 50% in cell exposed to 2.5mM SIN-1 for 24h in serum containing medium (Li *et al.*, 2006), similar cytotoxic effects were however seen only with 5-fold SIN-1 concentration in serum free medium (Konishi *et al.*, 2009). In this study, decrease in cell viability (Fig. 3.11; 15% FBS) and impairment of DNA synthesis by SIN-1 were significant only under medium condition of higher serum content (≥1.5% serum; Fig. 3.12). Thus the cytotoxic effects of 0.2, 2, or 20μM SIN-1 may be associated with a threshold serum concentration. Further work will be necessary to separate the cytotoxicies of SIN-1 generated ONOO- from that of the products of SIN-1 in serum containing culture medium.

3.5.4. Conclusion

The toxicity of SIN-1 was greater than that of ONOO- probably because of its longer duration of action. Although of fleeting existence, the study reports potent cytotoxic effects of authentic ONOO-. The study determined the threshold for the cytotoxic effects of ONOO- to be 2μM; at which apoptotic cell death may be caspase-3 dependent but independent of p38 or JNK activation. Cell death at >2μM ONOO- may involve activation of caspase-3 in both apoptotic and necrotic pathways. The data show initial evidence for pulmonary cell proliferation

CHAPTER 4

THE EFFECT OF SUB MICRO-MOLAR PEROXYNITRITE ON THE PROLIFERATIVE RESPONSE OF PULMONARY ARTERY ENDOTHELIAL AND SMOOTH MUSCLE CELLS

.

4.1. INTRODUCTION

Pulmonary hypertension is characterized largely by medial hypertrophy due to enhanced vascular smooth muscle cell proliferation or attenuated apoptosis and to endothelial cell hyper-proliferation, which can result in lumen obliteration (Mandegar *et al.*, 2004). In turn, this leads progressively to loss of pulmonary vascular compliance and the sustained increased in pulmonary vascular pressure which becomes a predominant pathological feature of the disease (Rubin, 1997). In addition, there is evidence that peroxynitrite formation is up-regulated in pulmonary hypertension (Bowers *et al.*, 2004). In works carried out in this laboratory, ubiquitous protein tyrosine nitration, a hallmark of peroxynitrite formation has been reported in lung sections of infants with pulmonary hypertension (Wadsworth *et al.*, 2004). Moreover, peroxynitrite formation was also observed in patients with long standing severe forms of the pulmonary disease (Bowers *et al.*, 2004). This indicated that the lungs of patients with pulmonary hypertension were likely under oxidative/nitrative stress.

Peroxynitrite research has classically focused on the role of the anion in disease pathology, perhaps because the anion is a strong nitrating agent. Consequently, there have been limited investigations into the activity of ONOO- at concentrations less than 5μM at which the anion will preferentially yield non-cytotoxic effects (Bolanos *et al.*, 2004; Klotz *et al.*, 2002; Mallozzi *et al.*, 1997). There are few reports on other possible biological effects of ONOO- such as stimulation of cell proliferation, cell survival or migration. Perhaps it has not been thought that low concentration ONOO- can be involved in disease progression or pathogenesis. There is no agreement in the literature estimates of the local in-vivo concentration of ONOO-. However, a central theme in the body of emerging evidence indicate that these concentrations must be lower than those widely reported as capable of cytotoxic effects (see chapter 3; Ichikawa *et al.*, 2008; El-Remessy *et al.*, 2007) . This present study therefore hypothesized that sufficiently low concentration of peroxynitrite are relevant to the pathological formation of the anion under oxidative stress and that local production of these levels of ONOO- in pulmonary arteries can stimulate endothelial and smooth muscle cell proliferation. Based on the determined threshold concentration for ONOO- cytotoxicity (2μM; Chapter 3), the effects of lower and non-cytotoxic concentration of the anion on pulmonary artery

endothelial (PAEC) and smooth muscle (PASMC) DNA synthesis and cell proliferation were investigated.

In addition, SIN-1 was used to mimic the in-vivo continuous formation of similar concentration range of authentic peroxynitrite. The choice of SIN-1 concentrations expected to mimic the biological effects of authentic peroxynitrite was based on the chemistry data (Chapter 2) and published evidence that showed authentic peroxynitrite and 10-fold SIN-1 concentration yielded comparable biological activity (Cao *et al.*, 2004; Cao and Li, 2004). Of note, studies reporting the peroxynitrite-like effects of SIN-1 also show that SIN-1 will produce superoxide (Darley-Usmar *et al.*, 1992; Dimmeler *et al.*, 1992; Hogg *et al.*, 1992). Thus SIN-1 is capable of producing 3 potent substances namely, peroxynitrite, NO and superoxide, and any effects of SIN-1 could potentially be due to any or a combination of these. Experiments were therefore designed to generate superoxide in-situ in pulmonary cell culture medium and to investigate the effects of various superoxide concentrations on pulmonary artery cells proliferation.

4.2. OBJECTIVE

To investigate the effect of low concentration (<2μM) peroxynitrite, SIN-1 and superoxide on endothelial and smooth muscle cell proliferation under normoxic (21% oxygen) culture conditions.

4.3. METHODS

4.3.1. Authentic and in-situ generated peroxynitrite

Peroxynitrite was supplied as a 170mM solution in 4.7% aqueous sodium hydroxide (NaOH) (Calbiochem, United Kingdom and Ireland; Cat #: 516620). Dilutions of the stock solution were made with 1M NaOH as vehicle, and aliquots were stored at -80^{0}C. All dilutions 8 days apart were discarded (Fig. 2.2; chapter 2). Peroxynitrite was quantified spectrophotometrically using the extinction coefficient at 302 nm = 1670M^{-1} cm^{-1} (Bohle *et al.*, 1994; Radi *et al.*, 1991a; Radi *et al.*, 1991b). Peroxynitrite was added directly to the side of culture and followed by rapid swirling. 3-morpholinosydnonimine (Sigma®; M184-25mg) was kept at -20^{o}C until needed. Stock solutions of SIN-1 in distilled water were made and added directly to cells with gentle swirling.

4.3.2. Pulmonary artery cell proliferation assays

4.3.2.1. DNA synthesis measured by [³H] Thymidine incorporation assay

DNA synthesis was used as a measure of PAEC and PASMC proliferation. The assay was conducted as described in Chapter 3 (section 3.3.8) and as previously described (Coats *et al.*, 2008). In control experiments, cells were exposed to equal volume NaOH 1M/or to decomposed ONOO- solution prepared by adjusted the pH of ONOO- solution to pH 7.4. or to ONOO- solution kept at room temperature for >30days (Fig. 2.2, Chapter 2). Preliminary experiments determined the effect of FBS alone on pulmonary cell proliferation. In separate experiments, pulmonary cells were stimulated with various superoxide concentrations with or without 0.2 or 2 20μM SIN-1.

4.3.2.2. Estimation of proliferation by cell counting using haemocytometer

Pulmonary endothelial or smooth muscle cell proliferation was also assessed by manual counting. Cells were seeded into 6 well plates and stimulated with 2nM or 0.2μM ONOO- or 2μM SIN-1 for 24h. The cells were thereafter detached by trypsin, centrifuged and re-suspended in labelled identical vials containing phosphate buffer solution (PBS). Vials were re-arranged and labels were replaced with random numbers by a non-participant in the study. A researcher blind to the treatment and control vials counted the numbers of cells in each vial by the use of a haemocytometer mounted on a phase contrast microscope (Nikon, Japan). Cell aliquots of 10μl was loaded onto haemocytometer and counted.

4.3.2.3. Assessments of cell proliferation by MTT

PAEC or PASMC were split at a density of 2×10^5 cells/ml in 24-well plates, 1ml suspension per well were cultured in medium comprising a 50:50 mix of Ham F-12 and Waymouth MB752 media (Invitrogen) made up with 15% foetal bovine serum (FBS). The cells were grown to 75% confluency, then quiesced for 24h at 0.1% FBS and thereafter stimulated with ONOO- for 24h. Exactly 100μl of 10mg/ml yellow MTT (3-(4,5-Dimethylthiazol-2-yl)-2,5-diphenyltetrazolium bromide, a tetrazole) was added and incubated for 2h. Culture medium was removed, 100μl DMSO was added to each well to dissolve the insoluble formazan, and the absorbance (OD) of the characteristic purple reaction product (formazan) was measured at 580nm using a microplate spectrophotometer (SpectraMax (M5), Molecular Devices Ltd™).

4.3.3. Chemiluminescence

Phosphate buffered solution (PBS) was used to make test solutions up to 1ml in clear plastic cuvettes. Lucigenin solution added to make a final cuvette concentration of 5μM was used for the detection of superoxide using a Berthold™ chemiluminometer. Measurements of superoxide generation from various xanthine concentrations combined with a fixed amount of xanthine oxide were recorded after chemiluminescence signal was observed for 70 seconds. Time dependent superoxide generation for a fixed combination of xanthine/xanthine oxidase was monitored every 20s for 15min. Sodium salt of xanthine dissolved in warm distilled water was used and the xanthine oxidase was dissolved in phosphate buffer solution. Measurements were charted as chemiluminescence signal in relative light units per second (RLU/s). Other experiments involved luminol (10^{-3}M)-enhanced chemiluminescence for the detection of hydrogen peroxide.

4.3.4. Drugs: Peroxynitrite was sourced as decribed above (section 4.3.1), bovine superoxide dismutase (cat.#: S2515-75KU), xanthine (cat.#: X0626-5G) xanthine oxidase (cat.#: X4376-5UN), bovine liver catalase (cat.#: C1345) and 3-morpholinosdynonimine (SIN-1; cat.#: M184-25mg) were purchased from Sigma® (UK).

4.4. RESULTS

4.4.1. Control experiments

4.4.1.1. Effect of FBS and the ONOO- vehicle: PAEC

Preliminary work demonstrated endothelial cells proliferation can be stimulated with foetal bovine serum (FBS) in a concentration-dependent manner (Fig. 4.1). Post hoc statistical evaluation of the proliferation induced by graded FBS concentration showed no significant differences in endothelial cell proliferation observed between 0.5% FBS and baseline stimulation (0.1% FBS). However, relative to baseline, 2.5 and 15% FBS showed significant stimulation of endothelial cell proliferation (Fig 4.1; $p<0.05$). Control experiments involved the administration of the ONOO- vehicle (0.5mM sodium hydroxide) to endothelial cells stimulated with varying FBS concentrations (results not shown). Sodium hydroxide (0.2-0.5mM) was present with each concentration of

authentic peroxynitrite solution applied to cells in this study; the addition of a 0.3µL NaOH/ONOO- solution to a 1ml cell culture medium was found to increase medium pH from 7.4±0.04 to 7.93±0.04 (See chapter 2, 3). The effect 0.5mM NaOH on pulmonary cell proliferation was not significant; in addition the associated pH change was transient since excess –OH was within the buffering capacity of cell culture medium (see chapter 2).

4.4.1.2. Determination of optimum growth and quiescing condition: PASMC

PASMC in serum free medium for 24h or in medium containing 0.1% serum for more than 30h became non-viable lifting off the culture plate (observation not shown) The areas showing cell 'lift-off' increased with quiescing period for both serum free and 0.1% serum in medium conditions. Based on these results, assessment of DNA synthesis in PASMC were done using cells quiesced for 24h in medium containing 0.1% serum since the cells tolerated this condition.

4.4.1.3. Effect of FBS on DNA synthesis: PASMC

Foetal bovine serum (FBS) stimulated PASMC DNA synthesis in a concentration dependent manner (Fig. 4.2). Maximum proliferation was seen with 15% FBS; this yielded over 10 fold increase compared with 0.1% FBS (Fig. 4.2) Exposure of cells to 2.5% FCS produced about 50% of sub-maximal increase in DNA synthesis (Fig. 4.2).

.

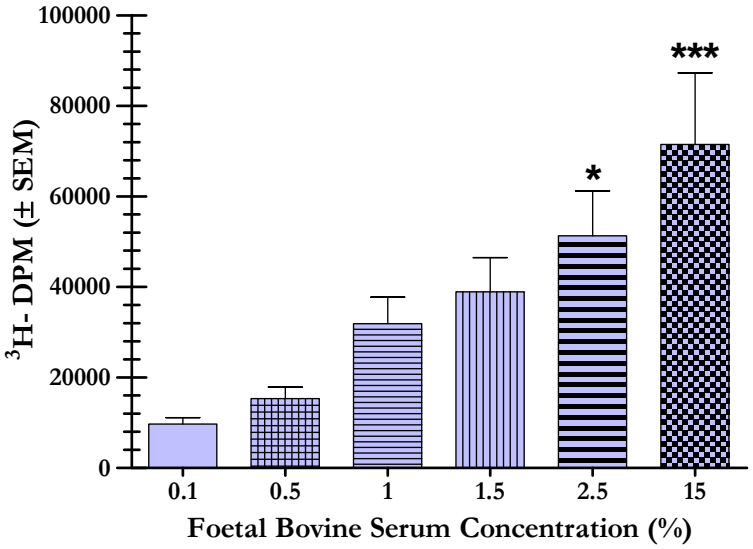

Figure 4.1: The Effect of Graded Foetal Bovine Serum Concentration Alone on Endothelial Cell Proliferation. DNA synthesis was evaluated using ^{3}H-thymidine incorporation assay. Counts were measured in DPMs (disintegrations per minute) and cell proliferation with graded FBS concentration was analysed using 1-way ANOVA. Post hoc investigations were by Bonferonnis test of multiple comparisons. Statistical significant is shown relative to control (0.1% FBS) *= $p < 0.05$; experiments were conducted in quadruplicates. n=6-7.

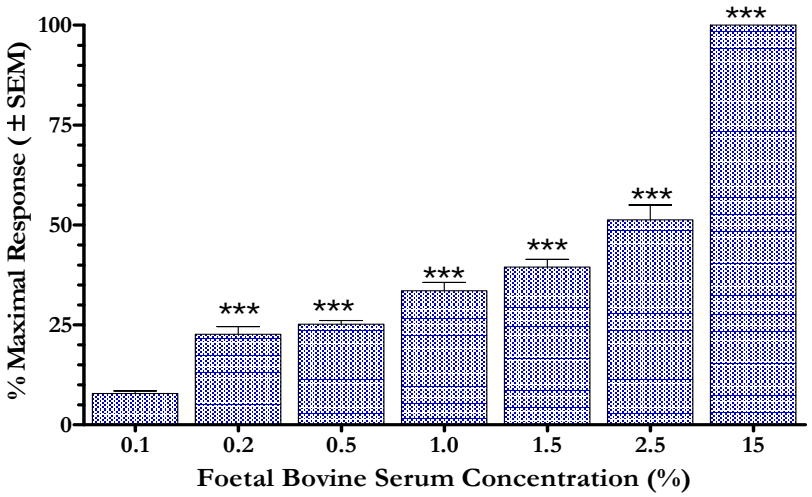

Figure 4.2: The Response of Pulmonary Artery Smooth Muscle Cells to Stimulation With Foetal Bovine Serum. DNA synthesis was measured by ^{3}H-thymidine incorporation assay. Counts were measured in DPMs (disintegrations per minute) and expressed as percentage proliferation (± SEM) relative to proliferation in cells stimulated with 15% FCS. Statistical evaluations were by 1-way ANOVA. Post hoc investigations were by Bonferonnis test of multiple comparisons *** = $p < 0.001$ relative to 0.1% FCS experiments were conducted in quadruplicates, n=8.

4.4.2. Effect of authentic peroxynitrite on pulmonary artery cell proliferation

4.4.2.1. Effect of authentic peroxynitrite on endothelial cell proliferation: ^{3}H-thymidine incorporation

Peroxynitrite [0.02-0.2μM] did not inhibit endothelial cell proliferation. In contrast, 0.2μM peroxynitrite significantly stimulated endothelial cell proliferation at three serum concentrations (basal stimulations), namely 0.1, 0.5 and 2.5% ($p<0.05$; Fig 4.3). Significantly the stimulatory effect of ONOO- was limited to conditions of 0.1, 0.5 and 2.5% FBS. The result suggests concentration dependent response of PAEC to ONOO- at 0.1 and 0.5% FBS (Fig. 4.3).

4.4.2.2. Effect of authentic peroxynitrite on smooth muscle cell proliferation: ^{3}H-thymidine incorporation

Low concentration ONOO- stimulated PASMC proliferation. The results which are shown in Figure 4.4 are so presented to reflect the design of the experiments in which there were as many controls as there were test groups for each FBS and ONOO- concentration tested. The life and activity of 0.2nM ONOO- was most transient amongst the concentrations tested (see Chapter 2); yet, this concentration of the anion remained able to significantly stimulate DNA synthesis in PASMC under 0.1% FBS (Fig. 4.4A). Also, the normalised data (Fig. 4.5) showed significant increase in DNA synthesis with 0.2nM ONOO- at 0.1% FCS when analysed in comparison with relevant controls (Paired t-test; $t=3.011$, $df=8$, 95% CI = -31.52 to -4.178; $p<0.05$). Figure 4.4B showed that 2nM ONOO- significantly stimulated PASMC at 2.5% FCS ($p< 0.01$). Peroxynitrite 0.2μM, showed greater ability to stimulate PASMC proliferation; with significant (at 15% FBS; $p < 0.05$, Fig. 4.4D) and about 100% increase in DNA synthesis (at 2.5% FBS; $p <0.01$, Fig. 4.4D) relative to the number of newly formed DNA in vehicle treated cells (Fig. 4.4D, 4.5). Also, proliferation was concentration dependent at 2.5% FBS (Fig. 4.5). At 2μM, ONOO- exhibited inhibitory effects on PASMC proliferation as earlier shown (see chapter 3); this effect was significant in cell under low, half-maximum and maximal baseline growth stimulus from FBS (Fig. 4.5; relate with Fig. 4.2). Again, the stimulatory effects of 2nM or 0.2μM ONOO- on PASMC was significant at specific FBS concentration (Fig. 4.4; 4.5); Also, the results at 15% FBS indicated that ONOO- can cause further stimulation of proliferation in cells under high serum concentration (Fig. 4.4D, 4.5). This perhaps was an early indication of a peroxynitrite stimulatory mode of action similar but distinguishable from serum. The study concluded that 0.2nM, 2nM, 0.02 μM or 0.2μM ONOO- can stimulate PASMC proliferation under specific well defined conditions.

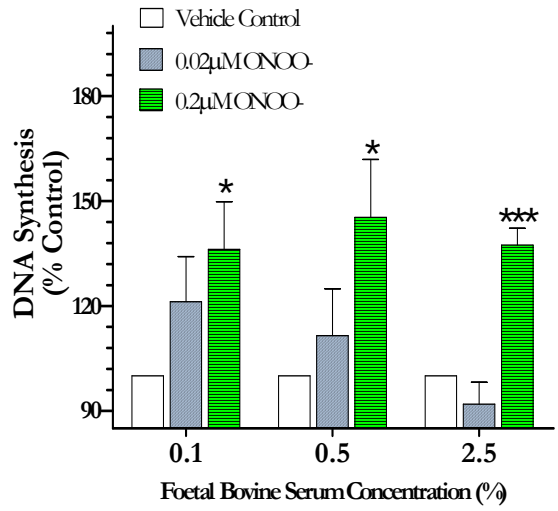

Figure 4.3: The Effect of 0.02 and 0.2μM Authentic Peroxynitrite (ONOO-) on Endothelial Cell Proliferation. Counts were measured in DPM (disintegrations per minute) and matched with the relevant controls at each FBS level. To make the effects of ONOO- clearer, DPMs were expressed as percentage fold proliferation (± SEM) relative to proliferation in respective control groups. Statistical evaluations of the normalised data were by 1-way analysis of variance at each FBS level. Post hoc investigations were by Dunnett's test that compares treatment columns with control. *** =p< 0.001 or *= p< 0.05 was considered significant; experiments were done in quadruplicates, n= 7-10.

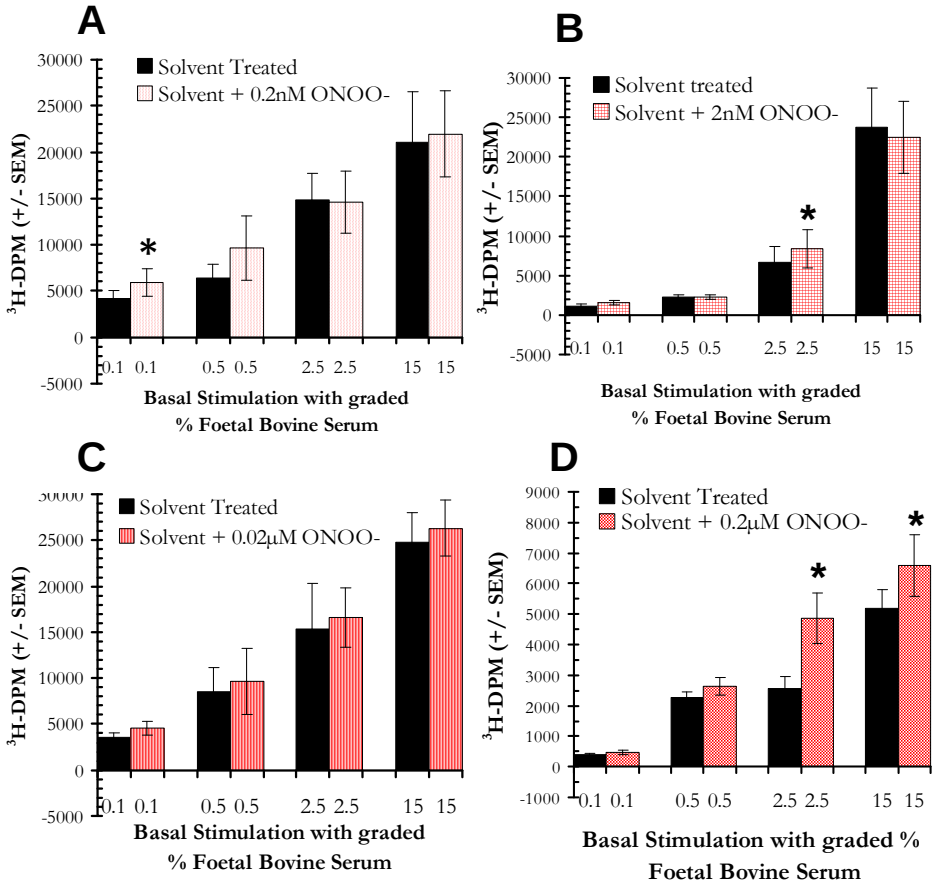

Figure 4.4: Effects of 0.2nM, 2nM, 0.02μM, 0.2μM and 2μM authentic ONOO on pulmonary artery smooth muscle cell proliferation: determined by ^{3}H- thymidine incorporation assay: Counts were measured in DPM (disintegrations per minute ± SEM) and matched with relevant controls (Fig. 5.4A-D). Pair-wise comparison by t-test was used to analyse the statistical significance of the changes in DPM in cell treated with ONOO- relative to their controls. ** =p< 0.01 or *= p< 0.05 was considered significant; experiments were conducted in quadruplicates, n=-6-9, 8-10, 6-8 & 8-10 4.4A, B, C D, respectively.

4.4.2.3. Effect of authentic peroxynitrite on smooth muscle cell proliferation: cell count method

Results from the determination of PASMC number under haemocytometer provided corroborative evidence for the stimulatory effects of low concentration ONOO-. The results (Fig. 4.6) showed increase in PASMC number following treatment with ONOO-. There were approximately 50 and 100% increase in PASMC number by 2nM ONOO- at 2.5 and 0.1% FBS, respectively (Fig. 4.6).

4.4.2.4. Effect of authentic peroxynitrite on smooth muscle cell proliferation: MTT assay

MTT (3-(4,5-Dimethylthiazol-2-yl)-2,5-diphenyltetrazolium bromide, a tetrazole) assay is a standard colorimetric assay for measuring the activity of enzymes that reduce MTT to formazan (such as mitochondrial dehydrogenases), giving a purple colour. This reduction reaction takes place mostly in the mitochondria; hence, the assay is largely taken as a measure of mitochondrial respiratory activity or activation. However, since the amount of formazan produced is directly proportional to the number of active cells in the culture, the assay has been repeatedly used to showed cell proliferation or inhibition (Hussain *et al.*, 1993; Mosmann, 1983).

The MTT assay provided supplementary evidence that ONOO- can cause increase in PASMC number (Fig. 4.7). Relative to vehicle treated PASMC, there were increases in mitochondrial activity with increasing ONOO- concentration. The results taken at 24 and 48h showed that this was significant at 2nM and 0.2μM ONOO- in PASMC under 0.1% FBS ($p < 0.01$; Fig. 4.7). Further analysis by 2-way ANOVA and Bonferroni's post-hoc test showed that the 24 and 48h growth curves of PASMC differed significantly following 2nM or 0.2μM ONOO- treatment ($p < 0.01$; Fig. 4.7). Following a one time (bolus) administration of 0.2μM ONOO- solution to PASMC, mitochondrial activity or cell number increased by 54% control and by 194% control at 24 and 48h, respectively (Fig. 4.7).

.

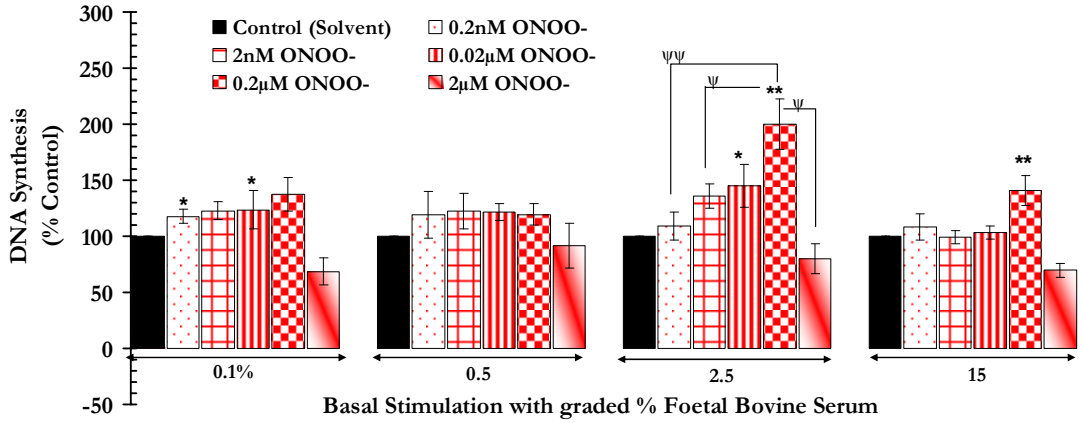

Figure 4.5: The effect of 0.2nM, 2nM, 0.02µM, 0.2µM and 2µM authentic peroxynitrite (ONOO) on bovine smooth muscle cell proliferation. This figure is a normalised plot of Figure 4.4. To make the effects of the intervention clearer, DPMs counts obtain in Figure 4.4 were expressed as percentage fold change in DNA synthesis (± SEM) relative to proliferation in respective control groups. Statistical evaluations of the normalised data were by 1-way analysis of variance at each FBS level. Post hoc investigations were by Bonferonnis test of multiple comparisons. Statistical significance is shown relative to control or as indicated; ** =p< 0.01 or *= p< 0.05 was considered significant; experiments were conducted in quadruplicates. Also, ψ indicates p< 0.05 in subgroup analysis by paired t-test comparing test with relevant solvent control; this followed the design of the experiment as shown in Figure 5.6. n=6-10.

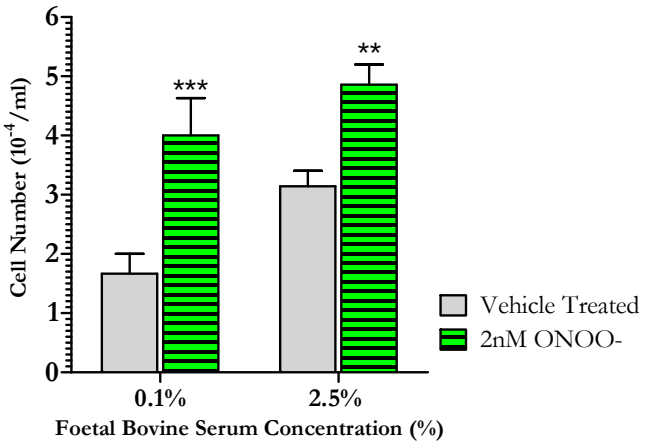

Figure 4.6: Increase in Pulmonary Artery Smooth Muscle Cell Number Following 2nM Peroxynitrite Treatment. PASMC were exposed to 2nM ONOO- and left for 24h. Cells were counted with the aid of an haemocytometer under a phase inversion microscope at x100 magnification. Statistical evaluations were by paired sample t-test at each FBS level; **= p< 0.01 for the pairwise comparison was considered significant; n=6-8.

.

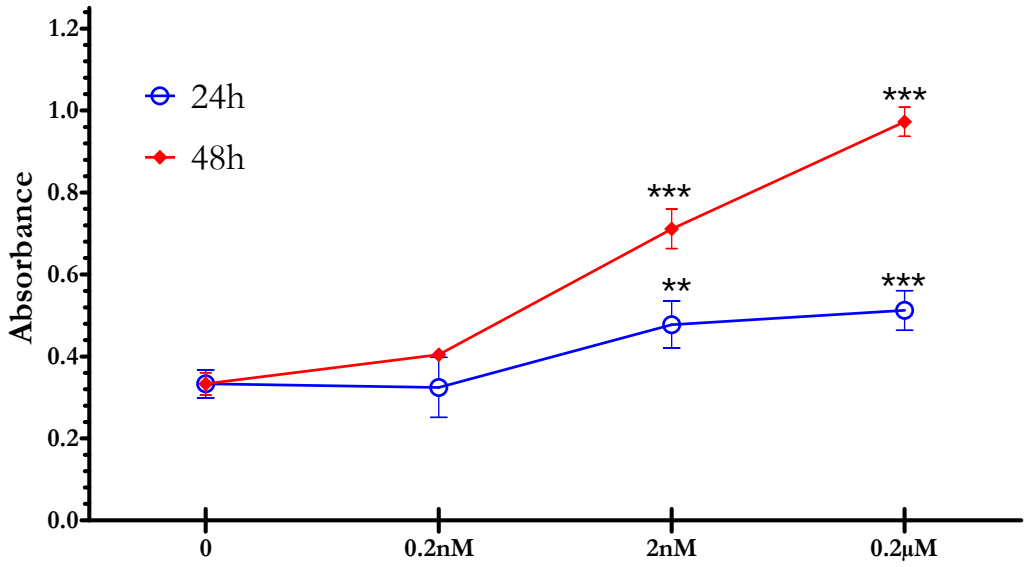

Figure 4.7: Effect Of Peroxynitrite on Pulmonary Artery Smooth Muscle Cell Proliferation: 24 and 48h Evaluation. Cells were maintained under condition of 0.1% foetal bovine serum. Assessment was by methyl thiazolyl tetrazolium (MTT) assay. Statistics was by 1-way analysis of variance (ANOVA) for each time observation; post-hoc test was by Dunnett's test comparing each concentration points with relevant vehicle treated. Changes in absorbance or formazan concentration with ONOO- relative to controls were considered very significant if =p< 0.01 (**); experiments were conducted in triplicates, n=7.

.

4.4.2.5. Effect of the peroxynitrite generator (SIN-1) on endothelial cell proliferation

Similar to authentic peroxynitrite (Fig. 4.3), 2μM SIN-1 stimulated PAEC proliferation (Fig 4.8). Similar to 0.2μM ONOO-, 2μM SIN-1 stimulated endothelial cell proliferation at 0.5 and 2.5% (Fig. 4.3; 4.8B). In addition, however, SIN-1 caused inhibitory effects on DNA synthesis at lower concentration (0.2μM; Fig 4.8A, 4.8C). Likely, this was not due to SIN-1 cytotoxicity since 2μM SIN-1 stimulated proliferation although both 0.2μM and 2μM SIN-1 showed similar toxic potential (see chapter 3; Fig. 3.10A). This dissimilar effect of 0.2μM SIN-1 was thus further investigated (see section 4.4.3)

4.4.2.6. Effect of SIN-1 on endothelial cell proliferation; assayed by cell count method

Following the observation that 2μM SIN-1 can stimulate DNA synthesis in endothelial cells, further experiments were conducted to investigate this effect on whole cell number. The results showed significant increases in whole cell number relative to control at each of the FBS concentrations chosen (0.1, 0.5 2.5 and 15%; results not shown). At 0.5% basal FBS, fold stimulations of PAEC proliferation by 2μM SIN-1 determined by cell counting with haemocytometer was 181.3 ± 17.6% control ($p<0.05$; $n=5$; results not shown). The observation was similar at 2.5% basal FBS concentration (187.7 ± 15.9% control; $p<0.01$; $n=5$).

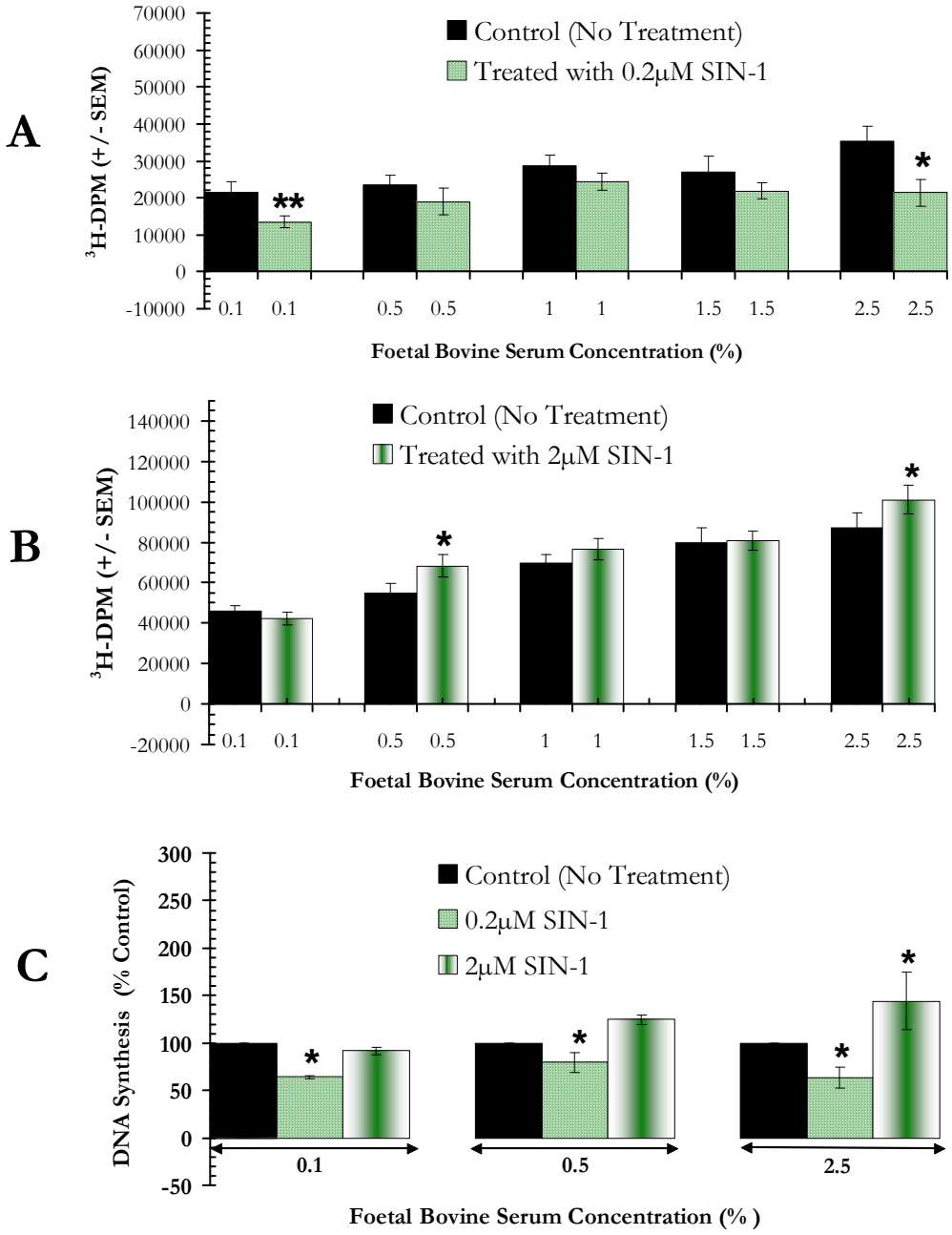

Figure 4.8: The Effect of 0.2 and 2μM 3-Morpholinosydnonimine (SIN-1: Peroxynitrite (Generator) on Endothelial Cell Proliferation. Counts were measured in DPM (disintegrations per minute) and matched with the relevant controls (Fig. 4.8A-B). Pair-wise comparison by t-test was used to analyse the statistical significance of the changes in DPM in cell treated with SIN-1 relative to their controls. To make the effects of the intervention clearer, DPMs were also expressed as percentage fold change in DNA synthesis (± SEM) relative to proliferation in respective control groups (Fig. 4.8C). Statistical evaluations of the normalised data (Fig. 4.8C) were by 1-way analysis of variance at each FBS level. Post hoc investigations were by Dunnett's test that compares treatments with control group. $p< 0.05$ (*) was considered significant; experiments were done in quadruplicates, n=6.

.

4.4.3. Proposition for the inhibitory effect of 0.2μM SIN-1: further experiments

4.4.3.1. The Supposition

SIN-1 necessarily dissociates into nitric oxide ($NO^{\bullet}$) before the generation of ONOO- (Chapter 1 or Scheme 1.1; Chapter 2 or Scheme 2.1), the significant inhibitions of cell proliferation by SIN-1 (Fig. 4.8A, 4.8C) may be due to the effect of nitric oxide produced from the dissociation of SIN-1 (Wedgwood and Black, 2003; Heller *et al.*, 1999; Kita *et al.*, 1994; Feelisch *et al.*, 1989) or to superoxide and not to the cytotoxicity of the molecule since the cytotoxic effect of SIN-1 did not differ significantly between 0.2 and 2μM (Fig. 3.10A; Chapter 3); also 2μM SIN-1 stimulated pulmonary cell proliferation (Fig. 4.8B). If the inhibitory effects were $NO^{\bullet}$ induced, it was anticipated that a co-application of exogenous superoxide with SIN-1 will cause superoxide to combine with any excess $NO^{\bullet}$ from the dissociation of SIN-1. This in turn will shift the reaction in favour of more ONOO- generation. In turn, this was expected to lead to further stimulation of endothelial cell proliferation than observed with SIN-1 alone at the same concentration or to stimulation at lower SIN-1 concentrations than previously observed. Further experiments were thus carried out to test this working hypothesis.

4.4.3.2. Superoxide and hydrogen peroxide generation

Initial experiments confirmed the generation of superoxide, using lucigenin chemiluminescence, from the reaction of xanthine and xanthine oxidase. The concentration relationship showed graded superoxide generation with 0.3μM - 10μM xanthine. The chemiluminescence signal was confirmed to be due to superoxide, since it was completely abolished by superoxide dismutase (Fig. 4.9A).

Maximum amount of superoxide was generated with 10^{-5}M xanthine and either xanthine oxidase concentrations (Fig 4.9A; 4.9B). Further increases in xanthine concentration beyond 10^{-5}M appeared to have resulted in corresponding decreases in superoxide generated possibly because xanthine quenches the radicals. It is also plausible that high concentration of xanthine generates hydrogen peroxide preferentially (Fig. 4.10). Over 75% of initial level of superoxide remained after 15min of real time decay (Fig. 4.9B). This indicated that there was significant amount of superoxide in the cell culture medium during experimentation.

It was confirmed that the xanthine-xanthine oxidase system generated not only superoxide but also hydrogen peroxide (H_2O_2). Luminol was used as it gives chemiluminescence in response to H_2O_2 as well as superoxide. The signals from these set of experiments which involved higher xanthine concentration were primarily due to H_2O_2, as shown by the near complete quenching with catalase (Fig. 4.10A). The residual chemiluminescence in the presence of catalase was presumably due to superoxide. The luminol signal was abolished by superoxide dismutase as expected, since superoxide is the primary product of the xanthine-xanthine oxidase reaction and is subsequently converted to H_2O_2. Levels of H_2O_2 were slowly declining when compared to superoxide level over the same period of time; declining only by 4-11% after a 15min real time (compare Fig. 4.9B and Fig. 4.10B). Although these experiments were not designed to calculate the number of units of superoxide and H_2O_2 generated by 1 unit of the enzyme at any concentration of xanthine, the results however suggests that the ratio of H_2O_2 to superoxide generated by this system may range from 1:1.6 to 1:2 (compare Fig. 4.9B and 4.10B).

.

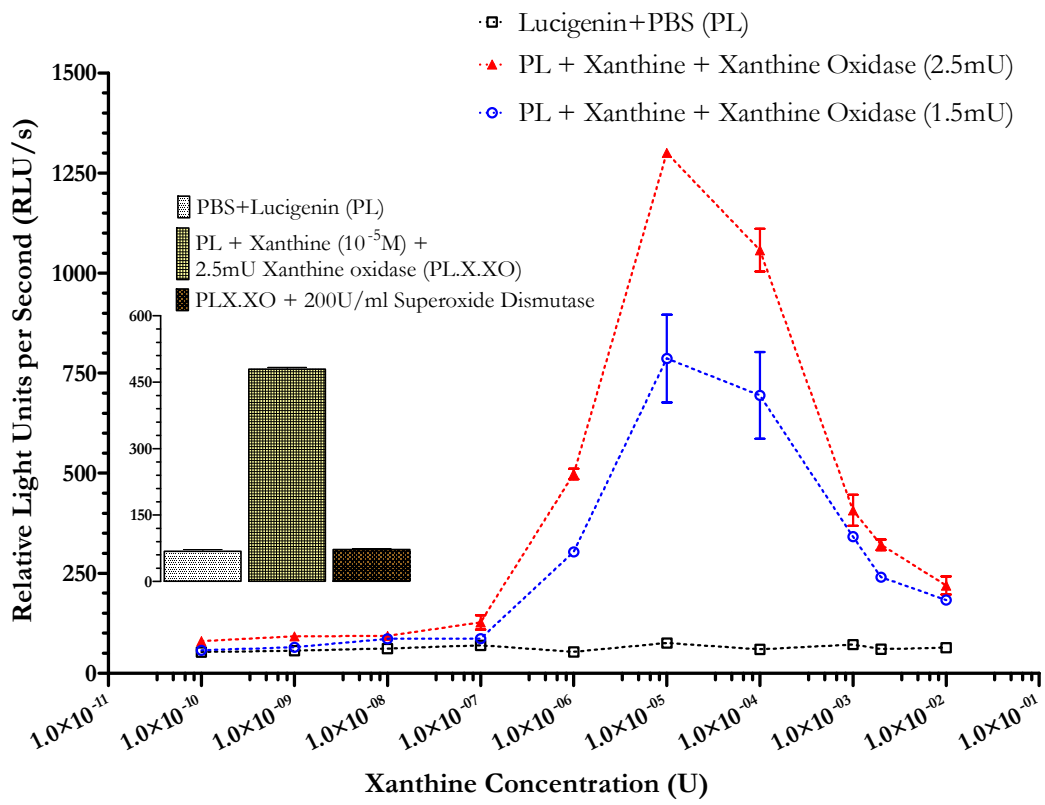

Figure 4.9A: Generation of Superoxide by Xanthine Oxidase with Graded Xanthine Concentration/1.5 or 2.5mU Xanthine Oxidase and the effect of Superoxide Dismutase 5µM Lucigenin enhanced chemiluminescence was used to detect superoxide production. Measurements were taken 60seconds following a 10 seconds delay after reactants have been added into vials and charted as chemiluminescence signal in relative light units per second (RLU/s). Inset show total obliteration of superoxide signal by 200U/ml Superoxide dismutase.

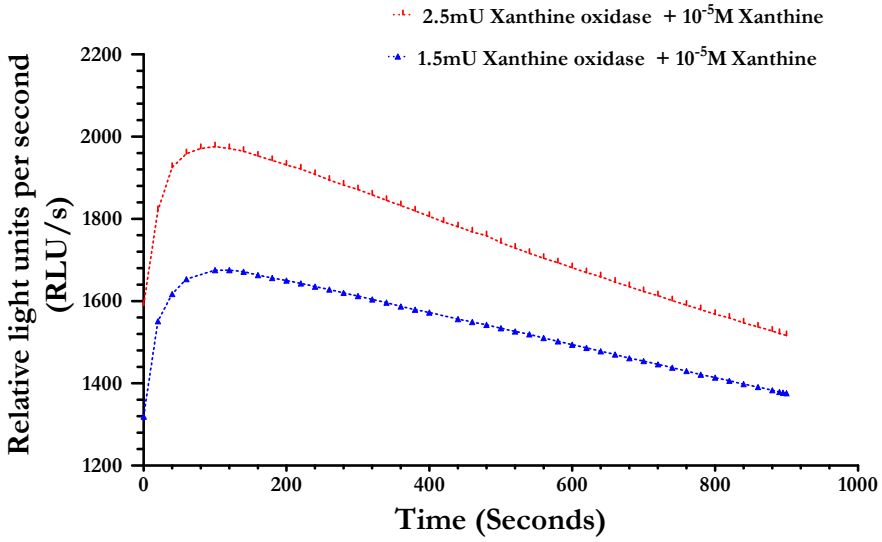

Figure 4.9B: Generation of Superoxide by 10^{-5}M Xanthine Combined with 2.5 or 1.5mU/ml Xanthine Oxidase: A 15min Real Time Observation. 5µM Lucigenin enhanced chemiluminescence was used to measure superoxide production. Measurements are charted as chemiluminescence signal in relative light units per second (RLU/s). Measurments were taken every 20 seconds.

4.4.3.3. Concentration dependent effects of superoxide on endothelial cell proliferation

Previous data from this laboratory showed that the activity of an aqueous solution of xanthine oxidase declined rapidly within a 7 day period when stock solution was maintained at 4^0C (data not shown). The dry stock of the enzyme however showed slower decline in activity with storage time (weeks). Each batch of xanthine oxidase solution was therefore assayed by measuring the superoxide production with fixed xanthine concentration through lucigenin chemiluminescence as previously described. The activity of each batch xanthine-xanthine oxidase combination was therefore expressed as relative light units per second; (RLU/s) rather than the concentrations of xanthine oxidase or xanthine involved. Alone, neither 10^{-6}M xanthine nor 2.5mU/ml xanthine oxidase had effect on endothelial cell proliferation in preliminary experiments. Together, they generated in these experiments, the highest concentration of superoxide (500RLU/s) and inhibited PAEC proliferation at all concentrations of serum investigated (Fig. 4.11). The effects of superoxide 150 RLU/s and 100 RLU/s generated from 10^{-7}M and 10^{-8}M xanthine, respectively on cell proliferation appeared to be insignificant, except under conditions of low growth factors (0.1% FBS; Fig. 4.11).

.

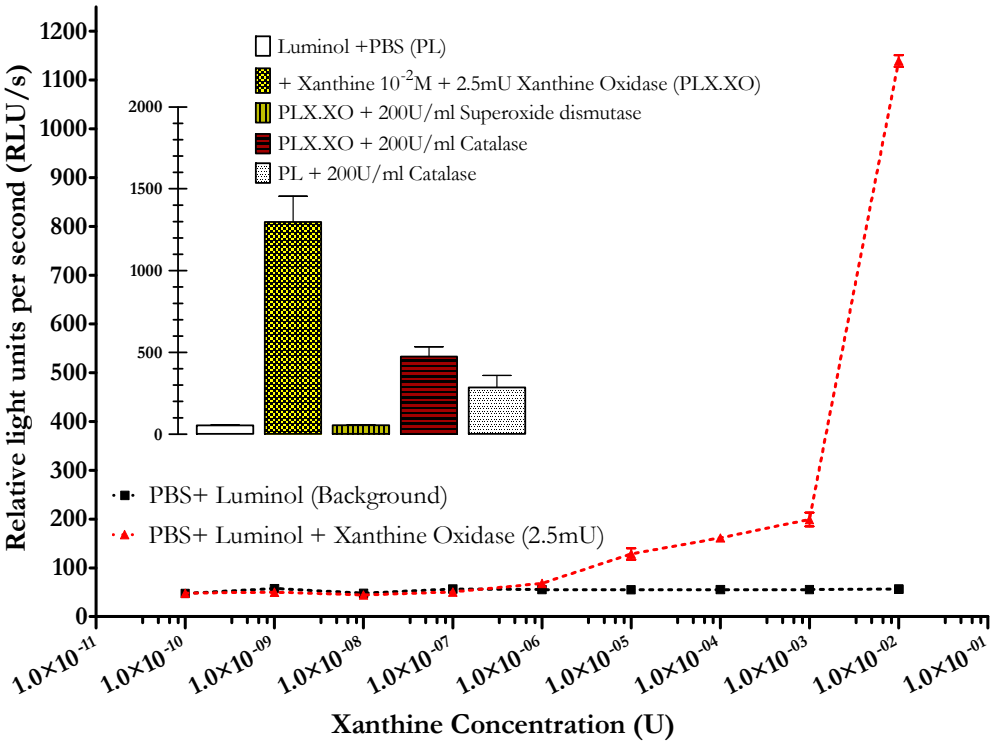

Figure 4.10A: Luminol Enhanced Chemiluminescence: The Generation and Blockade of Hydrogen Peroxide: Generation of hydrogen peroxide by graded xanthine concentration in combination with 2.5 xanthine oxidase. Chemiluminescence was enhanced by Luminol (10-3M). Measurements were taken 60 seconds following a 10 seconds delay after reactants have been added into vials and charted as chemiluminescence signal in relative light units per second (RLU/s). Insert shows total and partial obliteration of hydrogen peroxide signal by 200U/ml superoxide dismutase and Catalase respectively.

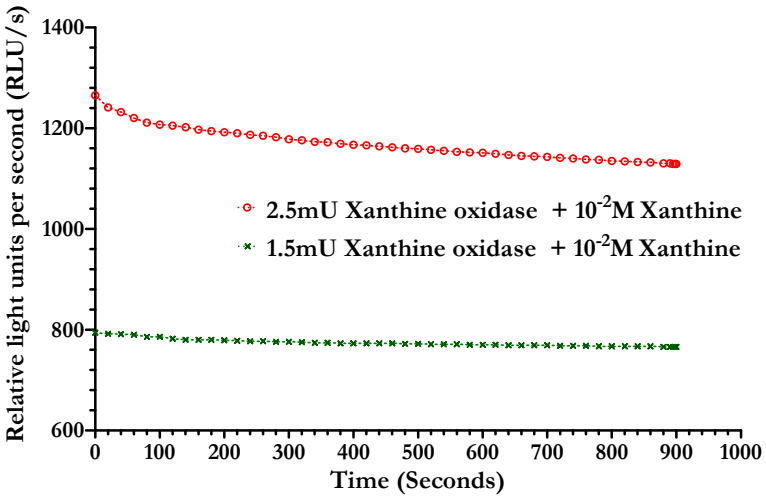

Figure 4.10B: Generation of Hydrogen Peroxide by 10-2M Xanthine Combined with 2.5 or 1.5mU Xanthine Oxidase: A 15min Real Time Observation of Luminol (10-3M) Enhanced Chemiluminescence. Measurements were taken every 20 seconds and charted as chemiluminescence signal in relative light units per second (RLU/s).

4.4.3.4. Inhibitory effects of xanthine/xanthine oxidase system: Mediators

The study confirmed that hydrogen peroxide (H_2O_2) was generated in addition to superoxide by the xanthine-xanthine oxidase system. Pre-treating PAEC with catalase and SOD combined completely abolished the inhibitory effects (Fig. 4.11) of xanthine-xanthine oxidase on PAEC proliferation at all FBS concentration investigated (Results not shown). In addition, the results showed that alone these amounts of either superoxide or H_2O_2 may produce growth inhibitory effect under conditions of low growth factors. The study also confirmed that a combination of superoxide and H_2O_2 was responsible for inhibition of cell proliferation by the xanthin/xanthine oxidase system at 500RLU/s. Cell were pretreated with catalase and superoxide dismutate prior to exposure to 10^{-6}M xanthine and 2.5mU/ml xanthine oxidase which together generated 500RLU/s product.

4.4.3.5. SIN-1 effect in the presence of high concentration superoxide: studies in PAEC

The study investigated the stimulatory effects of 2μM SIN-1 (Fig. 4.8) in the presence of high concentration superoxide. Endothelial cells were exposed to superoxide generated by 10^{-6}M xanthine and 2.5mU xanthine oxidase; this concentration has been established to cause significant inhibition of cell proliferation at all FBS baseline stimulation (Fig. 4.11).

The results (Fig. 4.12) showed that under conditions of high reactive oxygen species (ROS) concentration, 2μM SIN-1 remained able to stimulate DNA synthesis in viable PAEC; this effect was found to be significant at 0.5 ($p < 0.05$) and 2.5% ($p < 0.001$) FBS baseline stimulation. At 2.5% FBS, superoxide/H_2O_2 significantly inhibited endothelial cell proliferation to 33±2% control ($p<0.001$) however, SIN-1 remained able to stimulate proliferation to 63±4% control ($p<0.001$; Fig. 4.14) under the same condition. Similarly, at 0.5% FBS, superoxide/H_2O_2 significantly inhibited cell proliferation to 30.4±2.4% control ($p<0.001$) then again, SIN-1 remained able to stimulate proliferation to 51.1±7.6% control ($p<0.001$; Fig. 4.12) under the same condition. SIN-1 did not abolish the inhibitory effects of high levels of superoxide/H_2O_2 at any of the basal FBS concentration studied (Fig. 4.12).

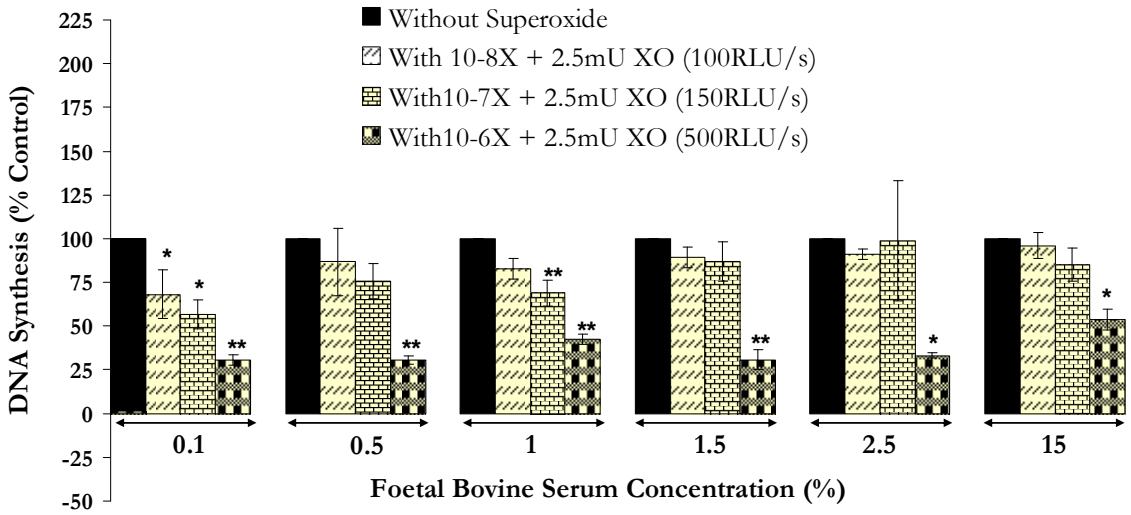

Figure 4.11: The Effect of 500, 150 and 100 RLU/s Superoxide Alone on Endothelial Cell Proliferation. Superoxide was generated by 10^{-6}, 10^{-7}, or 10^{-8}M xanthine (X) and 2.5mU xanthine oxidase (XO). Counts were measured in DPMs (disintegrations per minute) and expressed as percentage proliferation (± SEM) relative to proliferation in control cells. Statistical evaluations were by 1-way analysis of variance at each FBS concentration. Post hoc investigations were by Dunnett's test that compares treatments with control group. ** =p< 0.01 or *= p< 0.05 was considered significant; experiments were conducted in quadruplicate; n=4-5.

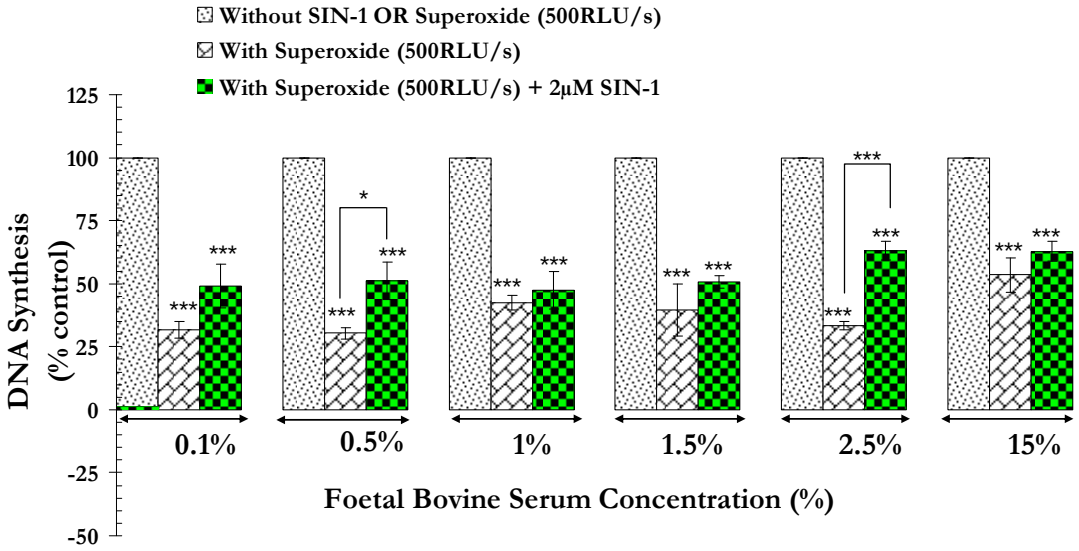

Figure 4.12: Effect of 2μM SIN-1 on Endothelial Cell Proliferation in The Presence of High Concentration Superoxide. Counts were measured in DPMs (disintegrations per minute) and expressed as percentage proliferation (± SEM) relative to proliferation in control media. High concentration (500 RLU/s) superoxide was generated by the combination of 10^{-6}M xanthine and 2.5mU xanthine oxidase added to cell culture medium. Statistical evaluations were by 1-way ANOVA at each FBS level. Post hoc investigations were by Dunnett's test that compares treatments with control group p< 0.001 (***) p< 0.01 (**), or p< 0.05 (*) was considered significant; experiment was conducted in quadruplicate; n=6.

4.4.3.6. SIN-1 effect in the presence of low concentration superoxide: PAEC

Since 10^{-6}M xanthine and 2.5mU xanthine oxidase generated 500RLU/s superoxide/H_2O_2 and caused marked inhibition of PAEC proliferation (Fig. 4.11), this complicates the interpretation of Fig. 4.8A to mean that 0.2μM SIN-1 generated excess $NO^{\bullet}$ which caused growth inhibitory effects . The Figure 4.8A experiments were therefore repeated using a 10^{-8}M xanthine and 2.5mU xanthine oxidase which generated low level of superoxide (100RLU/s). The combination of this level of superoxide (100RLU/s) with 0.2μM SIN-1 prevented the significant inhibition of proliferation previously seen with 0.2μM SIN-1 at 0.1, 2.5% serum (compare Fig. 4.8A and Fig. 4.13A). In addition, the combination increased the fold stimulation of proliferation induced by 2μM SIN-1 at 0.5% FBS from 119.1±7.3 to 135.1±15.3% control (compare Fig. 4.8B and Fig. 4.13B).

.

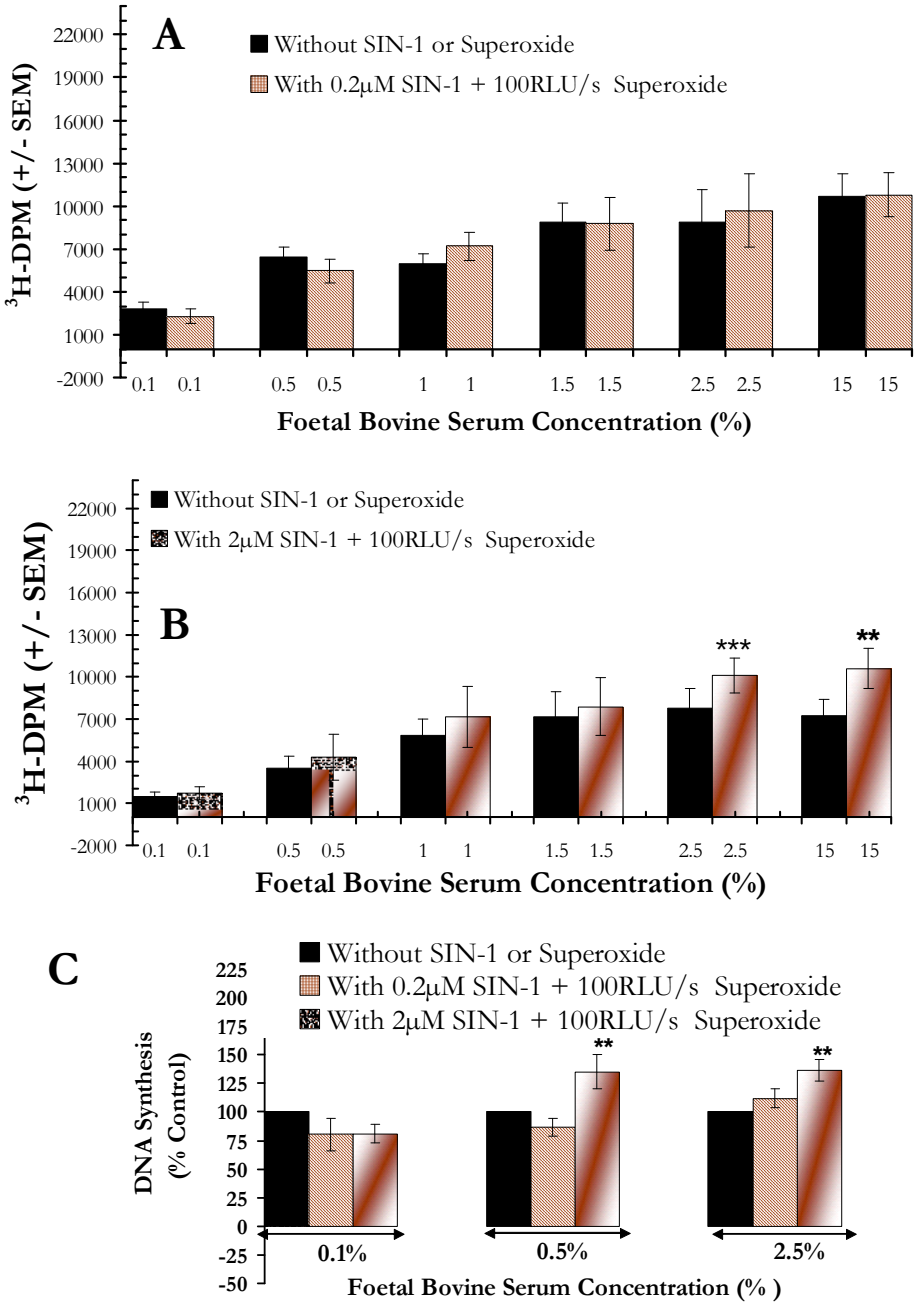

Figure 4.13: The Effect Of Low Concentration Superoxide On Pulmonary Artery Endothelial Cell Response to 3-Morpholinosydnonimine (SIN-1). Low concentration (100 RLU/s) superoxide was generated by the combination of 10-8M xanthine and 2.5mU xanthine oxidase added to cell culture medium. Counts were measured in DPM (disintegrations per minute) and matched with relevant controls (Fig. 4.13A-B). Pair-wise comparison by t-test was used to analyse the statistical significance of the changes in DPM in cell treated with SIN-1/superoxide- relative to their controls. To make the effects of the intervention clearer, DPMs were also expressed as percentage fold proliferation (± SEM) relative to respective control (Fig. 4.13C). Statistical evaluation of the normalised data (Fig. 4.15D) was by 1-way analysis of variance at each FBS level. Post hoc investigations were by Dunnett's test that compares treatment with control PAEC. $p < 0.01$ (**) was considered very significant; experiments were done in quadruplicates, n=8

4.5. DISCUSSION

4.5.1. Initial remarks and main findings

It is believed that cellular hyper-proliferation underlie the thickening of the pulmonary vascular medial layer and the formation of lesions obliterating vessel lumen in pulmonary hypertension (Rubin *et al.*, 2007; Balasubramaniam *et al.*, 2003; Humbert *et al.*, 1998). Hence, the control of pulmonary cell multiplicity is a current strategy for the resolution of vascular remodeling in pulmonary hypertension (Ghofrani *et al.*, 2005; Schermuly *et al.*, 2005). Using authentic (Fig. 4.3, 4.4, 4.5, 4.7) and in-situ generated ONOO- from SIN-1 (Fig. 4.8, 4.13), this study reports for the first time the stimulatory effects of 2-200nM ONOO- in pulmonary artery endothelial and smooth muscle cells. This response was confirmed by cell counting, ^{3}H-thymidine incorporation and MTT assays. The similar proliferative response of PAEC and PASMC to 2-200nM ONOO- suggests an action on a cell process common to both cells. In addition, studies involving xanthine/xanthine oxidase system showed that superoxide did not stimulate cell proliferation and confirmed that SIN-1 induced pulmonary cell proliferation was due to ONOO- but not $NO^{\bullet}$ or superoxide. The study thus suggests a role for ONOO- in pulmonary cell hyper-proliferation and vascular remodelling associated with pulmonary hypertension.

4.5.2. Peroxynitrite stimulates pulmonary artery endothelial cell proliferation

The proliferative responses of PAEC seen in this study followed transient exposures to low concentration ONOO- (see chapter 2). Under pathological conditions however, these levels of ONOO- may be achieved intermittently or sustained over longer period at the loci of production. In particular, the experiments with SIN-1 were an attempt to mimic this prolonged release profile under physiologic pH. The results showed that the stimulatory effects of authentic peroxynitrite on endothelial cell proliferation were mimicked (Fig. 4.8, 4.13). The initial inconsistency in the SIN-1 data (Fig 4.8) was probably due to a dual SIN-1 effect attributable to nitric oxide and ONOO- both of which are generated in-situ by the dissociation of SIN-1 (Kita *et al.*, 1994; Feelisch *et al.*, 1989). These caused both cell proliferation and inhibition (Fig. 4.8). This study however showed that co-application of low level exogenous superoxide (100RLU/s) with SIN-1 abolished most of the inhibitory effects of SIN-1 (Fig. 4.13). Jointly, 0.2μM SIN-1 and

100RLU/s superoxide may have generated a higher amount of ONOO- than would 0.2μM SIN-1 alone and rid the medium of excess $NO^{\bullet}$ which can inhibit endothelial cell proliferation (Wedgwood and Black, 2003; Heller *et al.*, 1999). It is not clear why ONOO- or SIN-1 concentration inducing proliferation at 0.1, 0.5, 2.5 or 15% FBS did not significantly increase DNA synthesis at other FBS concentration such as 1 or 1.5% FBS (Fig. 4.8, 4.13). It was however thought more important to further investigation on ONOO- effects only under condition enhancing its stimulatory actions on pulmonary cells.

4.5.3. Superoxide did not stimulate endothelial cell proliferation

This study provided evidence in PAEC that superoxide did not stimulate proliferation under condition of oxidative stress. On one hand, the presence of reactive oxygen specie (ROS) has been shown in some studies to promote endothelial cell proliferation; for example, treatment of rat coronary microvascular endothelial cell with pyrogallol or bovine aortic endothelial cells with glucose/glucose oxidase, both of which are ROS generators, resulted in increased cell number and increased DNA synthesis (Bayraktutan, 2004; Ruiz-Gines *et al.*, 2000). However, the superoxide and hydrogen peroxide generated in this study did not stimulate PAEC proliferation (Fig. 4.11). This on the other hand is in good agreement with the works of Zanetti and co workers (2001). These authors reported that either a deficiency or an excess of superoxide anions inhibited proliferation of human aortic and umbilical vein endothelial cell (Zanetti *et al.*, 2001). The present study demonstrate that alone, low (100RLU/s) and high (500RLU/s) levels superoxide with associated H_20_2 generated by the combination 10^{-8}M and 10^{-6}M xanthine with 2.5mU xanthine oxidase, respectively, did not stimulate bovine pulmonary endothelial cell proliferation (Fig. 4.11). Overall, the xanthine/xanthine oxidase experiments with endothelial cells provide further evidence that the proliferation response of PAEC with SIN-1 alone (Fig. 4.8) or with SIN-1 plus superoxide (Fig. 4.8) were due likely to ONOO-.

.

4.5.4. Peroxynitrite stimulates pulmonary artery smooth muscle cell proliferation

Transient exposures of PASMC to 2nM or 0.2μM ONOO- resulted in significant cell proliferation relative to un-exposed cells (Fig. 4.4, 4.5, 4.6, 4.7). As with PAEC, it is expected that the observed growth rate (Fig. 4.7) and extent of cell proliferation (Fig. 4.4, 4.5, 4.6) will be even more remarkable under local pathological conditions sustaining the formation of peroxynitrite. When compared with the proliferative response of PAEC, stimulatory effect of 0.2μM was twice as much in PASMC (compare Fig. 4.3 and Fig. 4.5). This revealed that PASMC were more sensitive or possessed greater proliferative potential in response to ONOO- stimuli in this model. This finding agreed with data which showed that 0.2 and 2nM stimulated PASMC proliferation under well defined serum condition (Fig. 4.5A, B) but remain unable to stimulate PAEC under these conditions or indeed under other serum concentrations investigated. Perhaps the importance of this unique response of PASMC to ONOO- lie in the evidence that PASMC play a greater role than PAEC in pulmonary artery medial hyperplasia (highly prevalent in small resistance arteries), hypertrophy (common to all human forms of pulmonary hypertension) and muscularisation that characterise pulmonary hypertension (Rabinovitch, 2008; Mandegar *et al.*, 2004; Durmowicz and Stenmark, 1999; Mckenzie *et al.*, 1984). In addition, PASMC in pulmonary hypertension can generate factors that stimulate the formation of connective tissues by other cells in the vessel wall (Mecham *et al.*, 1987; Mecham *et al.*, 1983). Taken with evidence that cells of the initimal layer of the pulmonary vasculature can modulate the growth and phenotype of adjacent cells (Eddahibi *et al.*, 2006; Heydarkhan-Hagvall *et al.*, 2003; Powell *et al.*, 1996), it is plausible that ONOO- induce a cascade of events that initiates changes leading to the pathological features of the pulmonary artery in pulmonary hypertension (Rabinovitch, 2008; Szabo *et al.*, 2007; Szabó *et al.*, 1996). This however will require further experiments to demonstrate. The data may also be interpreted to suggest that peroxynitrite increased cell survival in treated cells. This is based on results demonstrating 2-fold increase in whole cell number (Fig. 4.6) although DNA synthesis was 120-180% control (Fig. 4.4B) under the same condition. Taken together, the proliferative response of pulmonary cells to 2-200nM ONOO- provide at least part explanation for the clinical observation of pulmonary artery initimal and medial cell hyper-proliferation and the concomitant up-regulation of nitro-tyrosine in patients with pulmonary hypertension.

4.5.5. Stimulatory effects of peroxynitrite is independent of pulmonary cell quiescence

The percentage maximal stimulations in DNA synthesis reported with FBS alone in this study (Fig. 4.1) are typical of values in published papers (Shizukuda *et al.*, 1999). It was however noted that quiescing pulmonary artery cells under conditions of 0.1% FBS for 24h did not produce a consistent effect throughout the study. The results show considerable variation in the DNA synthesis in untreated cells under this condition. Cells were either partially or patently quiesced (Fig. 4.4A, 4.4C, 4.8A, 4.8B). More important though, is the response of pulmonary cells to ONOO- under these conditions. The results showed that the stimulatory effects of 0.2μM or lower ONOO- concentration can be demonstrated in patently quiesced (Fig. 4.4B, 4.4D), partially quiesced (Fig. 4.4A, 4.4C, 4.8A, 4.8B) and non quiesced pulmonary artery cells (Fig. 3.7B; Chapter 3). The signal transduction mechanism by which ONOO- stimulated pulmonary artery cell proliferation were explored and discussed in the next chapter.

4.5.4 Conclusion

The study reports for the first time that 0.2μM or lower peroxynitrite concentration can stimulate the proliferation of pulmonary artery endothelial and smooth muscle cells. This provide a novel link between pulmonary cell hyperplasia and the up-regulation of nitrotyrosine in pulmonary hypertension

.

CHAPTER 5

PEROXYNITRITE STIMULATES PULMONARY ARTERY CELL PROLIFERATION: SIGNAL TRANSDUCTION MECHANISM

.

5.1. INTRODUCTION

The present study has shown peroxynitrite and SIN-1 to stimulate the proliferation of endothelial and smooth muscle cells, the aim of the current chapter was to elucidate the signal transduction mechanisms utilised. The stimulatory effects of peroxynitrite (ONOO-) on members of the mitogen activated protein kinase family has been reported in vascular smooth muscle (Cao and Li, 2004; Upmacis *et al.*, 2004), endothelial (Clavreul *et al.*, 2006; Je *et al.*, 2004; Jiao *et al.*, 2003) as well as in other cell types (Zhang *et al.*, 2006; Pesse *et al.*, 2005b; Kaji *et al.*, 2002; Bapat *et al.*, 2001; Zhang *et al.*, 2000; Zouki *et al.*, 2000). Pesse et al., (2005) demonstrated in cardiomyocytes an increase in the phosphorylation of ERK 1/2 by 50-500μM ONOO-. ERK activation was found to be concentration and time-dependent and associated with Raf-1 dependent MEK-1 phosphorylation (Pesse *et al.*, 2005a). Also, exposure of Rat-1 Fibroblasts to 200μM ONOO- caused increase in phosphorylation of ERK1/2 via a Ca^{2+} dependent PKC but MEK independent pathway (Bapat et al., 2001). In addition, Zhang et al., (2000), reported that 1, 10 & 100μM ONOO- activated ERK in primary passage rat pulmonary myofibroblasts via MEK-1. In addition, the authors reported a concentration dependent decease in DNA synthesis following exposure of these cells to 1-1000μM (Zhang *et al.*, 2000). This effect was significantly reduced by MEK blockade (Zhang *et al.*, 2000). Independent works by Clavreul and co-authors showed that bolus addition of peroxynitrite (100μM) to bovine aortic endothelial cells increased phosphorylation of ERK (11±1.8- fold) and Akt (20±1.1-fold). This was noted as early as 1 min and peaked at 15 min and was dependent upon Ras activation (Clavreul et al., 2006). Since these signal molecules are well known to regulate cell proliferation pathways, ONOO- may therefore be capable of more than the widely reported cytotoxic (Cao and Li, 2004; Li *et al.*, 2002) or programmed cell death effects (Huang *et al.*, 2008; Szabó *et al.*, 1996). Accordingly, evidence pointing to a new role of peroxynitrite in vascular disease showed $cPLA_2$ activation and arachidonic acid release following bolus exposure to 100-500uM ONOO-. This effect was mediated via the MEK dependent activation of ERK in vascular smooth muscle cells (Upmacis *et al.*, 2004). In addition, a recent study showed that 1μM ONOO- or 100μM SIN-1 augmented fibroblast-mediated tissue remodelling in a model of airway remodelling (Ichikawa *et al.*, 2008).

Peroxynitrite also affects cellular signalling by causing dimerization of the epidermal growth factor receptor (EGFR) possibly through intermolecular dityrosine cross-linking (Van Der Vliet *et al.*, 1998). However, there is currently no consensus on whether ONOO- activation of ERK is growth factor receptor dependent (Jope *et al.*, 2000) or not (Pesse *et al.*, 2005a; Bapat *et al.*, 2001; Zhang *et al.*, 2000). Jope and co-workers showed that in PC-12 cells, ERK activation by ONOO- was mediated via the epidermal growth factor (EGF) receptor. Conversely, ONOO- mediated phosphorylation of ERK in rat lung fibroblasts though MEK dependent, occurred independent of EGF receptor (EGFR) (Zhang *et al.*, 2000). In a nutshell, the literature is replete with evidence for peroxynitrite activating the MAP kinase pathway, this is however based on high concentrations of the anion and there is contradiction between the papers as to the target/s for ONOO-. The present study however have demonstrated the growth stimulatory effects of 2-200nM ONOO- (chapter 4) and speculated in this chapter that these ONOO- concentrations might activate members of the MAP kinase signalling pathway directly and or via upstream activation of growth factor receptors. The investigations reported in this chapter focused on 0.2μM ONOO- since this stimulated both pulmonary artery endothelial (PAEC) and smooth muscle cells (PASMC). Although the kinetics of ONOO- and ONOO- from SIN-1 have been well described in this study (chapter 2), the signal transduction experiments involved authentic ONOO- alone as so prioritised. In addition, the effects on pulmonary cell proliferation were similar for SIN-1 and ONOO- (Chapter 4) and the chemistry data (chapter 2) showed that SIN-1 does release ONOO-.

5.2. OBJECTIVES

(1): To determine the time and peroxynitrite concentration dependent activation of ERK in PAEC and PASMC under conditions of cell growth stimulation, as shown in chapter 4. (2): To investigate by the use of specific inhibitors, the role of tyrosine kinase receptors, Ras, Raf-1 kinase, PKC and MEK in ONOO- induced pulmonary cell proliferation and or ERK activation. This group of signalling molecules has been reported as targets for ONOO-, albeit using high concentrations of ONOO-. Growth factor receptors were chosen because positive results were found with both ras and PKC, both of which can be activated as a result of growth factor receptor activation.

5.3. METHODS

5.3.1: Western blot analysis

Cell treatment, method of adding peroxynitrite, preparation of whole cell extracts, SDS-Polyacrylamide gel electrophoresis (SDS-PAGE), electrophoretic transfer of proteins to nitrocellulose membrane and immunological detection of proteins were carried out as described in chapter 3 (Section 3.3.). Selected details of the antibodies (Table 5.1) and specific inhibitors/stimulants (Table 5.2) used in this study are shown.

No	Name	Source/ Manufacturer /	Cat #
1	Phospho-ERK	Mouse/monoclonal; 1: 15000 Santa Cruz Biotechnology, INC.	pERK (E4):sc-7383
2	Total Erk	Rabbit polyclonal; 1: 15000 Santa Cruz Biotechnology, INC. ;	ERK 1 (K-23):sc-94
3	Phospho p38	Rabbit polyclonal, Biosource; 1: 15000	44-684G
4	Total p38	Rabbit polyclonal; 1: 15000 Santa Cruz Biotechnology, INC.	P38 (N-20):sc-728
5	Phospho-PDGF-Receptor β (Tyr751)	Rabbit polyclonal; 1: 10000 Cell Signaling	3161
6	Total Pdgf-R	Rabbit polyclonal, Upstate biotechonology, NY USA; 1: 10000	06-498
7	Ras	Rabbit polyclonal, Upstate;; 1: 10000	
8	HRP Anti-Phosphotyrosine	Mouse polyclonal; 1: 80000 BD Transduction Laboratories;	610011

Table 5.1: Details of antibodies: Invesstigation into the signalling mechanism of peroxynitrite induced pulmonary cell proliferation.

Name	Manufacturer	Cat #	Name	Manufacturer	Cat #
Ebselen	Calbiochem	324483	FTP inhibitor III	Calbiochem®	344154
U0126	Calbiochem	662005	FTP inhibitor II	Calbiochem®	344152
PD098059	BioMol, UK	EI360	Raf-1 kinase inhibitor	Calbiochem®	553008
SB203580	Calbiochem	559389	FTP inhibitor III	Calbiochem®	344154
AG-1296	Calbiochem	658551	Bisindolylmaleimide I	Calbiochem®	203290
AG-1478	Calbiochem	658552	Phorbol-12-myristate-13-acetate	Calbiochem®	524400
AG-1296	Calbiochem	658551	Epidermal growth factor (EGF)	Calbiochem®	324831
PDGF, BB homodimer	Calbiochem	521225	Imatinib, methanesulfonate salt.	LC laboratories	I-5508

Table 5.2: Details of specific inhibitors/stimulants: Invesstigation into the signalling mechanism of peroxynitrite induced pulmonary cell proliferation

5.3.2: DNA synthesis by ^{3}H-thymidine incorporation assay

DNA synthesis was used as a measure of PAEC and PASMC proliferation (see section 3.3.8).

5.4. RESULTS

5.4.1. Excluding the peroxynitrite and drug solvent effects

Sodium hydroxide (0.3-0.5mM) was used as vehicle control for peroxynitrite; in addition, the study involved the use of other solvents such as water and 0.1-0.5% dimethlyl sulfoxide (DMSO). These served as suitable solvents for inhibitors of specific proteins of the mitogen activated protein kinase (MAPK) proliferation pathways or of tyrosine receptor kinases. Experiments investigating the effects of these solvents on protein expression as well as pulmonary cell proliferation were carried out. DMSO did not significantly affect the expression of extracellular signal-regulated MAP kinases (ERK 1/2) or DNA synthesis in pulmonary cells up to a concentration of 0.5% (Results not shown); this was 5 times the concentration at which cells were routinely exposed to experimental drugs. Similarly, NaOH and decomposed ONOO- solvent did not significantly affect ERK expression or pulmonary artery cell proliferation (results not shown)

5.4.2. Serum as an ERK agonist in pulmonary artery cells

This study has demonstrated that low concentration peroxynitrite can stimulate the proliferation of bovine pulmonary artery cells in the presence of serum. Experiments were conducted to provide original data on the profile of serum induced expression of ERK 1/2 in pulmonary artery cells isolated for this study; and to establish whether or not inhibitors of ERK 1/2 will abolish serum induced ERK 1/2 activation and cell proliferation. The ensuing results elucidated on the activation of same pathway by ONOO-. The results showed that alone, serum at 2.5% caused 2.7±0.2 fold increase in the phosphorylation of p44/42 MAPK over baseline activation with 0.1% serum (results not shown). At 15%, serum caused marked activation of ERK. The MEK-1 inhibitor (PD 098059) and dual MEK-1/2 inhibitor (U0126) were used to investigate the contribution of MEK-ERK 1/2 pathway in serum induced cell proliferation and ERK 1/2 activation. U0126 is a highly selective inhibitor of both MEK 1 and MEK 2 which are MAPKK for the activation of ERK 1/2. Activation of ERK 1/2 by 2.5% FBS was reduced to 75.1±11.4% control by 50μM PD 098059 (n=3; results not shown) or 1.5μM U0126 (ERK 1/2 blocker; 63.3%±4.7 control; n=3) and was completely

abolished by ≥2.5μM U0126 (to 11.7%±1.5 control; n=3; result not shown) in PASMC. Pre-treatment of PASMC with U0126 caused significant attenuation of cell proliferation in a concentration dependent manner in cells under 0.1 or 2.5% FBS basal stimulus. At 0.1% FBS, 5μM U0126 caused approximately 36.1%.±2.8 control reduction in PAEC proliferation while growth appeared completely arrested with 12μM U0126 (2.6%±0.5 control; n=3). However, under 2.5% FBS, pre-treatment with 5 and 12μM U0126 reduced PAEC proliferation to 42.9%.±7.3 control and 32.5%±4.4 control, respectively (n=3; results not shown).

5.4.3. Effect of a Peroxynitrite Scavenger: Ebselen

Ebselen acts as a glutathione peroxidase mimic and is an excellent scavenger of peroxynitrite with a rate constant of 2 x $10^6 M^{-1}s^{-1}$ (Masumoto and Sies, 1996). Under basal stimulus condition of 0.1% FBS, 0.2μM ONOO- caused significant increase in PASMC DNA synthesis; this was approximately 2-fold the amount of new DNA synthesized in untreated cells (Fig. 5.1). When PASMC were pre-treated with ebselen 15min before exposure to 0.2μM ONOO-, the proliferative response was completely abolished (Fig. 5.1; $p<0.01$). This provided further evidence that PASMC hyper-proliferation was in response to ONOO-.

5.4.4. Effect of 0.2μM peroxynitrite on stress response pathways

Experiments were conducted to probe the activation of stress response pathway by peroxynitrite at the concentrations stimulating pulmonary cell proliferation. These concentrations of ONOO- did not activate p38 MAPK or stress activated JNK (see Chapter 3). Figure 5.2 showed that the phosphorylated state of p38 in PASMC was un-affected by treatment with 2μM peroxynitrite or lower concentration, although 0.2μM ONOO- caused significant increase in PAEC and PASMC proliferation under this condition (Chapter 4). In the same experiments, 10μM anisomycin significantly activated p38 MAPK. This indicated that the actions of ONOO- at these lower concentrations were not linked to cell stress pathways.

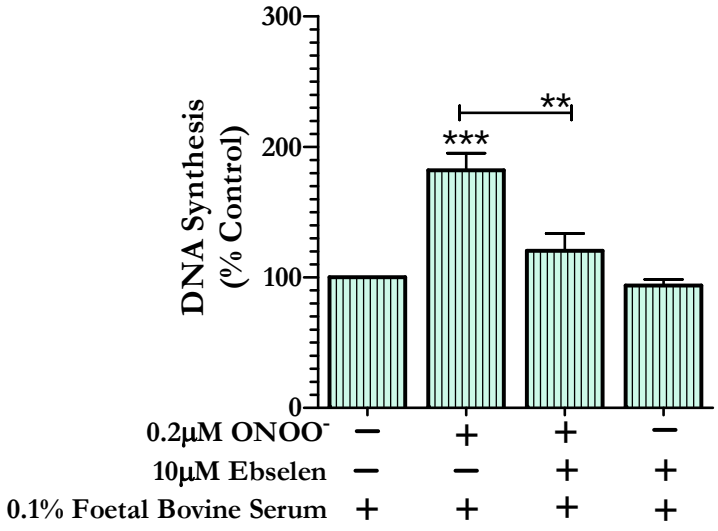

Figure 5.1: The Effect of Ebselen on the Stimulatory Actions of Peroxynitrite in Pulmonary Artery Smooth Muscle Cell. Cells were maintained at basal stimulation with 0.1% foetal calf serum. DNA synthesis was determined by ^{3}-H-thymidine incorporation assay. Counts were measured in DPMs and expressed as percentage proliferation (± SEM) relative to proliferation in untreated group. Statistical analysis was by 1-way ANOVA, post hoc test by Dunnett's test that compares treatments with control group; $p<0.001$ (***) was considered very significant; n=6

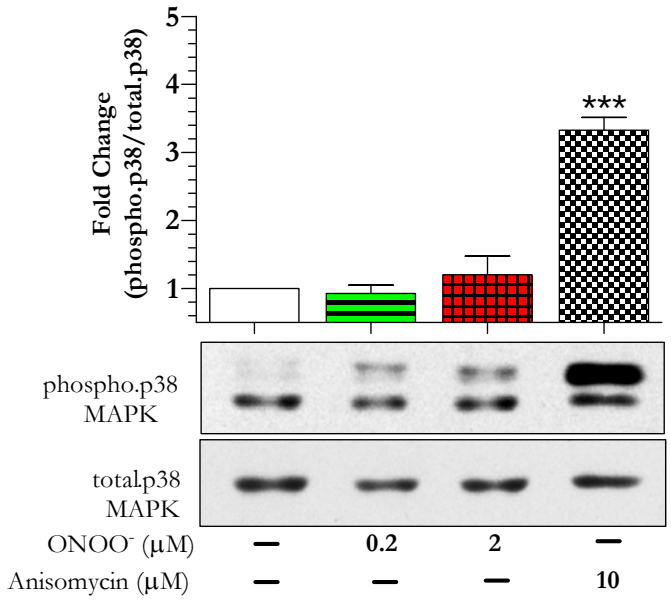

Figure 5.2: The Effect of ≤2μM Peroxynitrite on p38 MAPK Phosphorylation in Pulmonary Artery Smooth Muscle Cells. Cells were maintained under basal stimulation with 0.1% foetal calf serum and stimulated as shown for 15min. The 2 bands for phospho p38 MAPK represents the 2 isoforms of phospho p38 MAPK detected by the antibody. Expression of total and phosphorylated p38 MAPK were determined by western blotting; quantification was by densitometry. Statistical analysis was by 1-way ANOVA, post hoc test by Dunnett's test that compares treatments with control groups $p<0.01$ (**), was considered significant. n=3-5

5.4.5. Peroxynitrite Activates ERK 1/2 MAPK in Pulmonary Artery Cells

The results of this section provide biochemical evidence that peroxynitrite can further activate ERK 1/2 over basal serum stimulation in pulmonary artery cells.

5.4.5.1. Concentration dependent ERK 1/2 activation in PAEC and PASMC

Pulmonary artery endothelial cells exposed for 15min to a range of ONOO- concentration (2nM-20μM) showed a concentration dependent increase in phosphorylated ERK 1/2 up to 2μM (Fig. 5.3A). At 20μM ONOO-, ERK 1/2 activation decreased slightly relative to 2 or 0.2μM (Fig. 5.3A). Probe for total ERK 1/2 in these experiments confirmed that total ERK expression remained similar across treatment groups (Fig. 5.3A). Interestingly, ERK 1/2 activation was demonstrated at both ONOO- concentrations causing cell death (≥2 μM; chapter 3) and promoting cell growth (2nM-0.2μM; chapter 4). The presentation of the results in Figure 5.3A exemplifies the design of the experiments in this phase of the study. Probe for total protein (e.g ERK, p38, pDGFR) was conducted for every change in phosphorylated state investigated; and fold change shown was calculated from the ratio of phosphorylated ERK protein to total protein.

Similar to effect in PAEC, ONOO- caused increased in ERK 1/2 phosphorylation in PASMC. However, the concentration dependent activation evident in PAEC (Fig. 5.3A) was not apparent in these cells at the ONOO- concentration investigated (Fig. 5.3B). It is possible however; that these concentrations provided maximum ERK stimulation and smaller changes in ERK may be detectable with even lower ONOO- concentrations.

.

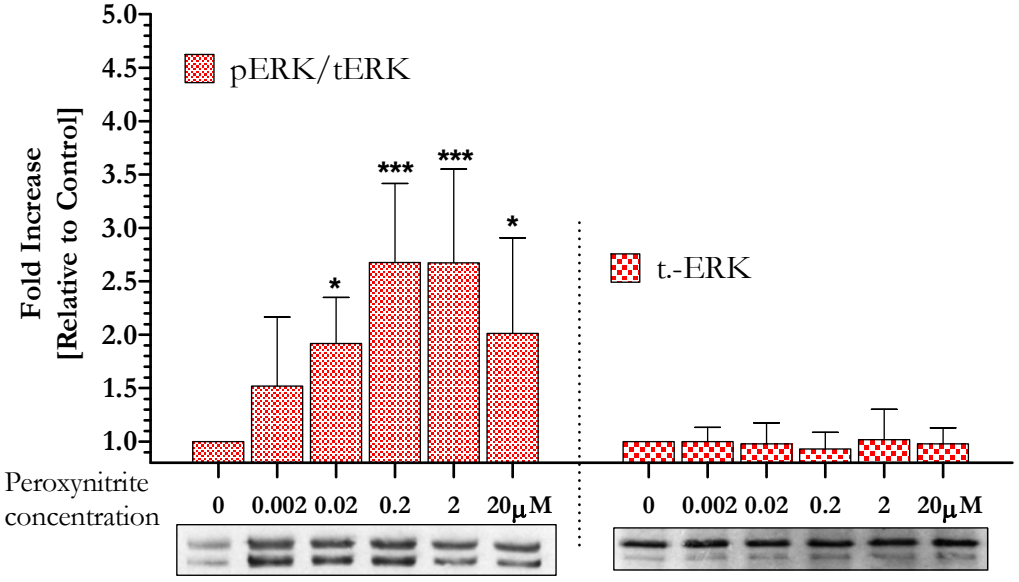

Figure 5.3A: Concentration Dependent Phosphorylation of ERK 1/2 in Cultured Pulmonary Artery Endothelial Cell. Cells were maintained at basal stimulation with 0.1% foetal calf serum. Expression of total (t-ERK) and phosphorylated mitogen activated protein kinase ERK 1/2 (pERK) were determined by western blotting; quantification was by densitometry. Statistical analysis was by 1-way ANOVA, post hoc test by Dunnett's test that compares treatments with control groups; $p<0.01$ (**), <0.001 (***) were considered significant. n=9.

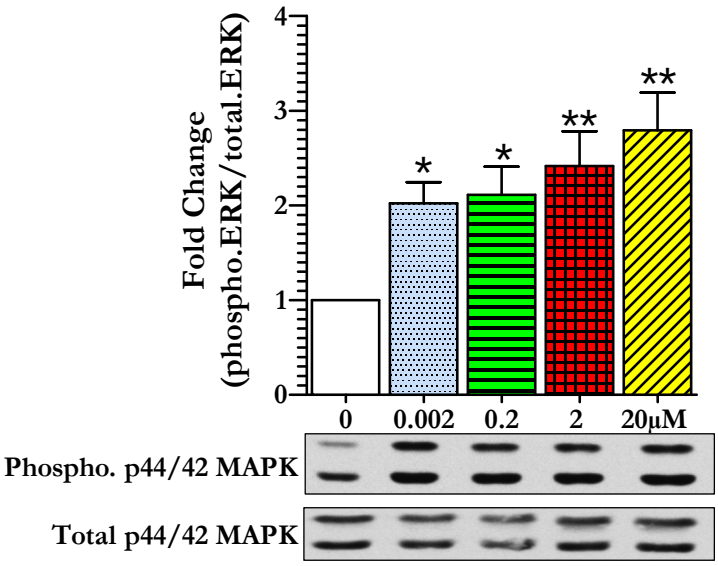

Figure 5.3B: Peroxynitrite Concentration Dependent Activation of ERK 1/2 in Cultured Pulmonary Artery Smooth Muscle Cells. Cells were maintained at basal stimulation with 0.1% foetal bovine serum. Expression of total and phosphorylated ERK 1/2 of mitogen activated protein kinase family was determined by western blotting; quantification was by densitometry. Statistical analysis was by Repeated measures ANOVA, post hoc test by Dunnett's test that compares treatment groups with relevant control $p<0.01$ (**) were considered significant; n=3

5.4.5.2. Time dependent ERK 1/2 activation- pulmonary artery endothelial and smooth muscle cells

The time course of ERK 1/2 activation by 0.2μM ONOO- was thus investigated. In response to 0.2μM ONOO-, PAEC showed time dependent increase in ERK 1/2 activation over a 60min period and phosphorylated ERK 1/2 levels remained significantly higher than in un-treated cells from 15th min of treatment and up to 1h (5.4A).

In PASMC, significant ERK 1/2 activation was sustained over a 12h period (Fig. 5.4B). Compared with PAEC (Fig. 5.4A), ERK activation was more rapid in PASMC (Fig. 5.4B). Relative to total ERK, significant activation in PASMC was seen at 2min after exposure to ONOO-. In addition, further increase in ERK 1/2 phosphorylation was observed up to 15min (Fig. 5.4B). This was followed by a slight decrease in ERK 1/2 expression; nonetheless, ERK levels were significantly higher than in untreated cells up to 12h (Fig. 5.4B).

5.4.6. The role of MEK 1/2 in peroxynitrite induced ERK 1/2 activation and pulmonary artery cell proliferation

The role of MEK 1/2, a regulatory kinase for the phosphorylation of ERK 1/2 in ONOO- induced pulmonary cell proliferation was examined. The stimulatory effects of ONOO- in PASMC under 2.5% FBS was observed in these experiments. Peroxynitrite at 0.2μM caused 148.6%±10.7 control increase in PASMC proliferation (Fig. 5.5A). Pre-treatment (1h) of control and ONOO- treated cells with 50μM PD09805 (MEK 1 inhibitor) resulted in significant inhibition of the proliferation recorded in both groups; 62.0%±5.4 and 55.7%±8.1, respectively (Fig. 5.5A). This suggests the involvement of activated MEK 1/2 in serum or ONOO- induced phosphorylation of ERK. In addition, it demonstrated that cellular hyper-proliferation reported in earlier experiments (chapter 4) was due to ERK activation. Initial experiments also showed that 0.2μM ONOO- further activated ERK 1/2 under high basal level of phosphorylated ERK 1/2 at 2.5% FBS (Fig. 5.5A; blot panel). Further experimentation involved the use of the dual MEK 1/2 inhibitor- U0126. The stimulatory effect of 0.2μM ONOO- at 0.1% serum (FBS) was completely abolished by 5μM U0126 (Fig 5.5B).

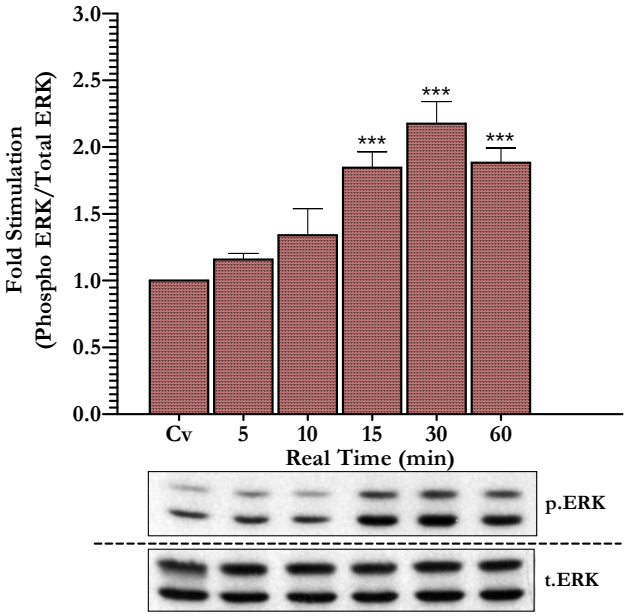

Figure 5.4A: Time Dependent Activation of ERK 1/2 by 0.2μM Peroxynitrite in Cultured Pulmonary Artery Endothelial Cells. Cells were maintained at basal stimulation with 0.1% foetal bovine serum. Expression of total and phosphorylated ERK 1/2 of mitogen activated protein kinase family was determined by western blotting; quantification was by densitometry. Statistical analysis was by 1-way ANOVA, post hoc test by Dunnett's test that compares treatment with control groups; $p<0.05$ (*), was considered significant. n=5.

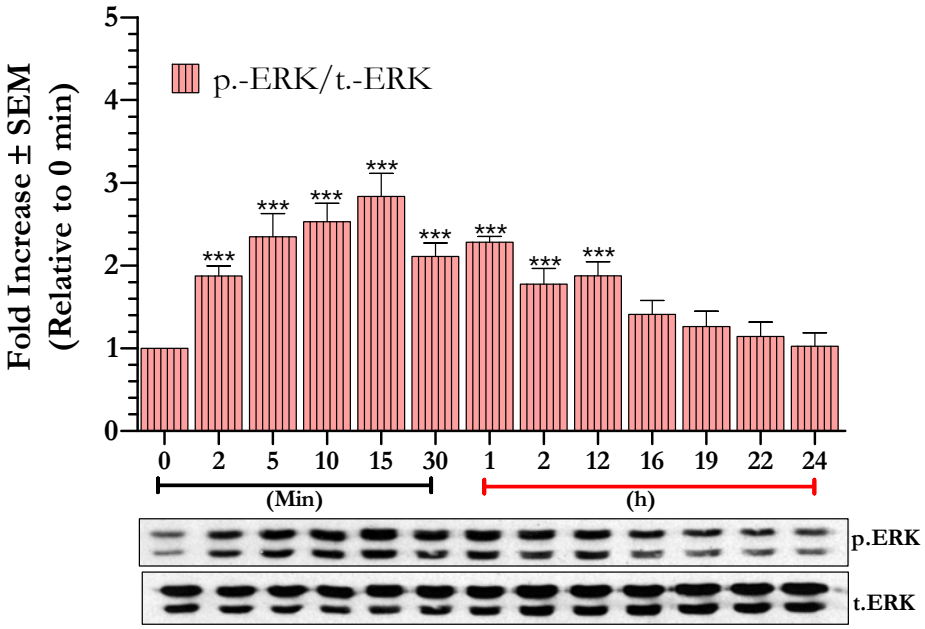

Figure 5.4B: Time Dependent ERK 1/2 Activation in Cultured Pulmonary Artery Smooth Muscle Cells. Cells were maintained at basal stimulation with 0.1% foetal bovine serum. Cells were stimulated with 0.2μM ONOO- for 0-24h. Expression of total and phosphorylated ERK 1/2 was determined by western blotting; quantification was by densitometry. Fold change in phosphorylated ERK for each treatment was calculated relative to the respective total ERK, and expressed as values normalised to control.. Statistical analysis was by 1-way ANOVA, post hoc test by Dunnett's test that compares treated with the untreated group (0min). $p<0.01$ (**) were considered significant. n=3

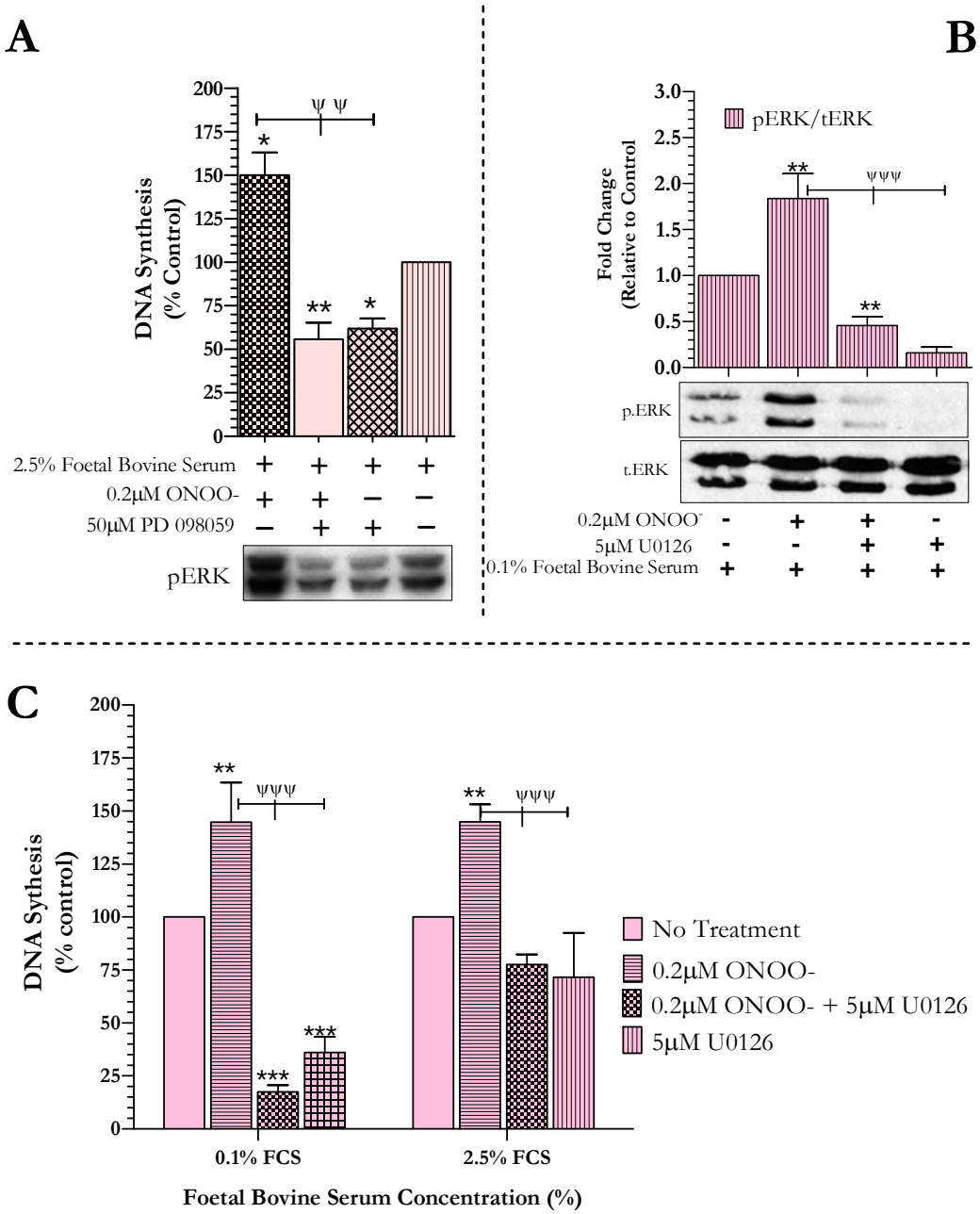

Figure 5.5: The Effect of MEK Inhibition on Peroxynitrite Induced ERK Phosphorylation and Pulmonary Cell Proliferation. (A): PASMC Cells were maintained at basal stimulation with 2.5% foetal bovine serum and stimulated as shown for 15min with or without 1h pre-treatment with PD098059, n=3. (B): PASMC Cells were maintained at basal stimulation with 0.1% foetal bovine serum and stimulated as shown for 15min with or without 1h pre-treatment with U0126. Expression of total and phosphorylated ERK 1/2 was determined by western blotting. Fold change in phosphorylated ERK for each treatment was calculated relative to the respective total ERK. Quantification was by densitometry and expressed as normalised to control; n=4 (Fig. A&B). (C): PAEC were stimulated as shown; DNA synthesis was determined by ^{3}-H-thymidine incorporation assay. Counts were measured in DPMs and expressed as percentage proliferation (± SEM) relative to proliferation in relevant control groups. Statistical analyses were by 1-way analysis of variance at each FBS concentration. Post hoc test was by Bonferroni's multiple comparison tests $p<0.05$ (*), <0.01 (**), <0.001 (***) were considered significant. Experiments in (C) were conducted in quadruplicates; n=4

Alone U0126 caused inhibition of ERK 1/2 activation in ONOO treated PASMC (Fig. 5.5B). Parallel experiments in PAEC showed that at 0.1% FBS, cell proliferation due to serum as well as the significant further increase in growth caused by 0.2μM ONOO- were together significantly attenuated by 5μM U0126 (Fig. 5.5C) to below baseline values. This demonstrates a significant effect of U0126 at 0.1% FBS (Fig. 5.5C). Under conditions of high growth factors, the ERK/proliferation inhibition effect of 5μM U0126 was expected to diminish. Accordingly, the effects of 5μM U0126 alone was not significant under 2.5% FBS; however, 0.2μM ONOO remained able to stimulate PAEC proliferation under this condition (Fig. 5.5C). Pre-treatment of ONOO treated PAEC with 5μM U0126 diminished cell proliferation but only to baseline values (Fig. 5.5C). Taken together, the western blot results demonstrated that both 0.1% serum and 0.2μM ONOO- stimulated PASMC proliferation via ERK 1/2 activation following upstream activation of MEK 1/2. However, the cell proliferation data with 2.5% serum is better evidence that ONOO- acts via stimulation of MEK.

5.4.7: Peroxynitrite induced ERK 1/2 activation and cell proliferation: effect of Raf-1 inhibition

Raf-1 is a serine-threonine protein kinase that functions in a protein kinase cascade important for mitogenic signaling (Avruch *et al.*, 1994). It is an up-stream kinase of MEK in the MAPK pathway of cell proliferation. The study investigated whether Raf-1 activation was pre-requisite for the mitogenic effects of peroxynitrite. The results are shown in Figure 5.6. The investigation involved the use of Raf-1 kinase inhibitor; this has been shown to disrupt the Raf-1/MEK1/2-ERK 1/2 signaling pathways, via Raf-1 kinase activity hereby abrogating the proliferation properties of this signaling pathway (Odabaei *et al.*, 2004). Pre-treatment of PASMC and PAEC with 10μM Raf-1 kinase inhibitor blunted ONOO- induced down-stream ERK 1/2 activation in PASMC (2.0±0.6 fold to 1.3±0.01 fold results not shown) and significantly inhibited proliferation in PAEC (Fig. 5.6).

.

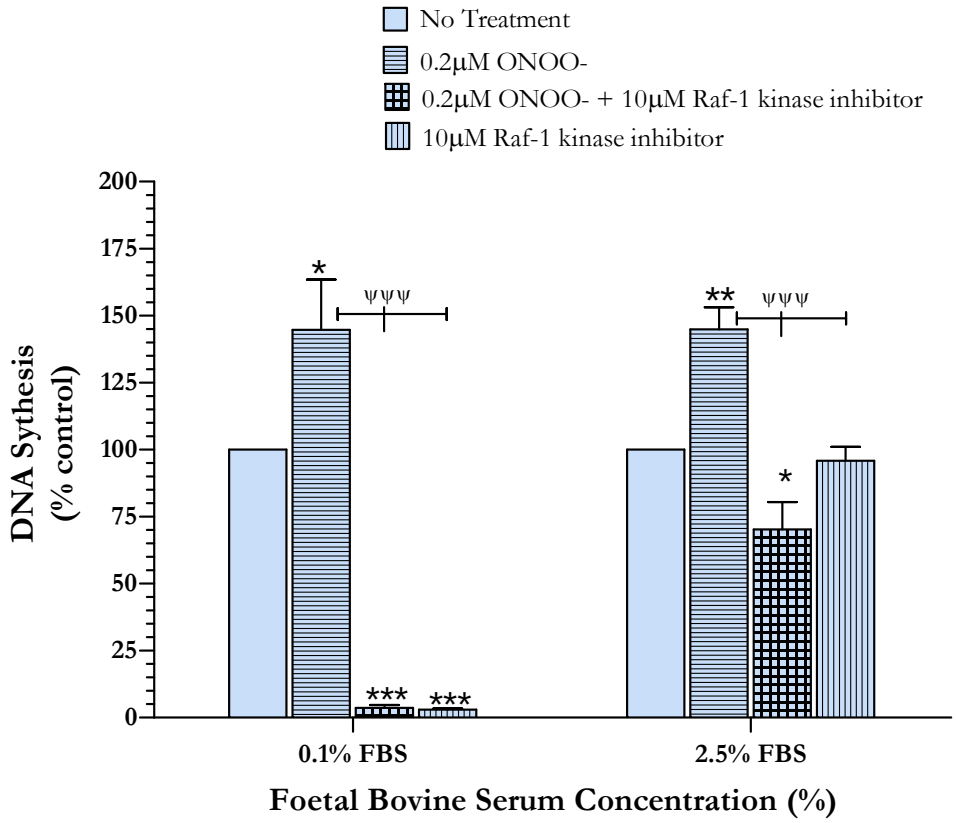

Figure 5.6: Peroxynitrite Induction of Pulmonary Artery Endothelial Cells Proliferation: the Effect of Raf-Kinase Inhibitor I. Cell were maintained at 0.1% and 2.5% foetal bovine serum (FBS). DNA synthesis was determined by ^{3}-H-thymidine incorporation assay. Counts were measured in DPMs and expressed as percentage proliferation (± SEM) relative to proliferation in relevant control groups. Statistical analyses were by 1-way analysis of variance at each FBS concentration. Post hoc test was by Bonferroni's multiple comparison tests $p<0.05$ (*), <0.01 (**), <0.001 (***) were considered significant. Experiments were conducted in quadruplicates; n=4

.

The changes in PAEC proliferation following exposure to ONOO- with or with pre-treatment with Raf-1 kinase inhibitor followed the pattern of proliferation reported for the U0126 experiments. At 0.1% FBS, 0.2μM ONOO- caused 144.7±18.7% control increase in PAEC ($p<0.05$; Fig. 5.6). This was diminished to 3.6± 1.1% control in the presence of 10μM Raf-1 kinase inhibitor ($p<0.01$; Fig. 5.6). Cell proliferation was equally reduced by the inhibitor in PAEC untreated with ONOO- (3.0±0.5% control; ($p<0.05$; Fig. 5.6). At 2.5% FBS, ONOO- remained able to stimulate cell proliferation (144.8±8.2% control; ($p<0.05$; Fig. 5.6). Raf-1 kinase inhibitor (10μM) significantly inhibited basal cell proliferation at 0.1 but not 2.5% FBS. In addition, this level of Raf-1 kinase inhibition significantly abolished the stimulatory effects of 0.2μM ONOO- in PAEC. Lower concentration of Raf-1 kinase inhibitor may have attenuated ONOO-induced proliferation with no effect on baseline growth at 0.1% FBS (Fig. 5.6). Again, the cell proliferation data with 2.5% serum is better evidence that ONOO- acts via stimulation of Raf-1.

5.4.8: Peroxynitrite induced ERK 1/2 activation and cell proliferation: effect of Ras inhibition

The role of Ras protein activation in mediating ONOO- induced stimulation of cell proliferation was investigated using a potent inhibitor of Ras activity. Ras is a critical component in cellular signal transduction associated with cell proliferation, however, without attachment to the cell membrane, Ras is not able to transfer signals from membrane receptors to intracellular signal molecules (Reuter *et al.*, 2000). The farnesyltransferase protein inhibitor (FTP II, III) target protein farnesyltransferase, block the transfer of farnesyl moiety to Ras which is necessary to attach Ras to the cell membrane. Under condition of 0.1% FBS, exposure of PASMC to 0.2μM ONOO- alone caused a 2.7 fold increase in PASMC proliferation (Fig. 5.7A; $p<0.01$). Though significant for the pathobiology of pulmonary hypertension, this is a modest increase in DNA synthesis compared with response of PASMC to growth factors. Alone platelet derived growth factor (PDGF) was used as positive control drug for the stimulation of the proliferation pathway; at 10ng/ml PDGF caused 156 fold increase in PASMC proliferation (Fig. 5.7A; $p<0.01$). In combination with 0.2μM ONOO-, proliferation increased further by 9-fold the growth in un-treated cells (Fig. 5.7A; $p<0.01$). Similar

proliferative responses of PASMC were recorded under condition of 2.5% FBS (results not shown). A 20h pre-treatment of PASMC with 25μM FTP III reduced the stimulatory effect of peroxynitrite and the combination with 10ng/ml PDGFto 0.51 and 0.63 fold relative to control, respectively (Fig. 5.7A; $p<0.01$). Pre-treatment of PAEC with FTP II prevented ONOO- or PDGF induced proliferative response (results not shown). Western blot analysis showed that both PDGF and ONOO- induced stimulation of PASMC proliferation were due to up-stream activation of Ras (Fig. 5.7B; $p<0.01$). Compared to un-treated PASMC, ERK 1/2 phosphorylation was approximately 2 and 4 fold higher in ONOO- and PDGF treated cells, respectively. However, the stimulatory effect of ONOO- but not PDGF was abolished by a 20h pre-treatment with 25μM FTP III. While Ras activity continued inhibited, it was puzzling that PDGF remained able to stimulate ERK 1/2 significantly in PASMC (Fig. 5.7B) without eliciting a proliferative response (Fig. 5.7A) in these cells.

.

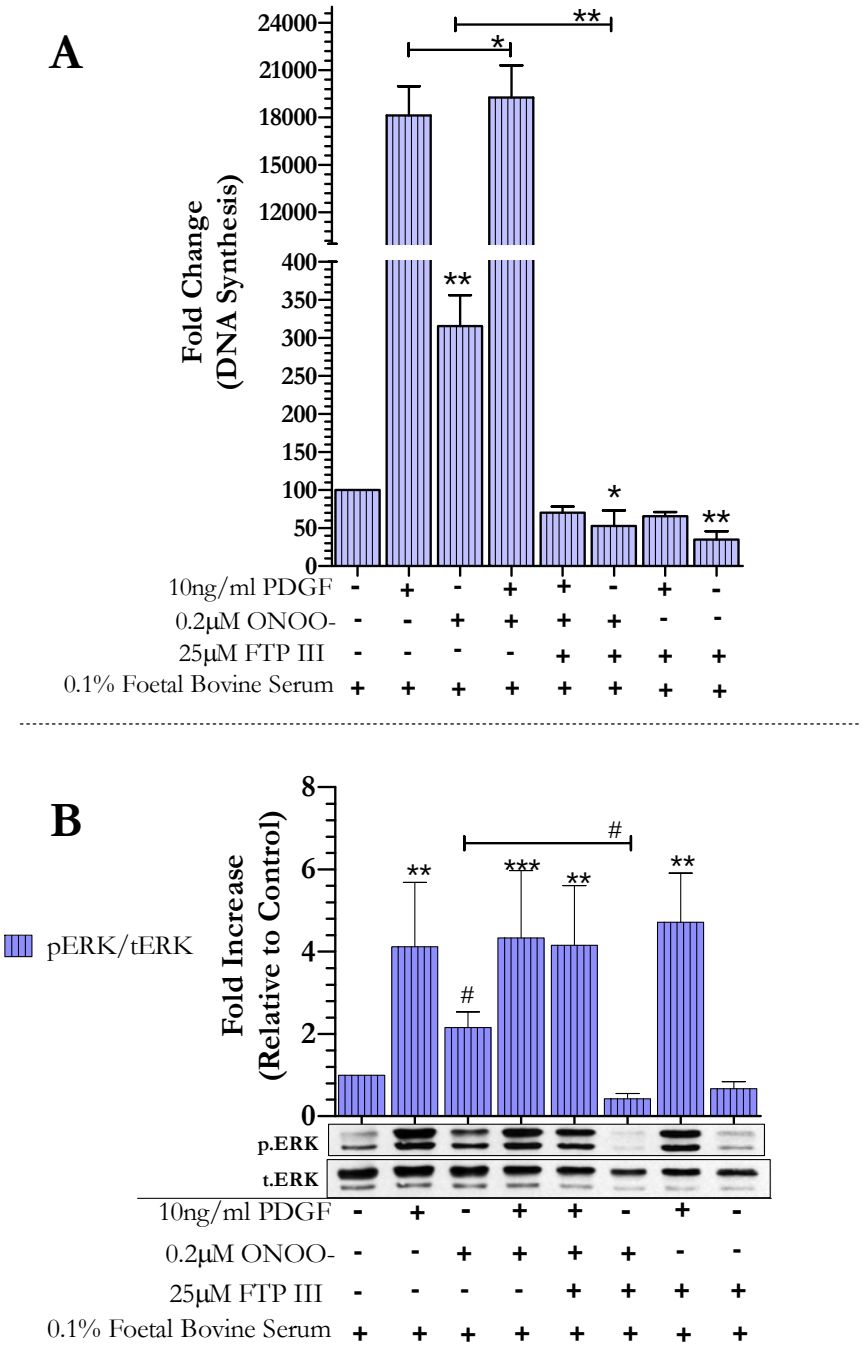

Figure 5.7: Peroxynitrite Induced Cell Proliferation and ERK 1/2 Activation: the Effect of Ras Inhibition. Pulmonary artery smooth muscle cells were maintained at 0.1% foetal bovine serum and received 20h pre-treatment with FTP III; cells were stimulated for 24h (A) or 15min (B) as shown. (A): DNA synthesis was determined by ^{3}-H-thymidine incorporation assay after 24h. Counts were measured in DPMs and normalised to untreated cells. (B): Expression of total and phosphorylated ERK 1/2 was determined by western blotting; quantification was by densitometry. Results were normalised to controls. Fold change in phosphorylated ERK for each treatment was calculated relative to the respective total ERK. Statistical analyses of figure A and B were by 1-way analysis of variance. Post hoc test was by Bonferonni's test of multiple comparison; $p<0.05$ (*), <0.01 (**), <0.001 (***) were considered significant; in Fig. A, n=4; in Fig. B, n=3; in Fig.B, # means significant were n=7.

5.4.9: PKC inhibition by Bisindolylmaleimide I (GF109203X): Effect on ERK 1/2 activation

The effects of inhibiting protein kinase C (PKC) in pulmonary cells stimulated to proliferate by ONOO- was investigated using bisindolylmaleimide I (GF109203X). This is a very potent and selective inhibitor of protein kinase C, selective for the α and β isoforms (Toullec *et al.*, 1991). The experiments also involved using downstream expression of ERK 1/2. PKC activation is closely linked with cell proliferation in several cell types. Using PMA as a PKC agonist, preliminary results showed concentration dependent activation of ERK in PASMC; 30nM PMA activated PKC the most (3.1 fold). This peaked at 5min and was followed by down-regulation of signal (to 20% maximum) over a 90 min period (results not shown). Further experiments in PAEC stimulated with 30nM PMA showed that 45min pre-treatment with GF109203X attenuated the downstream phosphorylation of ERK 1/2. The activation of ERK 1/2 by 30nM PMA was reduced to baseline by 10μM GF109203X (results not shown). In follow-up experiments, PAEC and PASMC were exposed to 0.2μM ONOO- with or without pre-treatmen with 10μM GF109203X. The result is shown in Figure 5.8. Peroxynitrite at 0.2μM stimulated PAEC proliferation following ERK 1/2 activation; these effects were significantly attenuated in cells pre-treated with 10μM GF109203X (Fig. 5.8A, B; $p < 0.05$). Alone, 0.2μM ONOO- caused 1.7±0.1 fold increase in ERK phosphorylation relative to untreated cells, however pretreatment of PAEC with PKC inhibitor decreased ONOO- induced ERK activation to baseline value (0.8±0.03 fold) (Fig. 5.8B).

.

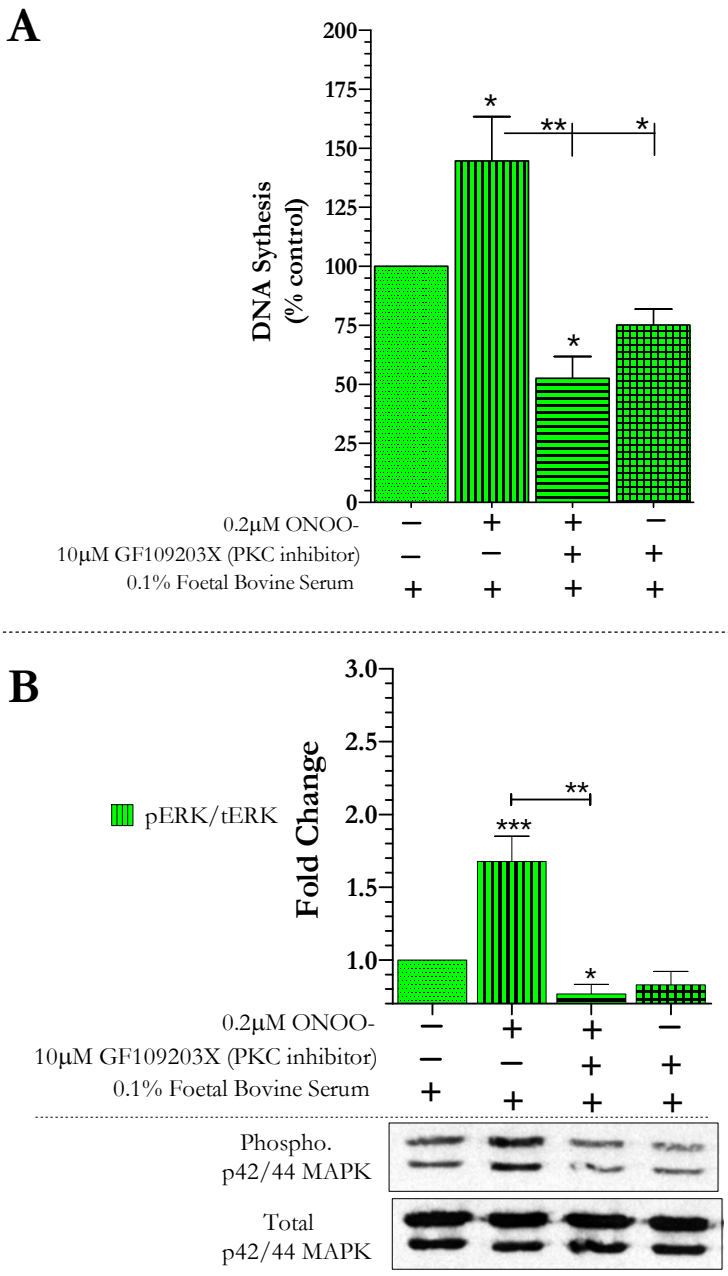

Figure 5.8 Peroxynitrite Induced ERK 1/2 Activation and Stimulation of Pulmonary Artery Endothelial Cell Proliferation: Effect of Inhibiting Protein Kinase C: (A): Peroxynitrite stimulation of pulmonary artery endothelial cells proliferation: the effects of protein kinase C inhibition. DNA synthesis was determined by ^{3}-H-thymidine incorporation assay. Counts were measured in DPMs and expressed as percentage proliferation (± SEM) relative to proliferation in relevant control groups. (B): Peroxynitrite activation of ERK 1/2 in pulmonary artery smooth muscle cells: the effects of protein kinase C inhibition. Cells were maintained at basal stimulation with 0.1% foetal bovine serum. Expression of total and phosphorylated ERK 1/2 was determined by western blotting; quantification was by densitometry. Results were normalised to controls. Fold change in phosphorylated ERK for each treatment was calculated relative to the respective total ERK. (Statistical analyses were by 1-way analysis of variance. Post hoc test was by Bonferroni's multiple comparison tests $p<0.05$ (*), <0.01 (**), <0.001 (***) were considered significant. n=3 for Fig.B. Experiments in Fig. A were conducted in quadruplicates; n=4.

5.4.10. The role of tyrosine kinase receptors in the initiation of peroxynitrite induced ERK 1/2 activation and stimulation of pulmonary cell proliferation

Using AG1296, a potent and selective inhibitor for platelet derived growth factor receptor (PDGFR) (Levitzki, 2004) and AG-1478 the selective inhibitor of epidermal growth factor receptor (EGFR) (Levitzki and Mishani, 2006), the study explored the role of growth factor receptors in the initiation of ONOO- induced activation of ERK 1/2 and the stimulation of proliferation in pulmonary cells.

5.4.10.1. The effect of inhibiting PDGF and EGF receptor tyrosine kinase activity

Platelet derived growth factor caused a significant 3-4 fold increase in ERK 1/2 activation and PASMC proliferation relative to untreated cells (Fig.5.9; $p<0.01$). The results were similar in PASMC treated with 100nM EGF (Fig.5.10; $p<0.01$). In both experiments, inhibition of the tyrosine kinase domain of the PDGF or EGF receptor by AG-1296 or AG1478, respectively resulted in the attenuation of ONOO- induced increase in cell proliferation and p42/44 phosphorylation (Fig.5.9; 5.10; $p<0.01$). Similarly, the tyrphostin AG-1296 and AG-1478 prevented the activation of ERK and the remarkable increase in PASMC proliferation caused by PDGF and EGF (Fig.5.9; 5.10; $p<0.01$), respectively

.

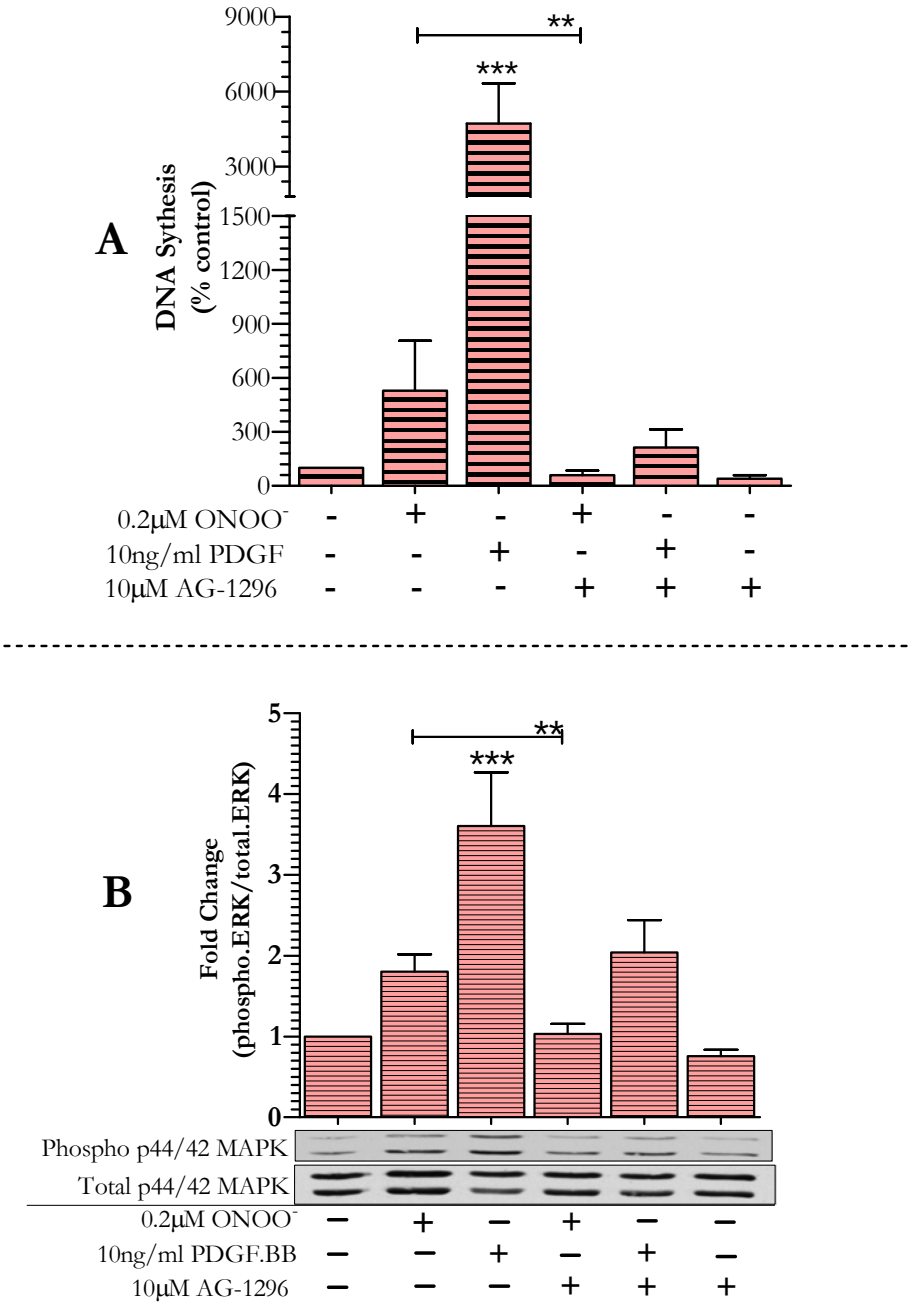

Figure 5.9: Peroxynitrite Induced ERK 1/2 Activation and Stimulation of Pulmonary Cell Proliferation: Effect of Inhibiting PDGF Receptor Tyrosine Kinase Activity (A):Peroxynitrite stimulation of pulmonary artery smooth muscle cells proliferation: the effects of inhibition by AG-1296. DNA synthesis was determined by ^{3}-H-thymidine incorporation assay. Counts were measured in DPMs (± SEM) (B): Peroxynitrite activation of ERK 1/2 in pulmonary artery smooth muscle cells: the effects of inhibition by AG-1296. Cells were maintained at basal stimulation with 0.1% foetal bovine serum. Expression of total and phosphorylated ERK 1/2 was determined by western blotting; quantification was by densitometry. Results were normalised to controls. Fold change in phosphorylated ERK for each treatment was calculated relative to the respective total ERK. Statistical analyses were by 1-way analysis of variance. Post hoc test was by Bonferroni's multiple comparison tests $p<0.05$ (*), <0.01 (**), <0.001 (***) were considered significant. n=4.

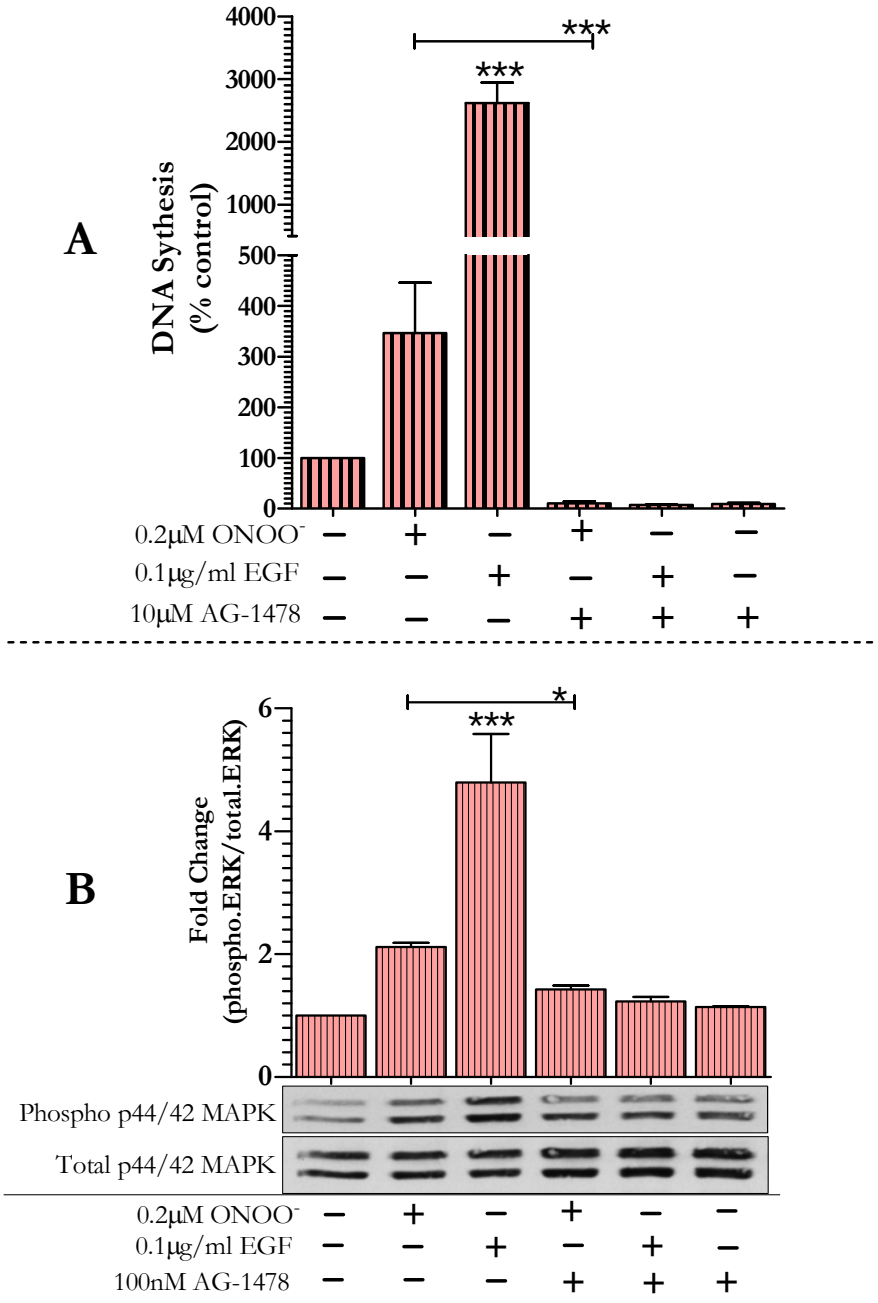

Figure 5.10: Peroxynitrite Induced ERK 1/2 Activation and Stimulation of Pulmonary Cell Proliferation: Effect of Inhibiting EGF Receptor Tyrosine Kinase Activity (A): Peroxynitrite stimulation of pulmonary artery smooth muscle cells proliferation: the effects of inhibition by AG-1478. DNA synthesis was determined by ^{3}-H-thymidine incorporation assay. Counts were measured in DPMs (± SEM) (B): Peroxynitrite activation of ERK 1/2 in pulmonary artery smooth muscle cells: the effects of inhibition by AG-1478. Cells were maintained at basal stimulation with 0.1% foetal bovine serum. Expression of total and phosphorylated ERK 1/2 was determined by western blotting; quantification was by densitometry. Results were normalised to controls. Fold change in phosphorylated ERK for each treatment was calculated relative to the respective total ERK. Statistical analyses were by 1-way analysis of variance. Post hoc test was by Bonferroni's multiple comparison tests $p<0.05$ (*), <0.01 (**), <0.001 (***) were considered significant. n=4.

5.4.10.2. The effect of Imatinib (STI-571) - A tyrosine kinase inhibitor

The therapeutic agent STI571 or Imatinib™ has been described as a rationally developed, potent, and selective inhibitor of the PDGF receptor tyrosine kinases which also inhibits abl tyrosine kinases, including bcr-abl (Druker and Lydon, 2000). It is currently licensed for the treatment of myeloid cells hyper-proliferation characteristic of chronic myelogenous leukemia (Mauro and Druker, 2001; Druker *et al.*, 1996). Imatinib is currently in clinical trial for the treatment of pulmonary hypertension (Novartis, 2009). In good agreement with the results from the tyrphostin AG-1296, AG-1478 (Fig. 5.9, 5.10), experimentation with Imatinib provided supportive evidence for the role of growth factor receptors in the initiation of ONOO- induced pulmonary cell proliferation and EKR 1/2 activation. Again, transient exposure of PAEC to 0.2μM ONOO- significantly increased cell proliferation relative to untreated cells (Fig 5.11A; $p<0.01$). However, a 1h pre-treatment of the cells with 5μM Imatinib completely abrogated this proliferative response (Fig 5.11A; $p<0.01$), without significantly affecting cell growth in untreated PAEC (Fig 5.11A). This confirmed that the proliferative effects of 0.2μM ONOO- can be effectively abrogated by the inhibition of PDGF tyrosine kinase activity.

5.4.10.2. Activity state of the PDGF receptor: probing for the effect of 0.2μM peroxynitrite

The PDGF receptor activity was assessed by a probe for phosphotyrosine formation at any of the tyrosine residues of the receptor (see inset Fig. 5.11B); this was termed 'global phosphotyrosine probe' (Fig. 5.11B). The expression of PDGF receptor phosphotyrosine was expected and examined at 190KDa. In PASMC, the result showed distinct and significant increase in phosphotyrosine formation following treatment with 0.2μM ONOO- or 10ng/ml PDGF, respectively (Fig. 5.11B, panel 1). This suggested receptor activation. In the same experiment, ONOO- or PDGF induced activation of the growth factor receptor was diminished by 10μM AG-1296- the PDGF tyrosine kinase inhibitor (Fig. 5.11B, panel 1). This provided further evidence that the phosphotyrosine formation was at the growth factor receptor site. Probe for PDGF receptor activation via phosphorylation at the 751 tyrosine residue confirmed activity for 10ng/ml PDGF but not 0.2μM ONOO- (Fig. 5.11, panel 2). The result suggests that while ONOO- remained able to activate growth factor receptor, its action is limited to specific receptor tyrosine residues. Further investigation will be required to determine the exact locus for ONOO- interaction with growth factor receptors

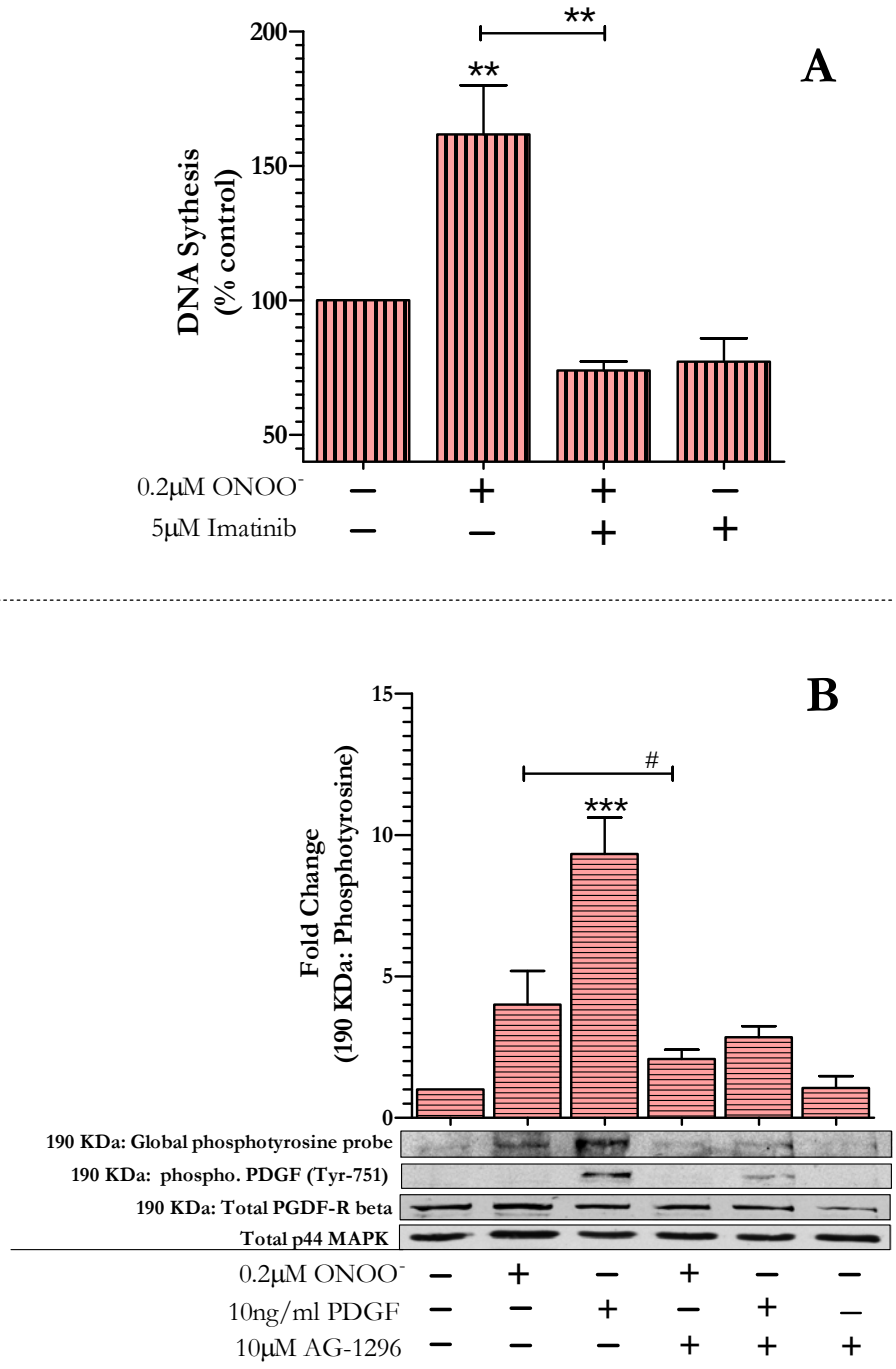

Figure 5.11: Peroxynitrite Induced ERK 1/2 Activation, Phosphotyrosine formation, and Stimulation of Pulmonary Cell Proliferation. Effect of Tyrosine Kinase Inhibition (A): Peroxynitrite stimulation of pulmonary artery endothelial cells proliferation: the effects of Imatinib. DNA synthesis was determined by ^{3}-H-thymidine incorporation assay. Counts were measured in DPMs and normalised to untreated cell (± SEM), n=4 (B): Probe for peroxynitrite activation of PDGF receptor in pulmonary artery smooth muscle cells; histogram show densitometry results for global phosphotyrosine probe. Cells were maintained at basal stimulation with 0.1% foetal bovine serum. Expression of phosphotyrosine, total ERK and total PDGF receptor was determined by western blotting; quantification was by densitometry. Results were normalised to controls. In Fig. A and B, statistical analyses were by 1-way analysis of variance. Post hoc test was by Bonferroni's multiple comparison tests $p<0.05$ (*), <0.01 (**), <0.001 (***) were considered significant. n=3-4; # means significant were n=12.

5.5. DISCUSSION

5.5.1. Preamble and main findings

The mitogen activated protein kinases mediate cellular responses to extra-cellular stimuli (MAPK; Robinson and Cobb, 1997). Of this family, the activation of extra-cellular signal regulated kinase 1 and 2 (ERK 1/2 or ERK) leads to cell survival and proliferation. For the first time, the current study demonstrated that at pathologically relevant yet scarcely reported low concentrations (2-200nM), $ONOO^-$ caused further activation of ERK and stimulated pulmonary cell proliferation over basal serum stimuli. Given the divergence of current evidence on the cascade of ONOO- induced events leading to ERK activation, this study provides converging evidence that ONOO- activates ERK by mechanisms involving activation of Ras, Raf-1 and MEK following growth factor receptor activation.

5.5.2. Peroxynitrite stimulates pulmonary cell hyper-proliferation independent of p38 MAPK and JNK

Experiments in which pulmonary cells were pre-treated with the ONOO- scavenger-ebselen confirmed the growth stimulatory actions of the anion (Fig. 5.1). In addition, the results suggest that ONOO- scavenging may prevent pulmonary cell hyper-proliferation under conditions of ONOO- induced oxidative stress. The current study also probed for the role of mitogen activated p38 MAPK and the stress activated protein kinase JNK in mediating the stimulatory action of ONOO-. Indeed, the molecular basis of some forms of pulmonary hypertension involve p38 MAPK activation (Weerackody *et al.*, 2009; Humbert *et al.*, 2004). However, the results of this study revealed that the potential role of ONOO- in provoking pulmonary cell hyperplasia or remodelling in pulmonary hypertension might not involve p38 MAPK or JNK activation. This is based on data, which showed that the ONOO- concentration stimulating pulmonary cell proliferation did not affect the activity state of p38 MAPK or JNK (Fig 5.2).

5.5.3. Peroxynitrite stimulates cell proliferation via Ras/ Raf-1/MEK/ ERK

The activation of ERK is a well established signal for cell proliferation in eukaryotic cells (Brown and Sacks, 2008; Robinson and Cobb, 1997; Geer *et al.*, 1994). Previous works have shown activation of ERK in various cell types, albeit by higher concentration peroxynitrite (Pesse *et al.*, 2005a; Kaji *et al.*, 2002; Bapat *et al.*, 2001; Jope *et al.*, 2000; Zhang *et al.*, 2000; Oh-Hashi *et al.*, 1999; Schieke *et al.*, 1999). The disparity in the reported mechanism by which ONOO- activated ERK is as varied as the cell type and ONOO- concentrations involved in these studies. For example, ERK activation by 50-1000μM ONOO– was shown to be dependent on Raf-1 in cardiomyocytes (Pesse *et al.*, 2005a) but not lung fibroblast (Zhang *et al.*, 2000). In the current study, ERK activation in pulmonary artery endothelial and smooth muscle cells was due to 2-200nM ONOO- (Fig. 5.3, 5.4). Separate experiments involving 0.2μM ONOO- showed that ERK phosphorylation was associated with the activation of Ras, Raf-1, MEK and PKC; the evidence is here evoked. Firstly, inhibition of MEK1/2 by U0126 and MEK-1 by PD098059 attenuated ERK activation and abolished the proliferative response of pulmonary cells to 0.2μM ONOO- (Fig. 5.5). PD98059 exerts its inhibitory effects by binding directly to the inactive or non-phosphorylated form of MEK thus blocking its activation by Raf (Favata *et al.*, 1998; Alessi *et al.*, 1995; Dudley *et al.*, 1995). U0126 however does not affect MEK phosphorylation but directly inhibits activation of ERK by MEK1 (Desilva *et al.*, 1998; Favata *et al.*, 1998). This confirmed that 0.2μM ONOO- induced ERK activation and the associated cell pulmonary cell proliferation were mediated via MEK. Secondly, the results in Figure 5.6 indicated that ERK activation and stimulation of pulmonary cell proliferation followed up-stream Raf-1 activation; since blocking Raf-1 kinase activity completely abolished both actions of ONOO-. Thirdly, ERK phosphorylation and cellular hyperproliferation were equally abrogated by the inhibition of the translocation of Ras by FTP II and III (Fig. 5.7), which are a highly selective and potent inhibitor of Ras farnesyltransferase. Taken together these results on one hand, demonstrate a pathway of ONOO- action in which the activation of an upstream principal target leads to the sequential phosphorylation of downstream kinases. This is in good agreement with published evidence that ONOO- activates ERK via Ras/Raf-1/MEK (Pesse *et al.*, 2005a; Upmacis *et al.*, 2004; Zhang *et al.*, 2000; Zouki *et al.*, 2000).

On the other hand, it is possible that ONOO- can directly activate these signalling molecules singly or in combination, although this study did not distinguish whether peroxynitrite was acting independently at these sites or at one site with consequential downstream effects. Nevertheless, several independent works has confirmed the direct effect of ONOO- on MAPK signalling molecules, albeit at higher concentration than tested in the current study. The effect of ONOO-on ERK 1/2 activity was measured by a kinase reaction which utilised Elk-1 fusion protein (a specific substrate of phospho-ERK 1/2); this showed that 50μM ONOO- activated ERK (Pesse *et al.*, 2005a). Also, Zhang et al., (2000) showed that ONOO- activated Raf-1 independent of upstream kinases. Furthermore, works in which Ras activity was measured have demonstrated increased Ras activity as a direct effect of 100μM peroxynitrite in endothelial cells (Clavreul *et al.*, 2006). In addition, ONOO– or SIN-1, induced activation of Ras in human neutrophils (Zouki *et al.*, 2000) and murine neural cells (Kaji *et al.*, 2002) has been reported. Studies have revealed that signaling by agents which modulate cellular redox status was prevented in cells in which Ras activity was blocked either through expression of a dominant negative mutant or by treating with a farnesyltransferase inhibitor (Oliveira *et al.*, 2003; Lander *et al.*, 1995). Given that ONOO- is a potent agent of oxidative stress (Szabo *et al.*, 2007), the direct activation of Ras by ONOO- is thus logical. Together, these findings also demonstrate the disparity in the literature evidence for the target of ONOO- action. The current study however showed that ONOO- activates them all namely; Ras, Raf-1, MEK, and ERK. In brief, this study opines that Ras, Raf-1 or MEK may be activated independently, or that one or more of these kinases could be the principal targets of ONOO-, which in turn activate downstream kinases.

5.5.4. The proliferative actions of ONOO-: growth factor dependent

The cascade of ERK phosphorylation involving the activation of growth factor receptors was observed in the pulmonary cells of this study. Exposure of PAEC and PASMC to PDGF, EGF or 0.2μM ONOO- stimulated cell proliferation and ERK phosphorylation; these effects were abrogated when cells were pretreated with AG-1296 (PDGFR inhibitor), AG-1478 (EGFR inhibitor), and AG-1296 or AG-1478, respectively (Fig. 5.9, 5.10). Given the selectivity of these inhibitors, these results

demonstrate that 0.2μM ONOO- activates PDGFR, EGFR or a very similar growth factor receptor. This result is in contrast to findings that effects of ONOO– on ERK were not influenced by AG-1478 in cardiomyocytes (Pesse *et al.*, 2005a) and hint that the specific pathway of ONOO- action may be ONOO- concentration and cell specific.

The current study showed that 0.2μM ONOO- caused 4.0±1.1 fold increase in the phosphorylation of PDGF receptor, in the same experiment PDGF alone caused a 9.3±1.3 fold increase (Fig 5.11B). In addition, both PDGF and ONOO- induced PDGFR phosphorylation were attenuated by AG-1296, which inhibits TKR activity. Together, these results revealed a principal target for ONOO-, the phosphorylation of which leads to the activation of downstream substrates. Previous works using much higher concentrations of peroxynitrite have shown that exposure to ONOO- can lead to the activation of both PDGF and EGF receptors and to the phosphorylation of ERK (Klotz, 2002). Exposure of human skin primary fibroblasts to 300μM peroxynitrite or 5mM SIN-1 led to the activation of phosphoinositide 3-kinase (PI-3K)/Akt pathway following the phosphorylation of EGFR, PDGFR-A and PDGFR-B (Klotz *et al.*, 2000). The authors demonstrated a clear induction rather than repression of tyrosine phosphorylation by peroxynitrite in the study in which the receptor were immunoprecipitated and examined for tyrosine phosphorylation by Western blotting (Klotz *et al.*, 2000). Further evidence for the involvement of PDGFR and EGFR were borne from data which showed that pre-treatment of cells with PDGFR kinase inhibitor AG-1295 or EGFR inhibitor AG-1478 before exposure to SIN-1 or peroxynitrite strongly inhibited the phosphorylation of Akt induced by either form of the anion (Klotz, 2002; Klotz *et al.*, 2000). In addition, a separate study found that peroxynitrite induced the dimerization of EGF receptors, an effect associated with EGF receptor activation, ERK phosphorylation and cellular hyper-proliferation (Van Der Vliet *et al.*, 1998). Together, these works have involved the use of >10μM ONOO, it is thus expected that the unreported biological consequences will include cell death (see chapter 3). While the present study has shown ERK activation at lethal ONOO- concentrations (≥2 μM; Fig. 5.3, chapter 3), it has also established hyper-proliferation and ERK activation in pulmonary cell exposed to 0.2μM and lower ONOO- concentrations (Fig. 5.1, 5.3). Interestingly, recent works have suggested the growth stimulatory (El-Remessy *et al.*, 2007) and tissue remodelling (Ichikawa *et al.*, 2008) potentials of 0.1 and 1μM

ONOO- in microvascular endothelial cells and human lung fibroblast, respectively. In stimulating cell proliferation, intracellular ONOO- acted as a signal molecule by sustaining the autophosphorylation of vascular endothelial growth factor receptor (El-Remessy *et al.*, 2007). Since protein tyrosine residues are targets for both nitration and oxidative phosphorylation, sufficiently low concentrations ONOO- may activate TKR by direct oxidative or nitrative interaction and promote a downstream cascade of events leading to cell proliferation. Independent evidence in NIH-3T3 cells confirmed that treatment with ONOO- can lead to receptor autophosphorylation (Yuen *et al.*, 2000). Taken together, these works provide supportive evidence that ONOO- is active, mitogenic and can activate growth factor receptors at the concentration investigated in the current study. This study has thus proposed a TKR dependent mechanism by which ≤ 0.2μM ONOO- might activate ERK and stimulate pulmonary cell proliferation (scheme 5.1). In addition, this study opines that the kinase activity of growth factor receptors is a suitable target for the control of ONOO- induced pulmonary cell hyper-proliferation.

All known protein tyrosine phosphatases (PTP) depend on the presence of a cysteine residue in their active site for action (Fauman and Saper, 1996). Oxidation of this cysteine residue inactivates the phosphatases, leading to a net increase in phosphorylation of proteins normally controlled by the phosphatases. Since ONOO- is cell permeable, it may act on pulmonary cell PTP and activate TKR by the transient inhibition of PTP sustained TKR dephosphorylation (scheme 5.1). A number of oxidants have been shown to activate growth factor signalling pathways and associated downstream events, at least in part, by this mechanism (Knebel *et al.*, 1996). In addition, peroxynitrite can inactivate a variety of phosphatases in-vitro (Takakura *et al.*, 1999). Accordingly and as previously demonstrated in vitro (Takakura *et al.*, 1999; Mallozzi *et al.*, 1997), ≤200nM ONOO- may activate tyrosine kinase receptors by oxidizing critical cysteinyl residue(s) of protein tyrosine phosphatases, leading to reversible catalytic inhibition of the phosphatases (Kappert *et al.*, 2005; Klotz *et al.*, 2002). This will be in good agreement with views that ONOO- induced oxidative inactivation of tyrosine phosphatases promote kinase activities (Ischiropoulos, 2002; Klotz et al., 2002) (scheme 5.1). PDGF-β receptors and other tyrosine kinases involved in smooth muscle cells proliferation and migration has been shown to be regulated by PTPs (Persson *et al.*,

2004; Östman and Böhmer, 2001). In addition, it was expected that the nitrating and oxidizing actions of peroxynitrite would lead to modification of receptors and other signalling molecules. Consequently, the pathway leading to phosphorylation of ERK and cell proliferation may become more readily stimulated due to inactivation of regulating enzymes (PTPs) (scheme 5.1).

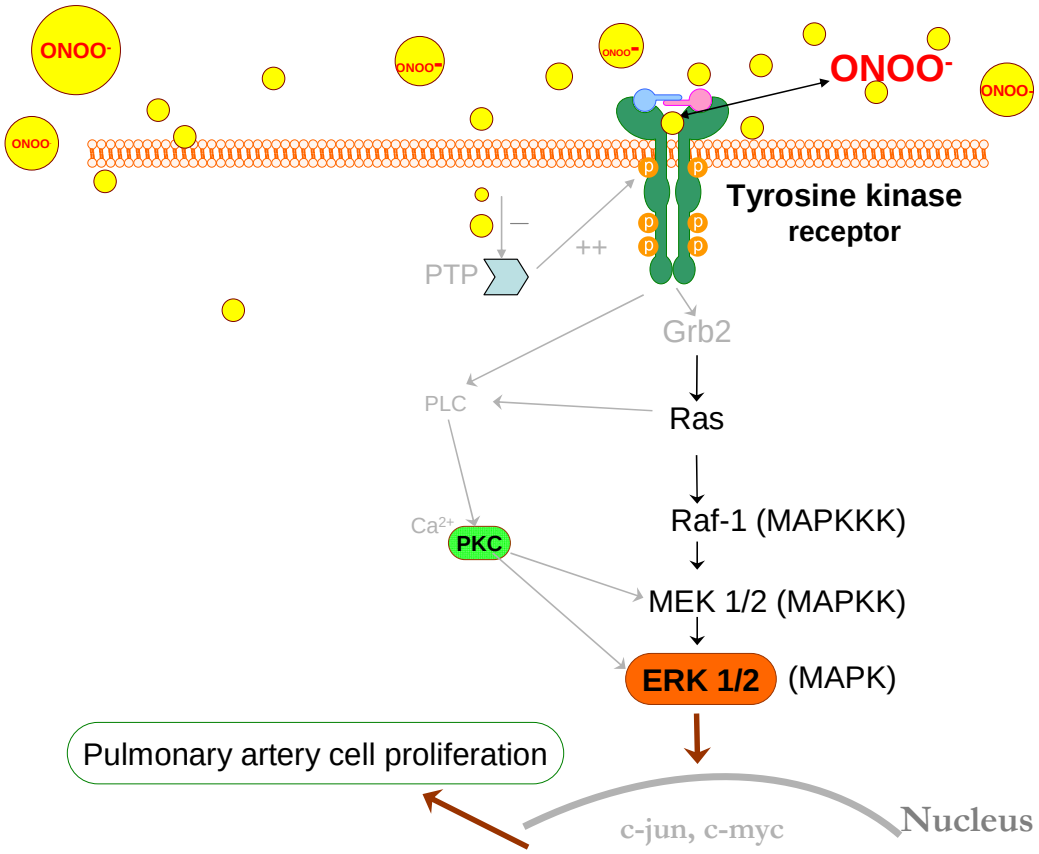

Scheme 5.1: Proposed tyrosine kinase receptor (TKR) dependent mechanism of peroxynitrite induced ERK activation and pulmonary cell hyper-proliferation. Peroxynitrite induced phosphotyrosine formation at specific tyrosine residue leads to receptor dimerisation and tyrosine kinase autophosphorylation. Likely following the phosphorylation of Grb-2, this leads to the activation of Ras-Raf-MEK-ERK and the requisite transcription factors for cell proliferation (c-myc, c-jun). PKC dependent ERK activation and cell proliferation might be Ras induced or following TKR activation of phospholipase C (PLC). Also, since ONOO- is cell permeable and can be intracellularly generated, it may act on pulmonary cell protein tyrosine phosphatises (PTP). Hence, peroxynitrite at ≤0.2μM ONOO- may activate tyrosine kinase receptors by oxidizing critical cysteinyl residue(s) of protein tyrosine phosphatises, leading to reversible catalytic inhibition of the phosphatases (Klotz *et al.*, 2002). Thus activating TKR by the inhibition of dephosphorylation.

.

5.5.5. The proliferative actions of ONOO-: by an ancillary mechanism

The present study provided data to suggest an auxiliary pathway independent of Ras/Raf-1 by which ONOO- may act to stimulate cell proliferation. Simultaneous inhibition of protein kinase C (PKC) abrogated the ERK activation and proliferative response of pulmonary cells to ONOO- (Fig. 5.8). This suggests that ONOO- may activate PKC directly or secondary to the activation of an upstream signalling molecule. Earlier works showed that ONOO- promoted the phosphorylation of ERK in rat-1 fibroblasts, via activation of calcium dependent PKC in a MEK independent pathway (Bapat *et al.*, 2001). Also, down regulation of PKC following 24h pretreatment with phorbol-12,13-dibutyrate caused significant reduction in ERK1/2 phosphorylation. Since MEK is the only physiological substrate of Raf-1 (Kyriakis *et al.*, 1992), this findings suggests a direct effect of PKC on ERK (scheme 5.1). On one hand, peroxynitrite induced PKC activation may be TKR dependent if acting via Ras (scheme 5.1) or phosphoinositide 3-kinase as separate evidence suggests that 50μM ONOO- may activate PKC via phosphoinositide 3-kinase dependent pathway in bovine aortic endothelial cells (Xie *et al.*, 2006). On the other hand, phospholipase A or C dependent but TKR independent activation of PKC may account for ERK activation independent of Ras/Raf-1 (scheme 5.1). Albeit at higher concentration, it has been reported that in response to peroxynitrite, smooth muscle cells initiated MEK/ERK cascade leading to cytosolic phospholipase A_2 ($cPLA_2$) activation (Upmacis *et al.*, 2004). In turn, phospholipase C (Yagasaki *et al.*, 2002; Stone *et al.*, 1988) or $cPLA_2$ (Chen *et al.*, 1999; Qiu and Leslie, 1994) has been shown to cause PKC activation. It is possible that even lower concentrations of ONOO- can act via one or more of these pathways as demonstrated in this study with ERK activation by both growth stimulating and cytotoxic concentrations of ONOO- (Fig. 5.3). The results of the current study suggest that PKC dependent ERK activation is a component of the proliferative action of peroxynitrite at the low concentration investigated. However, a key limitation in these experiments is the broad spectrum inhibitory action of PKC inhibitor (GF109203X) at 10μM. Further studies involving the effect of 0.2μM ONOO- on PKC activity will therefore be required to demonstrate the contribution of PKC to the proliferative actions of low concentration ONOO-.

5.5.6. Conclusion

The study reports on the novel finding that 0.2μM ONOO- activated PDGF or EGF receptor to cause further activation of ERK and stimulated cell proliferation over basal serum stimuli. This action was mediated by activated Ras, Raf-1 and MEK. The kinase activity of growth factor receptors is thus suggested as suitable target for the modulation of pulmonary cells hyperplasia in pulmonary hypertension.

.

CHAPTER 6

THE EFFECTS OF HYPOXIA ON THE PROLIFERATIVE RESPONSE OF PULMONARY ARTERY CELLS TO PEROXYNITRITE

.

6.1 INTRODUCTION

The World Health Organisation classification of pulmonary hypertension (Group 3) highlights the involvement of hypoxia in several forms of the disease (Simonneau *et al.*, 2004). Under hypoxic conditions, human PAEC reduce the production of vasodilatory and anti-mitogenic mediators such as nitric oxide (Takemoto *et al.*, 2002). In addition, PAEC produce vasoconstrictive and pro-proliferative factors such as endothelin (ET)-1, angiotensin II and thromboxane A_2 under hypoxic conditions (Humar *et al.*, 2002; Mukhopadhyay *et al.*, 1995; Kourembanas *et al.*, 1991). Similar effects of hypoxia has been reported in smooth muscle cells (Humar *et al.*, 2002; Eddahibi *et al.*, 1999). Alone, chronic hypoxia have stimulated the proliferation of endothelial cells of the main and pre-capillary pulmonary arteries (Howell *et al.*, 2003; Meyrick and Reid, 1979) and can lead to vascular wall thickening, eventually restriction of vessel lumen and increased vascular resistance (Pak *et al.*, 2007; Meyrick and Reid, 1979).

The literature is divergent on the effect of acute hypoxia on smooth muscle cells. On one hand, several published data report that acute hypoxia is a trigger for events culminating in smooth muscle cell proliferation (Michiels *et al.*, 1994; Vender, 1992). Hypoxia induced proliferation of PASMC have been associated with upregulation in the expression of the primary receptor for PDGF-β, activation of Rho protein and its downstream effector, Rho-kinase and the stimulation of protein kinase C (Cooper and Beasley, 1999; Frid *et al.*, 1997a; Frid *et al.*, 1997b; Dempsey *et al.*, 1991). On the other hand, some studies report that acute hypoxia had no effect (Lanner *et al.*, 2005) or decreased PASMC proliferation (Stiebellehner *et al.*, 2003; Eddahibi *et al.*, 1999). It is possible that these differences in the literature are in part due to interplay of different experimental conditions, such as different levels of hypoxia and different background stimulation. For example under basal stimulation from 5% FBS (Lanner *et al.*, 2005) or 10% FBS (Stiebellehner *et al.*, 2003), PASMC were not stimulated to proliferate in response to 3% O2 (PO2 = 23±2 mm Hg) hypoxia alone. Conversely, PASMC proliferation was demonstrated under conditions of 3% 02 and 0.1% FBS (Dempsey *et al.*, 1991) or 5% O_2, and 2% FBS (Cooper and Beasley, 1999). Using a range of basal stimulation conditions and oxygen concentrations, this study therefore aimed to provide baseline data for the effect of acute hypoxia on PASMC and PAEC. In addition, since peroxynitrite (ONOO-) is up-regulated in the lungs of patients with pulmonary

hypertension (Bowers *et al.*, 2004; Demiryürek *et al.*, 2000), the current study sought to simulate the effects of this powerful oxidizing and nitrating agent in hypoxic lung conditions. Currently this remains largely unknown. This study therefore hypothesized that the proliferative response of pulmonary cells to ONOO- (reported in chapter 4, 5) could be aggravated under experimental hypoxic condition.

6.2. OBJECTIVE

(1): To determine the responses of PAEC and PASMC to acute mild, moderate and severe levels of experimental hypoxia; which correspond to 10%, 5% and 1% (oxygen), respectively (2): To explore the effects of acute decline in ambient oxygen on the proliferative response of pulmonary artery cells to low concentration ONOO- (3): To investigate whether pulmonary artery cells generate ONOO- under experimental hypoxia conditions.

6.3. METHODS

6.3.1. Growth of Cells in Hypoxic and Normoxic Environment

Bovine PAEC or PASMC were seeded simultaneously into pairs of 24 well plates (WP) and quiesced under 0.1% foetal bovine serum (FBS) for 24h. Thereafter, each pair of 24 WP were split and assigned to normoxic or hypoxic treatment. Cells were maintained under 0.1, 0.5 and 2.5% FBS baseline growth conditions for 24h treatment period. The FBS concentrations were chosen to reproduce the conditions under which pulmonary cells were stimulated to proliferate in response to ONOO- (see chapter 4). Cells were stimulated with 2μM SIN-1 alone or combined with 100RLU/s superoxide generated by 10^{-8}M xanthine and 1.0mU xanthine oxidase or left un-stimulated. In parallel experiments, PASMC were stimulated with 2nM or 0.2μM ONOO- under conditions of 0.1, 0.5 and 2.5 FBS. Cells were then incubated under hypoxic conditions of 1% or 5% or 10% oxygen for 24h; these oxygen concentrations were chosen to represent experimental severe, moderate and mild hypoxia, respectively. Control experiments involved incubation of cells under normoxic conditions (21% oxygen) for the same period. The formation of new DNA was assessed by ^{3}H-thymidine incorporation assay as previously described (Chapter 3) and cell number was determined with the aid of haemocytometer as previously described in (Chapter 3).

6.3.2. Oxygen concentration determination and regulation

A humidified temperature-controlled incubator (RS.BIOTECH Galaxy oxygen-CO_2) was used as a hypoxic chamber. This incubator regulates as set, the internal oxygen levels within its chambers between 0 and 21% via the balance of influx of oxygen and nitrogen gases with CO_2 level maintained at 5%. The incubator was switched to hypoxia, i.e 1% or 5% or 10% oxygen during experimentation. Oxygen concentration within the incubator was read off the monitor; values within the cell culture medium were determined by immersing an oxygen electrode (Strathkelvin Instrument) via an aperture into cell culture flask in a separate experiment. The oxygen electrode was calibrated to zero before experimentation using sodium sulphite 100nM in disodium teraborate 10mM and to PO_2 at sea level by immersing the electrode into distilled water bubbled with 21% O_2, 5% CO_2, 75% N_2 gas mixture at 37^0C.

6.3.2. Western Blot Analysis

Using PASMC, Western blot analysis was carried as previously described in chapter 3. The primary antibody incubation step however involved the use of nitro-tyrosine antibody (cell signalling, cat#: 9691; at 1:1000 dilution).

.

6.4. RESULTS

6.4.1 Oxygen concentration measurement

The incubator oxygen level reached 5% set limit within 15min; however, the oxygen concentration in the pulmonary cell culture medium within the well plates with the lid closed did not reach the set value (5% O_2) until after 6h. Once attained oxygen levels within the cell culture medium and the incubator remained at equilibrium for 24h incubation period (data not shown).

6.4.2. The effect of acute exposure to 10% (oxygen) hypoxia

Newly formed DNA in bovine PAEC exposed to 10% hypoxia did not differ significantly from values in cells kept under normoxia (21% oxygen). The results were similar at all FBS concentrations investigated (Fig. 6.1A). Further experiments were conducted to investigate the effect of 10% hypoxia on the proliferative response of PAEC to 2μM SIN-1 (Fig. 4.8, chapter 4). The results (2μM SIN-1 = 109±4% control; 10% hypoxia= 100±9.4% control; 2μM SIN-1 + 10% hypoxia = 127.5±13% control; $p>0.05$) demonstrated that this level of hypoxia did not significantly affect PAEC response to 2μM SIN-1. Conversely, 10% (O_2) hypoxia alone caused significant stimulation of PASMC; this was significant at 0.5 and 2.5% FBS conditions, respectively (Fig. 6.1B). This result suggests a primary role for PASMC in the proliferative response of pulmonary artery cells to 10% (O_2) hypoxia.

6.4.3. The effect of acute exposure to 5% (oxygen) hypoxia: -

6.4.3.1. In pulmonary artery endothelial cells

Alone 5% (O_2) hypoxia stimulated the proliferation of PAEC significantly at 2.5% FBS; Fig. 6.2A). A similar effect was recorded in PAEC under 0.5% FBS (148±10% control). Again, SIN-1 was used to study the effects of 5% (O_2) hypoxia in PAEC exposed to sustained release of ONOO- (as previously demonstrated in chapter 2). As reported in chapter 4, 2μM SIN-1 stimulated PAEC proliferation to 144.4±4.2% control (Fig. 6.2A). Although the mean fold proliferation was highest in 2μM SIN-1 treated cells exposed to hypoxia (5% O_2), statistically this was not significantly different from SIN-1 or hypoxia induced increase in proliferation (Fig. 6.2A).

6.4.3.2. In pulmonary artery smooth muscle cells

Hypoxia alone (5% O_2) significantly stimulated the proliferation of PASMC under 0.1%, 0.5%, 2.5% and 15% serum conditions (Fig. 6.2B, 6.3; $p<0.05$). At 0.1 (5% hypoxia = 221±18% control; hypoxia + 0.2μM ONOO- =136±16% control) and 2.5% FBS condition (Fig. 6.2B), the proliferative response of PASMC to 0.2μM ONOO- under 5% (O_2) hypoxia was similar to the effects of 5% (O_2) hypoxia alone (Fig. 6.2B). Similar observations were made at 0.5 FBS in PASMC treated with 20nM SIN-1 (5% hypoxia = 198±49% control; hypoxia + 20nM SIN-1 = 251±9% control). Separate experiments were conducted to investigate the effect of 5% (O_2) hypoxia on PASMC exposed transiently to 2nM ONOO-. The result is shown in Figure 6.3. Alone hypoxia (5% O_2) remained able to significantly stimulate PASMC proliferation at 0.1, 0.5 and 2.5% FBS ($p<0.05$). In addition, 2nM ONOO- alone caused significant increase in cell proliferation at 0.5, 2.5 but not 0.1% FBS. Again, at 0.1, 0.5 or 2.5% FBS the proliferative response of PASMC to 2nM ONOO- under 5% (O_2) hypoxic condition was similar to effects of 5% (O_2) hypoxia alone (Fig. 6.3).

6.4.4. The effect of acute exposure to 1% (oxygen) hypoxia: -

Further reduction in oxygen concentration to 1% caused loss of the proliferative response of PAEC or PASMC to hypoxia alone or the combination with ONOO- (Fig. 6.4). Hypoxia at 1% (O_2) significantly inhibited the proliferation of PAEC (Fig. 6.4A; $p<0.01$) at 2.5% FBS but not PASMC at 0.1 or 2.5% FBS (Fig. 6.4B).

.

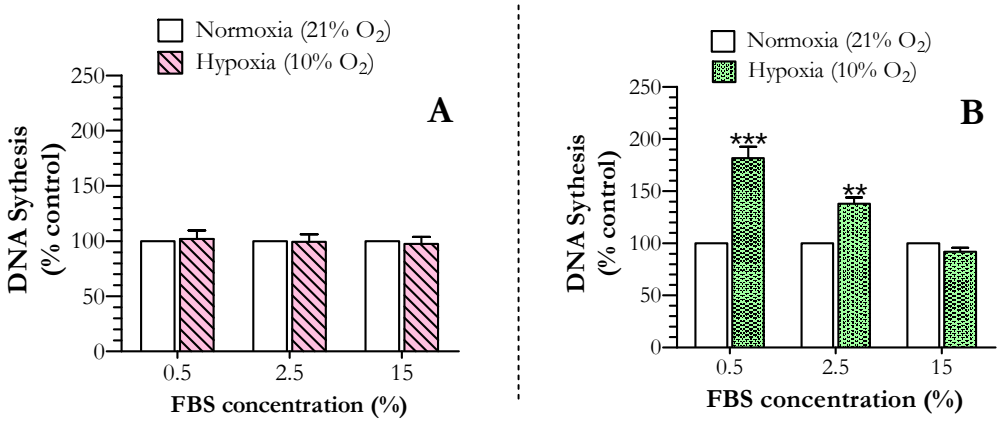

Figure 6.1: The Effect of Acute Exposure of Bovine Endothelial (A) and Smooth Muscle Cells (B) to Mild Hypoxia (10% Oxygen). DNA synthesis was determined by ^{3}H-thymidine incorporation assay. Counts were measured in DPMs (disintegrations per minute ± SEM) and normalised to DNA synthesis in control group (normoxia, 21% O_2). Statistical evaluations were by paired sample t-test at each FBS concentration. p<0.01 (**), <0.001 (***); n=5.

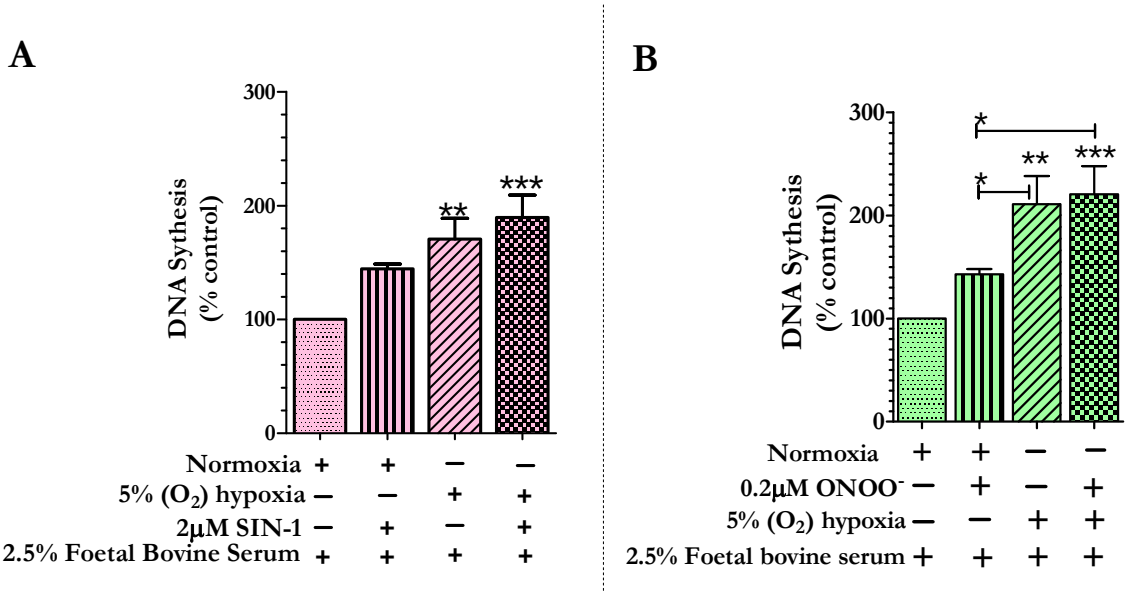

Figure 6.2: The Effect of 5% (Oxygen) Hypoxia on Pulmonary Artery Endothelial (A) and Smooth Muscle Cells (B) Treated With 2μM SIN-1 or Authentic Peroxynitrite (ONOO-). In A and B, cells were treated with the peroxynitrite generator, 3-Morpholinosydnonimine (SIN-1) or ONOO-, respectively. DNA synthesis was determined by ^{3}H-thymidine incorporation assay. Counts were measured in DPMs (disintegrations per minute ± SEM) and normalised to DNA synthesis in control group (normoxia, no ONOO- or SIN-1 treatment). Statistical evaluations were by one-way analysis of variance. A post hoc (analysis) investigation was by Boferonnis test of multiple comparison. ** =p< 0.01 or *= p< 0.05 was considered significant relative to control (normoxia, no ONOO- or SIN-1 treatment); experiments were conducted in quadruplicates (no of wells); n=7.

.

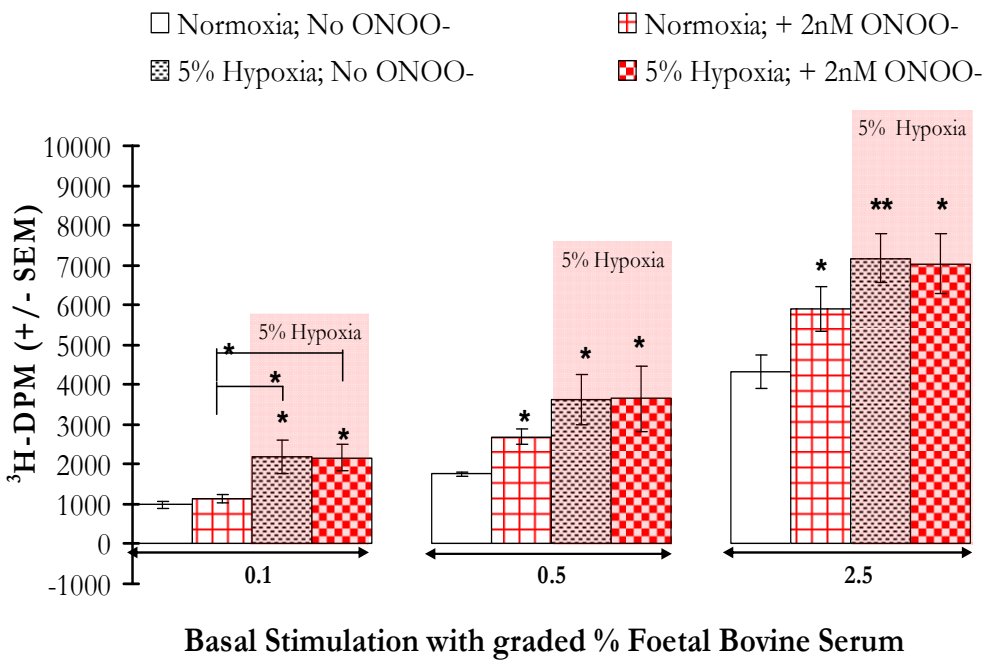

Figure 6.3: The Effect Hypoxia Alone (5% oxygen) and Combination With 2nM Peroxynitrite on Bovine Smooth Muscle Cell Proliferation. DNA synthesis was determined by ^{3}H-thymidine incorporation assay. Counts were measured in DPMs (disintegrations per minute ± SEM). Statistical evaluations were by 1-way analysis of variance at each FBS level. Post hoc investigations were by Bonferroni' test of multiple comparisons. ** =p< 0.01 or *= p< 0.05 was considered significant relative to control (normoxia, no ONOO- treatment); experiments were conducted in quadruplicate; n=7-8

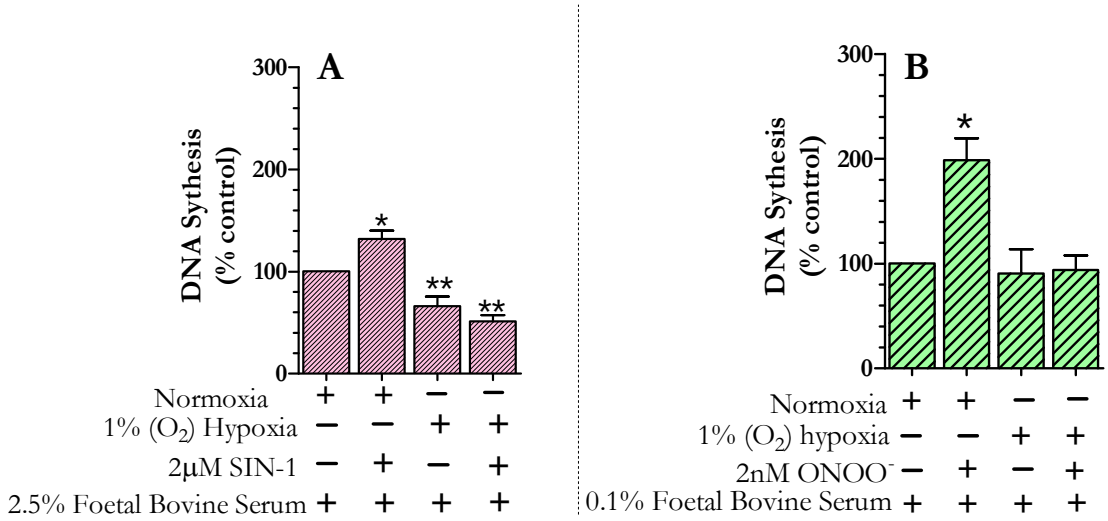

Figure 6.4: Effect of Severe Hypoxia (1% Oxygen) on the Proliferative Response of Pulmonary Artery Cells to Peroxynitrite. Pulmonary artery endothelial (A) or smooth muscle cells (B) were maintained under basal growth stimulus from 2.5% or 0.1% FBS, respectively and treated as shown. DNA synthesis was assessed by ^{3}H-thymidine incorporation assay. Counts were measured in DPMs (disintegrations per minute) and expressed as percentage proliferation (± SEM) relative to proliferation in un-stimulated cells under normoxia. Statistical evaluations were by 1-way analysis of variance. Post hoc investigations were by Bonferroni' test of multiple comparisons. *= p< 0.05 or *= p< 0.01 was considered significant relative to control (normoxia, no ONOO- treatment); experiments were conducted in quadruplicates; n=6

6.4.5. Pulmonary cell proliferative response to hypoxia: effect of scavenging peroxynitrite

The consequences of simultaneous treatment with a peroxynitrite scavenger on the proliferative response of pulmonary cells to ONOO- and or hypoxia were examined using ebselen (5uM). This drug is known to react with peroxynitrite (OONO-) and abolish its actions (Masumoto and Sies, 1996; Schewe, 1995). Cell proliferation increased by approximately 2-fold control values in PASMC stimulated with 0.2μM ONOO- (Fig. 6.5). Exposure of ONOO- treated PASMC to 5% (O_2) hypoxia significantly increased this response further to 4.5 fold control values (Fig. 6.5; $p<0.01$). However, this was not significantly different from the effects of 5% (O_2) hypoxia alone (Fig. 6.5; $p>0.05$). The proliferative response of PASMC to 0.2μM ONOO- (reported in Fig. 5.1; chapter 5) but also to 5% (O_2) hypoxia were attenuated by simultaneous treatment with 5μM ebselen (Fig. 6.5; $p<0.01$).

6.4.6. The formation of nitro-tyrosine in pulmonary artery cells under hypoxia

Treatment of PASMC with 0.2μM ONOO- caused significant increased in nitro-tyrosine formation (Fig. 6.6). Interestingly, PASMC exposed to moderate (5% O_2) hypoxia expressed nitro-tyrosine to similar extent and intensity as cells treated with authentic ONOO- alone (Fig. 6.6). For both treatments, the expression of nitro-tyrosine was prominent in 60-65 kDa band of proteins. In some experiments, this was also seen to increase at 9-12 kDa and 35-40 kDa of proteins, when compared to untreated cells (Fig. 6.6). In addition, the combination of ONOO- and hypoxia showed strong bands at 60-65 kDa indicating marked nitro-tyrosine formation (Fig. 6.6). Again, this was not significantly different from nitro-tyrosine formation due to 0.2μM ONOO- or 5% (O_2) hypoxia alone (Fig. 6.6).

.

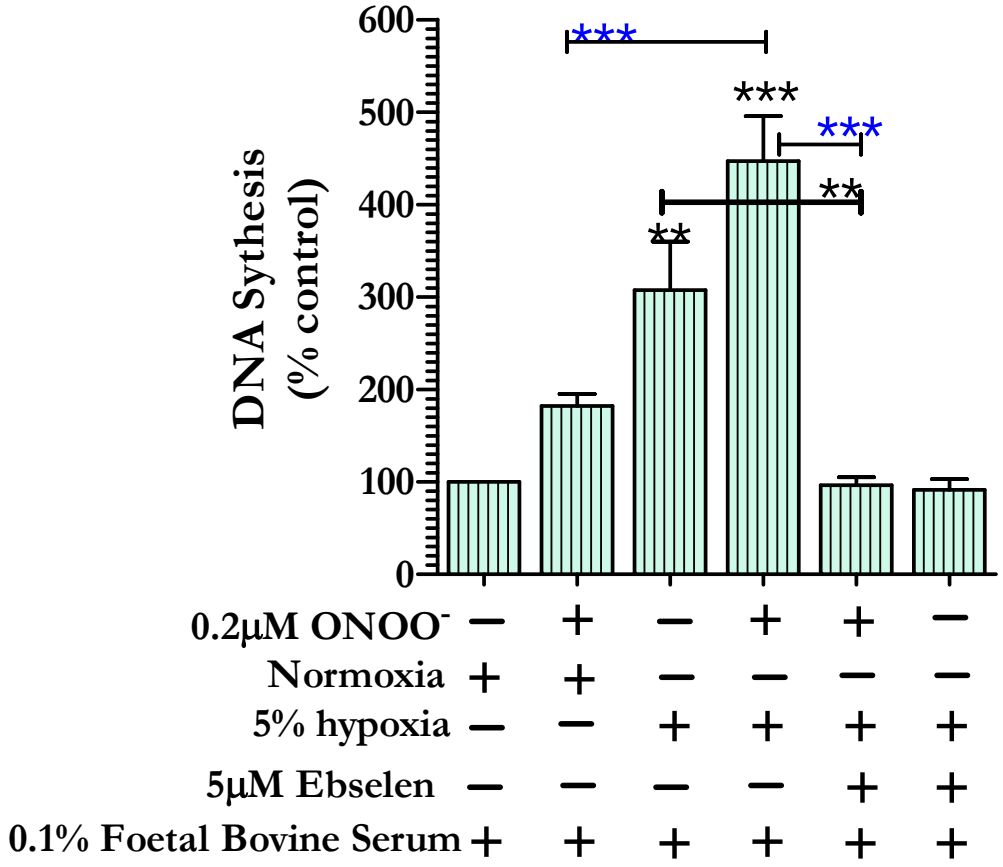

Figure 6.5: The Effect of Ebselen on the Proliferative Response of Pulmonary Artery Smooth Muscle cells to 5% (O_2) Hypoxia and or to 0.2µM Peroxynitrite. DNA synthesis was assessed by ^{3}H-thymidine incorporation assay and expressed as percentage proliferation (± SEM) relative to proliferation in un-stimulated cells maintained at normoxia (21% O_2). Statistical evaluations were by 1-way analysis of variance. Post hoc investigation was by Bonferroni' test of multiple comparisons. *** = $p < 0.001$; ** =$p< 0.01$ or *= $p< 0.05$ was considered significant relative to control (normoxia, no ONOO- treatment); n=6

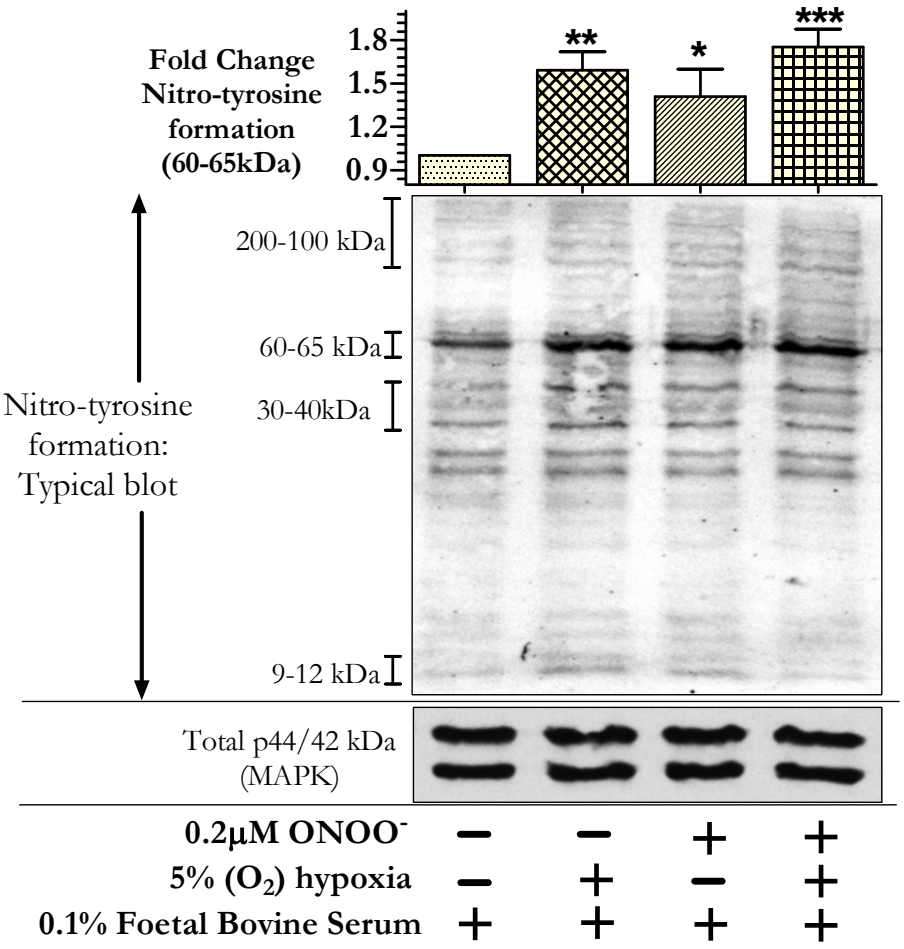

Figure 6.6: Probe for Nitro-tyrosine Formation in Pulmonary Artery Cell Exposed to Acute Hypoxia and or to Peroxynitrite. Pulmonary cells were either left un-stimulated or stimulated with peroxynitrite (ONOO-) for 15min or exposed to 5% (O_2) hypoxia for 24 or both. Expression of nitro-tyrosine and total p42/44 MAPK was determined by western blotting; quantification was by densitometry (Mean±SEM for 60-65 KDa is shown). Results were normalised to control (no hypoxia or ONOO- treatment). Statistical analyses were by one-way analysis of variance. Post hoc test was by Bonferroni's multiple comparison tests $p<0.05$ (*), <0.01 (**), <0.001 (***) were considered significant; n=3.

.

6.5. DISCUSSION

6.5.1. Foreword and main findings

Pulmonary hypertension is frequently associated with chronic hypoxic lung disease and is characterized by hyperplasia driven remodelling of the pulmonary artery walls (Meyrick and Reid, 1979). The current study reports the significant stimulation of PAEC and PASMC proliferation by a decline in ambient oxygen. For the first time, this study showed that hypoxia induced bovine pulmonary artery hyper-proliferation is linked to the intra-cellular formation of ONOO- in these cells.

6.5.2. The effect of experimental hypoxia on pulmonary artery cells

The results of this study show that bovine pulmonary artery endothelial cells (PAEC) exhibit variable response to different levels of hypoxia. Under 10%, 5% and 1% (O_2) experimental hypoxic conditions, the growth of PAEC was unaffected, enhanced and inhibited, respectively (Fig. 6.1, 6.2A, 6.4A). The inhibitory effect of 1% (O_2) on PAEC suggests that vital cellular functions were impeded (Fig. 6.4A). A previous study has demonstrated that exposure of bovine PAEC to acute (0% O_2) hypoxia led to a slowing of the cell cycle and decreased growth rate (Tucci *et al.*, 1997). In this study, the response of PASMC to 1% (O_2) was slightly different. The stimulatory response to ONOO- was reduced to baseline; however, unlike PAEC basal cell proliferation was not inhibited (Fig. 6.4). The lack of significant cell proliferation in PASMC exposed to 1% experimental hypoxia in this study suggests a lower limit of oxygen concentration for the mitogenic effect of hypoxia (compare Fig. 6.2B with Fig. 6.4B). In several cell types, studies have also demonstrated that 0-1% (O_2) hypoxia caused cessation of cell growth and cell cycle progression due probably to the activation of the G1 phase checkpoint of the cell cycle. The evidences also suggest that under these conditions, the cells conserved their capacity to divide or proliferate and when reoxygenated are capable of growth (Tucci *et al.*, 1997; Graeber *et al.*, 1994; Amellem and Pettersen, 1991; Wilson *et al.*, 199O). Arrest of PASMC DNA synthesis in response to extreme hypoxia may thus be a protective mechanism (Amellem and Pettersen, 1991).

Alone both 10 and 5% (O_2) experimental hypoxia caused significant increase in PASMC proliferation (Fig. 6.1B, 6.2B). Under 5% (O_2) experimental hypoxia, the proliferative response of cells pretreated with bolus 2nM or 0.2μM authentic peroxynitrite was similar to the effects of 5% (O_2) hypoxia alone (Fig. 6.2B, 6.5). There are several published data in support of the finding that hypoxia is a direct stimulus for PASMC proliferation. For example, exposure to hypoxia (5% O_2) alone enhanced proliferation of human and bovine PASMC (Cooper and Beasley, 1999; Frid *et al.*, 1997a). The current study thus provides baseline data for the mitogenic effect of 5% (O_2) experimental hypoxia in PASMC. In addition, this study provide evidence that hypoxia alone (5% O_2) can significantly stimulate the proliferation of PAEC (Fig. 6.2A, 6.4A). These results correlate with the histological changes seen in hypoxic pulmonary hypertension which in turn has been demonstrated to be similar to other forms of the disease (Meyrick and Reid, 1980, 1979). Indeed, the occlusion of pre-capillary pulmonary arteries by clusters of proliferating endothelial cells has been reported in pulmonary hypertension (Taraseviciene-Stewart *et al.*, 2001; Lee *et al.*, 1998). In addition, experimental model of pulmonary hypertension show that pulmonary cells proliferate within 24h of exposure to hypoxia (Meyrick and Reid, 1979). In this study, pulmonary smooth muscle cell proliferated in response to the least change in ambient oxygen (6.1B) investigated. In addition, the fact that the proliferative response of PAEC and PASMC to ONOO- alone differ significantly from 5% (O_2) hypoxia alone or ONOO- + 5% (O_2) hypoxia (Fig. 6.2B, 6.3@ 0.1% FBS, 6.5) suggests that hypoxia may activate an additional proliferation pathway and or stimulate the ONOO- proliferative pathway but for a longer period. The latter is discussed in section 6.5.4. While the cell growth stimulating concentration of ONOO- did not activate p38 MAPK (chapter 5), mounting evidence using pulmonary artery fibroblast show that hypoxia stimulates proliferation via p38 MAPK activation (Mortimer *et al.*, 2007; Welsh *et al.*, 2006). Taken together, the proliferation of PASMC and PAEC in response to decline in oxygen concentration is likely an important initial step in the cascade of events that may lead to deregulated cell growth seen in patients with hypoxic lung disease.

.

6.5.3. Physiologic relevance of experimental 1, 5, 10% (O_2) hypoxia

In this study, the normoxic growth condition of PAEC and PASMC simulate atmospheric pressure (760 mmHg or 760 torr) 21% of which is oxygen (≈159mmHg). However, blood from tissues reaching the lungs via the pulmonary arteries has a low PO_2 (40 mmHg). Consequently, oxygen exchange follows the diffusion of alveoli oxygen (100 mmHg) into pulmonary capillaries at 40 mmHg (Law and Bukwirwa, 1999; West, 1990). Accordingly, cell growth conditions of 10%, 5% and 1% (O_2) which correspond to 75, 38 and 8mmHg respectively, are hypoxic in relation to atmospheric pressure. In addition, these O_2 concentrations are also hypoxic in relation to in-vitro culture O_2 concentration since the pulmonary artery cells of this study were cultured and maintained at 21% O_2. Physiologically however, 10%, 5%, and 1% O_2 will represent hyperoxic, normoxic and hypoxic conditions, respectively when compared to pulmonary artery PO_2. Using physiologically relevant O_2 concentration, independent studies have investigated the response of pulmonary artery cells to O_2 gradient. Farber and co-workers (1991, 1990) maintained endothelial cells from bovine pulmonary artery for several months under 3% oxygen before the evaluation of the biological effect of exposure to acute short-term hypoxia (0% O_2). These works show that whether cultured at pulmonary arterial O_2 concentration or adapted to 21% O_2, the capacity of vascular endothelial cells to respond to decreases in oxygen concentration is carried by the cell throughout its existence (Farber, 1991; Farber and Rounds, 1990). The O_2 concentrations chosen for this study are widely used in-vitro culture conditions for the study of hypoxic diseases (Fletcher *et al.*, 2008; Wang *et al.*, 2007; Lanner *et al.*, 2005; Stiebellehner *et al.*, 2003; Demiryürek *et al.*, 2000; Cooper and Beasley, 1999). Concisely, the findings of the current study provide an indication of pulmonary artery cell response to acute decreases in ambient oxygen, which may occur in hypoxic lung disease.

6.5.4. The formation of peroxynitrite under hypoxic conditions

In this study, the proliferative response of PASMC to 0.2μM ONOO- (reported in chapter 5) but also to moderate 5% (O_2) hypoxia were attenuated by simultaneous treatment with 5μM ebselen (Fig. 6.5; $p<0.01$). In principle, this was an indication that PASMC may generate ONOO- under moderate experimental hypoxic condition. This was confirmed by further investigation, which revealed that exposure of PASMC to

0.2μM ONOO-, or 5% (O_2) experimental hypoxia caused significant increase in nitro-tyrosine formation (Fig. 6.6). Indeed, the intensity and extent of nitro-tyrosine formation was similar for both treatments (Fig. 6.6). This is the unique hallmark of the intracellular action of peroxynitrite (Wadsworth *et al.*, 2004) and has been reported independently in patients with pulmonary hypertension (Bowers *et al.*, 2004). Together, these results demonstrate that under conditions of moderate (5% O_2) experimental hypoxia, PASMC are induced to generate ONOO- intracellularly. This may have occurred over the period of acute hypoxia and accounted for the greater proliferative response to 5% (O_2) hypoxia than to transient exposure to 0.2μM ONOO- (Fig. 6.2B, 6.3 at 0.1% FBS, 6.5). The simultaneous upregulation of NADPH oxidase and eNOS in response to acute hypoxia has resulted in the simultaneous formation of superoxide and peroxynitrite in PAEC and PASMC (Muzaffar *et al.*, 2005). Also, using vascular endothelial growth factor, El-Remessy (2007) provided independent evidence for the intracellular generation of ONOO- under conditions producing $NO^{\bullet}$ and superoxide in concert. The current study is however first to demonstrate hypoxia induced nitro-tyrosine formation in bovine pulmonary artery smooth muscle cells. It is probable that corresponding decline in ambient O_2 is also able to sustain the generation of ONOO- locally within the pulmonary vasculature. Therefore, given the stimulatory effects of ONOO- on pulmonary cells (Chapter 4, Fig. 6.2, 6.5), acute decline in ambient O_2 may initiate and sustain a cycle of ONOO- induced events that represent an important mechanism for pulmonary cell hyper-proliferation.

6.5.5. Conclusion

While, cell proliferation appeared arrested under severe experimental hypoxia (1% O_2); moderate hypoxia (5% O_2) induced the intracellular formation of peroxynitrite and significantly stimulated pulmonary artery cell proliferation over the effects of ONOO- alone. Hypoxia may initiate and sustain a cycle of peroxynitrite induced proliferative events that represent an important mechanism for pulmonary artery hyperplasia in pulmonary hypertension.

.

CHAPTER 7
GENERAL DISCUSSION

.

7.1: FOREWARD

A review of relevant literature at the project onset revealed apparent gaps in the evidence for peroxynitrite action in pulmonary hypertension. It seems at odd that while the literature is replete with proof that ONOO- is potently cytotoxic, the anion is also up-regulated in the lungs of patients with pulmonary hypertension. Yet, cytotoxicity does not account for the histological changes in the pulmonary arteries of pulmonary hypertension patients. Notably, this involve PAEC and PASMC hyperplasia and arterial wall remodelling (Rabinovitch, 2008; Meyrick and Reid, 1979). This informed the 1st conjecture, that ONOO- is active below the lower limit for the widely reported cytotoxic effects. Accordingly, this study confirmed the cytotoxic effects of ONOO- in PAEC and PASMC but also determined for the first time, the cytotoxic threshold (2μM) of the anion in these cells. Further investigation confirmed for the first time, that a range of pathologically relevant concentrations of peroxynitrite (2-200nM; ONOO-) stimulated the proliferation of PAEC and PASMC (chapter 4). The signal transduction mechanism (chapter 5) underlying this effect hint on targets and options for the modulation of ONOO- action (chapter 5).

This study then further hypothesized that hypoxia can aggravate the ONOO- induced proliferative response of pulmonary cells. The results however did not prove this so (chapter 6). The extent of proliferation was similar in pulmonary cells exposed to hypoxia alone or to the combination of ONOO- and hypoxia (chapter 6). Overall, this study demonstrates the 2-edged effect of ONOO- in bovine pulmonary artery cells, namely the cytotoxic (≥2μM) and the growth stimulatory action (2-200nM). As a whole, this study advances current understanding of the disease-causing role of ONOO- by revealing the proliferative response of pulmonary cell to ONOO- and the potential of the anion to promote the arterial wall remodelling associated with pulmonary hypertension.

.

7.2. KNITTING THE EVIDENCE(S)

7.2.1. Life and activity of peroxynitrite: relevance to pulmonary hypertension pathobiology

Chapter 2 of the current study elucidated the life and activity of ONOO- under pulmonary artery cell growth conditions and highlighted the pathophysiological relevance of its biological activity in conditions of pulmonary hypertension. Evidence from this study (chapter 2) showed that 20μM SIN-1 generated approximately 1nM ONOO- over a 90min period (chapter 2). It is thus expected that stimulation of cell proliferation by 2μM SIN-1 will be associated with even lower steady state ONOO- concentration probably 0.1nM ONOO- sustained over an extended period. Authentic peroxynitrite also stimulated cell proliferation (chapter 4) but by the bolus kinetics of a transient exposure followed by significant loss of the anion (chapter 2). Even so, ONOO- sustained ERK activation for 12h in pulmonary artery cells (chapter 5) and stimulated cell proliferation significantly (chapter 4). Together these data suggests that exposure of pulmonary cells to both transitory and sustained levels of low concentration ONOO- will stimulate pulmonary cell hyper-proliferation. In addition, the collective evidence suggests that intermittent in-vivo generation of ONOO- may subject lung cells to proliferative stimuli long-term.

The physiological concentration of nitric oxide under basal conditions is about 100pM–5nM (reviewed in Hall and Garthwaite, 2009); it is expected that an equimolar concentration of superoxide is required for generation of peroxynitrite. It may seem that such level of ONOO- may be too low to have pathologic effect especially as the half-life of ONOO- under physiologic pH was 1.38 seconds (chapter 2). However, this study showed that transient exposure to 0.2nM or 2nM ONOO- stimulated PASMC proliferation (chapter 4). In addition, since the formation of superoxide is up-regulated in pulmonary hypertension (Demiryürek and Wadsworth, 1999), the disease state thus favours the formation of ONOO- (Ronson *et al.*, 1999). The potential for ONOO- to initiate and or progress arterial wall remodelling is supported by the potential of the anion to be formed within and to act on pulmonary cells of initimal, medial and adventitial origin (Kooy *et al.*, 1995; Squadrito and Pryor, 1995). The ability of ONOO- to cross cell membranes implies that peroxynitrite generated from a cellular source

could influence surrounding target cells within 1 to 2 cell diameters (≈ 5–20μm; Tanner et al., 2000; Wild et al., 1989). Accordingly, ONOO- generated in-vivo may stimulate the proliferation of both initimal and medial layer cells as shown in this study; but also has potential for a stimulatory effect on pulmonary fibroblasts. In turn, hyper-proliferation of pulmonary cells can result in the formation of plexiform lesions, which are commonly found in pathological examination of the pulmonary arteries of patients with pulmonary hypertension (Mandegar *et al.*, 2004; Stenmark and Mecham, 1997; Mecham *et al.*, 1987). In addition, endothelial cells are also responsible for producing a wide array of growth factors and vasoactive mediators which can affect PASMC growth and contractility (Eddahibi *et al.*, 2006; Heydarkhan-Hagvall *et al.*, 2003; Powell *et al.*, 1996). This may result in clinical consequences that include pulmonary vascular remodelling and hypertension (Mandegar *et al.*, 2004; Powell *et al.*, 1996).

7.2.1. Actions of peroxynitrite and hypoxia: relevance to pulmonary hypertension pathobiology

The proliferative response of cells from main and lobular pulmonary arteries to hypoxia and peroxynitrite reported in this study (chapter 4, 6) suggests the potential of both stimuli to cause pulmonary artery cell hyperplasia in pulmonary hypertension. This may lead to the occlusion of pre-capillary arteries and to loss of hypoxic pulmonary vasoconstriction (HPV) in these beds, which in turn will worsen the symptoms of pulmonary hypertension. This notion is based on evidence that regional acute HPV is crucial to ensure optimized adaptation of pulmonary perfusion to ventilation and that precapillary pulmonary arteries are vital to mediating this response (Dumas *et al.*, 1999; Nagasaka *et al.*, 1984; Kato and Staub, 1966).

7.2.3. Primary target of the proliferation actions of peroxynitrite: still unknown

It is interesting that this study demonstrated activation of PDGFR and EGFR by low concentration ONOO- (chapter 5). While the current work demonstrated increased phosphotyrosine formation at PDGFR, further work is required to elucidate the loci and scope of the interaction of ONOO- with growth factor receptors; and to confirm the interaction requisite for cell proliferation. Whilst ONOO- is capable of both oxidative and nitration action, it is not clear from the current study whether one or both

actions are directly linked with the growth stimulatory effects of the anion on pulmonary artery cells. Additionally, both low concentration ONOO- and PDGF caused increased global phosphotyrosine formation at PDGF receptors although response to PDGF was marked. However, while PDGF showed receptor activation via tyrosine 751 residue, ONOO- did not. This indicated specificity in the action of ONOO- on growth factor receptors; the data however, did not show the exact PDGF or EGF or similar growth factor receptor tyrosine residue phosphorylated by ONOO- (chapter 5). This remains unknown and future work may focus on this. Also, it remain unclear whether pulmonary cell growth factor receptor activation is a direct effect of low concentration ONOO- or secondary to ONOO- induced inhibition of enzymes inhibiting the TRK activity of these receptors. Further work is required to unravel this. These notwithstanding, the strong reactivity of ONOO- indicated that it can change the redox state of pulmonary cells (Beckman and Crow, 1993). In addition, ONOO- anion is small sized, diffuses easily, can be generated rapidly in response to extra or intra cellular stimuli, and is short-lived under physiological conditions. Together, these suggest that the molecule can act as an intracellular messenger although it is not likely that ONOO- actually binds to a receptor.

7.3: IMPLICATION OF NOVEL FINDINGS FOR THE TREATMENT OF PULMONARY HYPERTENSION

Hypoxia or pulmonary hypertension have been independently associated with the intra-cellular generation of ONOO- (chapter 6, Muzaffar *et al.*, 2005; Bowers *et al.*, 2004). Given that a large number of patient suffers pulmonary hypertension associated with hypoxia (Simonneau *et al.*, 2004); it is therefore of clinical relevance that this study has demonstrated significant stimulation in growth rates of pulmonary cells following acute exposure to ONOO- or to decline in ambient oxygen. In addition, given that current consensus is that pulmonary hypertension is a proliferative disease (reviewed in chapter 1), the success of future drugs for the treatment of this disease will therefore depend on their anti-proliferative properties. While current therapies for pulmonary hypertension involve drug with both vaoso-active and anti-proliferation properties, it is also becoming evident that the anti-proliferative agents target disease pathobiology and are vital for disease remission and improved quality of life (Rhodes *et al.*, 2009; Consensus, 2008; Rabinovitch, 2008).

7.3.1. Peroxynitrite action: a target for primary intervention

It is of interest that the proliferative response of pulmonary cells to ONOO- followed the activation of PDGFR and EGFR and was abolished by PDGF and EGF tyrosine kinase inhibitors (chapter 5). This suggests that PDGF, EGF or similar growth factor receptors could be target for the modulation of this peroxynitrite effect. Recent studies provide preclinical proof of concept for the clinical development of a TKR inhibitor as a targeted therapy for pulmonary hypertension. Acting via receptor tyrosine kinases, PDGF was shown to cause smooth muscle cell recruitment and endothelial cell proliferation and dysfunction (Barst, 2005). In addition, PDGF signalling has been shown to contributes to structural vascular remodelling in pulmonary hypertension (Balasubramaniam *et al.*, 2003). Also, lung tissue isolated from patients with pulmonary arterial hypertension show significant increase in expression of PDGF receptor mRNA (Humbert *et al.*, 1998). Besides acting alone to stimulate cell growth via PDGF or related growth factor receptors activation, it is possible that ONOO- causes the preponderance of PDGFRs. This can potentially amplifies the proliferative response of pulmonary cells to ONOO- over time. Hence, therapies of the future will be drugs selectively inhibiting TKR activity of PDGF and related growth factors. These will abolish the proliferative signals and effects of ONOO- as shown in this study (chapter 5). Accordingly, imatinib that act to inhibit PDGFR has been shown to have beneficial effects in models of pulmonary hypertension. In good agreement with the results of this study (chapter 5), treatment with imatinib caused reversal in pulmonary cell proliferation in monocrotaline and chronic hypoxia models of pulmonary hypertension in rat (Schermuly *et al.*, 2005). In addition, reduced right ventricular hypertrophy and right ventricular pressure and increased cardiac output were also observed outcomes. The clinical efficacy and safety of imatinib and other tyrosine kinase inhibitors such as sorafenib currently in clinical trials (Novartis, 2009), are thus awaited with keen interest.

.

7.3.2. Peroxynitrite action: a target for adjunct therapy

Clinical trials demonstrating the efficacy of combination therapies highlight the benefit of this regimen in the treatment of pulmonary hypertension (Adamali *et al.*, 2009). Antioxidants has been reported to decrease ligand and oxidants (H2O2) induced phosphorylation of PDGF receptor and MAPK p42/44 (Kappert *et al.*, 2006). Being a potent oxidant, the use of antioxidants or scavengers may limit the proliferative action of ONOO-. In this study, scavenging ONOO- with ebselen significantly attenuated the proliferative response of pulmonary cells exposed to the anion (chapter5). This finding provides experimental support for the therapeutic potentials of the use of antioxidants or ONOO- scavengers in the treatment of pulmonary hypertension.

7.4. GENERAL CONCLUSION

The proliferative response of pulmonary cells to 2-200nM ONOO- provide at least part explanation for the clinical observation of pulmonary artery initimal and medial cell hyper-proliferation and the concomitant up-regulation of nitro-tyrosine in patients with pulmonary hypertension. At pathologically relevant concentration, peroxynitrite phosphorylated growth factor receptors, activated MAPK pathway and stimulated pulmonary artery cell proliferation. Besides scavenging ONOO-, inhibiting its growth factor receptor activation by selective tyrosine kinase inhibitions demonstrated a viable option for the control of ONOO- induced pulmonary artery cell hyper-proliferation.

.

CHAPTER 8

REFERENCES:

Aaronson, P. I., Robertson, T. P., Knock, G. A., Becker, S., Lewis, T. H., Snetkov, V. & Ward, J. P. (2006) Hypoxic pulmonary vasoconstriction: Mechanisms and controversies. *J Physiol.,* 1(570(Pt 1)), 53–58.

Adamali, H., Gaine, S. P. & Rubin, L. J. (2009) Medical treatment of pulmonary arterial hypertension. *Semin Respir Crit Care Med,* 30(04), 484-492.

Adnot, S., Raffestin, B., Eddahibi, S., Braquet, P. & Chabrier, P. E. (1991) Loss of endothelium-dependent relaxant activity in the pulmonary circulation of rats exposed to chronic hypoxia. *J. Clin. Invest.,* 87(1), 155 - 162.

Alapati, V., Mckenzie, C., Blair, A., Kenny, D., A., M. & Am, S. (2007) Mechanisms of u46619- and 5-ht-induced contraction of bovine pulmonary arteries: Role of chloride ions. *Br J Pharmacol.,* 151(8), 1224-1234.

Alessi, D. R., Cuenda, A., Cohen, P., Dudley, D. T. & Saltiel, A. R. (1995) Pd 098059 is a specific inhibitor of the activation of mitogen-activated protein kinase kinase in vitro and in vivo. *J. Biol. Chem.,* 270(46), 27489-27494.

Ali, T. K., Matragoon, S., Pillai, B. A., Liou, G. I. & El-Remessy, A. B. (2008) Peroxynitrite mediates retinal neurodegeneration by inhibiting nerve growth factor survival signaling in experimental and human diabetes. *Diabetes,* 57(4), 889-898.

Alvarez, B. & Radi, R. (2003) Peroxynitrite reactivity with amino acids and proteins. *Amino Acids,* 25(3), 295.

Alvaro, G. E., Spear, N., Pelluffo, H., Kamaid, A., Barbeito, L. & J.S, B. (1999) Examining apoptosis in cultured cell after exposure to nitric oxide. *Methods in Enzymology,* 301393-402.

Amellem, O. & Pettersen, E. (1991) Cell inactivation and cell cycle inhibition as induced by extreme hypoxia: The possible role of cell cycle arrest as a protection against hypoxia-induced lethal damage. *Cell. Prolif.,* 24 127-141.

Ames, B. N., Shigenaga, M. K. & Hagen, T. M. (1993) Oxidants, antioxidants, and the degenerative diseases of aging. *Proceedings of the National Academy of Sciences of the United States of America,* 90(17), 7915-7922.

Anderson, H. C. C., S. Abbott, J. And Holtzer, H. (1970) The loss of phenotypic traits by differentiated cells in vitro. Vii. Effects of 5-bromodeoxyuridine and prolonged culturing on fine structure of chondrocytes. *Am J Pathol.,* 60(2), 289–312.

Asahi, Y., Shinozaki, K. & Nagaoka, M. (1971) Chemical and kinetic study on stabilities of 3-morpholinosydnonimine and its n-ethoxycarbonyl derivative. *Chem. Pharm. BUll.,* 191079-1088.

Avruch, J., Zhang, X. & Kyriakis, J. (1994) Raf meets ras: Completing the framework of a signal transduction pathway. *Trends Biochem Sci.,* 19(7)**,** 279-283.

Badesch, D., Tapson, V., Mcgoon, M., Brundage, B. H., Rubin, L. J., Wigley, F. M., Rich, S., Barst, R. J., Barrett, P. S., Kral, K. M., Jöbsis, M. M., Loyd, J. E., Murali, S., Frost, A., Girgis, R., Bourge, R. C., Ralph, D. D., Elliott, C. G. & Hill, N. S. (2000) Continuous intravenous epoprostenol for pulmonary hypertension due to the scleroderma spectrum of disease. A randomized, controlled trial. *Annals of internal medicine,* 132(6)**,** 425-434.

Balasubramaniam, V., Le Cras, T. D., Ivy, D. D., Grover, T. R., Kinsella, J. P. & Abman, S. H. (2003) Role of platelet-derived growth factor in vascular remodeling during pulmonary hypertension in the ovine fetus. *Am J Physiol Lung Cell Mol Physiol,* 284(5)**,** L826-833.

Bao, F. & Liu, D. (2002) Peroxynitrite generated in the rat spinal cord induces neuron death and neurological deficits. *Neuroscience,* 115(3)**,** 839-849 (811).

Bao, F. & Liu, D. (2003) Peroxynitrite generated in the rat spinal cord induces apoptotic cell death and activates caspase-3. *Neuroscience,* 11659-70(12).

Bapat, S., Verkleij, A. & Post, J. A. (2001) Peroxynitrite activates mitogen-activated protein kinase (mapk) via a mek-independent pathway: A role for protein kinase c. *FEBS Letters,* 499(1-2)**,** 21.

Barst, R. J. (2005) Pdgf signaling in pulmonary arterial hypertension. *The Journal of Clinical Investigation,* 115(10)**,** 2691-2694.

Barst, R. J., Langleben, D., Frost, A., Horn, E. M., Oudiz, R., Shapiro, S., Mclaughlin, V., Hill, N., Tapson, V. F., Robbins, I. M., Zwicke, D., Duncan, B., Dixon, R. A. F. & Frumkin, L. R. (2004) Sitaxsentan therapy for pulmonary arterial hypertension. *Am. J. Respir. Crit. Care Med.,* 169(4)**,** 441-447.

Barst, R. J., Mcgoon, M., Mclaughlin, V., Tapson, V., Oudiz, R., Shapiro, S., Robbins, I. M., Channick, R., Badesch, D., Rayburn, B. K., Flinchbaugh, R., Sigman, J., Arneson, C., Jeffs, R. & Beraprost Study, G. (2003) Beraprost therapy for pulmonary arterial hypertension. *J Am Coll Cardiol,* 41(12)**,** 2119-2125.

Barst, R. J., Rubin, L. J., Long, W. A., Mcgoon, M. D., Rich, S., Badesch, D. B., Groves, B. M., Tapson, V. F., Bourge, R. C., Brundage, B. H., Koerner, S. K., Langleben, D., Keller, C. A., Murali, S., Uretsky, B. F., Clayton, L. M., Jobsis, M. M., Blackburn, S. D., Shortino, D. & Crow, J. W. (1996) A comparison of continuous intravenous epoprostenol (prostacyclin) with conventional therapy for primary pulmonary hypertension. *N Engl J Med,* 334(5)**,** 296-301.

Bassil, M., Li, Y. & Anand-Srivastava, M. B. (2008) Peroxynitrite inhibits the expression of gi{alpha} protein and adenylyl cyclase signaling in vascular smooth muscle cells. *Am J Physiol Heart Circ Physiol,* 294(2)**,** H775-784.

Bauersachs, J., Bouloumie, A., Fraccarollo, D., Hu, K., Busse, R. & Ertl, G. (1999) Endothelial dysfunction in chronic myocardial infarction despite increased vascular endothelial nitric oxide synthase and soluble guanylate cyclase expression: Role of enhanced vascular superoxide production. *Circulation,* 100(3)**,** 292-298.

Bayraktutan, U. (2004) Nitric oxide synthase and nad(p)h oxidase modulate coronary endothelial cell growth. *Journal of Molecular and Cellular Cardiology,* 36(2)**,** 277 -286.

Beckman, J. & Crow, J. (1993) Pathological implications of nitric oxide, superoxide and peroxynitrite formation. *Biochem Soc Trans.,* 21(2)**,** 330-334.

Beckman, J. S., Beckman, T. W., Chen, J., Marshall, P. A. & Freeman, B. A. (1990) Apparent hydroxyl radical production by peroxynitrite: Implications for endothelial injury from nitric oxide and superoxide. *Proc Natl Acad Sci U S A.,* 87(4)**,** 1620–1624.

Bharani, A., Mathew, V., Sahu, A. & B, L. (2003) The efficacy and tolerability of sildenafil in patients with moderate-tosevere pulmonary hypertension. *Indian Heart,* 55 55–59.

Bogatcheva, N. V., Wang, P., Birukova, A. A., Verin, A. D. & Garcia, J. G. N. (2006) Mechanism of fluoride-induced map kinase activation in pulmonary artery endothelial cells. *Am J Physiol Lung Cell Mol Physiol,* 290(6)**,** L1139-1145.

Bohle, D. S., Hansert, B., Paulson, S. C. & Smith, B. D. (1994) Biomimetic synthesis of the putative cytotoxin peroxynitrite, onoo-, and its characterization as a tetramethylammonium salt. *J. Am. Chem. Soc.,* 116(16)**,** 7423-7424.

Bohn, H. & Schönafinger, K. (1989) Oxygen and oxidation promote the release of nitric oxide from sydnonimines. *J Cardiovasc Pharmacol.,* 14(Suppl 11)**,** S6-12.

Bolanos, J. P., Garcia-Nogales, P. & Almeida, A. (2004) Provoking neuroprotection by peroxynitrite. *Curr Pharm Des,* 10(8)**,** 867-877.

Bouloumie, A., Bauersachs, J., Linz, W., Scholkens, B. A., Wiemer, G., Fleming, I. & Busse, R. (1997) Endothelial dysfunction coincides with an enhanced nitric oxide synthase expression and superoxide anion production. *Hypertension,* 30(4)**,** 934-941.

Bowers, R., Cool, C., Murphy, R. C., Tuder, R. M., Hopken, M. W., Flores, S. C. & Voelkel, N. F. (2004) Oxidative stress in severe pulmonary hypertension. *Am. J. Respir. Crit. Care Med.,* 169(6)**,** 764-769.

Brimioulle, S., Julien, V., Gust, R., Kozlowski, J., Naeije, R. & Schuster, D. (2002) Importance of hypoxic vasoconstriction in maintaining oxygenation during acute lung injury. *Crit Care Med,* 30(4)**,** 874-880.

Brown, M. D. & Sacks, D. B. (2008) Compartmentalised mapk pathways. IN Klussmann, E., Scott, J. & Aandahl, E. M. (Eds.) *Protein-protein interactions as new drug targets.* Berlin, Springer.

Brunelli, L., Crow, J. P. & Beckman, J. S. (1995) The comparative toxicity of nitric oxide and peroxynitrite to escherichia coli. *Archives of Biochemistry and Biophysics,* 316(1)**,** 327-334.

Cai, L., Klein, J. B. & Kang, Y. J. (2000) Metallothionein inhibits peroxynitrite-induced DNA and lipoprotein damage. *J. Biol. Chem.,* 275(50)**,** 38957-38960.

Cao, Z., Hallur, S., Harry, Z. Q., Xingxiang, P. & Yunbo, L. (2004) Induction of endogenous glutathione by the chemoprotective agent, 3h-1,2-dithiole-3-thione, in human neuroblastoma sh-sy5y cells affords protection against peroxynitrite-induced cytotoxicity. *Biochemical and Biophysical Research Communications.,* 316 1043-1049.

Cao, Z. & Li, Y. (2004) Protecting against peroxynitrite-mediated cytotoxicity in vascular smooth muscle cells via upregulating endogenous glutathione biosynthesis by 3h-1,2-dithiole-3-thione. *Cardiovasc Toxicol.,* 4(4)**,** 339-353.

Carville, C., Adnot, S., Eddahibi, S., Teiger, E., Rideau, D. & Raffestin, B. (1997) Induction of nitric oxide synthase activity in pulmonary arteries from normoxic and chronically hypoxic rats. *Eur Respir J,* 10(2)**,** 437-445.

Chakraborti, S., Chowdhury, A., Kar, P., Das, P., Shaikh, S., Roy, S. & Chakraborti, T. (2009) Role of protein kinase c in nadph oxidase derived o2--mediated regulation of kv-lvocc axis under u46619 induced increase in [ca2+]i in pulmonary smooth muscle cells. *Archives of Biochemistry and Biophysics,* 487(2)**,** 123-130.

Channick, R. N., Simonneau, G., Sitbon, O., Robbins, I. M., Frost, A., Tapson, V. F., Badesch, D. B., Roux, S., Rainisio, M., Bodin, F. & Rubin, L. J. (2001) Effects of the dual endothelin-receptor antagonist bosentan in patients with pulmonary hypertension: A randomised placebocontrolled study. *The Lancet,* 358(9288)**,** 1119-1123.

Charles, L. H. & William, C. M. (2004) Signaling endosome hypothesis: A cellular mechanism for long distance communication. *Journal of Neurobiology,* 58(2)**,** 207-216.

Chen, B.-C., Lin, L.-L. & Lin, W.-W. (1999) Protein kinase c [var epsilon]-dependent pathway of extracellular signal-regulated protein kinase activation by p2y1 and p2y2 purinoceptors that activate cytosolic phospholipase a2 in endothelial cells. *European Journal of Pharmacology,* 373(1)**,** 101-110.

Chen, Z., Gibson, T. B., Robinson, F., Silvestro, L., Pearson, G., Xu, B.-E., Wright, A., Vanderbilt, C. & Cobb, M. H. (2001) Map kinases. *Chemical Reviews,* 101(8)**,** 2449.

Christman, B. W., Mcpherson, C. D., Newman, J. H., King, G. A., Bernard, G. R., Groves, B. M. & Loyd, J. E. (1992) An imbalance between the excretion of thromboxane and prostacyclin metabolites in pulmonary hypertension. *N Engl J Med,* 327(2)**,** 70-75.

Clavreul, N., Adachi, T., Pimental, D. R., Ido, Y., Schoneich, C. & Cohen, R. A. (2006) S-glutathiolation by peroxynitrite of p21ras at cysteine-118 mediates its direct activation and downstream signaling in endothelial cells. *FASEB J.,* 05-4875fje.

Coats, P., Kennedy, S., Pyne, S., Wainwright, C. L. & Wadsworth, R. M. (2008) Inhibition of non-ras protein farnesylation reduces in-stent restenosis. *Atherosclerosis,* 197(2)**,** 515-523.

Consensus (2008) National pulmonary hypertension centres: Consensus statement on the management of pulmonary hypertension in clinical practice in the uk and ireland. *Thorax,* 63(Suppl_2)**,** ii1-41.

Cooper, A. L. & Beasley, D. (1999) Hypoxia stimulates proliferation and interleukin-1alpha production in human vascular smooth muscle cells. *Am J Physiol Heart Circ Physiol,* 277(4)**,** H1326-1337.

Cotes, J. E. (1993) Distribution of ventilation and perfusion. IN Cotes, J. E. & Leathart, G. L. (Eds.) *Lung function.* 5th ed. Oxford, Blackwell Scientific Publications.

Crow, J. (2002) Peroxynitrite: Scavenging for survival: (The Virtual Free Radical School) Accessed: 23/07/09 http://www.healthcare.uiowa.edu/research/sfrbm/virtual.html#C

D'alonzo, G., Barst, R., Ayres, S., Bergofsky, E., Brundage, B., Detre, K., Fishman, A., Goldring, R., Groves, B. & Kernis, J. (1991) Survival in patients with primary pulmonary hypertension. Results from a national prospective registry. *Ann Intern Med.,* 115(5)**,** 343-349.

Darley-Usmar, V. M., Hogg, N., O'leary, V. J., Wilson, M. T. & Moncada, S. (1992) The simultaneous generation of superoxide and nitric oxide can initiate lipid peroxidation in human low density lipoprotein. *Free Radical Research,* 17(1)**,** 9 - 20.

Davies, R. J. & Morrell, N. W. (2008) Molecular mechanisms of pulmonary arterial hypertension: Role of mutations in the bone morphogenetic protein type ii receptor. *Chest,* 134(6)**,** 1271-1277.

Dawson, J. P., Berger, M. B., Lin, C.-C., Schlessinger, J., Lemmon, M. A. & Ferguson, K. M. (2005) Epidermal growth factor receptor dimerization and activation

require ligand-induced conformational changes in the dimer interface. *Mol. Cell. Biol.,* 25(17)**,** 7734-7742.

Demiryürek, A. T., Karamsetty, M. R., Mcphaden, A. R., Wadsworth, R. M., Kane, K. A. & Maclean, M. R. (2000) Accumulation of nitrotyrosine correlates with endothelial no synthase in pulmonary resistance arteries during chronic hypoxia in the rat. *Pulmonary Pharmacology & Therapeutics,* 13(4)**,** 157-165.

Demiryürek, A. T. & Wadsworth, R. M. (1999) Superoxide in the pulmonary circulation. *Pharmacology & Therapeutics,* 84(3)**,** 355-365.

Demiryurek, A., Wadsworth, R., Kane, K. & Peacock, A. (1993) The role of endothelium in hypoxic contraction of human pulmonary artery rings. *Am Rev Respir Dis.,* 147(2)**,** 283-290.

Demiryurek, A. T., Wadsworth, R. M. & Kane, K. A. (1991) Pharmacological evidence for the role of mediators in hypoxia-induced vasoconstriction in sheep isolated intrapulmonary artery rings. *European Journal of Pharmacology,* 203(1)**,** 1-8.

Dempsey, E. C., Mcmurtry, I. F. & O'brien, R. F. (1991) Protein kinase c activation allows pulmonary artery smooth muscle cells to proliferate to hypoxia. *American Journal of Physiology - Lung Cellular and Molecular Physiology,* 260(2)**,** L136-L145.

Dent, P., Haser, W., Haystead, T. A., Vincent, L. A., Roberts, T. M. & Sturgill, T. W. (1992) Activation of mitogen-activated protein kinase kinase by v-raf in nih 3t3 cells and in vitro. *Science,* 257(5075)**,** 1404-1407.

Desilva, D. R., Jones, E. A., Favata, M. F., Jaffee, B. D., Magolda, R. L., Trzaskos, J. M. & Scherle, P. A. (1998) Inhibition of mitogen-activated protein kinase kinase blocks t cell proliferation but does not induce or prevent anergy. *J Immunol,* 160(9)**,** 4175-4181.

Dewachter, L., Adnot, S., Guignabert, C., Tu, L., Marcos, E., Fadel, E., Humbert, M., Dartevelle, P., Simonneau, G., Naeije, R. & Eddahibi, S. (2009) Bone morphogenetic protein signaling in heritable versus idiopathic pulmonary hypertension. *Eur Respir J,* 09031936.00183008.

Dimmeler, S., Lottspeich, F. & Brune, B. (1992) Nitric oxide causes adp-ribosylation and inhibition of glyceraldehyde-3- phosphate dehydrogenase. *J. Biol. Chem.,* 267(24)**,** 16771-16774.

Druker, B. J. & Lydon, N. B. (2000) Lessons learned from the development of an abl tyrosine kinase inhibitor for chronic myelogenous leukemia. *J Clin Invest 2000,* 1053-7.

Druker, B. J., Tamura, S., Buchdunger, E., Ohno, S., Segal, G. M., Fanning, S., Zimmermann, J. & Lydon, N. B. (1996) Effects of a selective inhibitor of the abl tyrosine kinase on the growth of bcr−abl positive cells. *Nature Medicine,* 2561 - 566.

Du, L., Sullivan, C. C., Chu, D., Cho, A. J., Kido, M., Wolf, P. L., Yuan, J. X. J., Deutsch, R., Jamieson, S. W. & Thistlethwaite, P. A. (2003) Signaling molecules in nonfamilial pulmonary hypertension. *N Engl J Med,* 348(6)**,** 500-509.

Dudley, D. T., Pang, L., Decker, S. J., Bridges, A. J. & Saltiel, A. R. (1995) A synthetic inhibitor of the mitogen-activated protein kinase cascade. *Proc Natl Acad Sci.,* 92(17)**,** 7686–7689.

Dumas, J. P., Bardou, M., Goirand, F. & Dumas, M. (1999) Hypoxic pulmonary vasoconstriction. *General Pharmacology,* 33(4)**,** 289.

Durmowicz, A. G. & Stenmark, K. R. (1999) Mechanisms of structural remodeling in chronic pulmonary hypertension. *Pediatrics in Review,* 20(11)**,** 91e-102.

Eddahibi, S., Fabre, V., Boni, C., Martres, M. P., Raffestin, B., Hamon, M. & Adnot, S. (1999) Induction of serotonin transporter by hypoxia in pulmonary vascular smooth muscle cells: Relationship with the mitogenic action of serotonin. *Circ Res,* 84(3)**,** 329-336.

Eddahibi, S., Guignabert, C., Barlier-Mur, A. M., Dewachter, L., Fadel, E., Dartevelle, P., Humbert, M., Simonneau, G., Hanoun, N., Saurini, F., Hamon, M. & Adnot, S. (2006) Cross talk between endothelial and smooth muscle cells in pulmonary hypertension: Critical role for serotonin-induced smooth muscle hyperplasia. *Circulation,* 113(15)**,** 1857-1864.

El-Remessy, A. B., Al-Shabrawey, M., Platt, D. H., Bartoli, M., Behzadian, M. A., Ghaly, N., Tsai, N., Motamed, K. & Caldwell, R. B. (2007) Peroxynitrite mediates vegf's angiogenic signal and function via a nitration-independent mechanism in endothelial cells. *FASEB J.,* 21(10)**,** 2528-2539.

Emery, C. J., Teng, G. Q., Liu, X. & Barer, G. R. (2003) Vasoreactions to acute hypoxia, whole lungs and isolated vessels compared: Modulation by no. *Respiratory Physiology & Neurobiology,* 134115-129(115).

Estévez, A. G., Radi, R., Barbeito, L., Shin, J. T., Thompson, J. A. & Beckman, J. S. (1995) Peroxynitrite-induced cytotoxicity in pc12 cells: Evidence for an apoptotic mechanism differentially modulated by neurotrophic factors. *Journal of neurochemistry,* 65(4)**,** 1543-1550.

Evans, A. M. (2006) Amp-activated protein kinase underpins hypoxic pulmonary vasoconstriction and carotid body excitation by hypoxia in mammals. *Experimental Physiology,* 91(5)**,** 821-827.

Fagan, K., Fouty, B., Tyler, R., Morris, K., Hepler, L., Sato, K., Lecras, T., Abman, S., Weinberger, H., Huang, P., Mcmurtr, Y. I. & Rodman, D. (1999a) The pulmonary circulation of homozygous or heterozygous enos-null mice is hyperresponsive to mild hypoxia. *J Clin Invest,* 103291-299.

Fagan, K. A., Tyler, R. C., Sato, K., Fouty, B. W., Morris, K. G., Jr., Huang, P. L., Mcmurtry, I. F. & Rodman, D. M. (1999b) Relative contributions of endothelial, inducible, and neuronal nos to tone in the murine pulmonary circulation. *Am J Physiol Lung Cell Mol Physiol,* 277(3)**,** L472-478.

Farber, H. (1991) *Differences in pulmonary and systemic arterial endothelial cell adaptation to chronic hypoxia*, New York, Oxford University Press.

Farber, H. W. & Barnett, H. F. (1991) Differences in prostaglandin metabolism in cultured aortic and pulmonary arterial endothelial cells exposed to acute and chronic hypoxia. *Circ Res,* 68(5)**,** 1446-1457.

Farber, H. W. & Rounds, S. (1990) Effect of long-term hypoxia on cultured aortic and pulmonary arterial endothelial cells. *Experimental Cell Research,* 191(1)**,** 27-36.

Fauman, E. B. & Saper, M. A. (1996) Structure and function of theprotein tyrosine phosphatases. *Trends in Biochemical Sciences,* 21(11)**,** 413-417.

Favata, M. F., Horiuchi, K. Y., Manos, E. J., Daulerio, A. J., B, Stradley, D. A., Feeser, W. S., Van Dyk, D. E., Pitts, W. J., Earl, R. A., Hobbs, F., Copeland, R. A., Magolda, R. L., Scherle, P. A. & Trzaskos, J. M. (1998) Identification of a novel inhibitor of mitogen-activated protein kinase kinase. *J Biol Chem.,* 273(29)**,** 18623-18632.

Feelisch, M., Ostrowski, J. & Noack, E. (1989) On the mechanism of no release from sdynonimines. *Cardiovasc. Pharmacol.,* 14(14 (Supple11).)**,** S13-S22.

Fishman, A. (1976) Hypoxia on the pulmonary circulation. How and where it acts. *Circ Res.,* 38(4)**,** 221-231.

Fletcher, N. M., Jiang, Z. L., Diamond, M. P., Abu-Soud, H. M. & Saed, G. M. (2008) Hypoxia-generated superoxide induces the development of the adhesion phenotype. *Free Radical Biology and Medicine,* 45(4)**,** 530-536.

Frid, M. G., Aldashev, A. A., Dempsey, E. C. & Stenmark, K. R. (1997a) Smooth muscle cells isolated from discrete compartments of the mature vascular media exhibit unique phenotypes and distinct growth capabilities. *Circ Res,* 81(6)**,** 940-952.

Frid, M. G., Dempsey, E. C., Durmowicz, A. G. & Stenmark, K. R. (1997b) Smooth muscle cell heterogeneity in pulmonary and systemic vessels: Importance in vascular disease. *Arterioscler Thromb Vasc Biol,* 17(7)**,** 1203-1209.

Frödin, M. & Gammeltoft, S. (1999) Role and regulation of 90 kda ribosomal s6 kinase (rsk) in signal transduction. *Molecular and Cellular Endocrinology,* 151(1-2)**,** 65-77.

Gabbiani, G., Schmid, E., Winter, S., Chaponnier, C., De Ckhastonay, C., Vandekerckhove, J., Weber, K. & Franke, W. W. (1981) Vascular smooth muscle cells differ from other smooth muscle cells: Predominance of vimentin

filaments and a specific alpha-type actin. *Proceedings of the National Academy of Sciences of the United States of America,* 78(1)**,** 298-302.

Galie, N., Ghofrani, H. A., Torbicki, A., Barst, R. J., Rubin, L. J., Badesch, D., Fleming, T., Parpia, T., Burgess, G., Branzi, A., Grimminger, F., Kurzyna, M., Simonneau, G. & The Sildenafil Use in Pulmonary Arterial Hypertension Study, G. (2005) Sildenafil citrate therapy for pulmonary arterial hypertension. *N Engl J Med,* 353(20)**,** 2148-2157.

Galiè, N., Humbert, M., Vachiéry, J.-L., Vizza, C., Kneussl, M., Manes, A., Sitbon, O., Torbicki, A., Delcroix, M., Naeije, R., Hoeper, M., Chaouat, A., Morand, S., Besse, B. & Simonneau, G. (2002) Effects of beraprost sodium, an oral prostacyclin analogue, in patients with pulmonary arterial hypertension: A randomized, double-blind, placebo-controlled trial. *Journal of the American College of Cardiology,* 39(9)**,** 1496-1502.

Garg, H., Hales, C., Yu, L., Butler, M., Islam, T., Xie, J. & Linhardt, R. (2006) Increase in the growth inhibition of bovine pulmonary artery smooth muscle cells by an o-hexanoyl low-molecular-weight heparin derivative. *Carbohydr Res.,* 341(15)**,** 2607-2612.

Geer, P. V., Hunter, T. & Lindberg, R. A. (1994) Receptor protein-tyrosine kinases and their signal transduction pathways. *Annual Review of Cell Biology,* 10(1)**,** 251-337.

Ghofrani, H. A., Seeger, W. & Grimminger, F. (2005) Imatinib for the treatment of pulmonary arterial hypertension. *N Engl J Med,* 353(13)**,** 1412-1413.

Govers, R., Bevers, L., De Bree, P., Rabelink, Tj. (2002) Endothelial nitric oxide synthase activity is linked to its presence at cell-cell contacts. *Biochem J.,* 15(361(Pt 2))**,** 193-201.

Graeber, T. G., Peterson, J. F., Tsai, M., Monica, K., Fornace, A. J., Jr. & Giaccia, A. J. (1994) Hypoxia induces accumulation of p53 protein, but activation of a g1-phase checkpoint by low-oxygen conditions is independent of p53 status. *Mol. Cell. Biol.,* 14(9)**,** 6264-6277.

Green, D. & Kroemer, G. (1998) The central executioners of apoptosis: Caspases or mitochondria? *Trends in Cell Biology,* 8267-271.

Groves, B. M., Reeves, J. T., Sutton, J. R., Wagner, P. D., Cymerman, A., Malconian, M. K., Rock, P. B., Young, P. M. & Houston, C. S. (1987) Operation everest ii: Elevated high-altitude pulmonary resistance unresponsive to oxygen. *J Appl Physiol,* 63(2)**,** 521-530.

Gruetter, C. A. & Lemke, S. M. (1988) Bradykinin-induced endothelium-dependent relaxation of bovine intrapulmonary artery and vein. *Eur J Pharmacol.,* 122(3)**,** 363-367.

Haddad, I. Y., Crow, J. P., Hu, P., Ye, Y., Beckman, J. & Matalon, S. (1994) Concurrent generation of nitric oxide and superoxide damages surfactant protein a. *Am J Physiol Lung Cell Mol Physiol,* 267(3)**,** L242-249.

Hall, C. N. & Garthwaite, J. (2009) What is the real physiological no concentration in vivo? *Nitric Oxide,* 21(2)**,** 92-103.

Hampl, V., Archer, S. L., Nelson, D. P. & Weir, E. K. (1993) Chronic edrf inhibition and hypoxia: Effects on pulmonary circulation and systemic blood pressure. *J Appl Physiol,* 75(4)**,** 1748-1757.

Hampl, V. & Herget, J. (2000) Role of nitric oxide in the pathogenesis of chronic pulmonary hypertension. *Physiol. Rev.,* 80(4)**,** 1337-1372.

Hancock, J. F. (2006) Lipid rafts: Contentious only from simplistic standpoints. *Nat Rev Mol Cell Biol,* 7(6)**,** 456-462.

Harris, P. & Heath, D. (1986) *Influence of respiratory gases.,* London, Churchill Livingston.

Heller, R., Polack, T., Gräbner, R. & Till, U. (1999) Nitric oxide inhibits proliferation of human endothelial cells via a mechanism independent of cgmp. *Atherosclerosis,* 144(1)**,** 49.

Heydarkhan-Hagvall, S., Gisela, H., Bengt, R. J., Li, J. Y., Mattsson, E. & Risberg, B. (2003) Co-culture of endothelial cells and smooth muscle cells affects gene expression of angiogenic factors. *Journal of Cellular Biochemistry,* 89
(6)**,** 1250 - 1259.

Hicham, M., Hari, G. G. & Charles, A. H. (2009) Growth inhibition of bovine pulmonary artery smooth muscle cells following long-term heparin treatment. *Journal of Cellular Physiology,* 9999(9999)**,** n/a.

Higenbottam, T., Butt, A. Y., Mcmahon, A., Westerbeck, R. & Sharples, L. (1998) Long term intravenous prostaglandin (epoprostenol or iloprost) for treatment of severe pulmonary hypertension. *Heart,* 80(2)**,** 151-155.

Hodyc, D., Snorek, M., Brtnicky, T. & Herget, J. (2008) Superoxide dismutase mimetic tempol inhibits hypoxic pulmonary vasoconstriction in rats independently on either nitric oxide production or basal tone of pulmonary vessels. *FASEB J.,* 22(1_MeetingAbstracts)**,** 1174.1174-.

Hogg, N., Darley-Usmar, V. M., Wilson, M. T. & Moncada, S. (1992) Production of hydroxyl radicals from the simultaneous generation of superoxide and nitric oxide. *Biochem J.,* 15(281(Pt 2))**,** 419–424.

Holm, P., Kankaanranta, H., Metsä-Ketelä, T. & Moilanen, E. (1998) Radical releasing properties of nitric oxide donors gea 3162, sin-1 and s-nitroso-n-acetylpenicillamine. *European Journal of Pharmacology,* 346(1)**,** 97-102.

Howell, K., Preston, R. J. & Mcloughlin, P. (2003) Chronic hypoxia causes angiogenesis in addition to remodelling in the adult rat pulmonary circulation. *J Physiol,* 547(1)**,** 133-145.

Huang, J., Lin, S. C., Nadershahi, A., Watts, S. W. & Sarkar, R. (2008) Role of redox signaling and poly (adenosine diphosphate-ribose) polymerase activation in vascular smooth muscle cell growth inhibition by nitric oxide and peroxynitrite. *Journal of Vascular Surgery,* 47(3)**,** 599.

Huie, R. E. & Padmaja, S. (1993) The reaction of no with superoxide. *Free Radical Research,* 18(4)**,** 195 - 199.

Humar, R. O. K., Kiefer, F. N., Berns, H., Resink, T. J. & Battegay, E. J. (2002) Hypoxia enhances vascular cell proliferation and angiogenesis in vitro via rapamycin (mtor) -dependent signaling. *FASEB J.,* 16(8)**,** 771-780.

Humbert, M., Monti, G., Fartoukh, M., Magnan, A., Brenot, F., Rain, B., Capron, F., Galanaud, P., Duroux, P., Simonneau, G. & Emilie, D. (1998) Platelet-derived growth factor expression in primary pulmonary hypertension: Comparison of hiv seropositive and hiv seronegative patients. *Eur Respir J,* 11(3)**,** 554-559.

Humbert, M., Morrell, N. W., Archer, S. L., Stenmark, K. R., Maclean, M. R., Lang, I. M., Christman, B. W., Weir, E. K., Eickelberg, O., Voelkel, N. F. & Rabinovitch, M. (2004) Cellular and molecular pathobiology of pulmonary arterial hypertension. *Journal of the American College of Cardiology,* 43(12, Supplement 1)**,** S13-S24.

Humbert, M., Sitbon, O., Chaouat, A., Bertocchi, M., Habib, G., Gressin, V., Yaici, A., Weitzenblum, E., Cordier, J.-F., Chabot, F., Dromer, C., Pison, C., Reynaud-Gaubert, M., Haloun, A., Laurent, M., Hachulla, E. & Simonneau, G. (2006) Pulmonary arterial hypertension in france: Results from a national registry. *Am. J. Respir. Crit. Care Med.,* 173(9)**,** 1023-1030.

Hussain, R. F., Nouri, A. M. E. & Oliver, R. T. D. (1993) A new approach for measurement of cytotoxicity using colorimetric assay. *Journal of Immunological Methods,* 160(1)**,** 89.

Ichikawa, T., Sugiura, H., Koarai, A., Yanagisawa, S., Kanda, M., Hayata, A., Furukawa, K., Akamatsu, K., Hirano, T., Nakanishi, M., Matsunaga, K., Minakata, Y. & Ichinose, M. (2008) Peroxynitrite augments fibroblast-mediated tissue remodeling via myofibroblast differentiation. *Am J Physiol Lung Cell Mol Physiol,* 295(5)**,** L800-808.

Ip, Y. T. & Davis, R. J. (1998) Signal transduction by the c-jun n-terminal kinase (jnk) -- from inflammation to development. *Current Opinion in Cell Biology,* 10(2)**,** 205-219.

Ischiropoulos, H. (2002) Introduction to serial reviews: Reactive nitrogen species, tyrosine nitration and cell signaling. *Free Radical Biology and Medicine,* 33(6)**,** 727.

Je, J. H., Lee, J. Y., Jung, K. J., Sung, B., Go, E. K., Yu, B. P. & Chung, H. Y. (2004) Nf-[kappa]b activation mechanism of 4-hydroxyhexenal via nik/ikk and p38 mapk pathway. *FEBS Letters,* 566(1-3)**,** 183-189.

Jeffery, T. K. & Morrell, N. W. (2002) Molecular and cellular basis of pulmonary vascular remodeling in pulmonary hypertension. *Progress in Cardiovascular Diseases,* 45(3)**,** 173-202.

Jiao, J., Greendorfer, J. S., Zhang, P., Zinn, K. R., Diglio, C. A. & Thompson, J. A. (2003) Alternatively spliced fgfr-1 isoform signaling differentially modulates endothelial cell responses to peroxynitrite. *Archives of Biochemistry and Biophysics,* 410(2)**,** 187-200.

Johnson, S. R., Mehta, S. & Granton, J. T. (2006) Anticoagulation in pulmonary arterial hypertension: A qualitative systematic review. *Eur Respir J,* 28(5)**,** 999-1004.

Jones, P. L., Cowan, K. N. & Rabinovitch, M. (1997) Tenascin-c, proliferation and subendothelial fibronectin in progressive pulmonary vascular disease. *Am J Pathol,* 150(4)**,** 1349-1360.

Jope, R. S., Zhang, L. & Song, L. (2000) Peroxynitrite modulates the activation of p38 and extracellular regulated kinases in pc12 cells. *Archives of Biochemistry and Biophysics,* 376(2)**,** 365-370.

Kaji, T., Kaieda, I., Hisatsune, T. & Kaminogawa, S. (2002) 3-morpholinosydnonimine hydrochloride induces p53-dependent apoptosis in murine primary neural cells: A critical role for p21ras-mapk-p19arf pathway. *Nitric Oxide,* 6(2)**,** 125.

Kaneko, F. T., Arroliga, A. C., Dweik, R. A., Comhair, S. A., Laskowski, D., Oppedisano, R., Thomassen, M. J. & Erzurum, S. C. (1998) Biochemical reaction products of nitric oxide as quantitative markers of primary pulmonary hypertension. *Am. J. Respir. Crit. Care Med.,* 158(3)**,** 917-923.

Kappert, K., Peters, K. G., Bohmer, F. D. & Ostman, A. (2005) Tyrosine phosphatases in vessel wall signaling. *Cardiovasc Res,* 65(3)**,** 587-598.

Kappert, K., Sparwel, J., Sandin, A., Seiler, A., Siebolts, U., Leppanen, O., Rosenkranz, S. & Ostman, A. (2006) Antioxidants relieve phosphatase inhibition and reduce pdgf signaling in cultured vsmcs and in restenosis. *Arterioscler Thromb Vasc Biol,* 26(12)**,** 2644-2651.

Kato, M. & Staub, N. C. (1966) Response of small pulmonary arteries to unilobar hypoxia and hypercapnia. *Circ Res,* 19(2)**,** 426-440.

Kato, S., Endoh, H., Masuhiro, Y., Kitamoto, T., Uchiyama, S., Sasaki, H., Masushige, S., Gotoh, Y., Nishida, E., Kawashima, H., Metzger, D. & Chambon, P. (1995) Activation of the estrogen receptor through phosphorylation by mitogen-activated protein kinase. *Science,* 270(5241)**,** 1491-1494.

Kerkela, R., Grazette, L., Yacobi, R., Iliescu, C., Patten, R., Beahm, C., Walters, B., Shevtsov, S., Pesant, S., Clubb, F. J., Rosenzweig, A., Salomon, R. N., Van Etten, R. A., Alroy, J., Durand, J.-B. & Force, T. (2006) Cardiotoxicity of the cancer therapeutic agent imatinib mesylate. *Nat Med,* 12(8)**,** 908-916.

Kim, S. Y., Lee, J. H., Yang, E. S., Kil, I. S. & Park, J.-W. (2003) Human sensitive to apoptosis gene protein inhibits peroxynitrite-induced DNA damage. *Biochemical and Biophysical Research Communications,* 301(3)**,** 671-674.

Kissner, R., Beckman, J. & Koppenol, W. (1999) Peroxynitrite studied by stopped-flow spectroscopy. *Methods Enzymol,* 301342-352.

Kissner, R., Nauser, T., Bugnon, P., Lye, P. G. & Koppenol, W. H. (1997) Formation and properties of peroxynitrite as studied by laser flash photolysis, high-pressure stopped-flow technique, and pulse radiolysis. *Chem. Res. Toxicol.,* 10(11)**,** 1285-1292.

Kita, Y., Hirasawa, Y., Maeda, K., Nishio, M. & Yoshida, K. (1994) Spontaneous nitric oxide release accounts for the potent pharmacological actions of fk409. *European Journal of Pharmacology,* 257(1-2)**,** 123-130.

Klotz, L.-O., Schroeder, P. & Sies, H. (2002) Peroxynitrite signaling: Receptor tyrosine kinases and activation of stress-responsive pathways. *Free Radical Biology and Medicine,* 33(6)**,** 737.

Klotz, L. (2002) Oxidant-induced signaling: Effects of peroxynitrite and singlet oxygen. *Biological Chemistry,* 383(3-4)**,** 443-456.

Klotz, L. O., Schieke, S. M., Sies, H. & Holbrook, N. J. (2000) Peroxynitrite activates the phosphoinositide 3-kinase/akt pathway in human skin primary fibroblasts. *Biochem J,* 15(352 (pt 1))**,** 219–225.

Knebel, A., Rahmsdorf, H. J., Ullrich, A. & Herrlich, P. (1996) Dephosphorylation of receptor tyrosine kinases as target of regulation by radiation, oxidants or alkylating agents. *EMBO J.,* 15(19)**,** 5314–5325.

Kocher, O., Gabbiani, F., Gabbiani, G., Reidy, M.A., Cokay, M. S., Peters, H. & Hüttner, I. (1991) Phenotypic features of smooth muscle cells during the evolution of experimental carotid artery intimal thickening. Biochemical and morphologic studies. *Lab Invest.,* 65(4)**,** 459-470.

Kolch, W. (2005) Coordinating erk/mapk signalling through scaffolds and inhibitors. *Nat Rev Mol Cell Biol,* 6(11)**,** 827-837.

Kolch, W., Heidecker, G., Lloyd, P. & Rapp, U. R. (1991) Raf-1 protein kinase is required for growth of induced nih/3t3 cells. *Nature,* 349(6308)**,** 426-428.

Kolluru, G. K., Tamilarasan, K. P., Rajkumar, A. S., Geetha Priya, S., Rajaram, M., Saleem, N. K., Majumder, S., Jaffar Ali, B. M., Illavazagan, G. & Chatterjee, S. (2008) Nitric oxide/cgmp protects endothelial cells from hypoxia-mediated leakiness. *European Journal of Cell Biology,* 87(3)**,** 147-161.

Konishi, K., Watanabe, N. & Arai, T. (2009) Sin-1 cytotoxicity to pc12 cells is mediated by thiol-sensitive short-lived substances generated through sin-1 decomposition in culture medium. *Nitric Oxide,* 20(4)**,** 270 -278.

Konorev, E. A., Hogg, N. & Kalyanaraman, B. (1998) Rapid and irreversible inhibition of creatine kinase by peroxynitrite. *FEBS Letters,* 427(2)**,** 171-174.

Kooy, N. W., Royall, J. A., Ye, Y. Z., Kelly, D. R. & Beckman, J. S. (1995) Evidence for in vivo peroxynitrite production in human acute lung injury. *American journal of respiratory and critical care medicine,* 151(4)**,** 1250-1254.

Kourembanas, S., Marsden, P. A., Mcquillan, L. P. & Faller, D. V. (1991) Hypoxia induces endothelin gene expression and secretion in cultured human endothelium. *J Clin Invest.,* 88(3)**,** 1054–1057.

Kretzschmar, M., Doody, J. & Massagu, J. (1997) Opposing bmp and egf signalling pathways converge on the tgf-[beta] family mediator smad1. *Nature,* 389(6651)**,** 618-622.

Kyriakis, J. M., App, H., Zhang, X.-F., Banerjee, P., Brautigan, D. L., Rapp, U. R. & Avruch, J. (1992) Raf-1 activates map kinase-kinase. *Nature,* 358(6385)**,** 417-421.

Lander, H. M., Ogiste, J. S., Teng, K. K. & Novogrodsky, A. (1995) P21ras as a common signaling target of reactive free radicals and cellular redox stress. *J Biol Chem.*

Lanner, M. C., Raper, M., Pratt, W. M. & Rhoades, R. A. (2005) Heterotrimeric g proteins and the platelet-derived growth factor receptor-{beta} contribute to hypoxic proliferation of smooth muscle cells. *Am. J. Respir. Cell Mol. Biol.,* 33(4)**,** 412-419.

Law, R. & Bukwirwa, H. (1999) The physiology of oxygen delivery. IN (Online), U. I. A. (Ed.) *Update in Anaesthesia (online).* Nuffield Dept.of Anaesthetics, University of Oxford.

Lazarides, E. (1982) Intermediate filaments: A chemically heterogeneous, developmentally regulated class of proteins. *Annual Review of Biochemistry,* 51(1)**,** 219-250.

Le Cras, T., Xue, C., Rengasamy, A. & Johns, R. (1996a) Endothelial no synthase mrna and protein, and inducible no synthase mrna are upregulated in the rat lung following chronic hypoxia. *Am J Physiol,* 270(Lung Cell Mol Physiol 14)**,** L164–L170.

Le Cras, T. D., Xue, C., Rengasamy, A. & Johns, R. A. (1996b) Chronic hypoxia upregulates endothelial and inducible no synthase gene and protein expression in rat lung. *Am J Physiol Lung Cell Mol Physiol,* 270(1)**,** L164-170.

Leach, R. & Treacher, D. (1995) Clinical aspects of hypoxic pulmonary vasoconstriction. *Exp Physiol,* 80865-875.

Lee, S. D., Shroyer, K. R., Markham, N. E., Cool, C. D., Voelkel, N. F. & M, T. R. (1998) Monoclonal endothelial cell proliferation is present in primary but not secondary pulmonary hypertension. *J Clin Invest.,* 101(5)**,** 927-934.

Levitzki, A. (2004) Pdgf receptor kinase inhibitors for the treatment of pdgf driven diseases. *Cytokine & Growth Factor Reviews,* 15(4)**,** 229-235.

Levitzki, A. & Mishani, E. (2006) Tyrphostins and other tyrosine kinase inhibitors. *Annual Review of Biochemistry,* 75(1)**,** 93-109.

Li, C. Q., Trudel, L. J. & Wogan, G. N. (2002) Genotoxicity, mitochondrial damage, and apoptosis in human lymphoblastoid cells exposed to peroxynitrite generated from sin-1. *Chem. Res. Toxicol.,* 15(4)**,** 527-535.

Li, M.-H., Cha, Y.-N. & Surh, Y.-J. (2006) Peroxynitrite induces ho-1 expression via pi3k/akt-dependent activation of nf-e2-related factor 2 in pc12 cells. *Free Radical Biology and Medicine,* 41(7)**,** 1079-1091.

Liaudet, L., Soriano, F. & Szabo, C. (2000) Biology of nitric oxide signaling. *Crit Care Med,* 28N37–N52.

Lin, K.-T., Xue, J.-Y., Lin, M. C., Spokas, E. G., Sun, F. F. & Wong, P. Y. K. (1998) Peroxynitrite induces apoptosis of hl-60 cells by activation of a caspase-3 family protease. *Am J Physiol Cell Physiol,* 274(4)**,** C855-860.

Lin, K.-T., Xue, J.-Y., Sun, F. F. & Wong, P. Y. K. (1997) Reactive oxygen species participate in peroxynitrite-induced apoptosis in hl-60 cells. *Biochemical and Biophysical Research Communications,* 230(1)**,** 115-119.

Lipton, S. A., Choi, Y.-B., Pan, Z.-H., Lei, S. Z., Chen, H.-S. V., Sucher, N. J., Loscalzo, J., Singel, D. J. & Stamler, J. S. (1993) A redox-based mechanism for the neuroprotective and neurodestructive effects of nitric oxide and related nitroso-compounds. *Nature,* 364(6438)**,** 626-632.

Liu, C., Liu, K., Ji, Z. & Liu, G. (2006) Treatments for pulmonary arterial hypertension. *Respiratory Medicine,* 100(5)**,** 765-774.

Lomonosova, E. E., Kirsch, M., Rauen, U. & De Groot, H. (1998) The critical role of hepes in sin-1 cytotoxicity, peroxynitrite versus hydrogen peroxide. *Free Radical Biology and Medicine,* 24(4)**,** 522-528.

Lopez, B., Liu, G.-L., Christopher, T. & Ma, X.-L. (1997) Peroxynitrite, the product of nitric oxide and superoxide, causes myocardial injury in the isolated perfused rat heart. *Coron Artery Dis.,* 8(3-4)**,** 149–153.

Lu, Q., Patel, B., Harrington, E. O. & Rounds, S. (2009) Transforming growth factor-{beta}1 causes pulmonary microvascular endothelial cell apoptosis via alk5. *Am J Physiol Lung Cell Mol Physiol,* 296(5)**,** L825-838.

Majack, R. A. (1987) Beta-type transforming growth factor specifies organizational behavior in vascular smooth muscle cell cultures. *J. Cell Biol.,* 105(1)**,** 465-471.

Malan, D., Renzo, C., Levi, G., Alloatti, A., Marcantoni, I., Bedendi, M. & Pia, G. (2003) Cyclic amp and cyclic gmp independent stimulation of ventricular calcium current by peroxynitrite donors in guinea pig myocytes. *Journal of Cellular Physiology,* 197(2)**,** 284-296.

Mallozzi, C., Di Stasi, A. M. & Minetti, M. (1997) Peroxynitrite modulates tyrosine-dependent signal transduction pathway of human erythrocyte band 3. *FASEB J.,* 11(14)**,** 1281-1290.

Mandegar, M., Fung, Y. C., Huang, W., Remillard, C. V., Rubin, L. J. & Yuan, J. X. (2004) Cellular and molecular mechanisms of pulmonary vascular remodeling: Role in the development of pulmonary hypertension. *Microvasc Res,* 68(2)**,** 75-103.

Marsboom, G. R. & Janssens, S. P. (2004) Models for pulmonary hypertension. *Drug Discovery Today: Disease Models,* 1(3)**,** 289-296.

Marshall, B. E., Marshall, C., Benumof, J. & Saidman, L. J. (1981) Hypoxic pulmonary vasoconstriction in dogs: Effects of lung segment size and oxygen tension. *J Appl Physiol,* 51(6)**,** 1543-1551.

Marshall, C. J. (1995) Specificity of receptor tyrosine kinase signaling: Transient versus sustained extracellular signal-regulated kinase activation. *Cell,* 80(2)**,** 179-185.

Martin-Romero, F. J., Guti, Eacute, Rrez-Martin, Y., Henao, F., Guti, Eacute & Rrez-Merino, C. (2004) Fluorescence measurements of steady state peroxynitrite production upon sin-1 decomposition: Nadh versus dihydrodichlorofluorescein and dihydrorhodamine 123: Methods and applications of fluorescence spectroscopy, imaging and probes (mafs) august 24-27 2003, prague. *Journal of Fluorescence,* 1417-23(17).

Massague, J. & Chen, Y. G. (2000) Controlling tgf-β signaling. *Genes Dev.,* 14627-644.

Masumoto, H. & Sies, H. (1996) The reaction of ebselen with peroxynitrite. *Chemical Research in Toxicology,* 9(1)**,** 262-267.

Mauro, M. J. & Druker, B. J. (2001) Sti571: Targeting bcr-abl as therapy for cml. *Oncologist,* 6(3)**,** 233-238.

Mckenzie, J., Clancy, J. J. & Klein, R. (1984) Autoradiographic analysis of cell proliferation and protein synthesis in the pulmonary trunk of rats during the early development of hypoxia-induced pulmonary hypertension. *Blood Vessel,* 21(2)**,** 80-89.

Mclaughlin, V., Gaine, S., Barst, R., Oudiz, R., Bourge, R., Frost, A., Robbins, I., Tapson, V., Mcgoon, M., Badesch, D., Sigman, J., Roscigno, R., Blackburn, S., Arneson, C., Rubin, L. & Rich, S. (2003) Efficacy and safety of treprostinil: An epoprostenol analog for primary pulmonary hypertension. *J Cardiovasc Pharmacol,* 41(2)**,** 293-299.

Mecham, R., Madaras, J., Mcdonald, J. & U., R. (1983) Elastin production by cultured calf pulmonary artery endothelial cells. *J Cell Physiol.,* 116(3)**,** 282-288.

Mecham, R. P., Whitehouse, L. A., Wrenn, D. S., Parks, W. C., Griffin, G. L., Senior, R. M., Crouch, E. C., Stenmark, K. R. & Voelkel, N. F. (1987) Smooth muscle-mediated connective tissue remodeling in pulmonary hypertension. *Science,* 237(4813)**,** 423-426.

Meyrick, B. & Reid, L. (1979) Hypoxia and incorporation of 3h-thymidine by cells of the rat pulmonary arteries and alveolar wall. *Am J Pathol,* 96(1)**,** 51-70.

Meyrick, B. & Reid, L. (1980) Ultrastructural findings in lung biopsy material from children with congenital heart defects. *Am J Pathol,* 101(3)**,** 527-542.

Michiels, C., De Leener, F., Arnould, T., Dieu, M. & Remacle, J. (1994) Hypoxia stimulates human endothelial cells to release smooth muscle cell mitogens: Role of prostaglandins and bfgf. *Experimental Cell Research,* 213(1)**,** 43-54.

Minetti, M., Mallozzi, C. & Di Stasi, A. M. M. (2002) Peroxynitrite activates kinases of the src family and upregulates tyrosine phosphorylation signaling. *Free Radical Biology and Medicine,* 33(6)**,** 744.

Miyamoto, S., Nagaya, N., Satoh, T., Kyotani, S., Sakamaki, F., Fujita, M., Nakanishi, N. & Miyatake, K. (2000) Clinical correlates and prognostic significance of six-minute walk test in patients with primary pulmonary hypertension. Comparison with cardiopulmonary exercise testing. *Am. J. Respir. Crit. Care Med.,* 161(2)**,** 487-492.

Moncada, S., Palmer, R. M. & Higgs, E. A. (1991) Nitric oxide: Physiology, pathophysiology, and pharmacology. *Pharmacol Rev,* 43(2)**,** 109-142.

Mooi, W. J. & Grünberg, K. (2006) Histopathology of pulmonary hypertensive diseases. *Current Diagnostic Pathology,* 12(6)**,** 429-440.

Mor, A. & Philips, M. R. (2006) Compartmentalized ras/mapk signaling. *Annual Review of Immunology,* 24(1)**,** 771-800.

Morrell, N. W. (2006) Pulmonary hypertension due to bmpr2 mutation: A new paradigm for tissue remodeling? *Proc Am Thorac Soc,* 3(8)**,** 680-686.

Morrison, D. K. & Davis, R. J. (2003) Regulation of map kinase signaling modules by scaffold proteins in mammals*. *Annual Review of Cell and Developmental Biology,* 19(1)**,** 91-118.

Mortimer, H. J., Peacock, A. J., Kirk, A. & Welsh, D. J. (2007) P38 map kinase: Essential role in hypoxia-mediated human pulmonary artery fibroblast proliferation. *Pulmonary Pharmacology & Therapeutics,* 20(6)**,** 718-725.

Mosmann, T. (1983) Rapid colorimetric assay for cellular growth and survival: Application to proliferation and cytotoxicity assays. *Journal of Immunological Methods,* 65(1-2)**,** 55.

Mrc (1981) Long term domiciliary oxygen therapy in chronic hypoxic cor pulmonale complicating chronic bronchitis and emphysema: Report of the medical research council working party. *The Lancet,* 317(8222)**,** 681-686.

Mukhopadhyay, D., Tsiokas, L., Zhou, X.-M., Foster, D., Brugge, J. S. & Sukhatme, V. P. (1995) Hypoxic induction of human vascular endothelial growth factor expression through c-src activation. *Nature,* 375(6532)**,** 577.

Muzaffar, S., Shukla, N., Angelini, G. D. & Jeremy, J. Y. (2005) Acute hypoxia simultaneously induces the expression of gp91phox and endothelial nitric oxide synthase in the porcine pulmonary artery. *Thorax,* 60(4)**,** 305-313.

Nabeyrat, E., Jones, G. E., Fenwick, P. S., Barnes, P. J. & Donnelly, L. E. (2003) Mitogen-activated protein kinases mediate peroxynitrite-induced cell death in human bronchial epithelial cells. *Am J Physiol Lung Cell Mol Physiol,* 284(6)**,** L1112-1120.

Naeije, R. & Rondelet, B. (2004) Pathobiology of pulmonary arterial hypertension. *Bull Mem Acad R Med Belg,* 159(Pt 2)**,** 219-226.

Nagasaka, Y., Bhattacharya, J., Nanjo, S., Gropper, M. A. & Staub, N. C. (1984) Micropuncture measurement of lung microvascular pressure profile during hypoxia in cats. *Circ Res,* 54(1)**,** 90-95.

Nakazawa, N., Masatoshi, H., Hiroshi, O. & Hideaki, K. (1999) Mechanisms underlying the impairment of endothelium-dependent relaxation in the pulmonary artery of monocrotaline-induced pulmonary hypertensive rats. *British Journal of Pharmacology,* 1281098-1104.

Napoli, C. & Loscalzo, J. (2004) Nitric oxide and other novel therapies for pulmonary hypertension. *Journal of Cardiovascular Pharmacology and Therapeutics,* 9(1)**,** 1-8.

Nauser, T. D. & Stites, S. W. (2001) Diagnosis and treatment of pulmonary hypertension. *Am Fam Physician.,* 63(9)**,** 1789-1798.

Newman, J. H., Trembath, R. C., Morse, J. A., Grunig, E., Loyd, J. E., Adnot, S., Coccolo, F., Ventura, C., Phillips, J. A., Iii, Knowles, J. A., Janssen, B., Eickelberg, O., Eddahibi, S., Herve, P., Nichols, W. C. & Elliott, G. (2004) Genetic basis of pulmonary arterial hypertension: Current understanding and future directions. *J Am Coll Cardiol,* 43(12_Suppl_S)**,** 33S-39.

Novartis (2009) Imatinib in pulmonary arterial hypertension (impres) http://clinicaltrials.gov/ct2/show/NCT00902174

O'donnell, V. B., Chumley, P. H., Hogg, N., Bloodsworth, A., Darley-Usmar, V. M. & Freeman, B. A. (1997) Nitric oxide inhibition of lipid peroxidation: Kinetics of reaction with lipid peroxyl radicals and comparison with α-tocopherol. *Biochemistry,* 36(49)**,** 15216-15223.

Odabaei, G., Chatterjee, D., Jazirehi, A. R., Goodglick, L., Yeung, K., Bonavida, B. & George, F. V. W. A. G. K. (2004) Raf-1 kinase inhibitor protein: Structure, function, regulation of cell signaling, and pivotal role in apoptosis. *Advances in cancer research.* Academic Press.

Oh-Hashi, K., Maruyama, W., Yi, H., Takahashi, T., Naoi, M. & Isobe, K.-I. (1999) Mitogen-activated protein kinase pathway mediates peroxynitrite-induced apoptosis in human dopaminergic neuroblastoma sh-sy5y cells. *Biochemical and Biophysical Research Communications,* 263(2)**,** 504-509.

Oliveira, C. J. R., Schindler, F., Ventura, A. M., Morais, M. S., Arai, R. J., Debbas, V., Stern, A. & Monteiro, H. P. (2003) Nitric oxide and cgmp activate the ras-map kinase pathway-stimulating protein tyrosine phosphorylation in rabbit aortic endothelial cells. *Free Radical Biology and Medicine,* 35(4)**,** 381-396.

Olschewski, H., Simonneau, G., Galie, N., Higenbottam, T., Naeije, R., Rubin, L. J., Nikkho, S., Speich, R., Hoeper, M. M., Behr, J., Winkler, J., Sitbon, O., Popov, W., Ghofrani, H. A., Manes, A., Kiely, D. G., Ewert, R., Meyer, A., Corris, P. A., Delcroix, M., Gomez-Sanchez, M., Siedentop, H., Seeger, W. & The Aerosolized Iloprost Randomized Study, G. (2002) Inhaled iloprost for severe pulmonary hypertension. *N Engl J Med,* 347(5)**,** 322-329.

Orchard, C. H., Sanchez De Leon, R. & Sykes, M. K. (1983) The relationship between hypoxic pulmonary vasoconstriction and arterial oxygen tension in the intact dog. *J Physiol,* 338(1)**,** 61-74.

Orfanos, S. E., Mavrommati, I., Korovesi, I. & Roussos, C. (2004) Pulmonary endothelium in acute lung injury: From basic science to the critically ill. *Intensive Care Medicine,* 30(9)**,** 1702.

Östman, A. & Böhmer, F.-D. (2001) Regulation of receptor tyrosine kinase signaling by protein tyrosine phosphatases. *Trends in Cell Biology,* 11(6)**,** 258-266.

Pak, O., Aldashev, A., Welsh, D. & Peacock, A. (2007) The effects of hypoxia on the cells of the pulmonary vasculature. *Eur Respir J,* 30(2)**,** 364-372.

Paramothayan, N., Lasserson, T., Wells, A. & Eh., W. (2008) Prostacyclin for pulmonary hypertension in adults. *Cochrane Database of Systematic Reviews,* (3)**,** Art. No.: CD002994. DOI: 002910.001002/14651858.CD14002994.pub14651852.

Pearson, G., Robinson, F., Beers Gibson, T., Xu, B.-E., Karandikar, M., Berman, K. & Cobb, M. H. (2001) Mitogen-activated protein (map) kinase pathways: Regulation and physiological functions. *Endocr Rev,* 22(2)**,** 153-183.

Persson, C., Savenhed, C., Bourdeau, A., Tremblay, M. L., Markova, B., Bohmer, F. D., Haj, F. G., Neel, B. G., Elson, A., Heldin, C.-H., Ronnstrand, L., Ostman, A. & Hellberg, C. (2004) Site-selective regulation of platelet-derived growth factor {beta} receptor tyrosine phosphorylation by t-cell protein tyrosine phosphatase. *Mol. Cell. Biol.,* 24(5)**,** 2190-2201.

Pesen, D. & Hoh, J. H. (2005) Micromechanical architecture of the endothelial cell cortex. *Biophys. J.,* 88(1)**,** 670-679.

Pesse, B., Levrand, S., Feihl, F., Waeber, B., Gavillet, B., Pacher, P. & Liaudet, L. (2005a) Peroxynitrite activates erk via raf-1 and mek, independently from egf receptor and p21ras in h9c2 cardiomyocytes. *Journal of Molecular and Cellular Cardiology,* 38(5)**,** 765-775.

Pesse, B., Levrand, S., Feihl, F., Waeber, B., Gavillet, B., Pacher, P. & Liaudet, L. (2005b) Peroxynitrite activates erk via raf-1 and mek, independently from egf receptor and p21ras in h9c2 cardiomyocytes. *Journal of Molecular and Cellular Cardiology,* 38(5)**,** 765.

Pietra, G. G., Edwards, W. D., Kay, J. M., Rich, S., Kernis, J., Schloo, B., Ayres, S. M., Bergofsky, E. H., Brundage, B. H. & Detre, K. M. (1989) Histopathology of primary pulmonary hypertension. A qualitative and quantitative study of pulmonary blood vessels from 58 patients in the national heart, lung, and blood institute, primary pulmonary hypertension registry. *Circulation,* 80(5)**,** 1198-1206.

Powell, R. J., Cronenwett, J. L., Fillinger, M. F., Wagner, R. J. & Sampson, L. N. (1996) Endothelial cell modulation of smooth muscle cell morphology and organizational growth pattern. *Annals of Vascular Surgery,* 10(1)**,** 4.

Qiu, Z. H. & Leslie, C. C. (1994) Protein kinase c-dependent and -independent pathways of mitogen-activated protein kinase activation in macrophages by stimuli that activate phospholipase a2. *J Biol Chem. Jul 29,* 269(30)**,** 19480-19487.

Rabinovitch, M. (2008) Molecular pathogenesis of pulmonary arterial hypertension. *The Journal of Clinical Investigation,* 118(7)**,** 2372-2379.

Rabinovitch, M., Bothwell, T., Hayakawa, B. N., Williams, W. G., Trusler, G. A., Rowe, R. D., Olley, P. M. & Cutz, E. (1986) Pulmonary artery endothelial abnormalities

in patients with congenital heart defects and pulmonary hypertension. A correlation of light with scanning electron microscopy and transmission electron microscopy. *Lab Invest.,* 55((6)), 632-653.

Radi, R., Beckman, J., Bush, K. & Freeman, B. (1991a) Peroxynitrite-induced membrane lipid peroxidation: The cytotoxic potential of superoxide and nitric oxide. *Arch Biochem Biophys.,* 288(2), 481-487.

Radi, R., Beckman, J. S., Bush, K. M. & Freeman, B. A. (1991b) Peroxynitrite oxidation of sulfhydryls. The cytotoxic potential of superoxide and nitric oxide. *J. Biol. Chem.,* 266(7), 4244-4250.

Radi, R., Cassina, A., Hodara, R., Quijano, C. & Castro, L. (2002) Peroxynitrite reactions and formation in mitochondria. *Free Radical Biology and Medicine,* 331451-1464.

Reiter, C. D., Teng, R.-J. & Beckman, J. S. (2000) Superoxide reacts with nitric oxide to nitrate tyrosine at physiological ph via peroxynitrite. *J. Biol. Chem.,* 275(42), 32460-32466.

Reuter, C. W. M., Morgan, M. A. & Bergmann, L. (2000) Targeting the ras signaling pathway: A rational, mechanism-based treatment for hematologic malignancies? *Blood,* 96(5), 1655-1669.

Rey, F. E., Cifuentes, M. E., Kiarash, A., Quinn, M. T. & Pagano, P. J. (2001) Novel competitive inhibitor of nad(p)h oxidase assembly attenuates vascular o2- and systolic blood pressure in mice. *Circ Res,* 89(5), 408-414.

Rhodes, C. J., Davidson, A., Gibbs, J. S. R., Wharton, J. & Wilkins, M. R. (2009) Therapeutic targets in pulmonary arterial hypertension. *Pharmacology & Therapeutics,* 121(1), 69-88.

Richter, A., Yeager, M. E., Zaiman, A., Cool, C. D., Voelkel, N. F. & Tuder, R. M. (2004) Impaired transforming growth factor-{beta} signaling in idiopathic pulmonary arterial hypertension. *Am. J. Respir. Crit. Care Med.,* 170(12), 1340-1348.

Robbinson, R. A. & Stokes, R. H. (2002) *Electrolyte solutions,* London, Butterworth and Co Scientific Publications.

Robin, E., Theodore, J., Burke, C., Oesterle, S., Fowler, M., Jamieson, S., Baldwin, J., Morris, A., Hunt, S. & Vankessel, A. (1987) Hypoxic pulmonary vasoconstriction persists in the human transplanted lung. *Clin Sci (Lond),* 72(3), 283-287.

Robinson, M. J. & Cobb, M. H. (1997) Mitogen-activated protein kinase pathways. *Current Opinion in Cell Biology,* 9(2), 180-186.

Robinson, V. K., Sato, E., Nelson, D. K., Camhi, S. L., Robbins, R. A. & Hoyt, J. C. (2001) Peroxynitrite inhibits inducible (type 2) nitric oxide synthase in murine lung epithelial cells in vitro. *Free Radical Biology and Medicine,* 30986-991.

Ronson, R. S., Nakamura, M. & Vinten-Johansen, J. (1999) The cardiovascular effects and implications of peroxynitrite. *Cardiovascular Research,* 4447-59.

Roux, P. P. & Blenis, J. (2004) Erk and p38 mapk-activated protein kinases: A family of protein kinases with diverse biological functions. *Microbiol. Mol. Biol. Rev.,* 68(2)**,** 320-344.

Ruan, R.-S. (2002) Possible roles of nitric oxide in the physiology and pathophysiology of the mammalian cochlea. *Ann NY Acad Sci,* 962(1)**,** 260-274.

Rubanyi, G. M. & Vanhoutte, P. M. (1986) Oxygen-derived free radicals, endothelium, and responsiveness of vascular smooth muscle. *Am J Physiol Heart Circ Physiol,* 250(5)**,** H815-821.

Rubin, L., Badesch, D. & Barst, R. (2002) Bosentan therapy for pulmonary arterial hypertension. *N Engl J Med,* 346(16)**,** 1258-a-.

Rubin, L., Mendoza, J., Hood, M., Mcgoon, M., Barst, R. J., Williams, W., Diehl, J., Crow, J. & Long, W. (1990) Treatment of primary pulmonary hypertension with continuous intravenous prostacyclin (epoprostenol). Results of a randomized trial. *Ann Intern Med.,* 112(7)**,** 485-491.

Rubin, L. J. (1985) Calcium channel blockers in primary pulmonary hypertension. *Chest,* 88257S−260S.

Rubin, L. J. (1997) Primary pulmonary hypertension. *N Engl J Med,* 336(2)**,** 111-117.

Rubin, M., Tuder, M., C., J., Marecki, Amy Richtera, Iwona Fijalkowska & Flores, S. (2007) Pathology of pulmonary hypertension. *Clin Chest Med,* 28(1)**,** 23-42.

Ruiz-Gines, J., Lopez-Ongil, S., Gonzalez-Rubio, M., Gonzalez-Santiago, L., Rodriguez-Puyol, M. & Rodriguez-Puyol, D. (2000) Reactive oxygen species induce proliferation of bovine aortic endothelial cells. *J Cardiovasc Pharmacol,* 35109-113.

Runo, J. R. & Loyd, J. E. (2003) Primary pulmonary hypertension. *The Lancet,* 361(9368)**,** 1533-1544.

Sacks, D. B. (2006) The role of scaffold proteins in mek/erk signalling. *Biochem. Soc. Trans.,* 34(Pt 5)**,** 833-836.

Salganik, R. I. (2001) The benefits and hazards of antioxidants: Controlling apoptosis and other protective mechanisms in cancer patients and the human population. *J Am Coll Nutr,* 20(90005)**,** 464S-472.

Salgo, M. G., Bermudez, E., Squadrito, G. L. & Pryor, W. A. (1995a) DNA damage and oxidation of thiols peroxynitrite causes in rat thymocytes. *Archives of Biochemistry and Biophysics,* 322(2)**,** 500-505.

Salgo, M. G., Squadrito, G. L. & Pryor, W. A. (1995b) Peroxynitrite causes apoptosis in rat thymocytes. *Biochemical and Biophysical Research Communications,* 215(3)**,** 1111-1118.

Sato, K., Rodman, D. M. & Mcmurtry, I. F. (1999) Hypoxia inhibits increased etb receptor-mediated no synthesis in hypertensive rat lungs. *Am J Physiol Lung Cell Mol Physiol,* 276(4)**,** L571-581.

Schaeffer, H. J. & Weber, M. J. (1999) Mitogen-activated protein kinases: Specific messages from ubiquitous messengers. *Mol. Cell. Biol.,* 19(4)**,** 2435-2444.

Schermuly, R. T., Dony, E., Ghofrani, H. A., Pullamsetti, S., Savai, R., Roth, M., Sydykov, A., Lai, Y. J., Weissmann, N., Seeger, W. & Grimminger, F. (2005) Reversal of experimental pulmonary hypertension by pdgf inhibition. *The Journal of Clinical Investigation,* 115(10)**,** 2811-2821.

Schewe, T. (1995) Molecular actions of ebselen--an antiinflammatory antioxidant. *General Pharmacology: The Vascular System,* 26(6)**,** 1153-1169.

Schieke, S. M., Briviba, K., Klotz, L.-O. & Sies, H. (1999) Activation pattern of mitogen-activated protein kinases elicited by peroxynitrite: Attenuation by selenite supplementation. *FEBS Letters,* 448(2-3)**,** 301-303.

Schrammel, A., Pfeiffer, S., Schmidt, K., Koesling, D. & Mayer, B. (1998) Activation of soluble guanylyl cyclase by the nitrovasodilator 3-morpholinosydnonimine involves formation of s-nitrosoglutathione. *Mol Pharmacol,* 54(1)**,** 207-212.

Shizukuda, Y., Tang, S., Yokota, R. & Ware, J. A. (1999) Vascular endothelial growth factor–induced endothelial cell migration and proliferation depend on a nitric oxide–mediated decrease in protein kinase c{delta} activity. *Circ Res,* 85(3)**,** 247-256.

Simonneau, G., Galie, N., Rubin, L. J., Langleben, D., Seeger, W., Domenighetti, G., Gibbs, S., Lebrec, D., Speich, R., Beghetti, M., Rich, S. & Fishman, A. (2004) Clinical classification of pulmonary hypertension. *J Am Coll Cardiol,* 43(12_Suppl_S)**,** 5S-12.

Singh, R. J., Hogg, N., Joseph, J., Konorev, E. & Kalyanaraman, B. (1999) The peroxynitrite generator, sin-1, becomes a nitric oxide donor in the presence of electron acceptors. *Archives of Biochemistry and Biophysics,* 361(2)**,** 331-339.

Smith, A., Ramos-Morales, F., Ashworth, A. & Collins, M. (1997) A role for jnk/sapk in proliferation, but not apoptosis, of il-3-dependent cells. *Current Biology,* 7(11)**,** 893-896.

Song, Y., Jones, J. E., Beppu, H., Keaney, J. F., Jr., Loscalzo, J. & Zhang, Y.-Y. (2005) Increased susceptibility to pulmonary hypertension in heterozygous bmpr2-mutant mice. *Circulation,* 112(4)**,** 553-562.

Squadrito, G. L. & Pryor, W. A. (1995) The formation of peroxynitrite in vivo from nitric oxide and superoxide. *Chemico-Biological Interactions,* 96 203-206.

Stenmark, K. R. & Mecham, R. P. (1997) Cellular and molecular mechanisms of pulmonary vascular remodeling. *Annual Review of Physiology,* 59(1)**,** 89-144.

Steudel, W., Ichinose, F., Huang, P. L., Hurford, W. E., Jones, R. C., Bevan, J. A., Fishman, M. C. & Zapol, W. M. (1997) Pulmonary vasoconstriction and hypertension in mice with targeted disruption of the endothelial nitric oxide synthase (nos 3) gene. *Circ Res,* 81(1)**,** 34-41.

Steudel, W., Scherrer-Crosbie, M., Bloch, K., Weimann, J., Huang, P., Jones, R., Picard, M. & Zapol, W. (1998) Sustained pulmonary hypertension and right ventricular hypertrophy after chronic hypoxia in mice with congenital deficiency of nitric oxide. *J Clin Invest,* 101(11)**,** 2468-2477.

Stiebellehner, L., Frid, M. G., Reeves, J. T., Low, R. B., Gnanasekharan, M. & Stenmark, K. R. (2003) Bovine distal pulmonary arterial media is composed of a uniform population of well-differentiated smooth muscle cells with low proliferative capabilities. *Am J Physiol Lung Cell Mol Physiol,* 285(4)**,** L819-828.

Stone, R. M., Weber, B. L., Spriggs, D. R. & Kufe, D. W. (1988) Phospholipase c activates protein kinase c and induces monocytic differentiation of hl-60 cells. *Blood,* 72(2)**,** 739-744.

Szabó, C. (2003) Multiple pathways of peroxynitrite cytotoxicity. *Toxicology Letters,* 140-141105.

Szabo, C., Ischiropoulos, H. & Radi, R. (2007) Peroxynitrite: Biochemistry, pathophysiology and development of therapeutics. *Nat Rev Drug Discov,* 6(8)**,** 662.

Szabó, C., Zingarelli, B., O'connor, M. & Salzman, A. (1996) DNA strand breakage, activation of poly (adp-ribose) synthetase, and cellular energy depletion are involved in the cytotoxicity of macrophages and smooth muscle cells exposed to peroxynitrite. *Proc Natl Acad Sci U S A.,* 93(5)**,** 1753-1758.

Szabo, E., Virag, L., Bakondi, E., Gyure, L., Hasko, G., Bai, P., Hunyadi, J., Gergely, P. & Szabo, C. (2001) Peroxynitrite production, DNA breakage, and poly(adp-ribose) polymerase activation in a mouse model of oxazolone-induced contact hypersensitivity. 117(1)**,** 74-80.

Szöcs, K. (2004) Endothelial dysfunction and reactive oxygen species production in ischemia/reperfusion and nitrate tolerance. *Gen. Physiol. Biophys,* 23265-295.

Takakura, K., Beckman, J. S., Macmillan-Crow, L. A. & Crow, J. P. (1999) Rapid and irreversible inactivation of protein tyrosine phosphatases ptp1b, cd45, and lar by peroxynitrite. *Archives of Biochemistry and Biophysics,* 369(2)**,** 197-207.

Takemoto, M., Sun, J., Hiroki, J., Shimokawa, H. & Liao, J. K. (2002) Rho-kinase mediates hypoxia-induced downregulation of endothelial nitric oxide synthase. *Circulation,* 106(1)**,** 57-62.

Tan, P. B. O. & Kim, S. K. (1999) Signaling specificity: The rtk/ras/map kinase pathway in metazoans. *Trends in Genetics,* 15145-149.

Tanner, F. C., Meier, P., Greutert, H., Champion, C., Nabel, E. G. & Luscher, T. F. (2000) Nitric oxide modulates expression of cell cycle regulatory proteins: A cytostatic strategy for inhibition of human vascular smooth muscle cell proliferation. *Circulation,* 1011982-1989.

Taraseviciene-Stewart, L., Kasahara, Y., Alger, L., Hirth, P., Mc Mahon, G., Waltenberger, J., Voelkel, N. F. & Tuder, R. M. (2001) Inhibition of the vegf receptor 2 combined with chronic hypoxia causes cell death-dependent pulmonary endothelial cell proliferation and severe pulmonary hypertension. *FASEB J.,* 15(2)**,** 427-438.

Tarpey, M. M., Beckman, J. S., Ischiropoulos, H., Gore, J. Z. & Brock, T. A. (1995) Peroxynitrite stimulates vascular smooth muscle cell cyclic gmp synthesis. *FEBS Letters,* 364(3)**,** 314.

Thome, U., Lazrak, A., Chen, L., Kirk, M. C., Thomas, M. J., Forman, H. J. & Matalon, S. (2003) Novel sin-1 reactive intermediates modulate chloride secretion across murine airway cells. *Free Radical Biology and Medicine,* 35(6)**,** 662-675.

Thompson, B. T., Steigman, D. M., Spence, C. L., Janssens, S. P. & Hales, C. A. (1993) Chronic hypoxic pulmonary hypertension in the guinea pig: Effect of three levels of hypoxia. *J Appl Physiol,* 74(2)**,** 916-921.

Thomson, J. R., Machado, R. D., Pauciulo, M. W., Morgan, N. V., Humbert, M., Elliott, G. C., Ward, K., Yacoub, M., Mikhail, G., Rogers, P., Newman, J., Wheeler, L., Higenbottam, T., Gibbs, J. S. R., Egan, J., Crozier, A., Peacock, A., Allcock, R., Corris, P., Loyd, J. E., Trembath, R. C. & Nichols, W. C. (2000) Sporadic primary pulmonary hypertension is associated with germline mutations of the gene encoding bmpr-ii, a receptor member of the tgf-beta family. *J Med Genet,* 37(10)**,** 741-745.

Tom-Moy, M., Madison, J. M., Jones, C. A. & Brown, J. K. (1985) Characterization of freshly dispersed andcultured airway smooth muscle cells. *Chest,* 87160-161.

Toullec, D., Pianetti, P., Coste, H., Bellevergue, P., Grand-Perret, T., Ajakane, M., Baudet, V., Boissin, P., Boursier, E. & Loriolle, F. (1991) The bisindolylmaleimide gf 109203x is a potent and selective inhibitor of protein kinase c. *J. Biol. Chem.,* 266(24)**,** 15771-15781.

Tracey, W. R. & Eyre, P. (1988) Effects of bradykinin and leukotrienes b4 and d4 on the bovine bronchial artery in vitro: Role of the endothelium. *Agents and Actions,* 25(1)**,** 195-204.

Trackey, J. L., Uliasz, T. F. & Hewett, S. J. (2001) Sin-1-induced cytotoxicity in mixed cortical cell culture: Peroxynitrite-dependent and -independent induction of excitotoxic cell death. *Journal of Neurochemistry,* 79(2)**,** 445-455(411).

Tucci, M., Hammerman, S. I., Furfaro, S., Saukonnen, J. J., Conca, T. J. & Farber, H. W. (1997) Distinct effect of hypoxia on endothelial cell proliferation and cycling. *Am J Physiol Cell Physiol,* 272(5)**,** C1700-1708.

Tuder, R. M., Cool, C. D., Geraci, M. W., Wang, J. U. N., Abman, S. H., Wright, L., Badesch, D. & Voelkel, N. F. (1999) Prostacyclin synthase expression is decreased in lungs from patients with severe pulmonary hypertension. *Am. J. Respir. Crit. Care Med.,* 159(6)**,** 1925-1932.

Tuder, R. M., Cool, C. D., Yeager, M., Taraseviciene-Stewart, L., Bull, T. M. & Voelkel, N. F. (2001) The pathobiology of pulmonary hypertension. Endothelium. *Clin Chest Med,* 22(3)**,** 405-418.

Tyler, R. C., Muramatsu, M., Abman, S. H., Stelzner, T. J., Rodman, D. M., Bloch, K. D. & Mcmurtry, I. F. (1999) Variable expression of endothelial no synthase in three forms of rat pulmonary hypertension. *Am J Physiol Lung Cell Mol Physiol,* 276(2)**,** L297-303.

Upmacis, R. K., Deeb, R. S., Resnick, M. J., Lindenbaum, R., Gamss, C., Mittar, D. & Hajjar, D. P. (2004) Involvement of the mitogen-activated protein kinase cascade in peroxynitrite-mediated arachidonic acid release in vascular smooth muscle cells. *Am J Physiol Cell Physiol,* 286(6)**,** C1271-1280.

Van Der Vliet, A., Hristova, M., Cross, C. E., Eiserich, J. P. & Goldkorn, T. (1998) Peroxynitrite induces covalent dimerization of epidermal growth factor receptors in a431 epidermoid carcinoma cells. *J. Biol. Chem.,* 273(48)**,** 31860-31866.

Vanhoutte, P. M. (2000) Say no to et. *Journal of the Autonomic Nervous System,* 81(1)**,** 271-277.

Vender, R. (1992) Role of endothelial cells in the proliferative response of cultured pulmonary vascular smooth muscle cells to reduced oxygen tension. *In Vitro Cellular & Developmental Biology - Animal,* 28(6)**,** 403 - 409.

Virag, L., Marmer, D. J. & Szabó, C. (1998a) Crucial role of apopain in the peroxynitrite-induced apoptotic DNA fragmentation. *Free Radical Biology and Medicine,* 25(9)**,** 1075-1082.

Virag, L., Scott, G. S., Cuzzocrea, S., Marmer, D., Salzman, A. L. & Szabo, C. (1998b) Peroxynitrite-induced thymocyte apoptosis: The role of caspases and poly (adp-ribose) synthetase (pars) activation. *Immunology,* 93(4)**,** 345–355.

Virag, L. & Szabo, C. (2002) The therapeutic potential of poly(adp-ribose) polymerase inhibitors. *Pharmacol Rev,* 54(3)**,** 375-429.

Virág, L., Szabó, É., Gergely, P. & Szabó, C. (2003) Peroxynitrite-induced cytotoxicity: Mechanism and opportunities for intervention. *Toxicology Letters,* 140-141113-124.

Voelkel, N., Tuder, R. & Weir, E. (1997) *Primary pulmonary hypertension. Pathophysiology of primary pulmonary hypertension.,* New York, Marcel Dekker.

Wadsworth, R. M. (1994) Vasoconstrictor and vasodilator effects of hypoxia. *Trends Pharmacol Sci,* 1547-53.

Wadsworth, R. M., Hoehn, T., Mcphaden, A., Stiller, B. & Preston, A. (2004) Upregulation of nitrotyrosine, a marker for peroxynitrite, in pulmonary arteries of pulmonary hypertensive patients. IN Daniel Henrion, A., France (Ed.) *8th International Symposium on Resistance Arteries (June 20–23).* Angers, France, KARGER.

Walia, M., Samson, S. E., Schmidt, T., Best, K., Whittington, M., Kwan, C. Y. & Grover, A. K. (2003) Peroxynitrite and nitric oxide differ in their effects on pig coronary artery smooth muscle. *Am J Physiol Cell Physiol,* 284(3)**,** C649-657.

Wang, Y. F., Tian, H., Tang, C. S., Jin, H. F. & Du, J. B. (2007) Nitric oxide modulates hypoxic pulmonary smooth muscle cell proliferation and apoptosis by regulating carbon monoxide pathway. *Acta Pharmacol Sin,* 28(1)**,** 28-35.

Ward, J. P. T. (2007) Curiouser and curiouser: The perplexing conundrum of reactive oxygen species and hypoxic pulmonary vasoconstriction. *Experimental Physiology,* 92(5)**,** 819-820.

Ward, J. P. T. & Mcmurtry, I. F. (2009) Mechanisms of hypoxic pulmonary vasoconstriction and their roles in pulmonary hypertension: New findings for an old problem. *Current Opinion in Pharmacology,* 9(3)**,** 287-296.

Wedgwood, S. & Black, S. M. (2003) Molecular mechanisms of nitric oxide-induced growth arrest and apoptosis in fetal pulmonary arterial smooth muscle cells. *Nitric Oxide,* 9(4)**,** 201.

Weerackody, R. P., Welsh, D. J., Wadsworth, R. M. & Peacock, A. J. (2009) Inhibition of p38 mapk reverses hypoxia-induced pulmonary artery endothelial dysfunction. *Am J Physiol Heart Circ Physiol,* 296(5)**,** H1312-1320.

Wellbrock, C., Karasarides, M. & Marais, R. (2004) The raf proteins take centre stage. *Nat Rev Mol Cell Biol,* 5(11)**,** 875-885.

Welsh, D. J., Scott, P. H. & Peacock, A. J. (2006) P38 map kinase isoform activity and cell cycle regulators in the proliferative response of pulmonary and systemic artery fibroblasts to acute hypoxia. *Pulmonary Pharmacology & Therapeutics,* 19(2)**,** 128.

West, J. B. (1990) *Respiratory physiology*, Williams and Wilkins.

West, J. B., Dollery, C. T. & Naimark, A. (1964) Distribution of blood flow in isolated lung; relation to vascular and alveolar pressures. *J Appl Physiol,* 19(4)**,** 713-724.

Wild, L. M., Nickerson, P. A. & Morin Iii, F. C. (1989) Ligating the ductus arteriosus before birth remodels the pulmonary vasculature of the lamb. *Pediatr. Res.,* 25251-257.

Wilson, R. E., Keng, P. C. & Sutherland, R. M. (199O) Changes in growth characteristics and macromolecular synthesis on recovery from severe hypoxia. *Br. J. Cancer,* (61)**,** 14-21.

Wu, W., Platoshyn, O., Firth, A. L. & Yuan, J. X. J. (2007) Hypoxia divergently regulates production of reactive oxygen species in human pulmonary and coronary artery smooth muscle cells. *Am J Physiol Lung Cell Mol Physiol,* 293(4)**,** L952-959.

Xie, Z., Dong, Y., Zhang, M., Cui, M. Z., Cohen R.A., Riek, U., Neumann, D., Schlattner, U. & Zou, M. H. (2006) Activation of protein kinase cζ by peroxynitrite regulates lkb1-dependent amp-activated protein kinase in cultured endothelial cells. *J Biol Chem.,* 281(10)**,** 6366-6375.

Xue, C. & Johns, R. A. (1996) Upregulation of nitric oxide synthase correlates temporally with onset of pulmonary vascular remodeling in the hypoxic rat. *Hypertension,* 28(5)**,** 743-753.

Yagasaki, K., Morisaki-Tsuji, N., Miura, A. & Funabiki, R. (2002) Possible involvement of phospholipase c and protein kinase c in stimulatory actions of l-leucine and its keto acid, α-ketoisocaproic acid, on protein synthesis in rlc-16 hepatocytes. *Cytotechnology,* 40(1)**,** 151-154.

Yuen, E. C., Erik, C., Gunther, C. & Bothwe, M. (2000) Nitric oxide activation of trkb through peroxynitrite. *Neuroreport,* 113593-3597.

Zanetti, M., Zwacka, R. M., Engelhardt, J. F., Katusic, Z. S. & O'brien, T. (2001) Superoxide anions and endothelial cell proliferation in normoglycemia and hyperglycemia. *Arterioscler Thromb Vasc Biol,* 21(2)**,** 195-200.

Zhang, P., Wang, Y.-Z., Kagan, E. & Bonner, J. C. (2000) Peroxynitrite targets the epidermal growth factor receptor, raf-1, and mek independently to activate mapk. *J. Biol. Chem.,* 275(29)**,** 22479-22486.

Zhang, Y., Wang, H., Li, J., Dong, L., Xu, P., Chen, W., Neve, R. L., Volpe, J. J. & Rosenberg, P. A. (2006) Intracellular zinc release and erk phosphorylation are required upstream of 12-lipoxygenase activation in peroxynitrite toxicity to mature rat oligodendrocytes. *J. Biol. Chem.,* 281(14)**,** 9460-9470.

Zhuang, S. & Simon, G. (2000) Peroxynitrite-induced apoptosis involves activation of multiple caspases in hl-60 cells. *Am J Physiol Cell Physiol,* 279(2)**,** C341-351.

Zouki, C., Zhang, S.-L., Chan, J. S. D. & Filep, J. G. (2000) Peroxynitrite induces integrin-dependent adhesion of human neutrophils to endothelial cells via activation of the raf-1/mek/erk pathway. *FASEB J.,* 00-0521fje.